Investigation of the Microbial Diversity and Characterization of New Natural Products Produced by Fungi and Actinobacteria of Frobisher Bay

A Thesis

Submitted to the Graduate Faculty

In Partial Fulfillment of the Requirements

For the Degree of

Doctor of Philosophy

In the Department of Biomedical Sciences

Faculty of Veterinary Medicine

University of Prince Edward Island

Alyssa L. Grunwald

Charlottetown, Prince Edward Island

November 2017

THESIS/DISSERTATION NON-EXCLUSIVE LICENSE

Family Name: Grunwald	Given Name, Middle Name (if applicable): Alyssa Louise
Full Name of University: University of Prince Edward Island	
Faculty, Department, School: Department of Biomedical Sciences, Faculty of Veterinary Medicine	
Degree for which thesis/dissertation was presented: PhD	Date Degree Awarded: November 24, 2017
Thesis/dissertation Title: Investigation of the Microbial Diversity and Characterization of New Natural Products Produced by Fungi and Actinobacteria of Frobisher Bay	

In consideration of my University making my thesis/dissertation available to interested persons, I,

Alyssa Grunwald hereby grant a non-exclusive, for the full term of copyright protection, license to my University, the University of Prince Edward Island:

(a) to archive, preserve, produce, reproduce, publish, communicate, convert into any format, and to make available in print or online by telecommunication to the public for non-commercial purposes;
(b) to sub-license to Library and Archives Canada any of the acts mentioned in paragraph (a).

I undertake to submit my thesis/dissertation, through my University, to Library and Archives Canada. Any abstract submitted with the thesis/dissertation will be considered to form part of the thesis/dissertation.

I represent that my thesis/dissertation is my original work, does not infringe any rights of others, including privacy rights, and that I have the right to make the grant conferred by this non-exclusive license.

If third party copyrighted material was included in my thesis/dissertation for which, under the terms of the *Copyright Act*, written permission from the copyright owners is required I have obtained such permission from the copyright owners to do the acts mentioned in paragraph (a) above for the full term of copyright protection

I retain copyright ownership and moral rights in my thesis/dissertation, and may deal with the copyright in my thesis/dissertation, in any way consistent with rights granted by me to my University in this non-exclusive license.

I further promise to inform any person to whom I may hereafter assign or license my copyright in my thesis/dissertation of the rights granted by me to my University in this non-exclusive license.

Signature	**Date**

University of Prince Edward Island

Faculty of Veterinary Medicine

Charlottetown

CERTIFICATION OF THESIS WORK

We, the undersigned, certify that

candidate for the degree of

has presented her/his thesis with the following title

(as it appears on title page of thesis),

that the thesis is acceptable in form and content, and that a satisfactory knowledge of the field covered by the thesis was demonstrated by the candidate through an oral examination held on

Examiners

Dr.

Dr.

Dr.

Dr.

Dr.

Date

Abstract

Natural products (NPs) are an important source of pharmaceutical agents and are produced by a wide range of micro and macro organisms. Microorganisms, specifically bacteria within the order Actinomycetales and fungi, are prolific producers of NPs and are responsible for upwards of 70% of all clinically approved antibiotics. Due to the intensive investigation of these microorganisms, specifically from the terrestrial environment for NP discovery, the rate of reisolation of known compounds is high. One way to overcome this issue is to investigate unexplored and underexplored environments as a source of biodiverse microorganisms for natural product discovery.

Canada's Arctic remains a vast and largely undiscovered landscape due to its inaccessibility and harsh environment. Being so, the Arctic provides a unique niche, where members of the microbial community have evolved to "fit" this distinctive environment and must be capable of withstanding extreme cold, limited environmental resources and a range of other physical and biological factors. It is hypothesized Arctic microorganisms will have a unique secondary metabolome compared to their tropical counterparts based on environmental selection. Due to a lack of investigation of Canada's Arctic for natural products, Frobisher Bay was selected as the study location for this investigation. The aims of this thesis were to characterize the bacterial and fungal community of Frobisher Bay and to discover new NPs from these microorganisms.

In order to assess the microbial community within Frobisher Bay, 454-pyrosequencing of the 16S rRNA gene and ITS region was used to determine the bacterial and fungal diversity respectively within sediment samples from Frobisher Bay. In order to achieve greater sequencing depth within the prolific NP producing Actinobacteria, Actinobacteria-specific 16S rRNA primers were used in addition to universal 16S rRNA primers. Overall, sites within Frobisher Bay were found to host high levels of taxonomically diverse microorganisms. The presence of large numbers of unknown phylotypes and the immense taxonomic diversity uncovered, make this region an intriguing area to explore from a NPs perspective.

Using a variety of isolation techniques, Actinobacteria and fungi were cultured from sediment samples collected from Frobisher Bay. In total, 90 Actinobacteria representing 25 distinct species, and 354 fungal isolates representing 54 species were cultured from this region. Of the fungal isolates, 9 appeared to be putatively novel based on sequencing of barcoding genes and morphological investigations. These isolates were particularly interesting from a NPs perspective, as they offered an untapped resource for NP discovery.

In order to prioritize isolates based on the production of new NPs, an LC-HRMS based screening method was used. This resulted in the isolation and characterization of several new NPs including a new hirsutellic acid analog obtained from *Simplicillium aogashimaense* RKAG 563, a new reduced perylene quinone compound obtained from

Cadophora viticola RKAG 170 and two new cameronic acid analogs from *Botrytis caroliniana* RKAG 208. Investigation of the putatively novel fungal isolates was particularly fruitful for natural product discovery and resulted in the isolation of 17 new natural products. Investigation of *Mortierella* sp. RKAG 110 resulted in the characterization of mortiamides A-D, new cyclic heptapeptides containing five amino acids in the non-natural D-configuration. Examination of *Sesquicillium* spp. RKAG 571 and 186 led to the isolation of the new 11 residue peptaibols, tariuqins A-F containing the non-proteogenic amino acids (*R*)- and (*S*)-isovaline and aminoisobutyric acid, and to the isolation of the new cyclic decapeptides, auyuittuqamide A-D, containing three *N*-methylated amino acids. Lastly, exploration of putatively novel *Tolypocladium* species led to the isolation of several new tetramic acid containing compounds, iqalisetin A and B, and tolypoalbin.

Due to the permanently cold environment from which they were isolated, the effect of fermentation temperature on NP product production in Actinobacteria from Frobisher Bay was investigated. As most standard lab fermentations occur at a non-ecologically relevant temperature of 30˚C, fermentations at colder, more ecologically relevant temperatures (4˚C and 15˚C) was undertaken. Differences in NP production at each fermentation temperature were assessed using an LC-HRMS based chemical metabolomics method on a subset of cultured actinomycetes. Within the 15˚C fermentations, the *de novo* induction of actinomycin was observed in *Streptomyces* sp. RKAG 337 and the upregulated production of two new compounds, landomycin AA and AB from *Streptomyces* sp. RKAG 290 was observed. Due to this upregulation, sufficient material was produced to enable structural characterization of these two compounds. The use of fermentation temperature to induce or increase the production of NPs is a useful tool to access previously inaccessible chemical diversity.

Overall, Frobisher Bay is a rich resource for microorganisms as assessed by culture independent and dependent methods. The isolation of a large number of new NPs from microorganisms from this region, highlights the Arctic as a promising resource for NP discovery, reinforcing the notion that investigating unexplored environments for NP discovery is a very valuable tool in NPs research.

Acknowledgements

First and foremost, I would like to thank my supervisor Dr. Russell Kerr for first accepting me as a co-op student during my undergraduate degree and secondly for accepting me as a graduate student. Thank you for your mentorship, support and guidance over the last five years, and for allowing me to repeatedly say "sky's the limit!".

I would like to thank my research managers Brad Haltli, Dr. Fabrice Berrue and Dr. David Overy for all of their support over the years. Fabrice, thank you for teaching me all about natural products chemistry and how to solve NMR structures. Dave thank you for your guidance and insight and for teaching me all about fungal taxonomy. Brad thank you for all of your input into my project and teaching me way more than any person would ever want to know about actinomycetes!

I would also like to thank my supervisory committee members past and present including Dr. Chris Kirby, Dr. Jason McCallum, Dr. Spencer Greenwood, Dr. J. McClure and Dr. Junzeng Zhang. Your comments, guidance and support throughout my PhD have been greatly appreciated. Thank you to my examination committee Dr. Marya Ahmed, Dr. Spencer Greenwood, Dr. Andy Tasker and my external examiner Dr. John Sorensen for taking the time to read my thesis and be part of my exam.

Thank you to all who provided technical assistance during my project. Thank you to Dr. Jeff Lewis and Beatrice Despres for assisting with MALDI-TOF MS. To Kate McQuillan and Martin Lanteigne for running my biological assays. To Patricia Boland and Dr. Hebelin Correa for running my LC-HRMS and MS/MS experiments and to Hebelin for help with analysis. Thank you to Dr. Lloyd Kerry and Maike Fisher for running all of my NMR experiments. Thank you to Dr. Andreas Decken for running X-ray crystallography on my samples and to Dr. Gerry Wright for providing *Streptomyces* strains. I would like to thank Innovation PEI and NSERC for providing me with personal funding. Additionally I would like to thank Nunavut Tunngavik Inc. for allowing us to collect samples in Frobisher Bay.

Lastly I would like to thank my family and friends for their unwavering support and guidance. Thank you to my family, my parents, Pat and Albert for always being willing to move me across the country every time I got a new job or went to a new school, my brother Garrett and to Denise and Sophie, and to my Oma, Opa and Grandma. I am eternally grateful for all of you. Thank you to my parents away from home, Dennis and Diana for all of your kindness and encouragement and for making sure I never missed a holiday meal being so far from home. Thank you to all of my wonderful lab mates over the years (Malcolm, Andrew, Hebelin, Marieke, Gavin, Stacey, Amanda x 2, Logan, Leon, Hope, Vernon, Zach, Anna, Becca, Jen, Ghada, Doug, Beth, Nadia). You have made coming to the lab each day enjoyable and very entertaining. Thank you to the "Nautili", Noelle, Nick and Josh for answering all of my questions in the lab. A big thank you to Erin McCauley for always being ready to hang out with an endless supply of white wine…even if it was a Monday night. To Krista Gill, thank you for our daily 11:30 lunch dates and lifelong friendship. Thank you to Kate, Justine and Tara for your never-ending friendship and visits to PEI. To Nicole, thank you for inspiring me to live life to the fullest. Lastly, to Andrew, thank you for your love and unconditional support over the last five years (especially when I was busy doing thesis work and ignored you for multiple weeks at a time!).

Dedication

For my mom and dad

Table of Contents

List of Tables

List of Figures

Abbreviations

Å	angstrom
Ac	acetyl
Aib	aminoisobutyric acid
AOS	Arctic Ocean Survey
BFM	bacterial fermentation medium
BLAST	Basic Local Alignment Search Tool
bp	base pair
C_{18}	octadecylsilane
CD_3OD	deuterated methanol
$CDCl_3$	deuterated chloroform
CH_3CN	acetonitrile
CoA	coenzyme A
COSY	correlation spectroscopy
DEPT	distortionless enhancement by polarization
DMSO	dimethyl sulfoxide
DMSO-*d6*	deuterated dimethyl sulfoxide
DNA	deoxyribonucleic acid
E	Shannon equitability index
ELSD	evaporative light scattering detector
ESI	electrospray ionization
EtOAc	ethyl acetate
FA	formic acid
FACs	fungal artificial chromosomes
FDAA	1-fluoro, 2-4-dinitrophenyl-5-L-alanine amide
GTR+G	general time reversible (gamma distributed)
H’	Shannon diversity index
HCl	hydrochloric acid
HDAC	histone deacetylase
HEKa	human epidermal keratinocytes
HMBC	heteronuclear multiple bond correlation
HPLC	high performance liquid chromatography
HRMS	high-resolution mass spectrometry
HSQC	heteronuclear single quantum coherence
ICoMM	International Census of Marine Microbes
IC50	half-maximal inhibitory concentration
iCHIP	isolation chip
IO	instant ocean
ISP	International *Streptomyces* Project medium
ITS	internal transcribed spacer
Iva	isovaline
J	coupling constant
LC-HRMS	liquid chromatography high-resolution mass spectrometry
MALDI-TOF MS	matrix-assisted laser desorption/ionization time-of-flight mass spectrometry
MEGA	molecular evolutionary genetics analysis

MeOH	methanol
MNP	marine natural product
MRSA	methicillin resistant *Staphylococcus aureus*
MS/MS	tandem mass spectrometry
m/z	mass to charge ratio
NCBI	National Centre for Biotechnology Information
NGS	next generation sequencing
NMR	nuclear magnetic resonance
NOESY	nuclear Overhauser effect spectroscopy
NP	natural product
NRP	nonribosomal peptide
NRPS	nonribosomal peptide synthetase
OTUs	operational taxonomic units
PCR	polymerase chain reaction
PDA	photodiode array
PKS	polyketide synthase
ppm	parts per million
RiPP	ribosomally synthesized post-translationally modified peptide
ROESY	rotating frame Overhauser effect spectroscopy
rpm	revolutions per minute
rRNA	ribosomal ribonucleic acid
RP	reverse phase
R_T	retention time
S_{est}	Chao1 estimated species richness
S_{Obs}	observed species richness
TEF	transcription elongation factor
TOCSY	total correlated spectroscopy
WAC	Wright Actinomycete Culture Collection
UPGMA	unweighted paired group method with arithmetic mean
UV	ultraviolet
VRE	vancomycin resistant *Enterococcus*

CHAPTER 1: INTRODUCTION AND OBJECTIVES OF RESEARCH

1.1 What is a Natural Product?

Natural products (NPs), also known as secondary metabolites are compounds produced by living organisms (plants, animals, microorganisms, etc.) that are generally not required for the sustenance of life, but offer an evolutionary advantage to the producing organism[1]. NPs have evolved over billions of years to interact with biological targets and can function in chemical defense, aid in signalling and communication, function in nutrient transport, aid in reproduction or offer other competitive advantages. By determining the target and role of these compounds, these metabolites can be exploited as a source of pharmaceutical agents with benefits for human health[2].

NPs are structurally diverse accounting for their wide ranging biological activities and have been grouped into families based on structural features and biosynthetic origins. Generally NPs fall into four major classes including alkaloids, peptides, polyketides and terpenes[3] (Figure 1.1). Alkaloids are heterocyclic nitrogen containing compounds biosynthesized by modification of amino acid building blocks[4]. Terpenes are derived from the 5 carbon building block isoprene produced via the mevalonate pathway or the deoxyxylulose phosphate pathway (non-mevalonate pathway)[5]. Peptide NPs are composed of amino acids linked through peptides bonds which often contain non-proteogenic or modified amino acids. Peptides can either be biosynthesized via the ribosome to produce ribosomally synthesized post-translationally modified peptides (RiPPs)[6] or by large, multidomain non-ribosomal peptide synthetase enzymes (NRPs). Lastly, polyketides are typically composed of acetate and malonate subunits and are biosynthesized by large, multimodular polyketide synthase enzymes (PKS)[7]. The synthesis of hybrid NPs containing structural features of more than one class also contributes to the large structural diversity observed for these compounds.

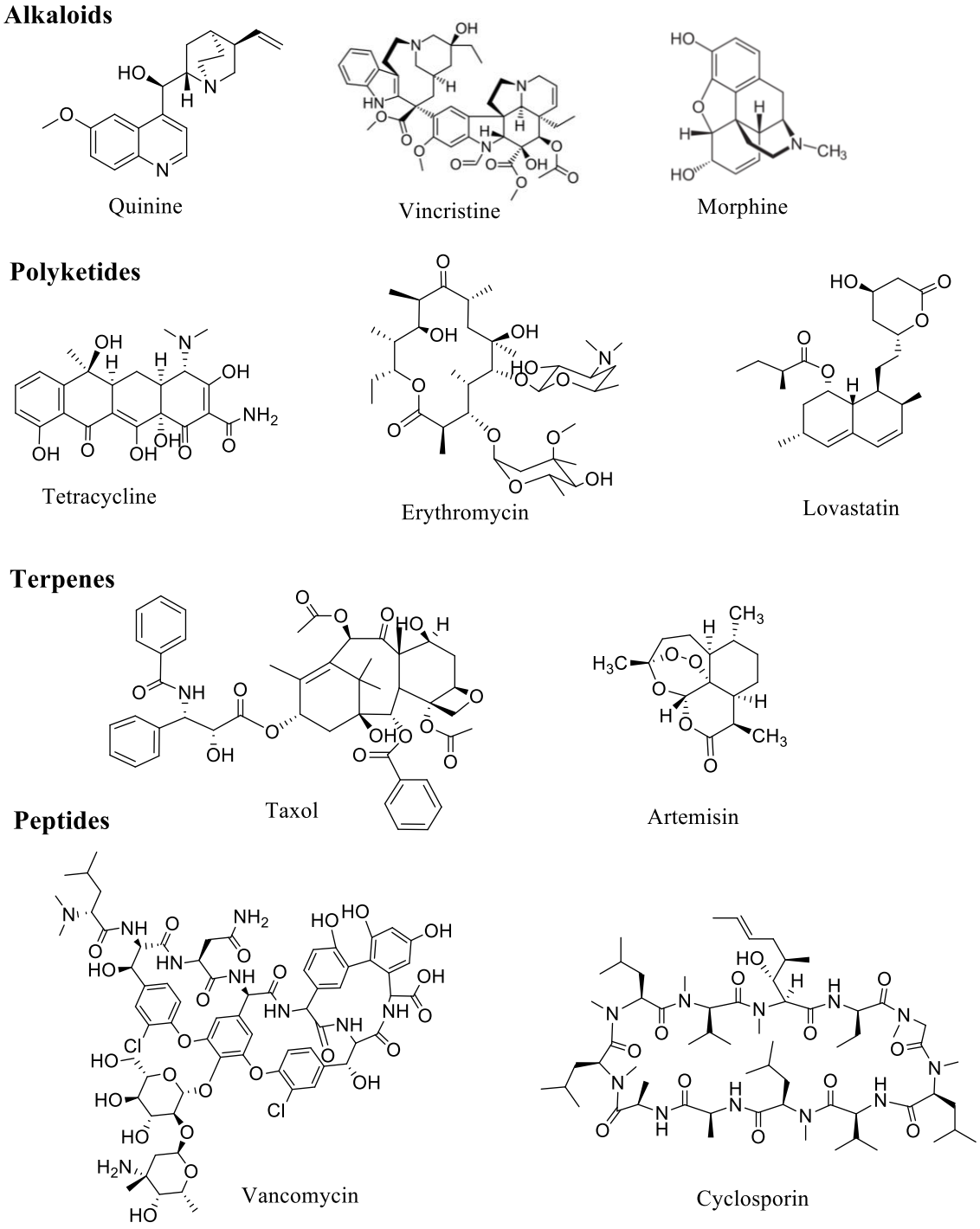

Figure 1.1. Classes of natural products.

1.2 Historically Important Natural Products

NPs have been used throughout millennia in the form of traditional medicines, remedies and oils. The use of several important NPs occurred in the 18th and 19th centuries (often long before the isolation of the active compound) including the cardiotonic glycoside digitoxin from *Digitalis purpurea* (foxglove), the anti-malarial drug quinine from the bark of *Cinchona succiruba*, morphine from the poppy *Papaver somniferum*, acetylsalicylic acid (aspirin) a synthetically derived compound of the NP salicin from the bark of the willow tree *Salix* and the alkaloid pilocarpine from the plant *Pilocarpus jaborandi* used for the treatment of glaucoma[2]. Although NPs have been used historically for thousands of the years, the field of modern NPs has only taken shape within the last 75 years.

The field of modern NPs was born from the discovery of penicillin in 1928 by Alexander Fleming from *Penicillium notatum* (now known as *Penicillium chrysogenum*) and the subsequent commercialization of penicillin in the early 1940s[8]. The success of this discovery prompted the large scale search for other bioactives from microorganisms heralding what is termed the "Golden Age" of antibiotic discovery (1950's-1960's). During this Golden Age, the majority of major classes of antibiotics were discovered including the aminoglycosides (e.g. streptomycin), amphenicols (e.g. chloramphenicol), ansamycins (e.g. rifamycin), cephalosporins (e.g. cefalotin), fusidanes (e.g. fusidic acid), glycopeptides (e.g. vancomycin), lincosamides (e.g. lincomycin), macrolides (e.g. erythromycin), penicillins (e.g. benzylpenicillin), polypeptides (e.g. bacitracin) and tetracyclines (e.g. chlorotetracycline)[9].

Not only were NPs utilized as antibiotics, they were also a source of anticancer agents. In the 1950's the alkaloid vincristine was discovered from the periwinkle

Catharanthus roseus and was later approved for the treatment of Hodgkin's disease and leukemia[10]. In 2013, the production of vincristine was determined to be by an endophytic fungus (*Fusarium oxysporum*) within the plant[11]. In 1971, paclitaxel was isolated from the Pacific Yew tree, *Taxus brevifolia*[12] (later shown to be produced by a fungal endosymbiont *Taxomyces andreanae*)[13] and approved for the treatment of a variety of cancers. Investigation of the bacterial genus *Streptomyces* resulted in the discovery of many FDA approved anticancer compounds including actinomycin in 1964, bleomycin in 1973, doxorubicin in 1974 and mitomycin C in 1974[14].

Besides antimicrobial and antineoplastic activity, NPs have found many other applications within human health including the cholesterol lowering statins (lovastatin, mevastatin) from *Penicillium citrinum* and *Monascus ruber*[15,16], Galantamine, an acetylcholinesterase inhibitor used to treat Alzheimer's Disease from the plant *Galanthus* spp.[17], artemisinin, an antimalarial drug from the plant *Artemisia annua*[18], cyclosporin, an immunosuppressant from the fungus *Tolypocladium inflatum*[19], ergometrine, a vasoconstrictor from the fungus *Claviceps purpurea*[20], asperlicin, for the treatment of anxiety from the fungus *Aspergillus alliaceus*[21], and ivermectin, the antiparasitic compound used for the treatment of river blindness and elephantiasis from *Streptomyces avermitilis*[22].

Today NPs play a prominent role in the clinic and of 1,562 new drugs approved between 1981 and 2013, 50.6% are NPs or synthetic compounds inspired by NPs. Of all NPs that are FDA approved, 45% are derived from plants, 29% from bacteria and 22% are from fungi[23]. Of 246 anticancer drugs approved from the late 1930's to 2014, 77% of compounds approved for the treatment of cancer are either derived or inspired by

NPs[24] and of all FDA approved antibiotics, 69% are derived from NPs. Strikingly of all NP-derived antibiotics, the vast majority are produced by microorganisms including bacteria (51%) and fungi (46%)[23] making these organisms a very important source of antibiotics.

1.3 Microorganisms as a Source of Natural Products

The link between biodiversity and chemical diversity is well established as it is known that taxonomically distinct organisms can produce different NPs[25,26]. As microorganisms are the largest reservoir of genetic diversity on Earth, they have great potential for natural product discovery[27]. The extensive taxonomic and metabolic diversity of microorganisms is shaped by adaptive pressures within their habitat and has led them to colonize every environment on Earth. Due to the immensely competitive environment in which they inhabit, microorganisms have a high propensity to produce bioactive NPs (especially antibiotics) compared to other sources including plants and animals. In terms of biological activity, microorganisms produce 80% of all bioactive NPs (80-100,000 total known bioactive NPs). Of the 60-80,000 known microbial metabolites, 36% exhibit antibiotic activity and 11% exhibit other biological activities. Fungi and members within the bacterial phylum Actinobacteria produce 36% and 44% of all bioactive microbial NPs respectively and are a tremendous resource for NP discovery[25].

The phylum Actinobacteria is one of the largest bacterial phyla and is a lineage of Gram-positive bacteria with high GC content in their DNA (50-75%). Actinobacteria are ubiquitous and inhabit the terrestrial, aquatic and marine environments. They are chemoorganotrophic, aerobic bacteria and many species are known to produce spores in

response to adverse environmental conditions[28,29]. Of all bioactive bacterial NPs, 77% are produced by Actinobacteria[25] and within the Actinobacteria, the genus *Streptomyces* is responsible for the production of the majority of these NPs. Extensive investigation of actinomycetes has been ongoing since the 1940's and has resulted in many important NPs which have been developed into drugs. These include, but are not limited to the antibiotics amphotericin B, erythromycin and vancomycin[30] and the anticancer compounds daunorubicin, bleomycin and mitomycin[14].

Within the fungal kingdom it is estimated that over 1.5 million species exist and of these only 25,000 have been formally characterized[31]. Within the environment, fungi act largely as decomposers, as pathogens, or as symbionts of other organisms[32]. Around 30,000 NPs have been discovered from fungi and of bioactive fungal NPs (15,600), 72% are produced by microscopic fungi such as *Aspergillus* and *Penicillium*, 23% are produced by the *Basidiomycetes* (mushrooms) and 2% by unicellular yeasts and slime moulds[25]. Almost all NPs produced by fungi are reported from members within the phyla Ascomycota and Basidiomycota and these phyla are responsible for the production of many commercially important NPs encompassing a wide range of activities including lovastatin (antilipidemic), cyclosporin and mycophenolic acid (immunosuppressants), penicillin (antibiotic), strobilurin (agricultural fungicide), echinocandin (antifungal), nodulisporic acid A (insecticidal) and PF1022A (anthelmintic)[33].

In addition to their propensity to produce bioactive NPs, microorganisms offer many advantages over other sources of NPs such as plants and animals. First, due to their enormous taxonomic biodiversity, the metabolic diversity of these microorganisms

is immense leading to a wide range of chemically diverse NPs. Secondly these NPs can be isolated in the lab in a nearly inexhaustible supply from the microorganism. In contrast, the use of plants and invertebrates for NP discovery often requires the large scale unsustainable harvest of the organism of interest. Often due to a lack of supply of the producing organism only limited quantities of the NP are obtained making characterization and future clinical development challenging. Thirdly, the relative ease of genetic manipulation of microorganisms allows for the manipulation of biosynthetic gene clusters to increase production, generate analogs or precursors of the NP, probe the biosynthesis of these compounds and/or heterologously express biosynthetic gene clusters from other organisms[34,35].

1.4 Current Challenges in Natural Products Research

Although microorganisms have been a prolific source of NPs, the continuous reisolation of known compounds is one of the largest challenges in the field of NP research. Extensive investigation of the terrestrial environment for NP producing microorganisms has led to the continued increase in the rate of reisolation of known NPs. This is especially true when studying members of the genus *Streptomyces*, as many species share the same biosynthetic gene clusters and produce the same metabolites causing the rate of reisolation to be extremely high. This trend is highlighted in the rate of discovery of new classes of antibiotics which has been in decline since the 1970's[9]. Due to the continued reisolation of known compounds and continued increase in the cost of discovering new antibiotics, big pharma has discontinued many of its NP discovery programs leaving a large void in the antibiotic clinical pipeline. When paired with the

increasing rise in multi-drug resistant microbes, there is a great need to discover new antibiotic classes.

One way to increase the odds of finding new NPs is to investigate previously unexplored geographic areas for NPs. The hypothesis that microbial diversity translates to chemical diversity is well established[25,26] and bioprospecting in underexplored, underrepresented and extreme habitats is increasing the probability of finding new NPs as new microbial diversity is uncovered. The terrestrial environment has been well studied as a source of microbial NPs, while the marine environment has largely been overlooked and under sampled. Within the marine environment, the immense diversity of ecological niches provides considerable opportunities for sampling and bacterial isolation, providing a largely untapped resource for the discovery of new NPs.

1.5 The Marine Environment as a Source of Natural Products

Oceans cover 70% of the area on Earth (360 million km^2) and host immense biodiversity. The diversity of ocean ecosystems and life within offers immense potential for the discovery of NPs. Exploration of the marine environment became enhanced with the introduction of SCUBA in the 1970s, manned submersibles in the 1980s and remotely operated vehicles (ROVs) in the 1990s. The isolation of over 28,000 structurally distinct NPs from many marine organisms including bacteria, fungi, algae, invertebrates (coral, sponges, tunicates, etc.) and vertebrates (fish) highlights the marine environment as an increasingly important source of new NPs[36]. Thus far, the global marine pharmaceutical pipeline consists of 7 compounds approved for clinical use (Figure 1.2), 26 NPs (or derivatives) in phase I-III of clinical trial and a large number of marine NPs in the preclinical pipelines[37].

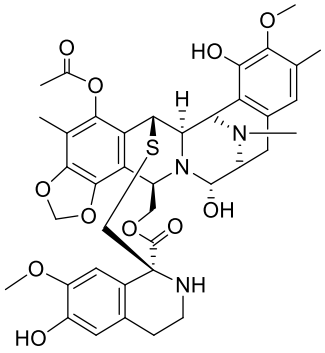

Trabectedein (Yondelis)

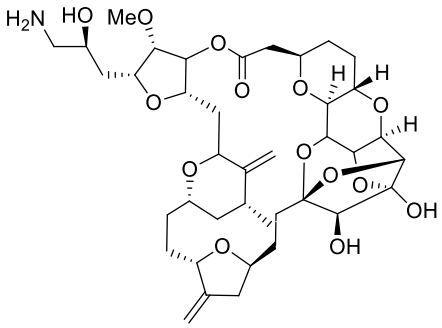

Eribulin mesylate (Halaven)

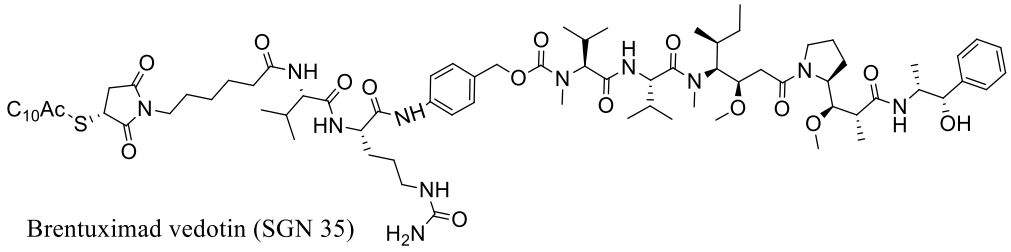

Brentuximad vedotin (SGN 35)

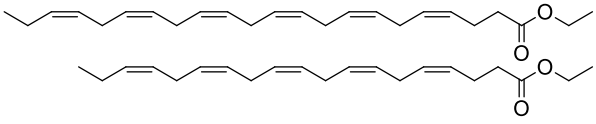

Omega-3-acid ethylesters (Lovaza)

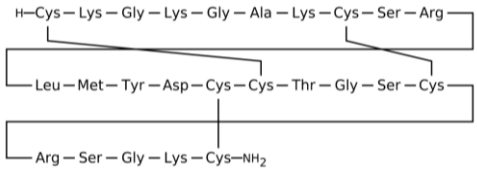

Ziconotide (Prialt)

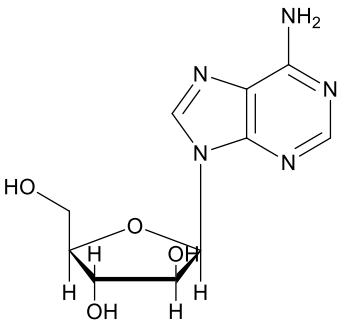

Cytarabine (Cytosar-U)

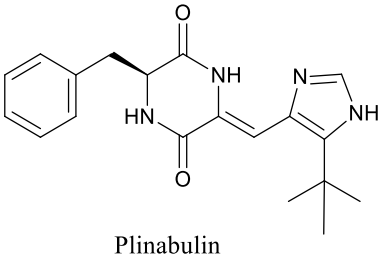

Plinabulin
(Phase II)

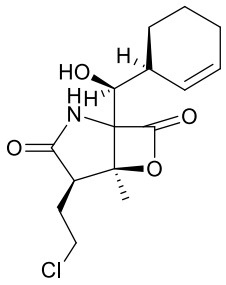

Salinosporamide A
(Phase I)

Figure 1.2. FDA approved marine natural products and fungal (plinabulin) and actinobacterial (salinosporamide) natural products in clinical trials.

The first marine NP to be developed for clinical use as an anticancer agent was Ara-C, a synthetic analog of a C-nucleoside from the Caribbean sponge, *Cryptotethya crypta* which was approved in 1969 for the treatment of acute myelocytic leukemia and non-Hodgkin's lymphoma[38]. Within the last 7 years, three additional anticancer compounds have been approved. These include trabectedin (Yondelis) from the tunicate *Ecteinascidia turbinata* for the treatment of soft tissue sarcomas and ovarian cancer[39], eribulin (Halaven), inspired by halichondrin A from the sponge *Halichondria okadai* for the treatment of breast cancer[40,41] and brentuximab vedotin (Adcetris), a dolastatin 10 drug-antibody conjugate for the treatment of Hodgkin's lymphoma and anaplastic large cell lymphoma[42]. Additional approved compounds include Ara-A (a synthetic analog of spongouridine from the sponge *Cryptotethya crypta* for the treatment of herpes simplex infections[43], ziconotide (Prialt) from the cone snail *Conus magus* for the treatment of chronic pain[44] and Lovaza, a lipid regulating agent consisting of fish oils[45]. Due to issues concerning the efficacy of Ara-A, this drug has been discontinued.

Prior to 1985, less than 100 NPs were discovered annually from the marine environment, increasing to 500 NPs per year from the 1990's to 2005 and currently upwards of 1,000 new marine NPs are described each year. Of these, 75% have been isolated from marine invertebrates belonging mainly to the phyla Porifera (sponges) and Cnidaria (corals)[46]. Increased reports within the literature suggesting the origin of many of these NPs are from microbial symbionts within the invertebrate host[47] and the amenability of microorganisms to lab culture has resulted in a shift of focus from the investigation of marine invertebrates to microorganisms for natural product discovery. Thus, the rate of isolation of new NPs from microorganisms is steadily increasing with

reports of Actinobacteria and fungi (within the phylum Ascomycota) contributing to increased reports of NPs from the marine environment within the last two decades[36,48]. Largely, NPs from microorganisms within the marine environment are still underrepresented in the NPs literature.

1.6 Marine Actinomycetes

Actinomycetes have been recovered from every explored marine niche, although their existence as true marine organisms was questioned for decades. It was unknown whether these isolates were metabolically active within the marine environment or were the result of dormant spores washed in from the terrestrial environment. Due to the doubt raised of their origin, the exploration of marine actinomycetes was largely ignored in favour of true marine organisms such as sponges and corals[49]. Although sampling for marine actinomycetes began in the 1960's[50], the first taxonomic description of a marine Actinobacteria, *Rhodococcus marinonascens* occurred in 1984[51]. In 2005, the first seawater obligate marine actinomycete genus was described, *Salinispora*, consisting of two species, *Salinispora tropica* and *S. arenicola*[52]. Continued work by Fenical and Jensen has uncovered at least 13 further marine lineages of Actinobacteria[49] and several other groups have contributed taxonomic descriptions of additional obligate marine Actinobacteria genera[53,54,55].

Marine actinomycetes have been an excellent resource for the discovery of new NPs with unique chemical scaffolds and interesting biological activity. Salinosporamide A isolated from *Salinispora tropica* is a β-lactone containing compound that irreversibly binds to and inhibits the 20S subunit of the proteasome resulting in the disruption of cellular processes, induction of apoptosis and inhibition of tumor growth and

angiogenesis[56]. Salinosporamide A is currently undergoing phase II clinical trials in patients with advanced solid tumor malignancies. Further chemical investigation of *S. tropica* led to the isolation of the polycyclic chlorine containing macrolides sporolide A and B[57] and the polyene macrolactam salinilactam A[58]. Additionally, the isolation of new compounds from other species within the genus *Salinispora* including *S. arenicola* (saliniketals A and B[59] and arenicolide A-C[60]) and *S. pacifica* (cyanosporaside A and B[61], salinipyrone A and B, and pacificanone A and B[62]) highlights the metabolic capabilities of this one marine genus.

Members within the family *Streptomycetaceae* are prolific producers of NPs in the terrestrial environment and have been readily cultured from marine samples, although most of these isolated strains are closely related or identical to terrestrial strains. The continued investigation of *Streptomyces* within the marine environment has led to the taxonomic characterization of marine *Streptomyces* including *S. ovatisporus*[63], *S. verrucosisporus*[64], *S. spongiicola*[65], *S. marinus*, *S. haliclonae*, and *S. tateyamensis*[66] to name a few. From these marine *Streptomyces* many new and unusual NPs have been uncovered and include the isolation of the marinoyrroles (densely halogenated bispyrroles)[67], actinoranone (dihydronapthalenone polyketide linked to a bicyclic diterpenoid)[68] and the mannopeptimycins (containing an unprecedented amino acid α-amino-β-[4‘-(2‘-iminoimidazolidinyl)]-β-hydroxypropionic acid)[69] (Figure 1.3).

Additionally, new genera within the family *Streptomycetaceae* have been uncovered including the marine clade *Marinospora* and the informally characterized marine clades MAR3, MAR4 and MAR8[49]. Chemical investigation of the genus *Marinospora* has led to the characterization of the macrolides, marinomycin A-D[70] and

marinisporolide A-E[71]. Investigation of the MAR3 clade has resulted in the isolation of the highly modified peptides, actinoramides A-C[72] and investigation of the MAR4 clade has resulted in the characterization of the hybrid polyketide-terpenoid marinone[73] and the N-isoprenoid bromo-phenazinone compounds, the marinocyanins[74].

Within the last 15 years, the rate of isolation of new metabolites from marine Actinobacteria has been rising. The continued isolation of new chemistry with unprecedented structures from marine lineages highlights the tremendous resource the marine environment is for NP discovery. The investigation of only a small proportion of the marine environment still leaves this as a largely uninvestigated resource for NP discovery.

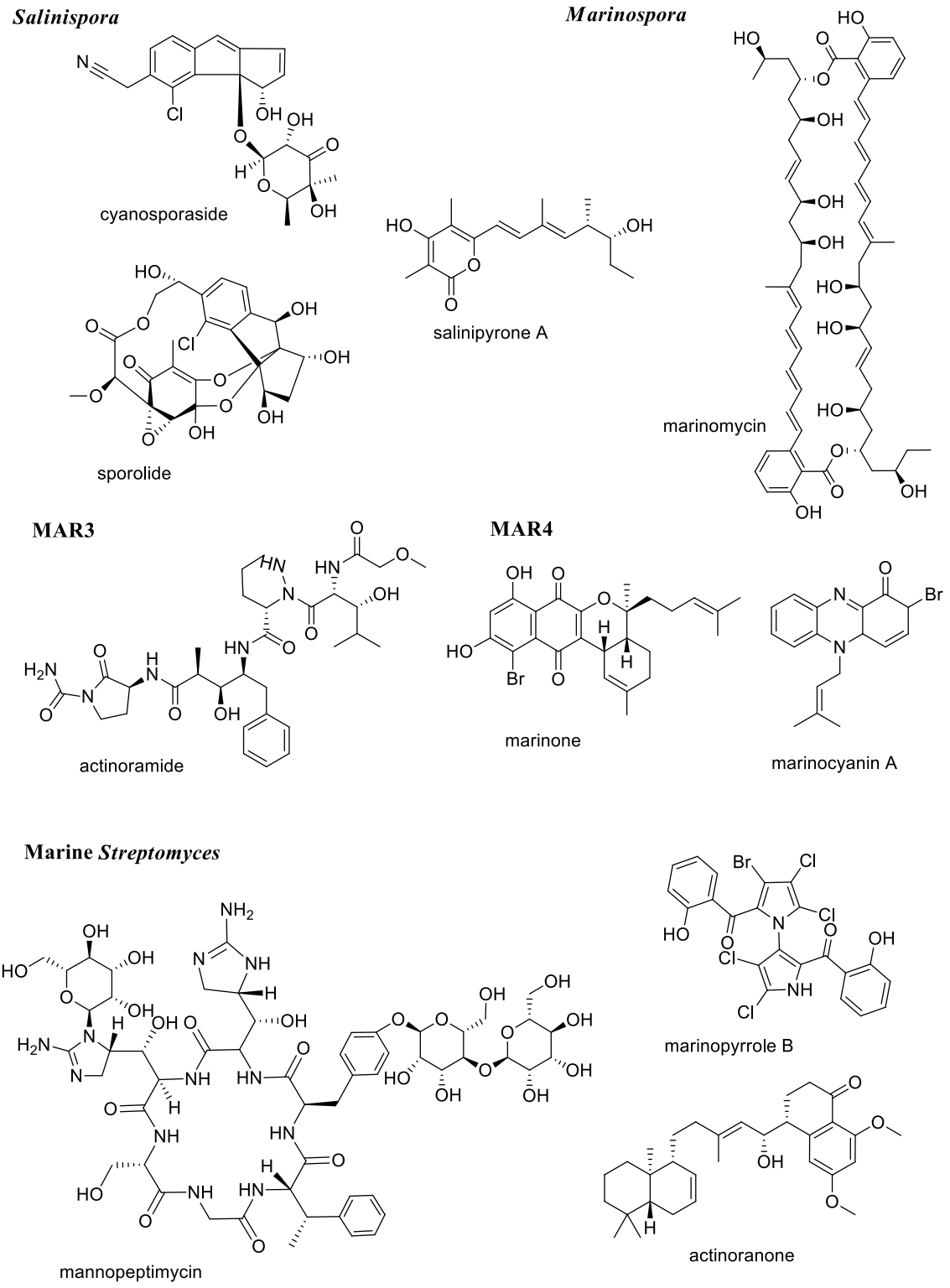

Figure 1.3. Select examples of natural products from marine derived actinomycetes.

1.7 Marine Fungi

The field of marine mycology began in the mid 1800's with the isolation of fungi from seaweed. Since this time, fungi have been shown to colonize virtually every marine niche including mangroves, sand, sediment, algae, estuary plants, invertebrates (sponges, corals, ascidians, bivalves, crustaceans and holothurians), vertebrates (mainly fish), plankton and the deep sea[75,76]. Like marine actinomycetes, the presence of true marine fungi was questioned as it was unknown whether fungi isolated from the marine environment was the result of dormant spores or propagules from the terrestrial environment, or whether these were indeed metabolically active as many isolated fungi were similar or identical to terrestrial species. The isolation of marine *sensu strictu* fungi which are entirely dependent on the marine environment for their survival proved the existence of marine fungi[77, 78]. Currently 1,100 species of marine *sensu strictu* fungi are described and many other lineages of marine fungi have been detected by environmental sequencing that remain uncultured[79].

Up until 1992, only 15 NPs were described from marine derived fungi. Since then, almost 2,000 NPs have been described and characterized from fungi collected from the marine environment[80,81,82]. The discovery of the antibiotic cephalosporin C in 1949 produced by a culture of a member of the genus *Cephalosporium* obtained from the Sardinian coast is one of the first examples of the isolation and characterization of a marine isolated fungal NP[83]. Currently the most promising fungal marine metabolite is the diketopiperazine halimide which was discovered by in 1992 from an *Aspergillus* sp. collected from the waters off the Philippine Islands[84]. This compounds displayed potent activity against multi-drug resistant human tumor cell lines by acting as a tubulin depolymerising agent. This molecule served as a lead structure for the closely related

synthetic analog Plinabulin (NPI-2358) which is currently undergoing phase III clinical trials in patients with advanced non-small cell lung cancer[85].

Within the last fifteen years, the isolation of metabolites from marine isolated fungi has been increasing, although the origins of many of these fungi are in question. Many fungi from the terrestrial environment are capable of growth within seawater and can inhabit both environments. These isolates are termed ubiquitous and a large number of reports of NPs within the literature from marine fungi has been the result of these ubiquitous fungi. In terms of NPs described from true marine fungi (marine *sensu stricto*), the number of NPs appears to be closer to 80[86]. Recent genome sequencing of several marine *sensu stricto* fungi is beginning to reveal the genetic capacity of these organisms and the NP diversity within, although formal characterization of these genomes has yet to be published. The field of NPs in terms of marine *sensu stricto* fungi is in its infancy and is a largely untapped resource for future NP discovery.

1.8 The Cold Marine Biosphere

The cold marine biosphere encompass Earth's polar marine environment, the deep sea environment and other marine environments with an average temperature less than 4˚C and is greatly underexplored in terms of NPs. This environment has often been overlooked due to the difficulty in accessibility and perception of being a low productivity environment[87]. Organisms inhabiting this region must be able to withstand extreme cold and low nutrient availability. In order to overcome these extreme conditions microorganisms have developed unique adaptations such as the synthesis of cold-adapted enzymes, production of cold shock and antifreeze proteins and the ability to increase membrane fluidity with decreasing temperature[88].

NPs isolated from the cold marine biosphere represent less than 3% of known marine NPs (605 total described NPs). Of these reported NPs, 51% are of microbial origin. The vast majority of reported NPs from the cold environment are from the deep sea. When looking at microbial NPs from Earth's northern polar marine environment, the number of NPs reported decreases drastically to around 23[87] (Figure 1.4). These include the isolation of the mixirins, cyclic peptides isolated from a psychrotolerant *Bacillus* sp. from sea mud near the Arctic pole[89], several aromatic nitro compounds from a *Salegentibacter* sp. isolated from the bottom of an ice flow from the Arctic Ocean[90], the diketopiperazine cyclo-(L-Pro-L-Met) from *Nocardiopsis* sp. isolated from an Arctic collected seaweed (*Undaria pinnatifida*)[91], N-(2-hydroxyphenyl)-2-phenazinamine from an Arctic Ocean sediment near Svalbard derived *Nocardia dassonviellei*[92], nitrosporeusines from *Streptomyces nitrosporeus* isolated from sediments of the Arctic Chukchi Sea[93], arcticosides from a sediment derived *Streptomyces* sp. isolated from the East Siberian continental margin[94], glaciapyrroles from a *Streptomyces* sp. isolated from Alaskan sediment[95] and the trichodin isolated from a *Trichoderma* sp. isolated from the Fram Strait[96]. As evident by Figure 1.5, the lack of NPs reported from this area is not due to a lack of productivity of these organisms, but instead due to the gross under sampling of this region. The Arctic marine biosphere represents an extremely unexplored resource for future NP discovery.

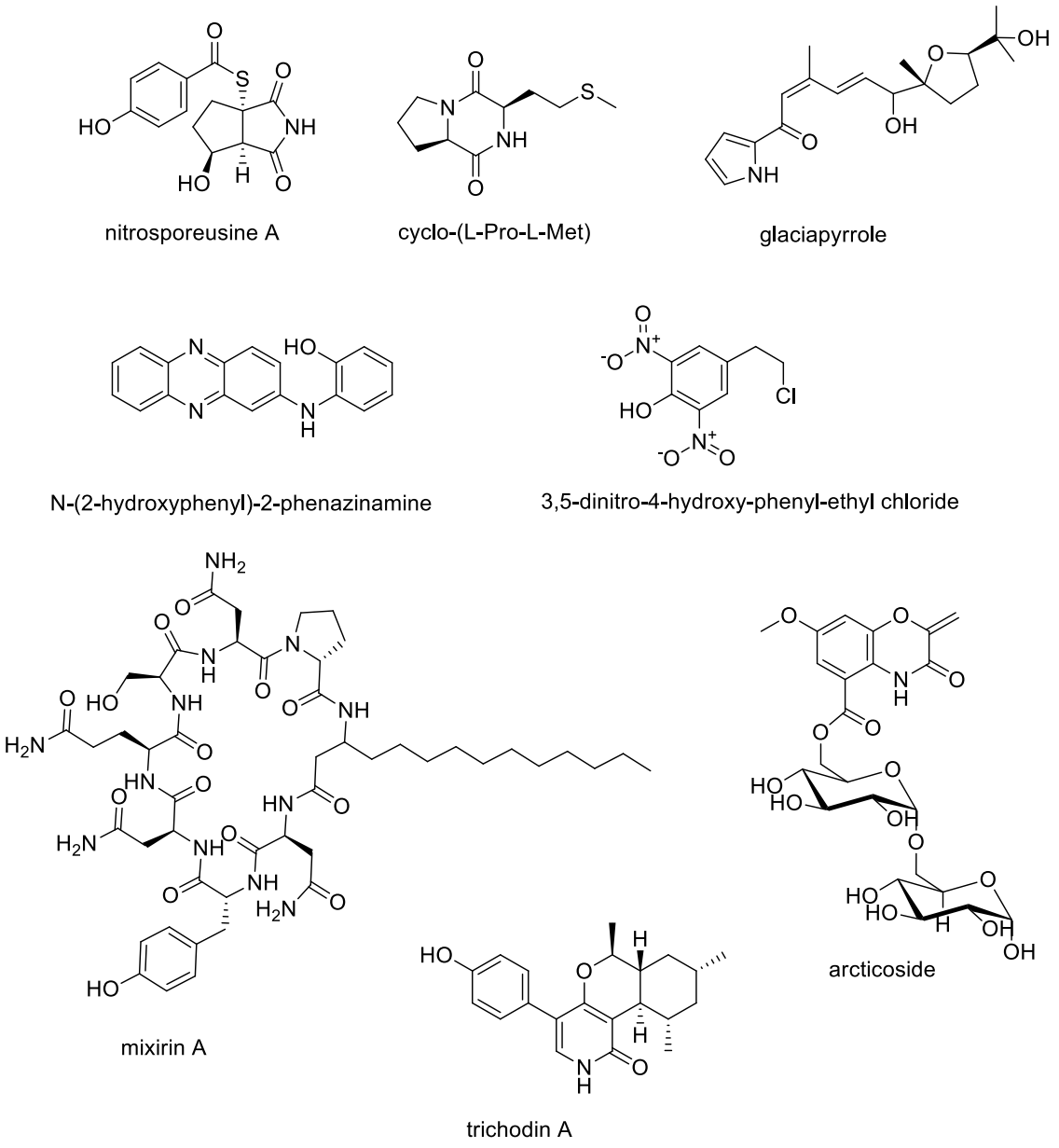

Figure 1.4. Natural products isolated from Arctic marine microorganisms.

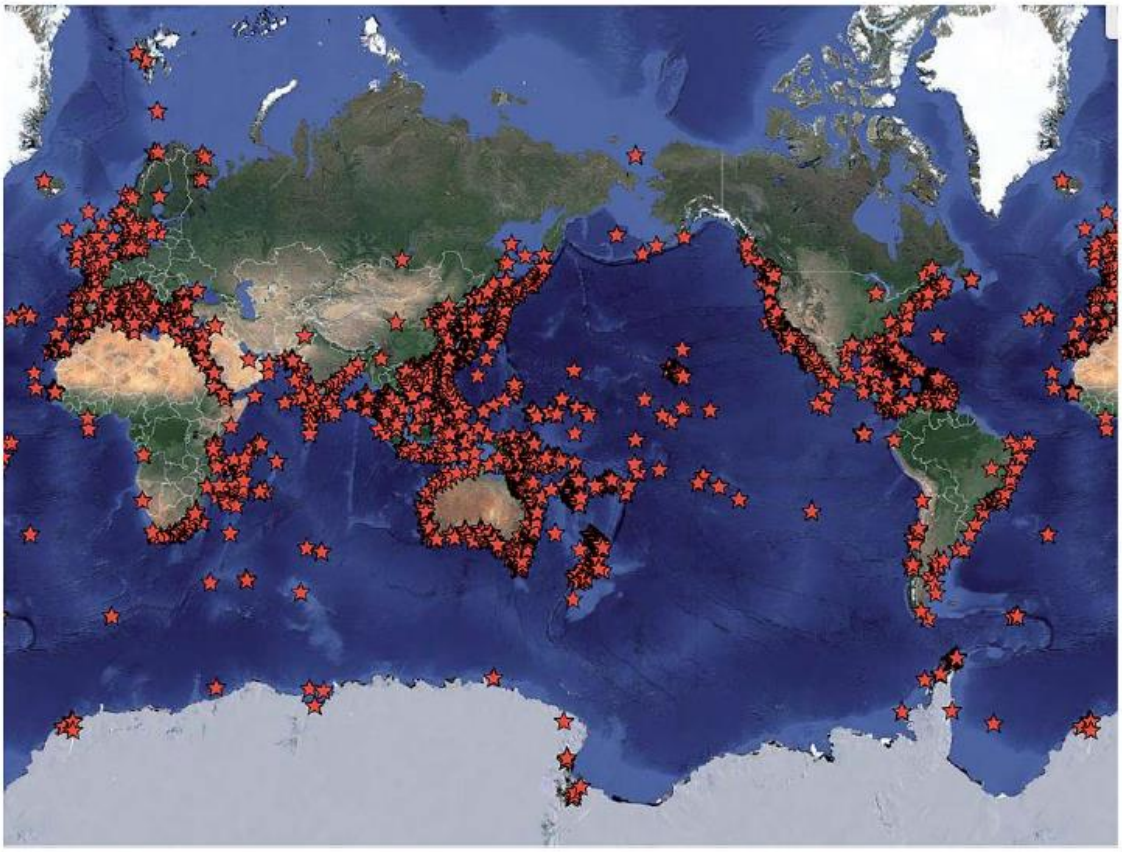

Figure 1.5. All collection sites for marine natural product discovery, 1965-2014. Figure created by J.W. Blunt.[48]

1.9 Canada's Arctic

Canada's Arctic encompasses an area of 1,424,500 km^2, covers 25% of the total land mass of the global Arctic and contains 162,000 km of coastline. It is bound by the Beaufort Sea on the west, the Arctic Ocean on the northwest, Baffin Bay and the Davis Strait on the east and Hudson Bay on the South. Canada's Arctic has never been investigated from a NPs standpoint. Due to the understudied nature of Arctic marine microorganisms and lack of investigation of Canada's Arctic, the purpose of this thesis was to investigate this region for the production of NPs by associated microorganisms.

Frobisher Bay is a 230 km inlet of the Labrador Sea located on Baffin Island and experiences some of the largest diurnal tidal variation in the world. This tidal variation results in some areas being completely uncovered during low tide and may exert significant environmental pressures on the organisms within. The influx of cold Arctic water from the Labrador Current into Frobisher Bay will also undoubtedly influence the microbial communities present within this region. Due to these reasons and the relative accessibility of Frobisher Bay in comparison to other Arctic regions, this area was selected as the study site for this thesis.

1.10 Research Objectives

Due to the desperate need for new NPs and the large untapped potential of the Arctic for NP discovery, bioprospecting in this region is a natural progression in NPs research. Organisms inhabiting the Arctic must be uniquely adapted in order to survive in this environment and it is presumed these uniquely adapted organisms will produce their own distinct set of NPs. Therefore the purpose of this thesis was to investigate

Frobisher Bay in terms of the microbial diversity present within this region and the NPs produced by these organisms.

The first objective of this research was to determine the bacterial and fungal communities present within sediment collected from Frobisher Bay using 454-pyrosequencing. In order to obtain greater sequencing depth within the prolific NP producing Actinobacteria, actinobacterial specific 16S rRNA primers were used[97] in addition to universal 16S rRNA primers for 454 pyrosequencing. The bacterial community analysis is described in Chapter 2. The fungal diversity was assessed using fungal specific internal transcribed spacer (ITS) primers in order to obtain greater sequencing depth than with standard ITS primers and is described in Chapter 4.

The second objective was to build a library of actinomycetes and fungi for subsequent NP discovery. Actinomycetes were isolated from sediment from five sites within Frobisher Bay using a selective pre-treatment and media for the isolation of actinomycetes. The cultured library of actinomycetes is described in Chapter 2. The construction of a fungal library from these same five sites is described in Chapter 4. A particle filtration method and multiple isolation media were used for the isolation of fungi resulting in the isolation of several putatively new species which are described in Chapters 6-8. In an attempt to obtain psychrophilic or psychrotolerant organisms, isolations occurred at 4˚C, in addition to 22˚C for both actinobacterial and fungal isolations.

The final objective was to screen the constructed fungal and actinobacterial libraries for the production of NPs. Due to the environment from which they were isolated, the effect of fermentation temperature on NPs was assessed within the

actinobacterial library. Using an LC-HRMS based chemical metabolomics analysis; differences in the secondary metabolomes of actinomycetes were characterized in response to fermentation temperature. The *de novo* production of actinomycins at colder fermentation temperatures is discussed, in addition to the isolation and characterization of two new compounds as a result of upregulated production in response to colder fermentation temperatures in Chapter 3. In Chapter 5, chemical screening of extracts generated from the fungal library by LC-HRMS are discussed as well as the isolation of several new compounds from taxonomically known fungi. The isolation of new natural products from putatively new fungal species are described in chapters 6-8.

CHAPTER 2: CULTURE INDEPENDENT AND DEPENDENT CHARACTERIZATION OF THE BACTERIAL DIVERSITY OF SEDIMENT OF FROBISHER BAY

2.1 Introduction

Bacteria are the greatest producers of bioactive NPs and are of immense importance for NP drug discovery[98]. Bioprospecting in unexplored geographic areas (e.g. the Arctic), increases the likelihood of finding new NPs due to the significant influence the environment has on bacterial speciation and on the production of NPs[26]. Microorganisms inhabiting polar environments have to contend with extreme environmental conditions including cold temperatures and seasonal UV fluctuations. In order to overcome these extreme conditions microorganisms have developed unique adaptations such as the synthesis of cold-adapted enzymes, production of cold shock and antifreeze proteins and the ability to increase membrane fluidity with decreasing temperature[88]. Distinctly polar lineages of bacteria[99-100] have been uncovered, highlighting this region as a source of unique taxonomy.

Advances in culture independent methods have allowed for high throughput sequencing of microbial barcoding genes allowing for the determination of the microbial community composition within a sample. Next generation sequencing technologies (454-pyrosequencing, Illumina sequencing, etc.) have allowed for microbial community surveys in a large variety of environments. Within the marine environment, many lineages of exclusively marine bacteria have been uncovered and the majority of these have evaded laboratory culture[101,102]. The roles, functions and NP capabilities of these uncultured organisms within the marine environment still remains largely unknown and offers an enormous untapped resource for NP discovery.

The Arctic Ocean Survey (AOS) and International Census of Marine Microbes (ICoMM) has provided the greatest depth of information on the microbial diversity of surface and deep water in the Arctic and North Atlantic Ocean[103]. Collectively these

surveys have assessed the bacterial diversity of water samples from the Labrador Sea, Laptev Sea, Chukchi Sea, Beaufort Sea, Russian Shelf, Baffin Bay, Hudson Bay and several sites within the Canadian archipelago. Comparisons of ICoMM study data from temperate and polar regions revealed only 5% of the operational taxonomic units (OTUs) detected are shared between the two marine environments and 70% of the OTUs from Arctic sites are unique to the Arctic[104]. Studies of the microbial diversity of cold polar sediment in the northern hemisphere have occurred in Russia[105] (Kara Sea Shelf), the Bering Sea[106] the Fram Strait[107] and Svalbard[108-109]. Within Arctic Canada, microbial diversity studies have included deep sea sediment (Baffin Bay, Chukchi Sea, deep Canada Basin)[110,111], sea ice associated bacteria (Chukchi Sea and Baffin Bay)[112,113], surface sea water (costal Beaufort Sea)[114] and pelagic seawater (Amundsen Gulf and Labrador Sea)[115,116]. Collectively these studies have revealed immense biodiversity within the Arctic and North Atlantic Ocean and revealed the presence of many unidentified bacterial lineages.

The microbial diversity of coastal sediment from polar waters has been understudied. Coastal regions represent a unique range of habitats within the marine environment and differ from the deep sea environment due to the influences of freshwater and organic matter from the terrestrial environment. Due to the influx of freshwater and organic nutrients, coastal sediment tends to be one of the most biodiverse marine regions due to the variety of ecological niches available for microorganisms[117]. Frobisher Bay is a 230 km inlet (20-40 km wide) of the Labrador Sea which is sea ice covered for most of the year and experiences diurnal tidal variations of 7-11 m each day.

The bacterial diversity of sediment from the intertidal region of Frobisher Bay has never been characterized and represents an interesting environmental niche for bioprospecting.

The aims of this study were to use 454-pyrosequencing to characterize the bacterial community composition of sediment samples from the intertidal region of Frobisher Bay and culture a library of Actinobacteria for NP discovery. In order to obtain deeper sequencing depth within the phylum Actinobacteria, actinobacterial specific 16S rRNA primers were used in addition to universal bacterial 16S rRNA primers to generate amplicons from environmental DNA for pyrosequencing analysis. The second aim of this study was to culture a library of Actinobacteria from sediment samples from Frobisher Bay using selective isolation techniques. This chapter will give an overview on the bacterial diversity of Frobisher Bay and discuss the cultivable Actinobacteria obtained from this region.

2.2 Experimental Procedures

2.2.1 Sample Collection and Processing

Thirteen sediment samples were collected over a five-day period in August and September 2011 from the intertidal zone of Frobisher Bay. Samples were collected from the following six locations, Iqaluit Harbour (IH1 and IH1, 63.741500, -68.521870), Apex Bay (AB1, AB2, AB3, 63.727789, -68.459801), Tarr Inlet (TI1, TI2, TI3, 63.726118, -68.424361), White Top Ledge Channel (WC1 and WC2, 63.721584, -68.531649), Qaummaarviit Island (QI, 63.71666, -68.68333) and Pugh Island (PI1 and PI2, 63.242269, -68.145086) by Brad Haltli (Kerr Lab, UPEI), Samples were collected aseptically using a LaMotte sediment sampler and sterile 50 mL conical tube. The samples were transported to the laboratory on ice, after which a portion (0.12-0.40 g)

was used for environmental DNA isolation and the remaining was used for culture isolation. Of these samples, ten were used for pyrosequencing analysis (AB1, AB2, IH1, IH2, PI1, PI2, QI, TI, WC1 and WC2) and five were used for the culture dependent portion of this study (AB3, PI1, QI, TI2 and TI3). Due to issues with DNA amplification and the culture dependent and independent portion of the study being completed in tandem, some of the sites included within the culture dependent portion were unable to be included in the culture independent portion of the study.

2.2.2 Environmental DNA Extraction and 16S rRNA Amplicon Pyrosequencing

Genomic DNA was isolated from sediment (0.12-0.40 g) using a Powersoil DNA Isolation kit (MoBio Laboratories, Carlsbad, USA) following the manufacturer's protocol. Recovered DNA was dissolved in sterile water (100 µL) and stored at -20˚C. DNA concentration was determined using a NanoDrop spectrophotometer (Fisher Scientific, Ottawa, ON).

Culture independent assessment of the bacterial and actinobacterial diversity of extracted DNA from ten sediment samples was undertaken using a bacterial-tag encoded GS-FLX amplicon pyrosequencing approach (Roche GS-FLX sequencer) performed by Genome Québec (McGill University, Montreal). Fusion primers were designed for each sample whereby Primer A (forward primer) consisted of a 454 FLX adaptor, a unique identifier barcode and a 16S rRNA primer (27F for bacterial primers[118] and S-C-Act-0235-a-S-20 for Actinobacteria-specific primers[97]) and Primer B (reverse primer) consisted of a 454 FLX adaptor and 16S rRNA primer (519R for bacterial primers[118] and Act-0878-a-A-19 for Actinobacteria[97]).

Amplicons were generated by polymerase chain reaction (PCR) from template gDNA (25 ng per 50 µl) using the 16S rRNA 27F and 519R fusion primers and AmpliTaq Gold 360 DNA polymerase (Applied Biosystems, Foster City, CA). PCR conditions were as follows; a hot start at 95˚C for 10 min followed by 15 cycles of 94˚C for 30 s, 54˚C for 40 s and 72˚C for 1 min with a final extension of 10 min at 72˚C. To generate Actinobacteria-specific16S rRNA amplicons, a nested PCR approach was used. Initially the full length 16S rRNA gene was amplified using universal 16S rRNA bacterial primers (27F and 1525R) with AmpliTaq Gold 360 DNA polymerase and the following conditions; 95˚C for 10 min followed by 15 cycles of 94˚C for 30 s, 54˚C for 40 s, 72˚C for 1 min and a final extension for 10 min at 72˚C. PCR products were purified using the QIAquick PCR purification kit (Qiagen, Toronto, ON) according to manufacturer's instructions. A nested PCR using 25 ng of purified DNA, AmpliTaq Gold 360 DNA polymerase and fusion primers S-C-Act-0235-a-S-20 and Act-0878-a-A-19 was performed with a hot start of 95˚C for 10 min followed by 10 cycles of 95˚C for 45 s, 72˚C* for 45 s, 72˚C for 45 s and a final extension for 10 min at 72˚C (*annealing temperature decreased by 0.5˚C each cycle). After purification using a QIAquick PCR purification kit, amplicons were pooled (three replicate PCR reactions) and DNA concentration was determined using a Quant-iT PicoGreen dsDNA Assay kit (Turner Biosystems, Sunnyvale, CA) according to manufacturer's instructions. Amplicons were then sent to Genome Québec for FLX-pyrosequencing.

2.2.3 16S rRNA Amplicon Pyrosequencing Analysis

Processing of the resulting pyrosequencing .sfff files was completed using Mothur v. 1.35.1[119]. Sequences were denoised using Mothur's implementation of

PyroNoise[120] (shhh.flows) and filtered for quality. Sequences were removed if they contained homopolymers greater than 8 bp in length, had more than one mismatch to the forward primer sequence or barcode or were shorter than 200 bp. Filtered sequences were aligned using the Silva v. 123 reference alignment[121], gaps were removed and sequences were preclustered allowing for two nucleotide differences between reads. Chimeras were identified using UCHIME[122] and removed. Singletons were removed using the split.abund command and remaining sequences were classified using the mother Bayesian classifier (80% confidence) using the Silva v. 123 database. Sequences identified as mitochondria, chloroplast and unknown lineages were removed from the analysis. In the case of Actinobacteria specific primers, non-Actinobacteria sequences were removed at this stage. The remaining sequences were clustered into species level operational taxonomic units (OTUs) with a pairwise identity of 97%. All alpha and beta diversity calculations were performed using Mothur on subsampled datasets. The Bray Curtis dissimilarity matrix[123] was created using the tree.shared command which clustered sites using the UPGMA algorithm. The resulting tree was visualized in MEGA v. 6.06[124].

2.2.4 Actinobacteria Isolation

A portion of each collected sediment sample was subjected to heat drying by incubation at 40˚C for 24 h[125]. Wet and dried sediment samples were placed in 50 mL sterile conical vials, frozen in liquid nitrogen and shipped to the University of Prince Edward Island. Dried sediment was stored at 4˚C and the wet sediment was stored at -80˚C. Five sediment samples were selected for Actinobacteria isolation; AB3, PI1, QI, TI2 and TI3.

Forty eight well plates containing one of five selective isolation media: raffinose-histidine (RH)[126], starch casein nitrate (SCN)[127], oligotrophic medium M5[128], *Streptomyces* isolation media (mSIM)[129] and chitin low nutrient (CH)[128] were inoculated with serial dilutions of wet sediment or stamped with heat dried sediment. All media were prepared with distilled water supplemented with Instant Ocean™ (18 g/L) and supplemented with nystatin (50 µg/ml), cyclohexamide (50 µg/mL) and/or nalidixic acid (10 µg/mL) to reduce the growth of fungi and non-actinomycete bacteria. Plates were incubated at 4˚C and 22˚C and monitored for the growth of actinomycete-like bacteria for four months. Actinobacteria were subcultured onto ISP2 and preserved at -80˚C in 10% (v/v glycerol).

2.2.5 Genomic DNA Extraction and PCR Amplification

Extraction of genomic DNA was carried out using a phenol/chloroform extraction[130]. PCR amplification of the partial 16S rRNA gene was conducted using the universal bacterial primers 27F and 530R with the following conditions: an initial denaturing step for 3 min at 95°C, followed by 35 cycles of 95°C for 1 min, 54 °C for 45s and 72°C for 1.5 min and a final extension of 5 min at 72°C. The presence of the correct PCR amplicon for bacteria was verified using gel electrophoresis (110 V, 40 min, Bio-Rad Laboratories, Mississauga, ON) using 1.0% agarose gel containing 0.001% ethidium bromide. PCR products were visualized using a UV transilluminator (Biospectrum, OptiChemi HR Camera, Upland, CA) and amplicons of the correct size (~500 bp) were sequenced by Eurofins MWG Operon (Huntsville, AL) using the 530R primer.

2.2.6 Phylogenetic Analysis

Sequences were trimmed and assembled using Contig Express (Vector NTI Advance 10.3.0, Invitrogen, Carlsbad, CA). Similar sequences were grouped into OTUs (99% sequence similarity) and identified using the Basic Local Alignment Search Tool (BLAST) using the BLASTn algorithm in the GenBank database[131]. Sequence alignment was completed using Clustal W in MEGA version 6.06[124]. Modeltest was used to determine the most appropriate nucleotide substitution model[132]. Phylogenetic trees were constructed using the GTR+G (general time reversible + gamma) model of evolution[133] and maximum-likelihood method[134] in MEGA v. 6.06. Bootstrap analysis was performed with 1000 replicates and values less than 60% were collapsed.

2.2.7 Comparison of Cultured Actinobacteria to Culture Independent Analysis

To compare the cultured actinobacterial isolates to the culture independent library, an NCBI local BLAST nucleotide database containing all unique culture independent Frobisher Bay bacterial and actinobacterial sequences was created in BioEdit version 7.2.5[135]. The cultured actinobacterial sequences were searched against this local database using an Expectation (E) value of $1.0E^{-100}$ and the Matrix BLOSUM64. Cultured sequences with high sequence similarity (≥99%) to members of the culture independent library were recorded.

2.3 Results and Discussion

2.3.1 Culture Independent Analysis: Universal 16S rRNA Bacterial Primers

2.3.1.1 Bacterial Alpha Diversity

Nine sediment samples collected from intertidal regions in Iqaluit Harbour (IH1 and IH2), Apex Bay (AB2), White Ledge Channel (WC1 and WC2), Pugh Island Channel (PI1 and PI2), Tarr Inlet (TI) and Qaummaarviit Island (QI) were chosen for

pyrosequencing analysis (Figure 2.1). Pyrosequencing of 16S rRNA amplicons from environmental DNA from each of these sites resulted in 86,706 high quality sequence reads spanning the V1, V2 and partial V3 region. Each sample contained between 3,339-13,049 sequence reads, averaging 337 bp in length. These sequence reads were clustered into operational taxonomic units (OTUs) according to their similarity to one another. Sequences were classified into OTUs at the species level, based on having ≥97% 16S rRNA gene similarity with one another. Bacterial diversity calculations were performed at the species level (97% sequence identity cutoff for OTUs) on a subsampled dataset of 3,300 reads per site (Table 2.1).

Observed bacterial richness is the simplest characterization of diversity within a sample and consists of a count of the total number of OTUs present within. Within Frobisher Bay bacterial richness at the species level (OTUs with ≥97% 16S rRNA gene sequence similarity) ranged from 545 OTUs (AB2) to 881 OTUs (PI1) (771 ± 110) [(average ± standard deviation)] per site. Often simple richness counts underestimate the true diversity present within a sample, as it is impractical/impossible to detect every member within a community with current sequencing technologies. Taking into account the richness and abundance data, various statistical estimators can be used to extrapolate the data set to uncover and estimate the true number of species present within a sample. One such estimate of species richness is the Chao1 estimator, which estimates the true species diversity present within a community by using the number of rare species as a way to calculate the likelihood that there are more undiscovered species. The Chao1 estimator takes into account the number of rare species found in a sample by the number of singletons (the number of species which had a single sequence read in the dataset)

and doubletons (the number of species with two sequence reads in the dataset) and uses it to estimate the total number of species present. The rationale behind this estimator is that if the community is being sampled and rare species are still being uncovered (singleton sequence reads), there are more likely still more rare species to be uncovered. As soon as all species have been detected at least twice (doubletons), there is likely no more new species to be uncovered[136]. Using the Chao1 estimator, the estimated richness at the species level and ranged from 572 OTUs (AB2) to 1,410 OTUs (PI1) (1,086 ± 304 OTUs) per site. At the species level, the number of OTUs predicted by the Chao1 estimator is much higher than the observed number of OTUs (observed richness) and additional richness at the species level would be observed with further sampling.

Good's coverage estimator is used as an estimator of the sequence coverage in a sample by calculating the percentage of OTUs present within a sample that consist of only a single sequence read[137]. Within sample sites, values for Good's coverage ranged from 87% to 94%, indicating 6% to 13% of reads per site are from OTUs that only consisted of a single sequence read in the sample. Further sequencing depth would be required to increase the coverage of singleton OTUs.

Rarefaction analysis is used to assess species richness (number of OTUs) as a result of increasing sample size and used to determine sampling adequacy. Rarefaction curves are generated by randomly resampling pools of *N* sequences multiple times and plotting the average number of OTUs found within a sample. As more sequences are sampled, the curve begins to plateau as only rare species remain to be sampled. Generation of rarefaction curves for each sample site showed most curves began to reach the plateau of their asymptote. Therefore sequencing depth was sufficient at most

sites to adequately describe the species level diversity (Figure 2.2), although further sampling would be required to detect rare species.

The Shannon diversity (H') index is a diversity index used to characterize species diversity in a community by taking into account the species richness and abundance of each species present within a sample. The Shannon equitability (E) index calculates the evenness of species within a samples, where 1 means complete evenness and 0 means complete unevenness[138]. This value indicates whether a community is dominated by a few highly abundant species (value closer to 0), or whether the community is composed of many equally abundant species (value closer to 1). Within sites from Frobisher Bay, the Shannon diversity index ranged from 5.32 (AB2) to 5.96 (IH1) (5.73 ± 0.21) and Shannon equitability index ranged from 0.84 (AB2) to 0.89 (IH1 and WC2) (0.86 ± 0.02). The high *H'* index values calculated indicates high bacterial diversity for all sediment samples within Frobisher Bay and the high *E* index values indicate a high level of community evenness within samples, whereby each sample is composed of many equally abundant species and is not dominated by a few species. The Shannon diversity and evenness values are higher than those reported from sediment samples collected from polar coastal[108,114] and polar deep sea marine sediment[105,139] and more similar to sediment collected from temperate coastal environments in New Brunswick[140] and Newfoundland[141]. Due to differences in sampling, methodology and analysis, accurate comparisons of diversity indices between studies cannot be made, although coastal sediment often displays higher variability within its microbial community compared to deep sea sediment due to the input of freshwater and nutrients from the surrounding terrestrial environment[142].

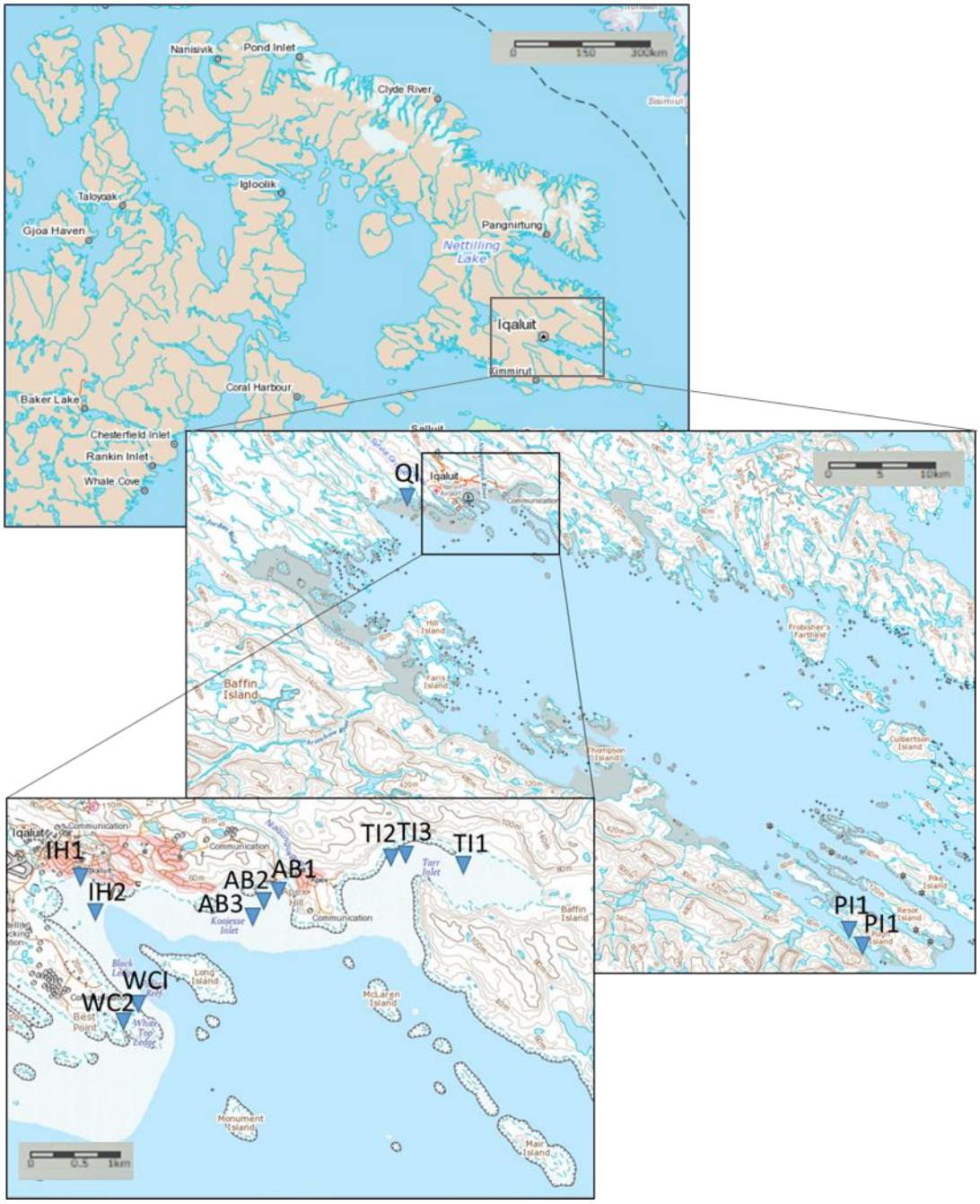

Source: Natural Resources Canada

Figure 2.1. Sample sites within Frobisher Bay.

Table 2.1. Bacterial richness and alpha diversity analysis using 16S rRNA primers on a subsampled dataset (3300 reads). OTUs were calculated at a distance of 0.03.

Sample	Sample Size	Richness (S_{obs})	Chao1 estimated richness (S_{est})	Good's Coverage *C* (%)	Shannon diversity index (*H'*)	Shannon equitability index (*E*)
QI	4,516	725	792	94	5.57	0.85
PI1	11,143	881	1337	87	5.80	0.85
PI2	10,912	878	1410	87	5.83	0.86
WC1	12,192	875	1351	87	5.89	0.87
WC2	12,626	774	1158	90	5.90	0.89
AB2	3,637	545	572	97	5.32	0.84
IH2	13,049	824	1338	88	5.79	0.86
IH1	15,292	795	1141	90	5.96	0.89
TI	3,339	641	675	96	5.47	0.85

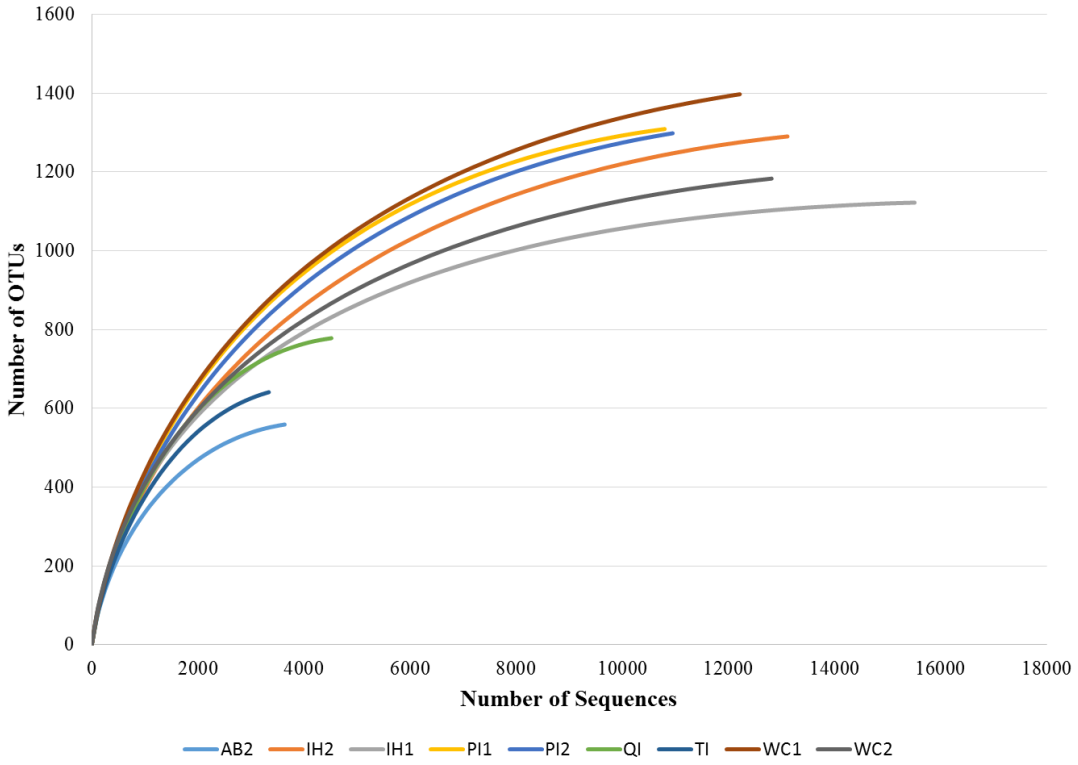

Figure 2.2. Rarefaction curve of sediment samples from Frobisher Bay (*D*=0.03)

2.3.1.2 Bacterial Beta Diversity

To determine the dissimilarity between the community structures of sediment samples from Frobisher Bay, the Bray-Curtis dissimilarity index was calculated between sites (Figure 2.3). This index is used to quantify the dissimilarity in community composition based on OTU abundance and the presence and absence of different OTUs between sites. Sites did not cluster based on sample location and were all quite dissimilar from one another (each site was greater than 50% dissimilar from other sites in the region). The lack of clustering between sites with multiple sampling locations (Iqaluit Harbour, Pugh Island and White Top Ledge Channel) indicates that these sites have quite different bacterial assemblages despite being geographically close. Prior pyrosequencing investigations within the Bay of Fundy (New Brunswick) and Bonne Bay (Newfoundland), have revealed bacterial assemblages are less influenced by geographic proximity within a region and more influenced by the physiochemical composition of the sample within a site[140,141]. Since the physiochemical composition of sediments collected from Frobisher Bay was not determined, inferences about the influence this may have on bacterial assemblages within this region cannot be made. Additionally, the bacterial assemblage within sites, specifically those that are near shore can be influenced by environmental factors from the terrestrial environment including nutrient and freshwater input and wash in of microorganisms and debris from the terrestrial environment. Pyrosequencing of samples from the terrestrial environment in tandem with those from the marine environment, would offer insight into how bacterial communities within the terrestrial environment have influenced those in the marine environment at the various locations.

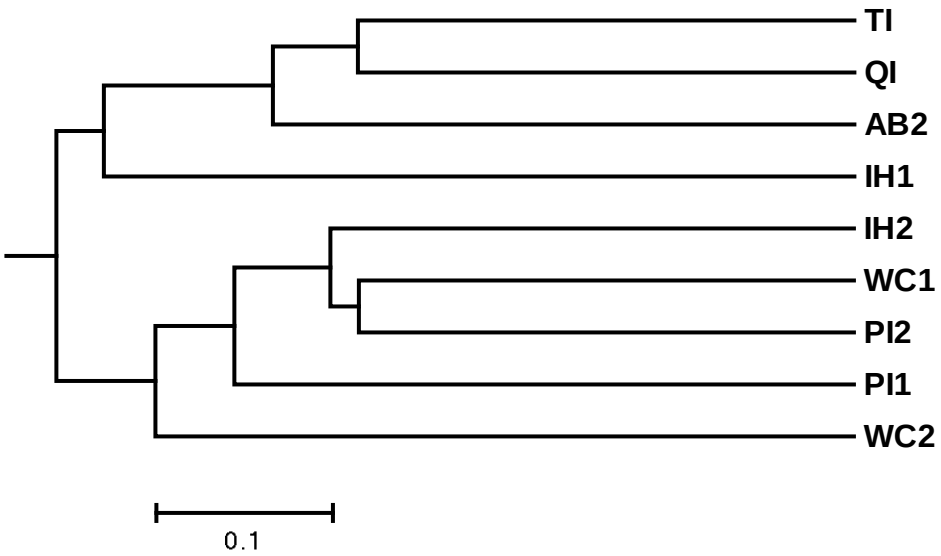

Figure 2.3. Bray-Curtis analysis dissimilarity analysis of sediment samples from Frobisher Bay (D = 0.03). Data was subsampled to 3300 reads.

2.3.1.3 Bacterial Taxonomic Composition

The Silva Classifier was used to classify the 86,706 sequence reads with a confidence threshold of 80%. Across all samples, 37 phyla were detected ranging from 13 (TI) to 30 (PI2) phyla detected per site (Figure 2.4). The dominant phyla at all sites were Proteobacteria and Bacteroidetes making up 39.1%-55.1% and 21.7%-39.7% of the total population of each sample respectively. Other phyla that were present at all sites were Actinobacteria (4.8%-13.8%), Planctomycetes (1.9%-19.9%) Acidobacteria (0.1%-2.1%), Lentisphaerae (0.1%-3.8%), Gemmatimonadetes (0.2%-1.24%), Verrucomicrobia (0.1%-1.3%), Nitrospirae (0.1%-0.9%) and Chloroflexi (0.4%-1.8%). Bacteria that could not be classified to a phylum level represented 2.2%-5.2% of all sequence reads per site.

At the class level, 100 classes were present across all samples and ranged from 42 (AB2) to 76 classes (PI2 and IH2) per site (Figure 2.4). The top four most abundant classes present amongst sites were Gammaproteobacteria (10.4% to 31.8%), Flavobacteria (8.8% to 26.0%), Deltaproteobacteria (2.4% to 21.9%) and Alphaproteobacteria (3.7% to 10.5%). The majority of sequences within Gammaproteobacteria were classified as *Woeseia* (29.6%), unclassified BD7-8 marine group (17.34), *Marinicella* (13.6%), unclassified Gammaproteobacteria (13.1%) or *Granulosicoccus* (12.82%). Within Flavobacteria most sequences represented unclassified Flavobacteriaceae (33.0%), *Maribacter* (10.3%), *Ulvibacter* (8.3%), *Winogradskyella* (7.8%), *Lutibacter* (4.7%) and *Maritimimonas* (4.5%). Within the Deltaproteobacteria most reads corresponded to *Desulfopila* (15.0%), *Desulfobacula* (11.5%), unclassified SVA1033 (8.4%), unclassified *Desulfobacula* (8.0%), *Geopsychrobacter* (7.3%), *Desulfobulbus* (7.5%), or *Desulforhopalus* (5.1%).

Alphaproteobacteria reads were mainly unclassified *Rhodobacteraceae* (33.8%), unclassified Alphaproteobacteria (12.6%), *Octadecabacter* (5.1%) and *Sulfitobacter* (3.4%). Other classes that were present in all samples included Acidimicrobiia (0.8% to 12.7%), Betaproteobacteria (0.2% to 10.9%), Sphingobacteria (0.7% to 5.4%), Planctomycetacia (0.8% to 18.6%), Cytophagia (0.6% to 6.0%), OM190 (0.3% to 2.8%), Opitutae (<1.3%), Gemmatimonadetes (<1.2%), Acidiobacteria (<1.1%), Holophagae (<1.2%), Phycisphaerae (<1.2%), Nitrospira (<0.9%), Anaerolineae (<0.3%) KD4-96 (<0.3%) and PLA4 (<0.2%). Additionally sequences representing unclassified Bacterioides (0.6% to 4.0%), unclassified Proteobacteria (0.5% to 1.4%), unclassified Lentisphaerae (<0.2%), unclassified Planctomycetes (<0.3%) and unclassified bacteria (2.2% to 5.2%) were present across all samples. All of the abundant genera identified have been described as marine lineages[143] . The distribution of the major phyla and classes follows the same pattern of distribution observed for coastal benthic environments worldwide where Gammaproteobacteria, Flavobacteria, Deltabacteria and Alphabacteria are the most abundant members within these sediments[142]. This same pattern has been observed in regional studies of coastal marine sediment off Svalbard[108-109], New Brunswick[140] and Newfoundland[141].

A)

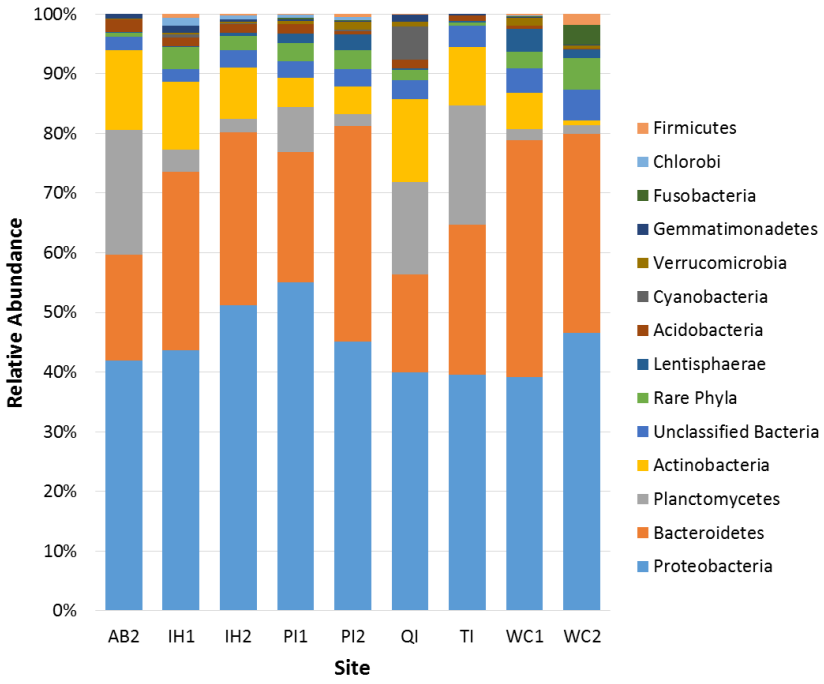

B)

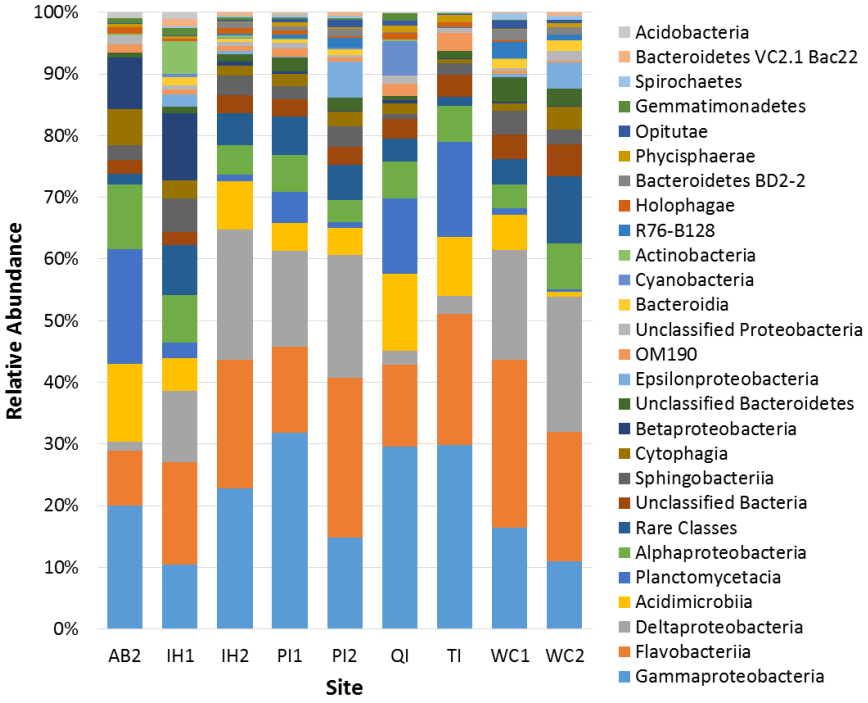

Figure 2.4. Microbial taxonomic diversity of Frobisher Bay on non sub-sampled data. All phyla and classes below 1% abundance are collapsed within rare phyla or class category. **A)** Phylum level diversity. **B)** Class level diversity.

Twenty-seven OTUs were detected at all sites in varying abundance (0.05%-2.6% of all reads) (Table 2.2). Preliminary identification of these OTUs using BLAST resulted in the identification of many marine genera (e.g. represented by the following species; *Woeseia oceani*, *Granulosicoccus antarcticus*, *Desulfopila inferna*, *Geopsychrobacter electrodiphilus*, *Ulvibacter litoralis*, *Algibacter lectus*, *Sulfitobacter undariae* and *Jannaschia faecimaris*), however due to the short sequence lengths, these identifications remain tentative. The most abundant OTUs observed corresponded to an unknown *Woeseia* species (2.6%), *Granulosicoccus antarcticus* (2.2%), an unknown *Desulfopila* species (1.8%), an unknown Gammaproteobacteria (1.7%), *Geopsychrobacter electrodiphilus* (0.9%) and *Ulvibacter litoralis* (0.9%).

In total, 5.3% of all sequence reads had OTUs with significant similarity to *Woeseia oceani* XK5 (NR_147719.1). Members of the *Woeseiaceae* family have been identified as ubiquitous core members of marine sediments worldwide and have been shown to be one of the most abundant OTUs present in marine sediment in NGS studies, making up on average 5% of all total reads[117]. Within Frobisher Bay, OTUs corresponding to the family *Woeseiaceae* made up 5.3% of all total reads. The family *Woeseiaceae*, has only one cultured member, *Woeseia oceani* XK5 which was demonstrated to be an obligate chemoorganoheterotroph[144]. Metagenomic analysis of uncultured members of the *Woeseia* have revealed them to have the genetic potential for chemolithoautotrophy powered by sulfur or hydrogen oxidation[145]. The ability of members of this family to be heterotrophs and autotrophs may explain their success in marine sediments worldwide. Further isolation of members within this family will help to shed light on the roles and function of this family within the marine environment.

Table 2.2. Most abundant and shared OTUs (*D* = 0.03)

OTU	Total Read %	% coverage	% identity	Closest accessioned strain
1[a]	2.58	100	96	*Woeseia oceani* XK5 (CP016268.1)
2[a]	2.19	100	100	*Granulosicoccus antarcticus* NBRC 10264 (NR114178.1)
3[a]	1.82	100	98	*Desulfopila inferna* JS_SRB250Lac (NR_115066.1)
4	1.71	100	91	*Sedimenticola thiotaurini* (CP011412.1)
5	1.02	100	96	*Desulfopila inferna* JS_SRB250Lac (NR_115066.1)
6[a]	0.92	100	98	*Geopsychrobacter electrodiphilus* A1 (NR_042768.1)
7[a]	0.90	99	97	*Ulvibacter litoralis* KMM 6715 (NR_025731.1)
8	0.89	87	94	*Halmonas anticariensis* FP35 (NR_029113.1)
9	0.84	87	94	*Halmonas anticariensis* FP35 (NR_029113.1)
10[a]	0.82	100	93	*Ilumatobacter coccineus* YM16-304 (NR_112714.1)
11	0.78	100	93	*Desulfopila inferna* JS_SRB250Lac (NR_115066.1)
12[a]	0.73	99	93	*Ilumatobacter fluminsis* YM22-133 (NR_041633.1)
13[a]	0.71	100	98	*Woeseia oceani* XK5 (CP016268.1)
14	0.67	100	96	*Winogradskyella damuponensis* F081-2 (NR109095.1)
15	0.61	100	93	*Sulfurovum lithotrophicum* ATCC BAA-797 (CP011308.1)
16	0.60	100	96	*Desulfosarcina ovata* Oxy51 (NR_037125.1)
17	0.56	100	92	*Aequorivita viscosa* 8-1b (NR_109011.1)
18	0.54	95	100	*Ilyobacter psychrophilius* (AJ877255.1)
19	0.54	100	97	*Maribacter aesturaii* GY20 (NR_109501.1)
20	0.54	95	99	*Thiomicrospira arctica* SVAL-E (NR_0421055.1)
21	0.52	100	91	*Maribacter polysiphoniae* (NR_042612.1)
22	0.47	100	98	*Cocleimonas flava* KMM3898 (NR_112909.1)
23[a]	0.46	100	95	*Woeseia oceani* XK5 (CP016268.1)
24[a]	0.46	100	95	*Woeseia oceani* XK5 (CP016268.1)
25[a]	0.45	100	94	*Woeseia oceani* XK5 (CP016268.1)
Shared OTUs[b]				
48	0.33	100	96	*Ilumatobacter fluminsis* YM22-133 (NR_041633.1)
55	0.30	100	89	*Maribacter aesturaii* GY20 (NR_109501.1)
58	0.28	100	97	*Algibacter lectus* p13 (JQ661172.1)
63	0.27	99	94	*Ilumatobacter fluminsis* YM22-133 (NR_041633.1)
69	0.25	100	95	*Oceanicola antarcticus* Ar-45 (NR_134107.1)
81	0.23	100	89	*Coxiella brunetii* ATCC VR-615 (NR_104916.1)
99	0.20	100	87	*Rhodopirellula baltica* U1 (NR_043384.1)
111	0.18	100	94	*Woeseia oceani* XK5 (CP016268.1)
115	0.16	100	96	*Rhodopirellula baltica* UC47 (HQ845529.1)
140	0.15	100	89	*Rhodopirellula rosea* LHWP3 (NR_132692.1)
158	0.13	100	100	*Sulfitobacter undariae* W-BA2 (KM275624.1)
242	0.09	100	91	*Nitrospira marina* Nb-295 (HQ686084.1)
263	0.08	100	99	*Jannaschia faecimaris* HD-22 (NR_133766.1)
302	0.08	100	96	*Woeseia oceani* XK5 (CP016268.1)
314	0.07	89	82	*Rhodopirellula lusitana* UC49 (HQ845530.1)
443	0.05	100	93	*Labrenzia marina* BBCC2160 (KY787129.1)

[a]OTU detected at every sample site [b]not in most abundant, detected at every sample site

2.3.1.4 Actinobacterial Diversity

Members within the phylum Actinobacteria are of immense interest in the field of NPs due to their unrivalled ability to make bioactive NPs[98]. Sequence reads within the Actinobacteria accounted for 7.1 % of the total bacterial diversity within Frobisher Bay and made up 0.8% (WC2) to 13.8% (QI) (avg. 8.1% ± 4.1%) of the relative abundance at each site, which is comparable to levels observed in other next generation sequencing studies from the marine environment. For example, Actinobacteria abundance has been observed to range from 1-9.5% in the Bay of Fundy[140], 0.3-5.9% in Bonne Bay, Newfoundland[141], ~5% in Arctic deep sea sediment[146] and 2-4% in polar seawater[104]. The total number of actinobacterial reads ranged from 103 (WC2) to 1735 (IH1) sequences per site (Table 2.3). The Shannon diversity index ranged from 2.08 (WC2) to 3.98 (IH1) and Shannon equitability index ranged from 0.70 (WC2) to 0.82 (IH1) on non-subsampled data. At the family level, 26 families were observed with sequence reads being dominated by *Acidimicrobiaceae* (26.97%-85.44%), followed by uncultured marine actinobacterial clades OM1 (4.59%-21.08%) and Sva0996 (2.78%-19.57%). Within the family *Acidimicrobiaceae* all reads corresponded to the genus *Ilumatobacter* (54% of all total reads). In total, four OTUs were shared amongst all sites and were identified as members of the genus *Ilumatobacter*.

Ilumatobacter is a recently described obligate marine genus within the Actinobacteria[53] consisting of three formally described members isolated from sediment in Japan[147]. Genome sequencing of *Ilumatobacter coccineum* revealed the presence of two type 1 PKS gene clusters within the genome that most likely encode omega-3 polyunsaturated fatty acid synthase gene clusters. No type II or III PKS or NRPS gene

clusters were found within the genome making this group of bacteria rather uninteresting from a NPs perspective[148].

Members within the order Streptomycetales are prolific producers of NPs[98] and are of extreme interest in terms of bioprospecting. Within this study members of the order Streptomycetales were only detected as singleton isolates. *Streptomyces* are frequently isolated in culture dependent studies from a wide range of marine habitats[140,149] and are readily cultivable from most substrates, yet are often not detected or detected in low abundance by culture independent methods[141,140]. There are several reasons why Actinobacteria are often underestimated in pyrosequencing studies. The first reason is that Actinobacteria are often more resilient to cell lysis than other bacteria[150], causing underestimation of their abundance during pyrosequencing. The second reason is that due to the high GC content of their DNA (50-70%), dissociation of their DNA during PCR can often be hindered, resulting in underestimation of their abundance[151]. Thirdly, universal 16S rRNA bacterial primers are sometimes not capable of amplifying this gene from all bacteria[152]. One way to overcome this issue is to use taxon specific primers which have high specificity and coverage to a taxon of interest. Actinobacteria-specific primers have been designed that offer greater coverage and specificity for Actinobacteria than universal 16S rRNA primers[97]. In order to increase the sequencing depth within the Actinobacteria, amplicons were also generated using Actinobacteria-specific primers for pyrosequencing.

2.3.2 Culture Independent Analysis: Actinobacteria-Specific 16S rRNA Primers

2.3.2.1 Actinobacterial Alpha Diversity

Using Actinobacteria specific primers 129,690 reads were obtained from ten sites (Table 2.4). After removal of non-actinobacterial sequences, 88,748 reads

remained. Reads were subsampled to 7,000. The observed number of OTUs (*D*=0.03) ranged from 36 (TI) to 82 (QI) (58 ± 17) and the number of estimated OTUs (Chao1) ranged from 36 (TI) to 84 (QI) (62 ± 16). The coverage at each site was above 99.8% and all rarefaction curves reached an asymptote indicating sequencing depth was sufficient to explain the diversity at these sites (Figure 2.5). The Shannon diversity index ranged from 0.99 (WC2) to 2.76 (AB1) and evenness ranged from 0.26 (WC2) to 0.64 (AB1). Sites with evenness below 0.45 (PI1, PI2, WC1, WC2, TI and IH2) were dominated by reads corresponding to the genus *Ilumatobacter* (61.2% to 84.2% of total reads per site) accounting for the unevenness observed within these sites.

2.3.2.2 Actinobacterial Beta Diversity

The similarity between sites was calculated using a Bray Curtis dissimilarity matrix (Figure 2.6). Sites from White Top Ledge Channel and Pugh Island clustered closely in this analysis (10% maximum dissimilarity between sites WC1, WC2, PI1 and PI2) and formed a larger cluster with samples TI and IH2 (28.3% dissimilar from each other and 34.9% dissimilar to WC1 cluster). The clustering of these sites together is largely a result of the significant number of sequence reads corresponding to *Ilumatobacter* (OTU 1) which ranged from about 50% of sequence reads (TI and IH2) to over 70% of sequence reads (WC1, WC2, PI1 and PI2). The remaining sites (IH1, AB1, AB2 and QI) all formed a cluster with each other and had a maximum dissimilarity of 50.8%. Within this cluster *Ilumatobacter* (OTU 1) was far less abundant and ranged from 5.8% to 12.3% of total reads per site. Compared to the dissimilarity analysis of the bacterial diversity where each site was quite distinct from each other, the sites are more similar in terms of their actinobacterial diversity.

Table 2.3. Actinobacteria richness and alpha diversity analysis using universal 16S rRNA bacterial primers (*D*=0.03).

Sample	Sample Size	Richness (S_{obs})	Chao1 estimated richness (S_{est})	Good's Coverage *C* (%)	Shannon diversity index (*H'*)	Shannon equitability index (*E*)
121	624	80	81	99	3.42	0.78
132	536	48	50	99	3.06	0.79
136	504	54	62	98	3.08	0.77
241	739	63	72	98	2.99	0.72
253	103	19	25	92	2.08	0.70
3112	486	57	58	99	3.21	0.79
3122	1119	85	93	98	3.39	0.76
3123	1735	126	127	100	3.98	0.82
381	327	50	52	98	3.01	0.77

Table 2.4. Actinobacteria richness and alpha diversity analysis using Actinobacteria specific 16S rRNA bacterial primers (*D*=0.03).

Sample	Sample Size	Richness (S_{obs})	Chao1 estimated richness (S_{est})	Good's Coverage *C* (%)	Shannon diversity index (*H'*)	Shannon equitability index (*E*)
121	9554	82	84	99.99	2.35	0.53
132	9409	38	42	99.99	1.02	0.28
136	8428	49	52	99.87	1.16	0.30
241	9429	41	53	99.80	1.05	0.28
253	9970	45	59	99.79	0.99	0.26
3111	9757	73	77	99.86	2.76	0.64
3112	7711	74	76	99.91	2.45	0.57
3122	8675	63	63	99	1.62	0.39
3123	7064	74	74	99	2.73	0.64
381	8751	36	36	99	1.62	0.45

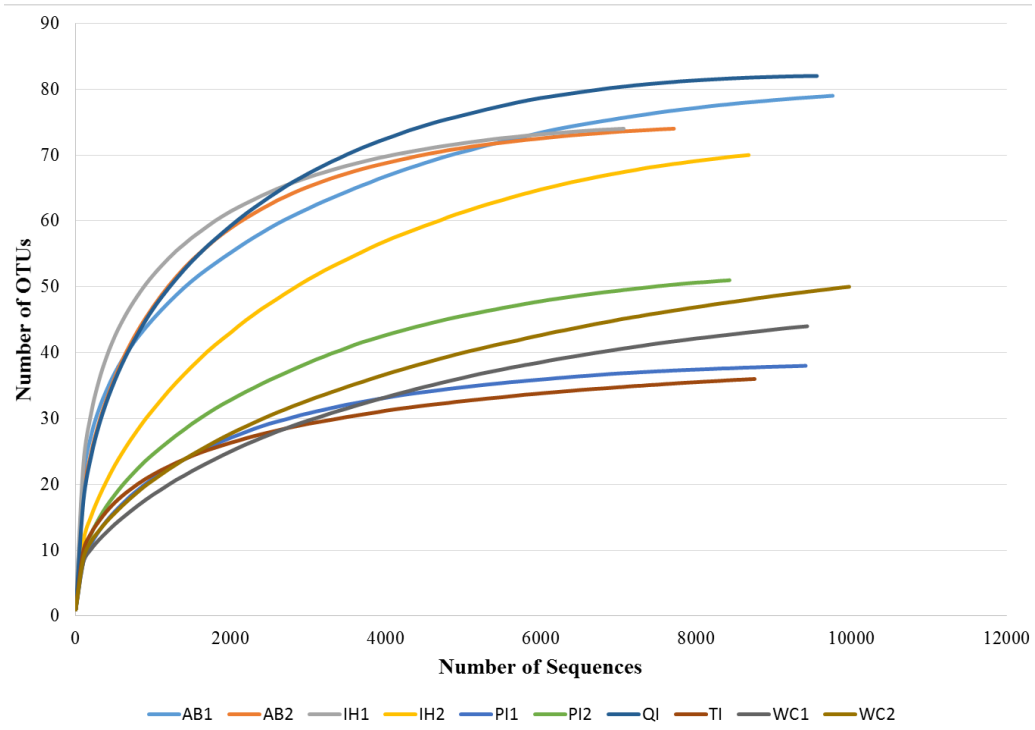

Figure 2.5. Rarefaction curve of sediment samples from Frobisher Bay using Actinobacteria-specific primers (*D* =0.03).

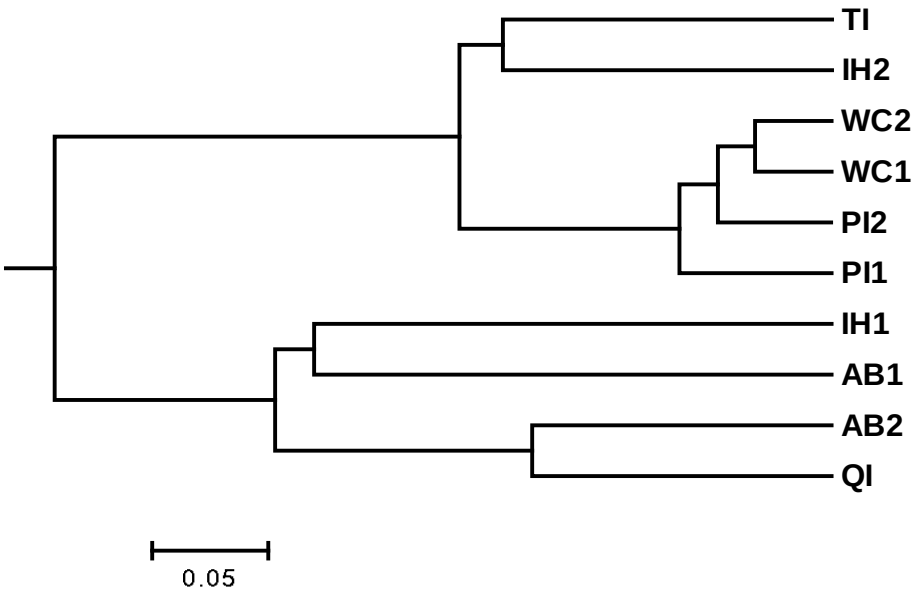

Figure 2.6. Bray Curtis dissimilarity analysis of actinobacterial diversity between sites (*D* =0.03).

2.3.2.3 Actinobacterial Taxonomic Composition

The 88,748 reads were classified using the Silva v. 123 reference database[121]. At the family level, 34 different families were observed with the dominant family being *Acidimicrobiaceae*, representing 19.47% to 84.26% of sequence reads per site (Figure 2.7). The majority of these reads (99.4%) corresponded to the genus *Ilumatobacter*. Families that were present at all sites included members within the uncultured marine actinobacterial clades OM1 (0.4%-28.4%) and Sva0996 (0.2%-26.6%), *Nocardioidaceae* (0.02%-32.7%), *Streptomycetaceae* (0.2%-6.6%), *Acidimicrobiales incertae sedis* (0.1%-4.2%) and unclassified *Acidimicrobiales* (0.1%-3.4%). Within *Nocardiaceae*, the majority of reads corresponded to the genera *Nocardioides* (66.2%), *Marmoricola* (22.1%) and *Aeromicrobium* (11.2%). Within the *Streptomycetaceae*, all of the reads corresponded to the genus *Streptomyces*.

Ten OTUs were shared between all sites (Table 2.5). Three of the OTUs corresponded to the genus *Ilumatobacter* whereas the others corresponded the genus *Iamia* (2 OTUs), *Streptomyces* (1 OTU), *Nocardioides* (1 OTU) and an unknown Acidiobacteria (3 OTUs). The genus *Ilumatobacter* and *Iamia* are obligate marine Actinobacteria[53,153] whereas the genera *Nocardioides* and *Streptomyces* are ubiquitous in the marine and terrestrial environments. The most abundant OTU present corresponded to *Ilumatobacter fluminis* (45.7% of all sequence reads). Of the remaining abundant OTUs, members identified belong to genera that contain both terrestrial and marine species (*Aeromicrobium*[154,155], *Kineococcus*[156,157] *Nocardioides*[158,159], *Janibacter*[160,161]. *Marmoricola*[162,163], *Streptomyces*[164,66], *Pseudarthrobacter*[165] and *Microlunatus*[166,167]).

A)

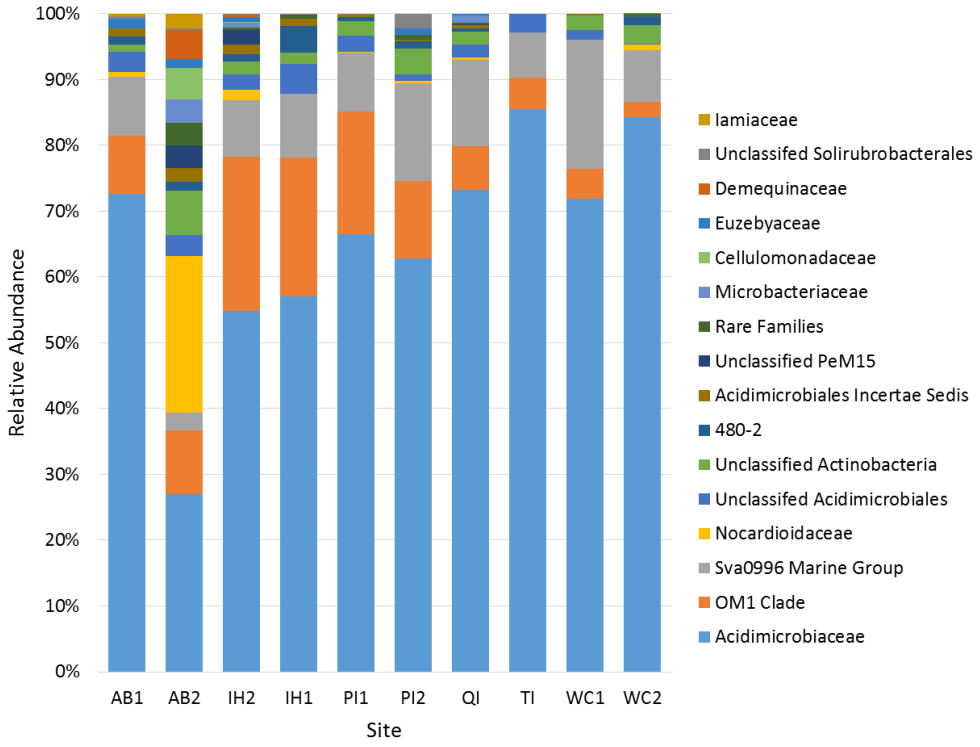

B)

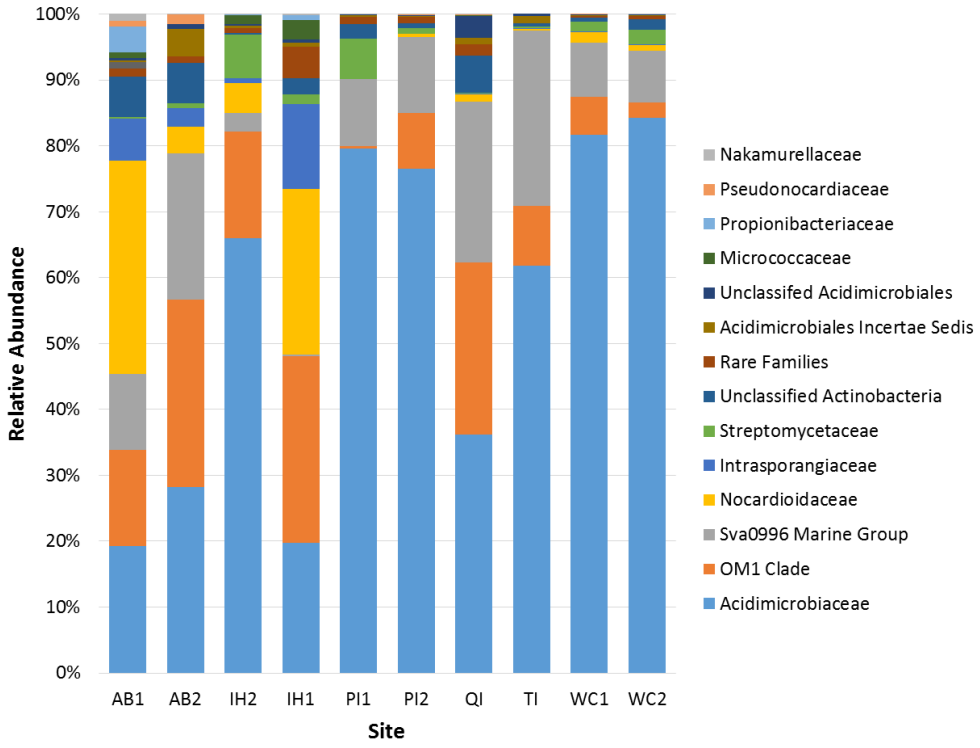

Figure 2.7. Family level actinobacterial diversity using **A)** universal 16S rRNA bacterial primers and **B)** Actinobacteria-specific 16S rRNA primers.

Table 2.5. Most abundant OTUs and shared OTUs between sites detected using Actinobacteria-specific primers (*D*=0.03).

OTU	Total Read %	% Coverage	% Identity	Closest accessioned strain
1[a]	45.70	100	99	*Ilumatobacter fluminis* YM22-133 (NR_041633.1)
2[a]	13.09	99	91	*Acidithrix ferrooxidans* Py-F3 (KC208497.1)
3[a]	10.19	98	94	*Acidithrix ferrooxidans* Py-F3 (KC208497.1)
4[a]	8.67	100	98	*Ilumatobacter fluminis* YM22-133 (NR_041633.1)
5	2.53	100	99	*Nocardioides kribbensis* CB-281548 (JX841083.1)
6[a]	2.11	100	96	*Streptomyces aomiensis* M24DSO4 (NR_112998.1)
7[a]	2.02	100	98	*Ilumatobacter nonamiensis* YM16-303 (NR_112713.1)
8	1.81	100	99	*Aquipuribacter hungaricus* IV-75 (NR_108458.1)
9[a]	0.91	100	99	*Iamia majanohamensis* F12 (JQ899225.1)
10	0.86	100	94	*Aquihabitans daechugensis* CH22-21 (NR_132289.1)
11[a]	0.82	99	98	*Nocardioides salsibiostraticola* PAMC 26527 (NR_109738.1)
12	0.79	100	97	*Nocardioides aquaticus* EL-17K [NR_044903.1]
13	0.78	100	99	*Aeromicrobium qinsengisoli* CB-281479 (JX841017.1)
14[a]	0.71	98	94	*Aciditerrimonas ferrireducens* IC-180 (NR_112972.1)
15	0.67	100	94	*Aciditerrimonas ferrireducens* IC-180 (NR_112972.1)
16	0.52	100	97	*Nocardioides tritolerans* MSL-14 (NR_044227.1)
17	0.48	100	99	*Marmoricola aquaticus* B374 (JN615437.2)
18	0.44	100	99	*Microlunatus aurantiacus* (NR_044306.1)
19	0.41	100	100	*Pseudarthrobacter defluvii* 52-OD12 (KU647245.1)
20	0.39	96	94	*Angutibacter aerolatus* 7402J-48 (NR_109610.1)
21	0.30	100	93	*Iamia majanohamensis* F12 (JQ899225.1)
22	0.28	100	94	*Ilumatobacter fluminis* YM22-133 (NR_041633.1)
23	0.28	100	99	*Janibacter anopheles* VN2013-66 (KX449293.1)
24	0.28	100	99	*Kineococcus xinjiangensis* S2-20 (NR_044522.1)
25	0.25	100	96	*Iamia majanohamensis* F12 (JQ899225.1)
Shared OTUs				
84	0.07	98	92	*Iamia majanohamensis* NBRC 102561 (NR_041634.1)

[a]OTU detected at every sample site

[b]Not in most abundant, detected at every sample site

2.3.2.4 Comparison of Universal and Actinobacteria-Specific 16S rRNA Primers

The use of Actinobacteria-specific primers for 454-pyrosequencing resulted in greater sequencing depth within the Actinobacteria. Of the 116,534 reads obtained, 76.2% were Actinobacteria. The remaining reads corresponded to unclassified bacteria (18.8%), Gemmatimonadales (2.2%), OM190 (1.3%) and DUNssu371 (1.5%). The non-actinobacterial sequences obtained belonging to Gemmatimonadetes, OM190 and DUNssu371 are unsurprising, as their 16S rRNA gene has only one or two nucleotide mismatches with the forward and reverse actinobacterial primers used. Despite the amplification of these bacteria, the high specificity of these primers for Actinobacteria allowed for greater sequencing depth within this phylum than using universal bacterial primers.

By using Actinobacteria-specific primers, 34 genera were detected that were not detected by universal bacterial primers whereas only 8 genera were detected by universal bacterial primers that were not detected by Actinobacteria-specific primers. The 8 genera not detected by Actinobacteria-specific primers were further investigated for their primer specificity by comparing their 16S rRNA gene sequences to the sequence of the Actinobacteria-specific primers in MEGA v 6.0[124]. All of these genera had at most, only 1 bp difference between their 16S rRNA gene sequence and the forward and reverse Actinobacteria-specific primers, so it is surprising they were not detected. This may be because they represent rare phylotypes within the environment as they were detected in low abundance (less than 2-50 sequences) within the total 16S rRNA bacterial dataset. Of the 34 genera not detected by the universal primers, several genera were detected in high abundance using Actinobacteria-specific primers including *Streptomyces* (1800 reads) and *Aquipuribacter* (1600). From a bioprospecting

perspective, the use of both primer sets is complementary as the use of more specific primers allows deeper sequence depth within the prolific NP producing Actinobacteria and the use of universal primers allows for the assessment of relative abundance of Actinobacteria to other phyla.

2.3.3 Culture Dependent Analysis

In order to develop an actinobacterial library for NP discovery, five sediment samples were selected for further investigation. In the initial experimental design, sites selected for culture dependent analysis were to also be analyzed by 454-pyrosequencing. As both of these experiments occurred in tandem, not all sites selected for the culture dependent portion of the analysis were suitable for pyrosequencing due to low quality DNA or an inability to obtain PCR amplicons for pyrosequencing. Therefore, only sites QI and PI1 were included in both portions of the study. For the culture dependent portion, two additional sites from Tarr Inlet (TI2 and TI3) and an additional site from Apex Bay (AB3) were included.

A portion of the sediment sample from each of the five sites was heat-dried to select for spore forming actinomycetes[125]. The dried sediments were stamped onto 48 well plates containing selective actinomycete medium (RH, M5, SCN, CH or mSIM) supplemented with antibiotics and antifungals to inhibit the growth of Gram negative bacteria and fast growing fungi. Serial dilutions of wet sediment were also plated onto 48 well plates in the same manner. Plates were incubated at 22˚C and 4˚C and monitored for growth of Actinobacteria-like morphologies for three months. Incubation at the colder temperature was designed to help select for psychrophilic or psychrotolerant bacteria.

In total, 90 isolates were obtained from these five sediment samples (Table 2.6). Forty-five isolates were obtained from TI2, 18 from TI3, 20 from QI, 7 from AB3 and none from PI1. The isolates were grouped using a 99% sequence similarity cutoff of their 16S rRNA resulting in 11 OTUs containing multiple isolates and 14 singleton isolates which were identified using BLAST (Figure 2.8). The majority of the isolates were taxonomically assigned to the genus *Streptomyces* which is unsurprising given the selective isolation methodology used. Of note, several contigs showed sequence similarity to *Streptomyces fildesensis*, a streptomycete isolated from Antarctic soil from Fildes Peninsula on King George Island[168]. Non-*Streptomyces* genera obtained included *Actinomadura, Amycolatopsis, Kribella, Rhodococcus* and *Streptosporangium*.

All selective media yielded large numbers of bacteria exhibiting Actinobacteria-like morphology. Seventy-eight isolates were obtained using the dry stamp method, compared to 12 by plating of wet sediment. Twelve unique isolates were obtained by using the dry stamp method and five were obtained by direct plating of wet sediment. In terms of media, nine unique isolates were obtained using RH medium, two unique isolates were obtained using M5 medium and two unique isolates were obtained using SCN medium. Twelve isolates were obtained at 4˚C representing five *Streptomyces* spp. These 12 isolates were shown to be capable of growth at both 4˚C and 22˚C and were classified as psychrotolerant.

Table 2.6. Identification of cultured Actinobacteria using 16S rRNA gene sequence similarity.

Contig	# of isolates	Rep. Isolate	Seq. Length (bp)	Closest Blast Hit	Query Coverage	ID
1	2	RKAG 290	970	*Streptomyces brevispora* BK 160 [NR_117081.1]	98	99
2	5	RKAG 421[a]	1485	*Streptomyces cirratus* CSSP 547 [NR_043356.1]	99	99
3	9	RKAG 346	1415	*Streptomyces cyaneofuscatus* CSSP 436 [NR_115383.1]	100	100
4	7	RKAG 278	1410	*Streptomyces fildesensis* GW 25-5 [NR_115761.1]	100	99
5	13	RKAG 425[a]	1382	*Streptomyces fildesensis* GW 25-5 [NR_115761.1]	99	99
6	2	RKAG 309	816	*Streptomyces graminifolii* JL-22 [NR_134196.1]	98	99
7	2	RKAG 592	1442	*Streptomyces laculatispora* BK 166 [NR_117082.1]	99	99
8	2	RKAG 319	1024	*Streptomyces microflavus* NRRL B2156 [NR_043854.1]	97	99
9	3	RKAG 334	1429	*Streptomyces prunicolour* NBRC 13075 [NR_043501.1]	100	99
10	10	RKAG 542	1446	*Streptomyces rubiginosohelvolus* NBRC 12912 [NR_041093.1]	100	100
11	14	RKAG 427[a]	1461	*Streptomyces sampsonii* ATCC 25495 [NR_025870.1]	99	99
12	6	RKAG 428[a]	1479	*Streptomyces sampsonii* ATCC 25495 [NR_025870.1]	99	99
13	3	RKAG 602	1445	*Streptomyces stramineus* NBRC 16131 [NR_041198.2]	100	98
	1	RKAG 353	364	*Actinomadura sediminis* YIM M 10931 [NR_118114.1]	99	97
	1	RKAG 318	1343	*Amycolatopsis saalfeldensis* 2406-001 [NR_043964.1]	99	99
	1	RKAG 296	903	*Kribella antibiotica* YIM 31530 [NR_029048.1]	100	99
	1	RKAG 543	1480	*Rhodococcus qinqshengii* djl-6 [NR_043535.1]	100	99
	1	RKAG 312	862	*Streptomyces beijiangensis* YIM6 [NR_028825.1]	99	98
	1	RKAG 297	1029	*Streptomyces fildesensis* GW 25-5 [NR_115761.1]	99	99
	1	RKAG 337	811	*Streptomyces fildesensis* GW 25-5 [NR_115761.1]	99	99
	1	RKAG 534	1564	*Streptomyces microflavus* NRRL-B2156 [NR_043854.1]	95	98
	1	RKAG 536	1490	*Streptomyces niveus* NRRL B-24297 [NR_115784.1]	95	99
	1	RKAG 357	953	*Streptomyces sampsonii* ATCC 25495 [NR_025870.1]	99	99
	1	RKAG 419[a]	936	*Streptomyces scopuliridis* [NR_116098.1]	99	99
	1	RKAG 538	1475	*Streptosporangium corydalis* NAEU-Y6 [NR_146367.1]	99	99

[a]Isolated at 4˚C

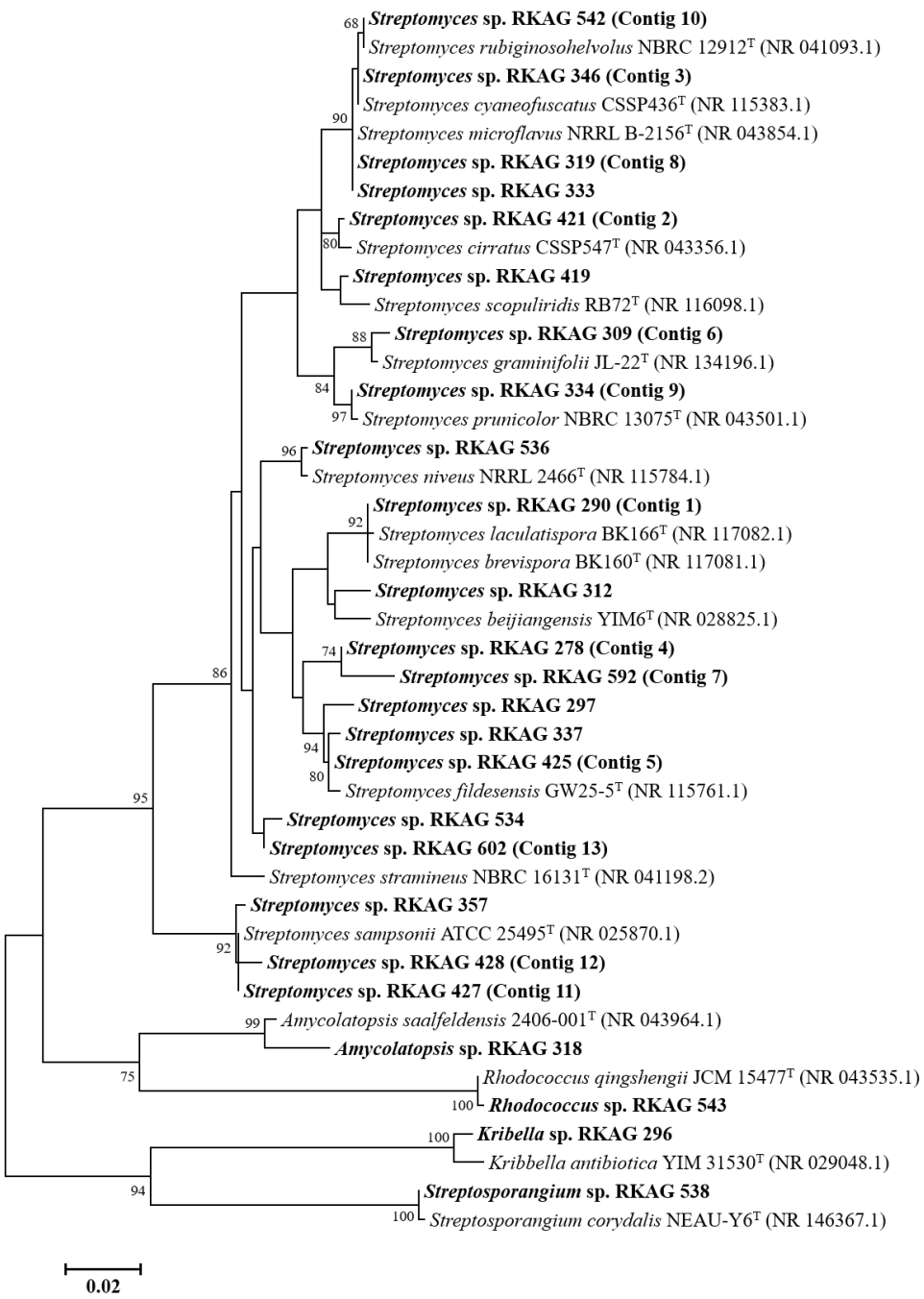

Figure 2.8. Maximum likelihood analysis of 16S rRNA gene sequences of cultured Actinobacteria isolates and reference strains. Alignment was based on a total of 960 nucleotide positions. Phylogram was constructed using the GTR+G model of DNA substitution and 1000 bootstrap iterations. Node support below 50% is collapsed.

2.3.4 Comparison of Cultured Actinobacteria to Culture Independent Analysis

The cultured bacterial 16S rRNA sequences were compared to the culture independent 16S rRNA sequences using a local BLAST search. Only six cultured bacterial isolates were detected in the pyrosequencing analysis using universal bacterial 16S rRNA primers as singletons (RKAG 543, 337, 290, 425, 309, and 297). Using Actinobacteria-specific 16S rRNA primers every cultured isolate was detected, albeit with low read abundance (<20 reads). Whether these isolates are indeed active members within the community or present as dormant spores is unknown, as the isolation method (dry stamp) used strongly favoured spore forming actinomycetes. Further meta-transcriptomics analysis would shed light onto the active members of the Actinobacteria within the community.

The cultured Actinobacteria obtained only represent a small proportion of the total actinobacterial diversity present within Frobisher Bay. The genus *Ilumatobacter* was prevalent across all sites within Frobisher Bay by 454-pyrosequencing, yet was not cultured. This highlights a large issue with bacterial cultivation from environmental sources; many organisms that are prevalent in the environment as determined by next generation sequencing have not been cultured in the lab, due largely to a lack of understanding of their growth requirements. Some microorganisms require the metabolic cooperation of others to grow, where one bacterial species provides the other with necessary growth factors to survive[169,170], while others have very fastidious growth requirements and require specific nutrients, pH, temperature or oxygen levels for growth. The development of more innovative isolation methods should continue to be developed in order to culture these “unculturables”.

2.4 Conclusions

In summary, this study provides the first overall view of bacterial and actinobacterial diversity within Frobisher Bay using culture independent and culture dependent methodologies. Using 454-pyrosequencing it was shown that Frobisher Bay harbours high levels of taxonomically distinct microorganisms, providing a rich resource of microorganisms for natural product discovery. The use of Actinobacteria-specific 16S rRNA primers paired with 454-pyrosequencing represents the first use of these primers with this sequencing technology and offered deeper sequencing reads within the Actinobacteria. Increased diversity was uncovered using these primers and allowed for a more thorough characterization of Actinobacteria present within Frobisher Bay. Within sediment from Frobisher Bay, Actinobacteria made up a small, but significant portion of the diversity at each site.

This study provides the first report of bacterial diversity within Frobisher Bay and can be used to further guide the isolation of bacteria for NP discovery or as a starting point for ecological studies within the area. In terms of NPs, Frobisher Bay is an excellent resource for taxonomically distinct bacteria as assessed by pyrosequencing. The presence of large numbers of putatively novel bacteria is especially interesting from a NP perspective, as the metabolic capabilities of these isolates are unknown and these isolates may be capable of producing new NPs. Due to the selective isolation strategies used, and the lack of understanding of the growth requirements of these isolates, they remain uncultured. Despite this, a taxonomically distinct library of Actinobacteria was isolated and provides a resource for NP discovery. Investigation into the NPs produced by these bacteria is described in Chapter 3.

CHAPTER 3: EFFECT OF FERMENTATION TEMPERATURE ON NATURAL PRODUCT PRODUCTION OF ACTINOMYCETES FROM FROBISHER BAY AND ISOLATION OF TWO NEW LANDOMYCIN NATURAL PRODUCTS

3.1 Introduction

Actinobacteria are one of the most prolific producers of bacterial NPs and are ubiquitous in the terrestrial and marine environment[76]. *Streptomyces* is a genus of filamentous bacteria within the Actinomycetales and one of the most productive producers of NPs within the order[98]. Many clinically relevant antibiotics including tetracycline[171], streptomycin[172] and daptomycin[173] are produced by *Streptomyces* species. Genome sequencing of some *Streptomyces* species has revealed upwards of 20-30 different biosynthetic gene clusters that could be capable of producing NPs, but only a handful of NPs have been isolated from these strains[174,175]. There are several reasons why these gene clusters may be silenced. The gene clusters may either be non-functional or may not be active under the unnatural cultivation conditions within the lab. Enormous untapped potential lies within these isolates and turning on these previously silenced secondary metabolite gene clusters.

It is well-known that switching fermentation parameters including media composition, pH, and aeration can have a large impact on NP production and has been used as a tool to activate silent natural product gene clusters. This is because subtle changes in the environment can have drastic impacts on the transcriptome, proteome and in turn the metabolome. Finding ways to alter the metabolome by changing fermentation parameters is known as the "One Strain –Many Compounds" approach[176] (OSMAC) and has successfully been applied to many microorganisms including *Streptomyces*. Using this approach *Streptomyces* sp. strain c34, isolated from the Chilean Atacama Desert showed distinct LCMS metabolite profiles when cultured on ten different fermentation media. The production of chaxamycin C and D was observed only in fermentations in

modified ISP2 medium whereas the production of three new macrolactone compounds, chaxalactin A-C was only observed using a defined medium[177]. Through the alteration of media components within this *Streptomyces* isolate, differential production of metabolites was observed.

Less studied is the effect of temperature on NP production. The vast majority of fermentations are conducted at 30°C, which may not be ecologically relevant for most microorganisms, especially those from cold environments. Previous work with *Streptomyces griseus* subspecies *psychrophilus* led to the isolation of the new peptide compound cryomycin which was only produced when the fermentation temperature was below 20°C[178]. At fermentation temperatures above 20°C the production of cryomycin ceased and the production of the peptide M-81 was observed[179]. Further investigation into the thermoregulation of cryomycin and M-81 has not been undertaken. The effect of high fermentation temperature on secondary metabolite production has also been investigated. At fermentation temperatures above 37°C the production of validamycin A by *Streptomyces hygroscopicus* is markedly increased than at fermentations between 28-35°C[180]. Transcriptomic analysis revealed enhanced expression of SHJGO322, a SARP-family transcriptional regulator that was confirmed to be associated with the thermo-regulation of validamycin by gene inactivation/complementation[181]. These two fermentation temperature studies highlight that changes in temperature can affect the production of NPs.

Chemical metabolomics is a useful tool to visualize differences between extracts and has been used to dereplicate microbial strains[182], highlight strains producing unique chemistry[183] and look at changes in the metabolome associated with co-culture between

organisms[184]. The use of LC-HRMS to analyze extracts provides information on the mass and polarity of the components within an extract. By using the *m/z* ratio and retention time generated from the LC-HRMS chromatograms, chemical barcodes of an extract can be generated[182] and allow for the quick visualization of differences amongst microbial strains or fermentation conditions[141]. The use of chemical barcodes to quickly look for differences in metabolite production between two conditions can be especially useful for identifying compounds that are differentially expressed between different conditions[185].

The aim of this work was to investigate the effect of fermentation temperature on the production of NPs from a subset of actinomycetes isolated from Frobisher Bay. Due to the cold environment from which they were isolated, fermentations at 30°C are not ecologically relevant for these organisms, and it was hypothesized fermentations at colder, more ecologically relevant temperatures may stimulate the production of silent natural products. Chemical metabolomics was used to observe differences between extracts generated from variations in fermentation temperatures. The differences in the metabolome of select isolates when fermented at different temperatures 4°C (cold temperature), 15°C (moderate temperature) and 30°C (high temperature) will be discussed, as well as the isolation and characterization of two new landomycin analogs as a result of upregulated production in fermentations conducted at 15°C.

3.2 Experimental Procedures

3.1.1 Small-Scale Fermentation of RKAG Library

A subset of 44 actinomycetes were selected for fermentation based on taxonomy and isolation site. Each strain was streaked onto an ISP2 agar plate and incubated for 7

days at 30°C. A 1 cm x 1cm scraping of cells was used to inoculate 7 mL of BSM1 broth supplemented with Instant Ocean™ (18 g/L) and cultivated for 3 days at 30°C and agitated at 200 rpm. A second stage seed medium was inoculated with 1 mL of stage one seed medium and incubated at 30°C at 200 rpm for 24 h. A 3% (v/v) of second stage seed culture was used to inoculate fermentation media (BFM2, BFM3, BFM4 and BFM11). Fermentations were conducted in 25 x 150 mm culture tubes (7 mL/tube) and incubated at both 15°C and 30°C with shaking at 200 rpm for 10 days. After 10 days, Diaion HP20 (5% w/v) was added to each fermentation tube and uninoculated medium blanks and shaken for 1 h. Cells and resin were harvested by centrifugation and the pellets were washed twice with 25 mL ddH_2O. Washed pellets were freeze dried and extracted twice with 10 mL MeOH. Extracts were concentrated *in vacuo* and dissolved in MeOH (700 µL, 10X concentration relative to fermentation volume) for bioactivity testing and chemical analysis using LC-HRMS.

3.1.2 LC-HRMS and Metabolomic Analysis

Crude extracts were analyzed by LC-HRMS using a Thermo Q Exactive HPLC system with a Core Shell 100 Å C_{18} column (Kinetex 1.7 µm C18 100 Å 50 × 2.1 mm). A linear solvent gradient from 95 % H_2O/0.1 % formic acid (FA) (solvent A) and 5 % CH_3CN/0.1 % FA (solvent B) to 100 % solvent B over 4.8 min was followed by an isocratic elution with 100% solvent B for 3.2 min at a flow rate of 500 µL/min. Eluate was detected by +ESI-HRMS monitoring (*m/z* 200–2,000), an evaporative light scattering detector (ELSD; Sedex; Sedere, Alfortville, France) and PDA (200–600 nm).

LC-HRMS files (.RAW) were converted to netCDF files using Xcalibur and processed within MZmine as previously described[182]. Briefly, peak lists were generated

containing a mass-to-charge ratio (*m/z*), retention time and intensity for each metabolite present within the LC-HRMS chromatogram. Mass detection (1E5 threshold), chromatogram building, deisotoping, and bucketing alignment (mass tolerance ± 0.005 and retention time tolerance ± 0.1 min) were also performed within MZmine. Processed data was exported as a CSV file and further processed using Microsoft Excel. All buckets detected in media blanks, reserpine and MeOH blanks were eliminated from the dataset. Scatterplots were generated from the dataset to observe differences in metabolite production between fermentation temperatures. Chemical barcodes were generated in Excel by changing all non-zero intensity values to one and colour coding each fermentation temperature for easier visualization.

3.1.3 Antimicrobial Testing

Crude extracts were tested for antimicrobial activity according to Clinical Laboratory Standards Institute testing standards in a 96-well plate microbroth dilution assay against the human microbial pathogens, methicillin resistant *Staphylococcus aureus* ATCC 33591 (MRSA), vancomycin resistant *Enterococcus faecium* EF379 (VRE), *Staphylococcus warneri* ATCC 17917, *Proteus vulgaris* ATCC 12454, *Pseudomonas aeruginosa* ATCC 14210, and *Candida albicans* ATCC 14035 by Martin Lanteigne (Kerr Lab, UPEI)[186]. Pathogens were grown for 18 h in cation-adjusted Mueller Hinton broth (CAMH), bovine heart infusion broth (BHI) or synthetic defined medium broth (SD, 067% yeast nitrogen base, 2% glucose) and diluted to $5x10^5$ CFU/mL for use in the assay. Optical density was recorded at T_{zero} and T_{final} using a Thermo Scientific Varioskan Flash plate reader to determine growth inhibition after incubation for 22 h. Extracts were considered active if they inhibited the growth of the

test organism by 60% or more. Landomycin AA and AB were tested in triplicate in the same assay at seven concentrations ranging from 1 µg/mL to 64 µg/mL.

3.1.4 Growth Curves and Metabolite Production of RKAG 337 and RKAG 290

Streptomyces sp. RKAG 290 and RKAG 337 were streaked onto ISP2 agar plates and incubated for 7 days at 30°C. A 1 cm x 1cm scraping of cells was used to inoculate 7 mL of clarified BFM3m broth and cultivated for 3 days at 30°C and agitated at 200 rpm. A second-stage seed medium was inoculated with 1 mL of the stage one seed medium and incubated at 30°C at 200 rpm for 24 h. A 3% (v/v) of second-stage seed culture was used to inoculate 7 mL tubes of clarified BFM3m medium. Tubes were grown in triplicate at 4°C, 15°C and 30°C. Samples were collected every 24 h. The cells were centrifuged at 10,000 *g* in a microcentrifuge for five min, the supernatant discarded and the cells washed with ddH_2O. Cells were freeze dried and weighed to determine the dry cell weight. To monitor the production of actinomycin by RKAG 337 and landomycin by RKAG 290 over time, fermentations were set up in triplicate in BFM11 and incubated at 4°C, 15°C and 30°C. Fermentations were carried out over 10 days as described in section 3.1.1. Prior to LCMS analysis a dioctyl phthalate internal standard (200 µL) was added to the extract. The total peak area corresponding to actinomycin or landomycin and the internal standard in the mass spectrometry chromatogram was determined in Xcalibur. The ratio between total peak area and the internal standard was reported.

3.1.5 Fermentation and Actinomycin Production in WAC strains

Three *Streptomyces* strains with 99% 16S rRNA gene sequence similarity to *Streptomyces* sp. RKAG 337 were obtained from Dr. G. Wright's Actinomycete

Collection (WAC library) at McMaster University. These isolates were fermented in duplicate at 15°C and 30°C as described in section 3.1.1. Dioctyl phthalate (200 µL) was added as an internal standard to each extract prior to LC-HRMS submission. Peak area for actinomycin B2, D and C3 (*m/z* 1255.6337, 1269.6143 and 1283.6672 $[M+H]^+$) was determined for each extract and the ratio between total peak area for all three detected actinomycins to the internal standard was reported.

3.1.6 Large Scale Fermentation of RKAG 290 and Purification of Landomycins AA and AB

Streptomyces sp. RKAG 290 was inoculated into 10 mL of ISP2 liquid seed at 30°C and agitated at 200 rpm for five days. The seed culture (200 µL) was used to inoculate six 1 L fermentations of BFM11 fermentation media and grown for 10 days at 15 °C. The liquid cultures were extracted with EtOAc, evaporated *in vacuo* and partitioned between 80% CH_3CN and 100% hexane. The CH_3CN layer was collected and evaporated to dryness *in vacuo* to give a crude extract (890 mg). The crude extract was fractionated using automated reversed-phase flash chromatography on a Teledyne Combiflash RF^+ system with a linear gradient from 20% aqueous MeOH to 100% MeOH over 15 min on a 15.5 g C_{18} column (High Performance GOLD RediSep Rf) with a flow rate of 30 mL/min. The semi-pure fraction eluting at 18 min was subjected to reversed-phase HPLC (flow rate 3 mL/min) using a Thermo Surveyor HPLC system coupled with an evaporative light scattering detector (Sedex 55) and photodiode array (PDA) detector. Using a Gemini 110Å C18 column (5µm 250 x 10 mm, Phenomenex) and 30 min isocratic elution in 55% aqueous MeOH, compounds **1** (10.4 mg) and **2** (1.5 mg) were purified. Tandem mass spectrometry analysis was performed using a Thermo LTQ Orbitrap Velos mass spectrometer and MS/MS spectra were obtained by direct

infusion at a rate of 2 µL/min using a collision induced dissociation energy of 35 eV. NMR spectra were obtained on a 600 MHz Bruker Avance III spectrometer equipped with a cryoprobe. Chemical shifts (δ) were referenced to the $CDCl_3$ residual peaks at δ_H 7.24 ppm and δ_C 77.0 ppm. Optical rotations were measured on a Rudolph Autopol III polarimeter using a 50 mm microcell (1 mL). The infrared spectrum was recorded using attenuated total reflectance on a Bruker Alpha FT-IR spectrometer.

Landomycin AA **(1)** Red powder; $[\alpha]^{25}_D$ -115.6 (c = 0.1, MeOH); IR (film) ν_{max} 3385, 2971, 2936, 2877, 1630, 1445, 1366, 1251, 1119, 1080, 1064, 1012, 981 cm^{-1}; (+) HRESIMS *m/z* $[M+Na]^+$, (calcd for $C_{74}H_{106}O_{29}$, 1481.6712).

Landomycin AB **(2)** Orange powder; $[\alpha]^{25}_D$ -132.4 (c = 0.1, MeOH); IR (film) ν_{max} 3409, 2965, 3931, 2889, 1644, 1605, 1448, 1365, 1262, 1117, 1063, 1013, 986cm^{-1}; (+) HRESIMS *m/z* 1481.6724 $[M+Na]^+$, (calcd for $C_{74}H_{106}O_{29}$, 1465.6763).

3.1.7 Cytotoxicity Testing

Compounds **1** and **2** were tested for cytotoxicity by Kate McQuillan (Nautilus Biosciences) using human foreskin BJ fibroblast cells (ATCC CRL-2522), adult human epidermal keratinocytes (HEKa), Vero kidney cells (ATCC CL-81), human breast adenocarcinoma cells (ER-) (ATCC HTB-26) and human breast adenocarcinoma cells (ER +) (ATCC MCF-7) in triplicate in a 96-well cell culture plate. Cells were grown in 15 mL of Eagle's minimal essential medium supplemented with 10% fetal bovine serum, 100 µU penicillin and 0.1 mg/mL streptomycin in cell culture flasks at 37˚C in a humidified atmosphere of 5% CO_2. Once cells reached 80% confluency, the cells were counted, diluted and plated into 96 well culture plates (cell density of 10,000 cells per well in 90 µL of growth medium without antibiotics). The cells were incubated at 37˚C

in a humidified atmosphere of 5% CO_2 to allow cells to adhere to the plate 24 h before treatment. Cell viability was determined after treatment using the redox dye Alamar Blue to extrapolate cell viability. Fluorescence was monitored using a Thermo Scientific Varioskan Flash plate reader at 560/12 excitation, 590 nm emission both at time zero and 4 h after Alamar blue addition. Landomycin AA and AB were tested at seven concentrations ranging from 1 µg/mL to 64 µg/mL.

3.3 Results and Discussion

3.3.1 Strain Selection

A subset of 44 actinomycetes from the Frobisher Bay actinomycete library constructed in Chapter 2 were selected for further chemical investigation. Isolates were first selected based on partial 16S rDNA sequences (~500 bp). The fourteen singleton isolates and representatives from the thirteen OTUs described in Chapter 2 were included. If an OTU contained isolates obtained from multiple study site locations, a representative isolate was chosen from each study site to be included. If an OTU contained members that were isolated at 4˚C, a representative of this isolation temperature was also included since it was known these isolates had the ability to grow at cold temperatures. This resulted in the inclusion of 44 actinomycetes for this study and included a single isolate from the genus *Kribella*, *Amycolatopsis, Actinomadura, Streptosporangium* and *Rhodococcus* and 39 isolates from the genus *Streptomyces* (Figure 3.1).

3.3.2 Metabolomic Analysis and Bioactivity Profiling of Crude Extracts

Due to the cold environment from which they were isolated, standard laboratory fermentations of 30°C are not ecologically relevant when screening Arctic

Actinobacteria for natural product production. Within Frobisher Bay, the average mean temperature throughout the year is -8.8°C, but temperatures within this region briefly approach 15°C during the summer months. In order to thrive within this environment, microorganisms must be able to survive over a wide range of cold and moderate temperatures. It was hypothesized in response to temperature change, these bacteria would produce different suites of natural products at different temperatures in order to aid in survival during seasonal temperature fluctuations. Within the Actinobacteria library, slow growth was observed amongst these organisms at 4°C and more robust growth was observed at 15°C. Therefore initial fermentation temperatures were selected to observe the effect of moderate (15°C) and high (30°C) temperature fermentations. Based on prioritization of isolates due to differences observed between these two fermentation temperatures, additional fermentations at cold (4 °C) fermentation temperatures were undertaken for select isolates. The subset of isolates selected for further investigation, was fermented in four different fermentation media at two different temperatures (15°C and 30°C) by Noelle Duncan (Nautilus Biosciences). Multiple fermentation media were chosen since it is known that a microorganism can produce different subsets of metabolites by altering fermentation conditions known as the one strain many compound (OSMAC) approach[176]. Ethyl acetate crude extracts for each fermentation condition were analyzed by LC-HRMS and submitted for antimicrobial screening.

Each of the crude extracts was submitted for antimicrobial testing against methicillin resistant *Staphylococcus aureus* ATCC 33591 (MRSA), vancomycin resistant *Enterococcus faecium* EF379 (VRE), *Staphylococcus warneri* ATCC 17917,

Proteus vulgaris ATCC 12454 and *Candida albicans* ATCC 14035. Crude extracts exhibiting growth inhibition of any of the tested pathogens over 60% were considered active. Overall, 73% of the strains exhibited bioactivity against at least one or more pathogens (Figure 3.1). Anti-VRE activity was most prevalent (19 isolates) followed by activity against MRSA (17 isolates), *S. warneri* (11 isolates), *P. vulgaris* (16 isolates) and *C. albicans* (7 isolates). Fifty percent of the strains tested showed differential antibiosis against one or more pathogens when fermented at 15°C vs. 30°C whereas 11% of the strains tested showed differential antibiosis at 30°C vs. 15°C. Nine isolates had activity observed only in the 15°C fermentations (RKAG 286, 287, 290, 309, 318, 337, 425, 534 and 543) whereas only one isolate (RKAG 296) exhibited activity exclusively at 30°C.

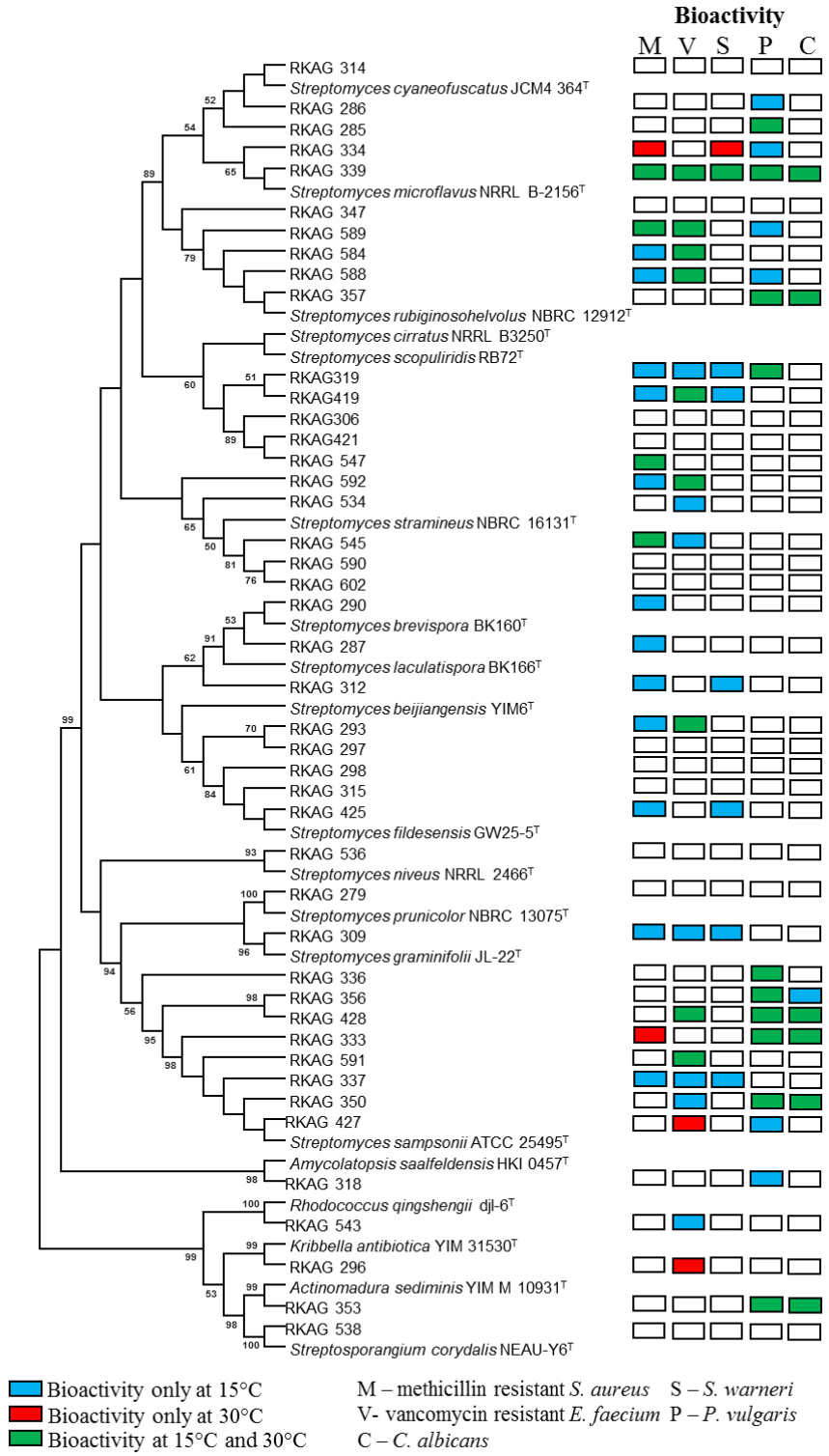

Figure 3.1. Antimicrobial screening of actinomycete library against five microbial pathogens when fermented at 15˚C and 30˚C.

Metabolomic profiling of the LC-HRMS data of the EtOAc crude extracts for each of the isolates was performed using MZmine 2.10. LC-HRMS data was grouped into two-dimensional buckets consisting of a retention time-*m/z* (*m/z* ± 0.005 *m/z* units and retention time ± 0.1 min) as one dimension and ion intensity as the other. A 1E5 ion intensity cut-off was used for peak detection to reduce the number of buckets associated with artifacts. Buckets detected in media components, MeOH blanks and internal reserpine calibration standards were removed from the analysis. Chemical barcodes and scatterplots were generated for each isolate to visualize differences in metabolite production at each fermentation temperature. Depending on the isolate 85-1051 buckets were observed with an *m/z* ratio ranging from 190.6243 to 1909.0372 and retention times ranging from 1.00 to 8.50 min. All isolates showed differential metabolite production with temperature and tentative identification of these metabolites was given based on database searches (Antibase 2014 and SciFinder). Those isolates displaying chemical novelty or high levels of induction of known NPs were prioritized for further investigation. The following isolates were prioritized based on the production of unknown compounds exclusively at 15°C; RKAG 592 *m/z* 1141.2253 $[M+Na]^+$, RKAG 425 *m/z* 570.2272 $[M+H]^+$, *m/z* 584.2425 $[M+H]^+$ and *m/z* 598.2587 $[M+H]^+$, RKAG 590 *m/z* 1029.0651 $[1/2M+H]^+$, RKAG 319 *m/z* 813.4035 $[M+H]^+$, RKAG 287 and 290 *m/z* 1481.6724 $[M+H]^+$ and *m/z* 1465.6754 $[M+H]^+$ and RKAG 285 and 286 *m/z* 1107.5410 $[M+H]^+$ and *m/z* 870.4899 $[M+NH_4]^+$. Isolate RKAG 337 was also prioritized due to the *de novo* induction of actinomycins when fermented at 15°C (Figure 3.2).

A)

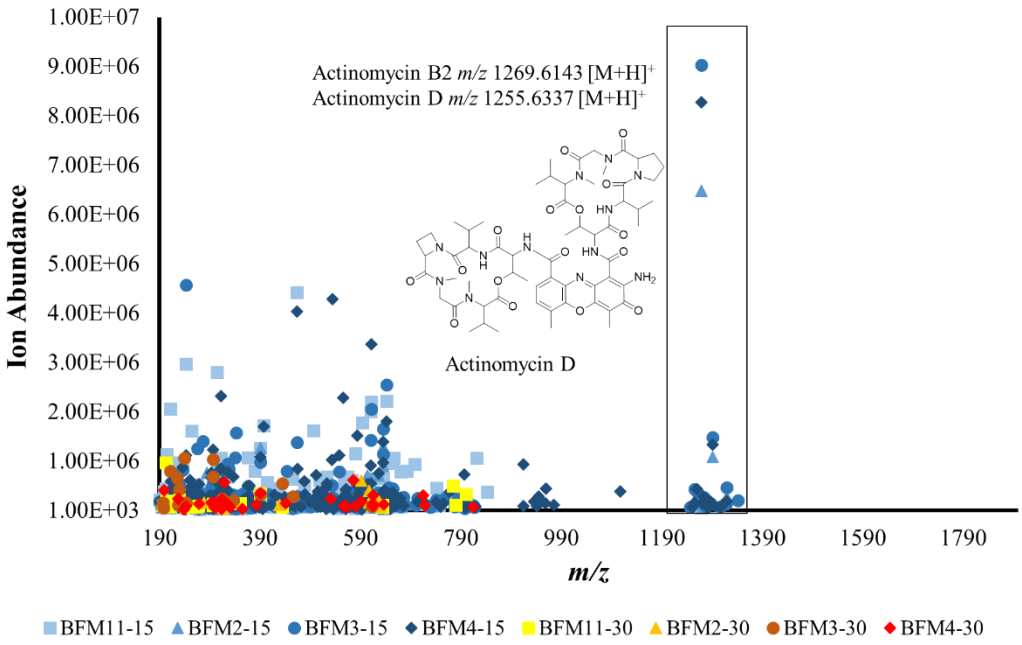

B)

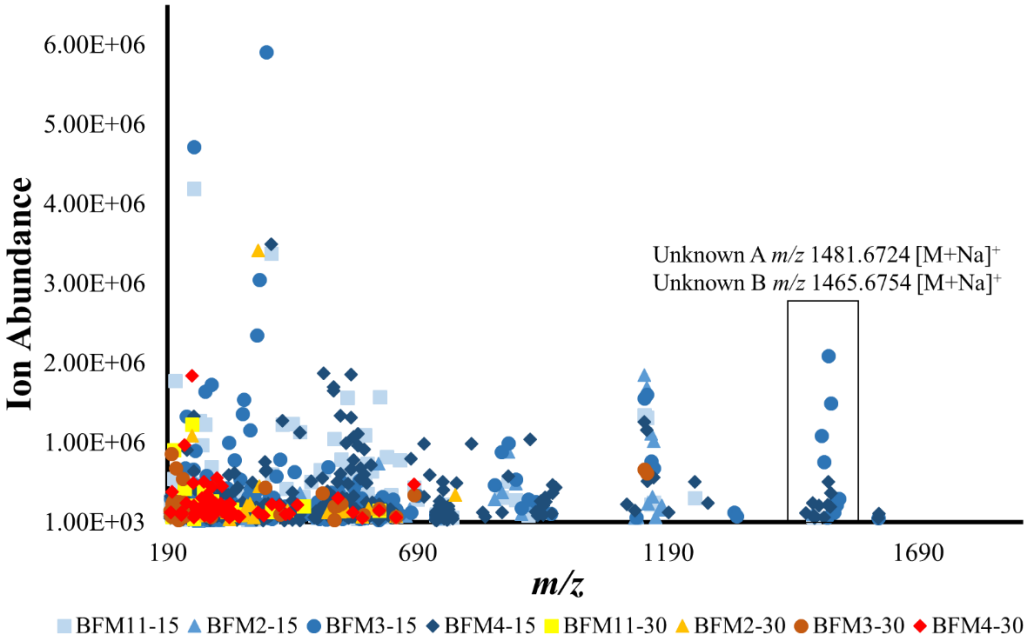

Figure 3.2. Chemical scatterplots of A) RKAG 337 and B) RKAG 290.

Since the metabolomics analysis only offered a snapshot of the fermentation process at day 10, it was unknown whether the difference in metabolite production observed was truly a result of differential metabolite production between the two fermentation temperatures. Since these isolates were obtained from the Arctic, the differences observed between the two fermentation temperatures could be the result of an inability of the organism to grow at 30°C or a growth retardation at 30°C. Likewise the organism may be able to grow more rapidly at 30°C and produce the compounds of interest before day 10 whereby they could be broken down and no longer detectable by day ten. In order to further investigate what was occurring growth rates for isolates of interest were monitored for ten days at 4°C, 15°C and 30°C and fermentations were simultaneously carried out to monitor the production of metabolites over the ten day period. Triplicate extractions were performed every two days and monitored by LC-HRMS. Growth curves were generated using dry cell mass for each isolate. Single ion monitoring for the compounds of interest was done for each extract. These experiments were completed by a Master's thesis student Courtney Gallant and undergraduate student Nick Mulligan with the prioritized isolates from the metabolomics study. For the purposes of this thesis only the results from isolate RKAG 337 and RKAG 290 will be further discussed.

3.3.3 Actinomycin Production of RKAG 337 and WAC strains

Streptomyces sp. RKAG 337 was of interest for further investigation due to the antimicrobial activity observed against MRSA, VRE and *S. warneri* when the 15°C crude extracts were tested and the induction of actinomycins at 15°C. Analysis of the chemical barcode of RKAG 337 revealed the presence of 402 buckets associated with

the 15°C fermentation and only 16 buckets associated with the 30°C fermentation. Analysis of the scatterplot of RKAG 337 revealed the presence of compounds corresponding to *m/z* values of 1269.6143 and 1255.6337 $[M+H]^+$ which were identified in Antibase 2012 as actinomycin B2 (Δ= -0.63 ppm, *m/z* calcd for $C_{62}H_{85}N_{12}O_{17}^+$) and actinomycin D (Δ= -1.67 ppm, *m/z* calcd $C_{62}H_{87}N_{12}O_{16}^+$) that were only observed when the isolate was fermented at 15°C. The actinomycins are a family of bicyclic chromopeptide lactones originally isolated in 1940 from *Streptomyces antibioticus* and have potent antimicrobial[187] and anticancer activity[188]. The antimicrobial activity of the actinomycins may be responsible for the differential bioactivity observed when this isolate was fermented at 15°C.

To determine if the production of actinomycin was due to a lack of growth of the isolate at 30°C, the growth rate (measured by dry cell mass) was monitored every 24 h for ten days at 4°C, 15°C and 30°C. It was determined that this isolate was psychrotolerant as it was capable of growth at all three temperatures. The isolate showed robust growth at 15°C and 30°C and experienced slower growth at 4°C. The production of actinomycin was followed over ten days by carrying out fermentations simultaneously with the growth rate. Extractions were performed every two days and a dioctyl phthalate internal standard was added to each extract. Extracts were monitored by LC-HRMS and single ion monitoring of actinomycins showed they were exclusively produced in the 15°C fermentation (Figure 3.3) and were not observed as a result of a lack of growth of the isolate at 30°C, but due to the fermentation temperature.

In order to further investigate if temperature dependent production of actinomycin is unique to the Arctic *Streptomyces* sp. RKAG 337, or is prevalent across

other non-Arctic actinomycin producing *Streptomyces*, three actinomycin producing *Streptomyces* strains were obtained from the WAC culture collection (Wright Actinobacteria Culture Collection) at McMaster University. Each of the obtained isolates (*Streptomyces* sp. 7652, 8892 and 8910) exhibited >99% 16S rRNA gene sequence similarity to *Streptomyces* sp. RKAG 337. The WAC isolates were fermented by Brad Haltli (Kerr Lab, UPEI) in four fermentation media at 15°C and 30°C in duplicate. Comparison of actinomycin production between strains is reported as a ratio of the sum of the peak area of all detected actinomycins to an internal standard (dioctyl phthalate) (Figure 3.3). None of the WAC *Streptomyces* strains exhibited temperature dependent actinomycin production as actinomycin production occurred at both 15°C and 30°C fermentation temperatures. The lack of temperature dependent regulation of actinomycin in the WAC strains highlights the unique temperature dependent regulation of actinomycin within *Streptomyces* sp. RKAG 337 and provides proof of concept for the use of decreased fermentation temperature for the discovery of natural products from bacteria isolated from cold environments. Further investigation of the regulation of actinomycin in all four *Streptomyces* strains is warranted to determine how fermentation temperature is causing the differential expression of the actinomycins in the Arctic *Streptomyces* sp. RKAG 337, but not in the non-Arctic *Streptomyces* isolates from the WAC collection.

A)

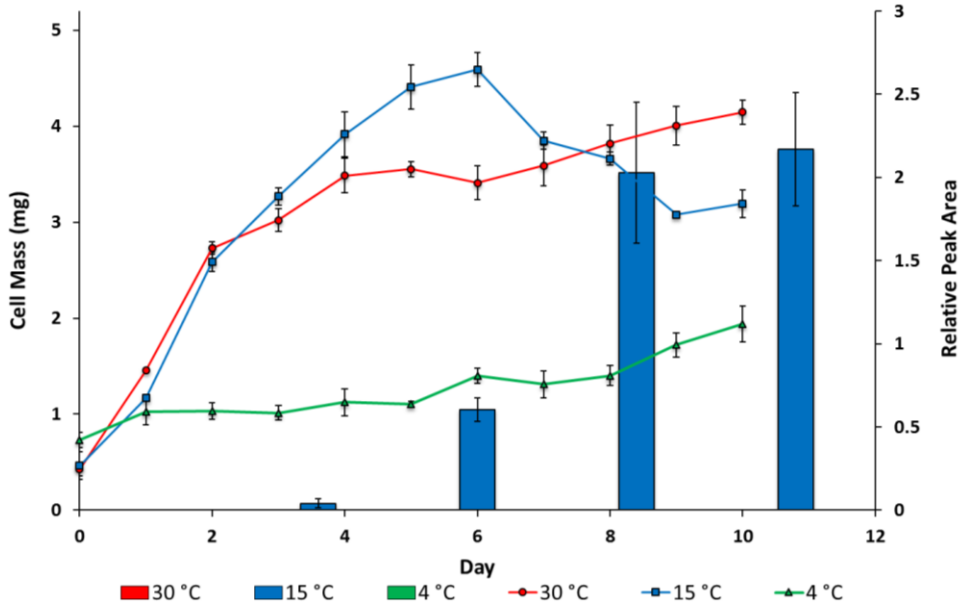

B)

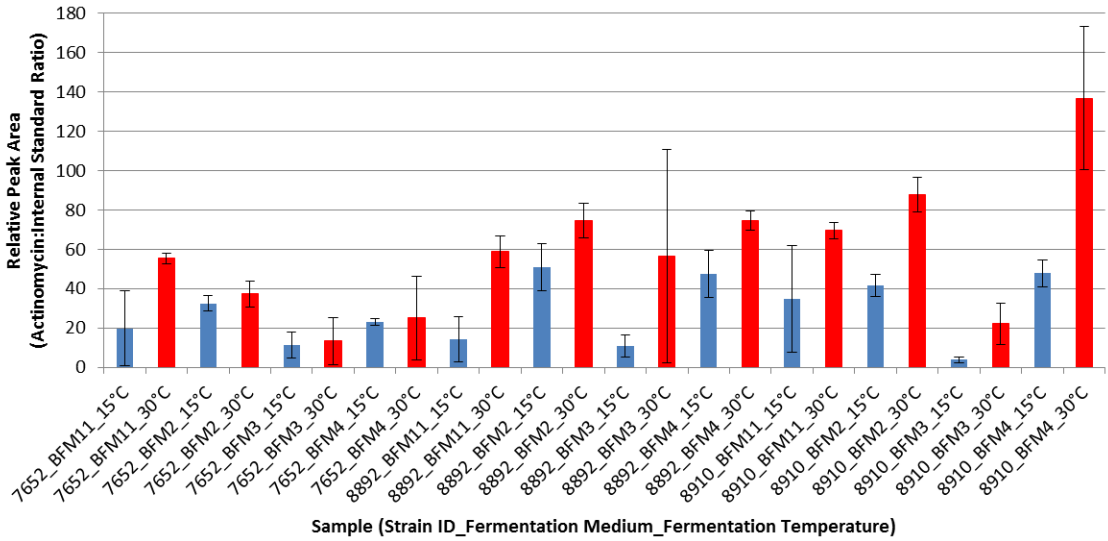

Figure 3.3. A) Growth rate and actinomycin production of RKAG 337 over ten days (relative peak area is the ratio of the peak area of actinomycin to a dioctyl phthalate internal standard monitored by LC-HRMS). **B)** Actinomycin production by WAC strains after ten days.

3.3.4 Growth Rate and Metabolite Production of RKAG 290

Due to the differential metabolite production observed for *Streptomyces* sp. RKAG 337 as a result of fermentation temperature, isolates producing unknown metabolites were of interest for further investigation. *Streptomyces* sp. RKAG 290 was selected from the prioritized isolates because it produced 'purifiable' quantities of the unknown compounds of interest as judged by the ELSD chromatogram and had antimicrobial activity exclusive to the extracts associated with the 15°C fermentations. Metabolomic analysis of RKAG 290 revealed 432 buckets associated with the 15°C fermentation and 56 buckets associated with the 30°C fermentation. Analysis of these buckets revealed the presence of two buckets associated with an *m/z* of 1481.6724 $[M+Na]^+$ and *m/z* 1465.6754 $[M+Na]^+$ produced only at 15°C with no likely hits when searched in natural product databases. Growth curves and fermentations were carried out in the same manner as for RKAG 337. Fastidious growth of RKAG290 at 15°C and 30°C and slower growth at 4°C was observed. Single ion monitoring of the unidentified compounds over ten days (Figure 3.4) revealed small amounts of *m/z* 1481.6724 $[M+Na]^+$ being produced in the 30°C fermentation. The production of the unknown compounds is reported as a ratio of the sum of the peak area to an internal standard (dioctyl phthalate). The production of this compound was six fold higher in the 15°C fermentation over the 30°C fermentation by day 10. In order to determine the identity of the unknown compounds, a large-scale fermentation at 15°C was undertaken in order to obtain enough material for structure elucidation.

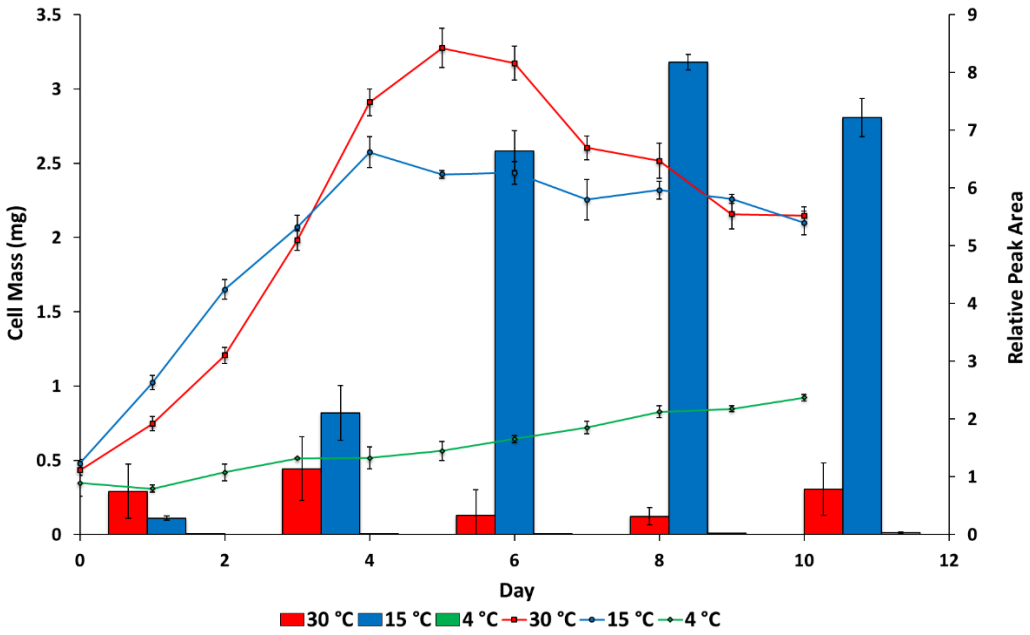

Figure 3.4. Growth rate of RKAG 290 and production of *m/z* 1481.6724 $[M+Na]^+$ over ten days (relative peak area is the ratio of the peak area of *m/z* 1481.6724 $[M+Na]^+$ to a dioctyl phthalate internal standard monitored by LC-HRMS).

3.3.5 Isolation and Structure Elucidation of Landomycin AA and AB

A 6 L liquid fermentation of RKAG 290 was extracted with EtOAc, dried *in vacuo* and partitioned between 100% hexane and 80% CH_3CN. The CH_3CN soluble portion was subjected to flash chromatography yielding a fraction eluting between 18 and 19.5 min consisting of 37 mg of semipure material. Reversed-phase HPLC purification using a C18 column with 55% MeOH resulted in the separation of two compounds, one at 12.2 min (1.5 mg) and the other at 20.9 min (10.5 mg) representing *m/z* 1465.6754 $[M+Na]^+$ and 1481.6724 $[M+Na]^+$ respectively.

Compound **1** was obtained as a red powder and the molecular formula was assigned as $C_{74}H_{106}O_{29}$ (*m/z* 1481.6724 $[M+Na]^+$, Δ = -0.81 ppm) by HRESIMS indicating 22 degrees of unsaturation (Table 3.1, Appendix Figures A.1 and A.2). The HSQC spectrum revealed the presence of nine anomeric protons (δ_H 4.44-5.04, δ_C 97.4-101.5) consistent with nine saccharide moieties as well as 28 methine, 15 methylene and 10 methyl signals (Figure 3.5). Four of the methine signals were for multiple highly substituted aromatic ring systems. Two ortho coupled aromatic signals at δ_H 7.24 (d, *J*=9.4 Hz) and δ_H 7.51 (d, *J*= 9.4 Hz) revealed the first substituted aromatic ring system and two broad aromatic signals at δ_H 6.79 and δ_H 6.75 revealed another highly substituted aromatic ring. DEPTQ-135 revealed the presence of two quinone carbonyls (δ_C 182.8 and δ_C 192.8) and COSY experiments revealed an oxymethine signal (δ_H 5.06) directly next to a methylene group (δ_H 3.05 and δ_H 2.87). An aromatic bound ethyl group was observed due to correlations between H-13 (δ_H 2.60) and H-14 (δ_H 1.23) and was localized to the A ring by correlations from H-13 (δ_H 2.60) to C-2 (δ_C 118.9), C-3 (δ_C 150.0) and C4 (δ_C 122.7). Correlations from H-2 (δ_H 6.79) to C-11 (δ_C 155.4) and C-

13 (δ_C 28.6); and H-4 (δ_H 6.75) to C-4a (δ_C 137.0), C-5 (δ_C 36.6) and C-12b (δ_C 113.6) connected the A ring to the B ring. HMBC correlations from H-6 (δ_H 5.06) to C-6a (δ_C 139.0), C-7 (δ_C 182.8), and C-12a (δ_C 147.1) connected the B ring to the C ring. Lastly HMBC correlations from H-9 (δ_H 7.51) to C-7 (δ_C 182.8), C-7a (δ_C 119.3), and C-8 (δ_C 150.9) and from H-10 (δ_H 7.24) to C-11 (δ_C 159.9), C-11a (δ_C 115.1) and C-12 (δ_C 192.8) connected the D ring to the C ring and confirmed the presence of an angucyclinone core. This core structure was similar to the previously reported landomycin family of compounds[189] and differed by the presence of an ethyl group within the angucyclinone core at C-3 as opposed to a methyl group. Due to the similarity in structure and similar coupling constant observed for H-6 (apparent triplet, *J*=4.4 Hz), the *R* configuration at this stereocentre was tentatively assigned since all reported landomycins have *R* stereochemistry at this location[189-190].

The proton, DEPTQ-135 and HSQC spectra revealed the presence of nine saccharide moieties (δ_H 4.44-5.04, δ_C 97.4-101.5) consisting of two different deoxy sugars. The planar structure of the sugars was determined using TOCSY and COSY experiments and the relative configuration of the sugar residues was determined by NOESY correlations confirming the identity of the sugars as olivose and rhodinose in a five to four ratio. The anomeric protons of olivose showed large coupling constants (*J*=9.1-9.7 Hz) and represented β-D-olivose. The anomeric protons corresponding to rhodinose showed small coupling constants (*J*=1.5 Hz) and represented α-L-rhodinose. It was determined that the sugars were connected as a linear nonasaccharide chain to the 3-ethyl-landamycinone core through HMBC and NOESY correlations and MS/MS analysis. The first sugar within the chain, olivose was connected to the angucyclinone

core at C-8 due to $^{3}J_{C\text{-}H}$ long range coupling between the anomeric proton (δ_H 5.04) and C-8 (δ_C 150.9). HMBC correlations from H-1B (δ_H 4.49) to C-4A (δ_C 88.0) confirmed olivose as the second sugar in the chain. Rhodinose was assigned as the third sugar in the chain due to HMBC correlations from H-1C (δ_H, 4.91) to C-3B (δ_C 80.7). The remaining sugars alternated between olivose and rhodinose and were assigned by HMBC correlations from H-$4_{E, G}$ of rhodinose (δ_H 3.51) to the anomeric carbon of olivose D, F and H (δ_C 101.5) and from the anomeric proton of rhodinose E and G (δ_H 4.91) to C-$3_{D, F, H}$ of olivose (δ_C 81.0). The terminal sugar rhodinose was assigned by HMBC correlations from H-1I (δ_H 4.92) to C-3H (δ_C 81.0). Tandem mass spectrometry (Appendix Figure A.3) confirmed the order of the sugars by the successive loss of masses corresponding to rhodinose and olivose from the terminal end of the saccharide chain. The presence of β-D-olivose and α-L-rhodinose was consistent with those saccharides previously reported for the landomycins[189]. Due to the similarity in structure to the landomycins, this compound was named landomycin AA.

A second compound was obtained as an orange powder and the molecular formula was assigned $C_{74}H_{106}O_{28}$ (*m/z* 1465.6754 $[M+Na]^+$, Δ = -0.61 ppm) by HRESIMS indicating 22 degrees of unsaturation (Table 3.1, Appendix Figures A.4 and A.5). The molecular mass of **2** was 16 amu less than **1** and analysis of the ^{1}H and ^{13}C NMR data revealed **2** differed by **1** by the loss of a phenolic OH singlet (δ_H 12.30) and the gain of an additional aromatic proton signal (δ_H 7.95) (Table 3.1). COSY correlations between H-11 (δ_H 7.95) and H-10 (δ_H 7.66) and HMBC correlations from H-11 (δ_H 7.95) to C-11a (δ_C 120.8) and C-12 (δ_C 189.7) confirmed that ring D was deoxygenated at position C-11 compared to **1**. Analysis of COSY, HSQC, HMBC and

NOESY data confirmed the remainder of **2** had the same structural and stereochemical features as **1** and was named landomycin AB (Figure 3.6). MS/MS was used to confirm the order of sugars within the nonasaccharide chain (Appendix Figure A.6)

The isolation of landomycin AA and AB represent two new analogs within the landomycin family. The landomycins are a large group of type II polyketides and consist of an angucyclinone core decorated with a single deoxyoligosaccaride chain. The saccharide chain has previously been shown to contain up to six sugars and consists of the sugar moieties, rhodinose and olivose and rarely amicetose[189,190]. To date all members within this family have been isolated from three *Streptomyces* strains, *S. globisporus* 1912[191], *S. cyanogenus* S-136[192,193,194,195] and *S. cyanogenus* K62[190]. The isolation of landomycins AA and AB from *S. brevispora* RKAG 290 represents a new source for landomycins and the first examples of landomycins containing a nonasaccharide chain. Previous investigation into landomycin A biosynthesis has revealed the *lan* gene cluster contains four glycosyltransferase enzymes responsible for attaching six deoxy sugars. LanGT1 and LanGT4 work iteratively and attach one sugar residue twice whereas LanGT2 and LanGT3 attach one sugar each[194]. Due to the iterative nature of these glycosyltransferases, the addition of another three sugars is not implausible. The change from a methyl to an ethyl moiety at position C-3 within landomycin AA and AB is also not unreasonable. In landomycin biosynthesis a type II polyketide synthase enzyme uses acetyl CoA as a starter unit and malonyl CoA as extender units to establish the decaketide backbone[196]. In the case of landomycin AA and AB, a propionate starter unit can be used instead which would result in the appearance of an ethyl group at C-3 instead of a methyl.

A

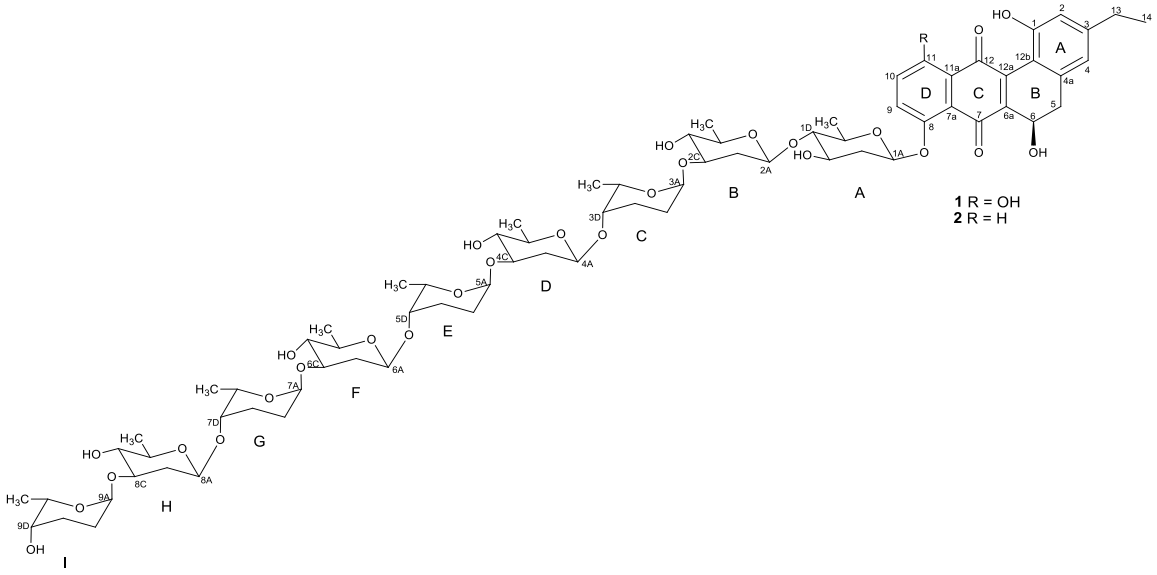

B

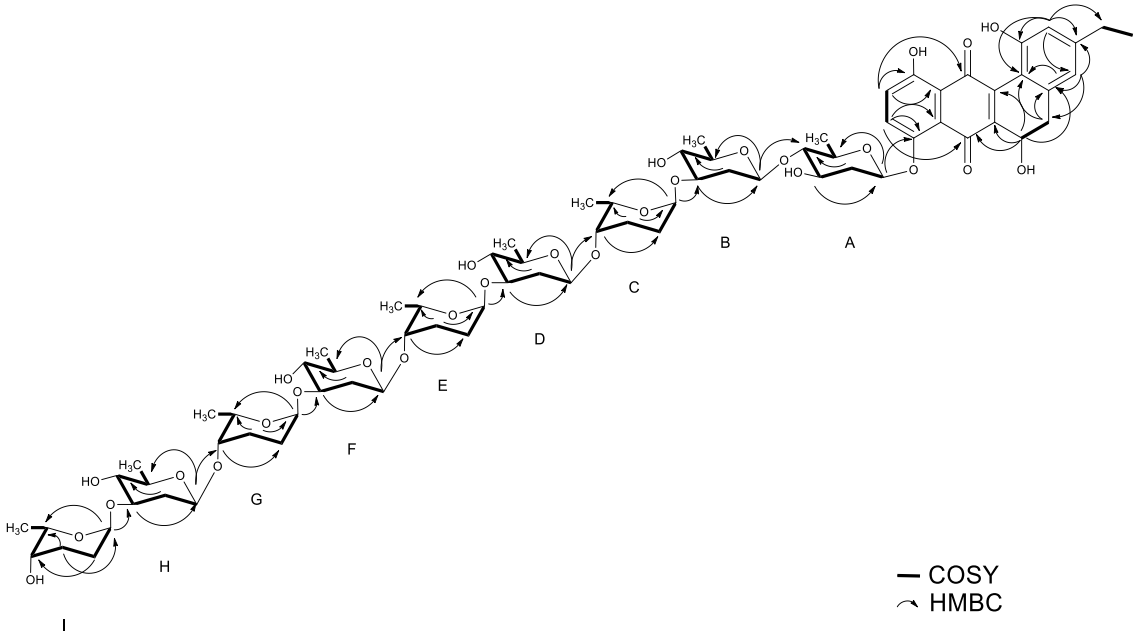

Figure 3.5. A) Structure of landomycin AA (**1**) and AB (**2**). **B)** Key COSY and HMBC correlations to determine the structure of **1. C)** Key NOESY correlations to determine the structure of **1**.

C

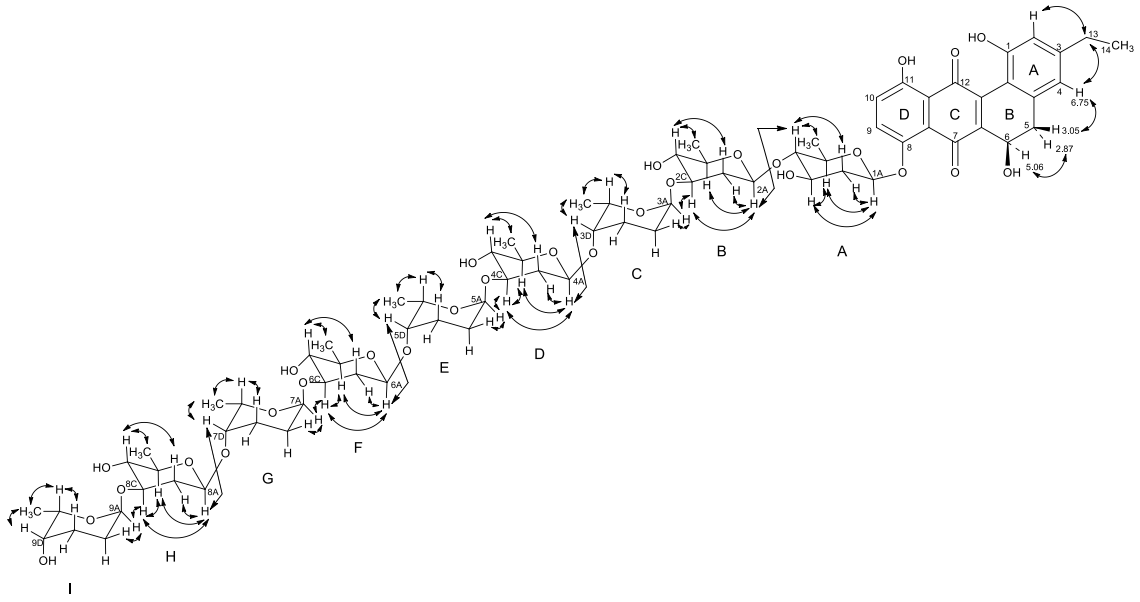

Figure 3.5. Continued from previous page

A

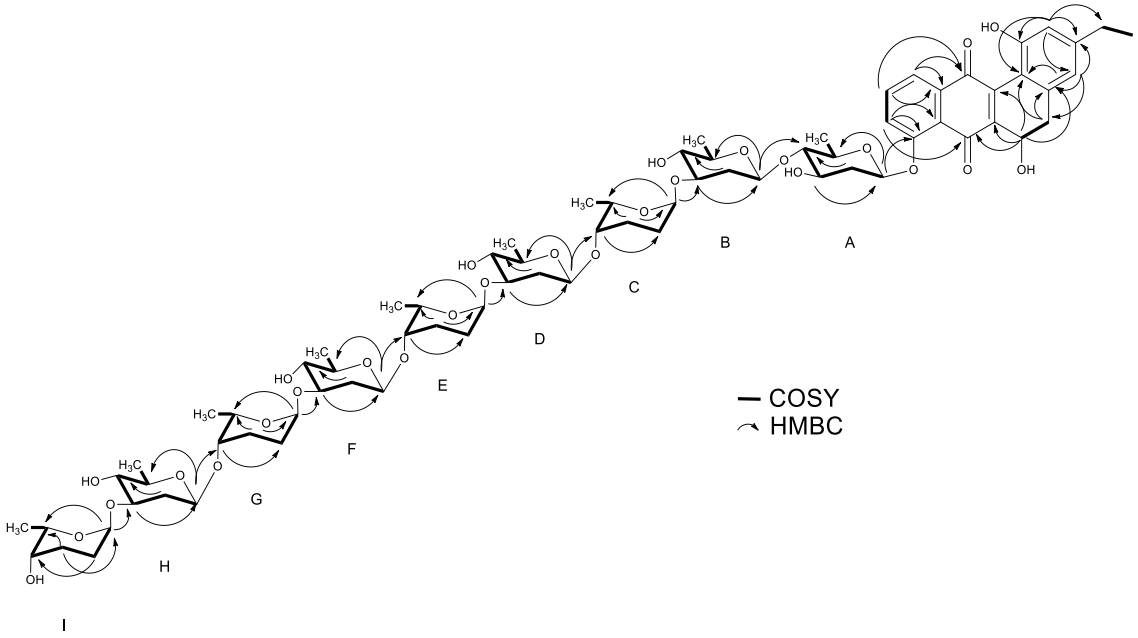

B

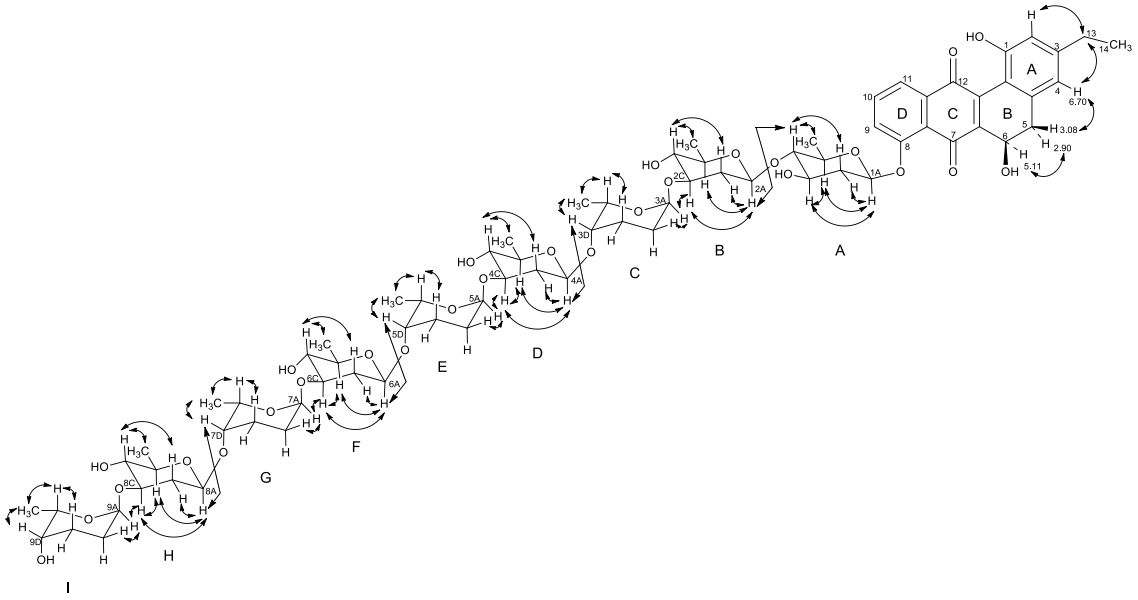

Figure 3.6. A) Key COSY and HMBC correlations to determine the structure of landomycin AB. **B)** Key NOESY correlations to determine the structure of landomycin AB.

Table 3.1. ^{1}H (600 MHz) and ^{13}C (150 MHz) NMR data of landomycin AA (1) and landomycin AB (2) in $CDCl_3$.

	Landomycin AA (1)			**Landomycin AB (2)**	
Position	δ_H	δ_C		δ_H	δ_C
1-OH	8.84, bs		1-OH	9.53, bs	
1		155.4	1		156.0
2	6.79, s	118.9	2	6.80, s	119.0
3		150.0	3		150.1
4	6.75, s	122.7	4	6.70, s	122.5
4a		137.0	4a		136.8
5_α	2.87, dd (4.2, 15.9)	36.6	5_α	2.90, dd (16.0, 4.5)	36.6
5_β	3.05, m		5_β	3.08, m (complex)	
6	5.06, t (4.4)	62.4	6	5.11, t (4.6)	62.3
6a		139.0	6a		145.9
7		182.8	7		183.9
7a		119.3	7a		134.8
8		150.9	8		156.4
9	7.51, d (9.4)	132.7	9	7.49, d (8.4)	125.4
10	7.24, d (9.4)	126.9	10	7.66, dd (8.4, 7.8)	134.9
11-OH	12.30, bs		11-OH	-	
11		159.9	11	7.95, d (7.8)	123.2
11a		115.1	11a		120.8
12		192.8	12		189.7
12a		147.1	12a		138.8
12b		113.6	12b		113.5
13	2.60, dt (7.7, 7.5)	28.6	13	2.60, dt (7.7, 7.5)	28.7
14	1.23, t (7.6)	14.9	14	1.23, dd (7.7, 7.5)	14.9
Sugar A, β-D-olivose					
1A	5.04, dd (9.4, 1.2)	99.8	1A	5.21, dd (9.6, 2.0)	98.7
$2A_a$	1.89, m	37.8	$2A_a$	2.00, m (complex)	37.8
$2A_e$	2.68, ddd (6.4, 5.0, 1.3)		$2A_e$	2.67, ddd (7.2, 5.2, 2.0)	
3A	3.67, ddd (12.0, 8.4, 5.5)	69.4	3A	3.71, ddd (12.0, 8.3, 5.2)	69.5
3A-OH	4.70, brs		3A-OH	4.70, brs	
4A	3.05, m (complex)	88.0	4A	3.11, m (complex)	88.0
5A	3.36, m (complex)	71.0	5A	3.46, m (complex	71.1
6A	1.26, d (6.1)	18.0	6A	1.29, m	17.9
Sugar B, β-D-olivose					
1B	4.49, dd (9.1, 1.6)	101.0	1B	4.52, dd (10.1, 1.5)	101.1
$2B_a$	1.67, m (complex)	37.	$2B_a$	1.64, m (complex)	37.4
$2B_e$	2.21, m (complex)		$2B_e$	2.20, m (complex)	
3B	3.48, m (complex	80.7	3B	3.48, m (complex)	80.8
4B	3.05, m (complex)	75.4	4B	3.09, m (complex)	75.5
4B-OH	4.18, brs		4B-OH	4.15, brs	

5B	3.36, m (complex)	72.5	5B	3.38, m	72.6
6B	1.37, d 6.0)	18.0	6B	1.38, d (6.1)	18.1
Sugar C, α-L-rhodinose					
1C	4.91, brs	97.8	1C	4.93, brs	97.8
$2C_a$	1.50, m (complex)	25.3	$2C_a$	1.50, m (complex)	25.3
$2C_e$	2.09, m (complex)		$2C_e$	2.10, m (complex)	
$3C_a$	1.50, m (complex)	24.6	$3C_a$	1.51, m (complex)	24.7
$3C_e$	1.94, m (complex)		$3C_e$	1.90, m (complex)	
4C	3.51, m	76.0	4C	3.51, brs	75.9
5C	4.05, m (complex)	67.7	5C	4.05, m (complex)	67.8
6C	1.16, (complex)	17.2	6C	1.17, m	17.2
Sugar D, β-D-olivose					
1D	4.44, dd (9.7, 2.0)	101.5	1D	4.45, dd (9.7, 1.8)	101.5
$2D_a$	1.67, m (complex)	37.4	$2D_a$	1.65, m (complex)	37.2
$2D_e$	2.21, m (complex)		$2D_e$	2.23, m (complex)	
3D	3.44, m (complex	81.0	3D	3.45, m (complex)	81.1
4D	3.05, m (complex)	75.8	4D	3.05, m (complex)	76.1
4D-OH	4.35, brs		4D-OH	4.35, brs	
5D	3.21, m (complex)	72.0	5D	3.21, m (complex)	72.0
6D	1.29, (complex)	18.3	6D	1.31, m (complex)	18.3
Sugar E, α-L-rhodinose					
1E	4.91, brs	97.8	1E	4.93, brs	97.8
$2E_a$	1.50, m (complex)	25.3	$2E_a$	1.50, m (complex)	25.3
$2E_e$	2.09, m (complex)		$2E_e$	2.10, m (complex)	
$3E_a$	1.50, m (complex)	24.6	$3E_a$	1.51, m (complex)	24.7
$3E_e$	1.94, m (complex)		$3E_e$	1.90, m (complex)	
4E	3.51, m	76.0	4E	3.51, brs (complex)	75.9
5E	4.05, m (complex)	67.7	5E	4.05, m (complex)	67.8
6E	1.16, (complex)	17.2	6E	1.17, m	17.2
Sugar F, β-D-olivose					
1F	4.44, (dd 9.7, 2.0)	101.5	1F	4.45, dd (9.7, 1.8)	101.5
$2F_a$	1.67, m (complex)	37.4	$2F_a$	1.65, m (complex)	37.2
$2F_e$	2.21, m (complex)		$2F_e$	2.23, m (complex)	
3F	3.44, m (complex	81.0	3F	3.45, m (complex)	81.1
4F	3.05, m (complex)	75.8	4F	3.05, m (complex)	76.1
4F-OH	4.35, brs		4F-OH	4.35, brs	
5F	3.21, m (complex)	72.0	5F	3.21, m (complex)	72.0
6F	1.29, (complex)	18.3	6F	1.31, m (complex)	18.3
Sugar G, α-L-rhodinose					
1G	4.91, (brs)	97.8	1G	4.93, brs	97.8
$2G_a$	1.50, m (complex)	25.3	$2G_a$	1.50, m (complex)	25.3
$2G_e$	2.09, m (complex)		$2G_e$	2.10, m (complex)	
$3G_a$	1.50, m (complex)	24.6	$3G_a$	1.51, m (complex)	24.7
$3G_e$	1.94, m (complex)		$3G_e$	1.90, m (complex)	
4G	3.51, brs	76.0	4G	3.51, brs	75.9
5G	4.05, m (complex)	67.7	5G	4.05, m (complex)	67.8

6G	1.16, m (complex)	17.2	6G	1.17, m	17.2
Sugar H, β-D-olivose					
1H	4.44, dd (9.7, 2.0)	101.5	1H	4.45, dd (9.7, 1.8)	101.5
$2H_a$	1.67, m (complex)	37.4	$2H_a$	1.65, m (complex)	37.2
$2H_e$	2.21, m (complex)		$2H_e$	2.23, m (complex)	
3H	3.44, m (complex	81.0	3H	3.45, m (complex)	81.1
4H	3.05, m (complex)	75.8	4H	3.05, m (complex)	76.1
4H-OH	4.49, brs		4H-OH	4.35, brs	
5H	3.21, m (complex)	72.0	5H	3.21, (complex)	72.0
6H	1.29, (complex)	18.3	6H	1.31, (complex)	18.3
Sugar I, α-L-rhodinose					
1I	4.92, brs	97.4	1I	4.93,	97.5
$2I_a$	1.53, m (complex)	24.3	$2I_a$	1.56, m (complex)	24.4
$2I_e$	1.99, m (complex)		$2I_e$	2.01, m (complex)	
$3I_a$	1.74, m	25.7	$3I_a$	1.73, m	25.9
$3I_e$	2.00, m (complex)		$3I_e$	2.00, m (complex)	
4I	3.60, m	67.3	4I	3.62, m	67.4
5I	4.10, dt (6.7, 6.5)	67.7	5I	4.12, dt (6.8, 6.7)	67.9
6I	1.18, d (6.6)	17.2	6I	1.19, m	17.3

3.3.6 Antimicrobial and Cytotoxic Activity of Landomycin AA and AB

Compounds **1** and **2** were assayed for biological activity against methicillin resistant *Staphylococcus aureus* (ATCC 33591), vancomycin resistant *Enterococcus faecium* (EF379), *Proteus vulgaris* (ATCC 12454), *Staphylococcus warneri* (ATCC 17917), *Pseudomonas aeruginosa* (ATCC 14210), and *Candida albicans* (ATCC 14035) (Figure 3.7). Both landomycin AA and AB exhibited weak bioactivity against MRSA, *S. warneri* and VRE. This observed antimicrobial activity may have been responsible for the activity observed against *S. warneri* and MRSA observed only in the initial 15°C fermentation. No activity was observed against *Proteus vulgaris*, *Pseudomonas aeruginosa* or *Candida albicans*.

Compounds **1** and **2** were also tested for cytotoxicity against keratinocyte, fibroblast, HTB-26 and MCF-7 breast cancer cell lines. Significant activity was seen by both compounds against HTB-26 and MCF-7 breast cancer cell lines down to the lowest concentration tested (1 µg/mL). Due to the potent activity observed (>60% inhibition) at the lowest concentration tested (1 µg/mL), IC_{50} values could not be calculated against MCF-7 and HTB-26 cell lines. Cytotoxic activity was also observed against HEKa and Vero cell lines albeit much lower cytotoxic activity. The bioactivity observed for **1** and **2** is consistent with previously reported antibacterial activity[189] and cytotoxic activity for the landomycins[190]. It was noted that **1** exhibited more potent anticancer activity against both MCF-7 and HTB-26 cell lines than **2** which must be due to the presence of the 11-OH. The lack of an 11-OH appears (**2**) to greatly decrease the cytotoxicity against Vero and HEKa cell lines. Previous testing of the landomycins has shown that the 11-OH group is important for increased bioactivity. Additionally, landomycin activity has been reported to increase with increasing saccharide chain length[190] and increase by having a

non-aromatic B ring with a hydroxylation at position C-6[195]. The landomycin family of compounds has potent anticancer activity against a variety of cancer cell lines, but toxicity in laboratory animals and solubility issues have prevented them from getting into clinical trials[197]. The mode of action of this family of compounds remains unknown.

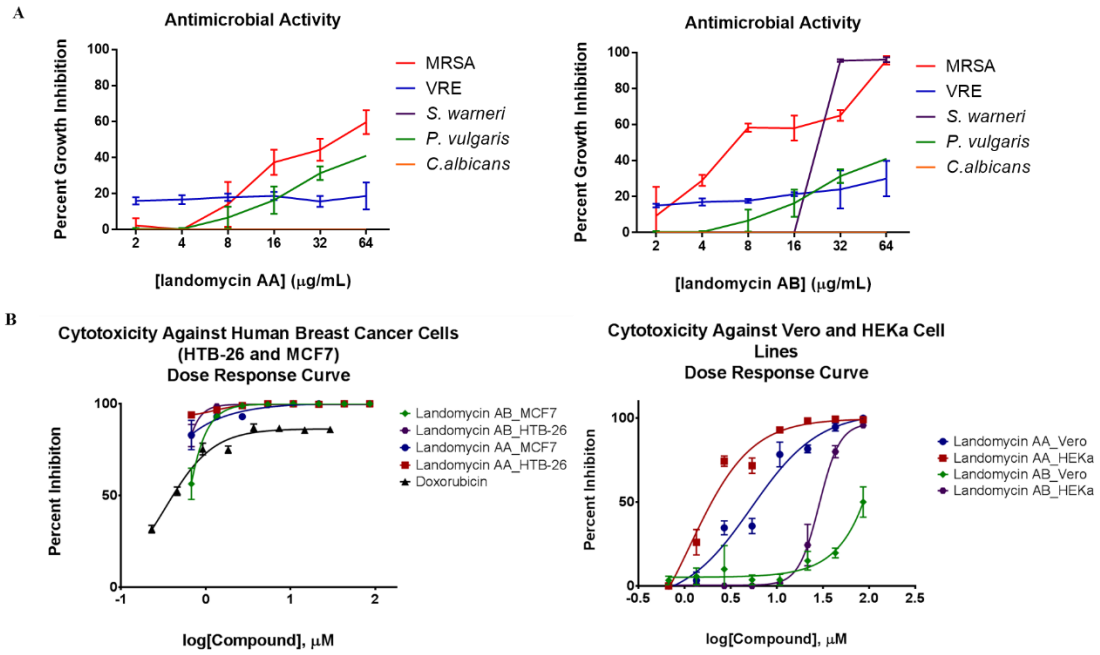

Figure 3.7. A) Antimicrobial activity of landomycin AA and AB. **B)** Cytotoxicity of landomycin AA and AB.

3.4 Conclusions

Arctic actinomycetes are a largely underexplored resource for NPs discovery. A library of actinomycetes isolated from Frobisher Bay was investigated for the production of NPs. Due to the cold environment from which they were isolated, fermentations were initially conducted at both 30°C (standard lab fermentation temperature) and a more ecologically relevant 15°C (maximum summer temperature for Frobisher Bay). Using LC-HRMS metabolomics, differences between the two fermentations temperatures was observed. All isolates exhibited varying degrees of differential metabolite production between the two fermentation temperatures. *Streptomyces* sp. RKAG 337 and *Streptomyces* sp. RKAG 290 were selected for further investigation based on their biological activity and differential production of metabolites between the two fermentation temperatures. Subsequent fermentations at 4°C (cold temperature), 15°C (moderate temperature) and 30°C (high temperature) of these isolates were undertaken to further probe the differential production of metabolites of these isolates. *Streptomyces* sp. RKAG 337 produced members of the actinomycin family only when fermented at 15°C. Analysis of the growth rate and production of actinomycin over a 10 day time course revealed the production of these compounds was a result of fermentation temperature. Further investigation of other actinomycin producing *Streptomyces* from the WAC culture collection revealed the temperature dependent production of actinomycin was unique to the Arctic *Streptomyces* sp. RKAG 337 and suggests Arctic Actinobacteria have developed unique mechanisms to control natural product production via temperature.

Investigation of *Streptomyces* sp. RKAG 290 revealed increased production of two new polyketide NPs, landomycin AA and AB when fermented at 15°C. These

compounds are new to the landomycin family and are unique members as they have the longest reported sugar chain of the family. These two compounds displayed potent anticancer activity against two different breast cancer cell lines.

This study indicates that fermentation temperature can have a large impact on NP production within the actinomycetes and is a useful tool for discovering new NPs. The *de novo* production of actinomycin and upregulated production of landomycin AA and AB as a result of fermentation temperature, demonstrates the ability of fermentation temperature to effect the production of natural products within Arctic Actinobacteria. The mechanism by which the production of secondary metabolites is affected by cold temperature is unknown. During periods of cold, membrane fluidity and enzyme activity decrease and transcription and translation are reduced. In order to circumvent these issues, bacteria have evolved numerous mechanisms for dealing with cold temperatures. The production of cold shock proteins (Csp) in response to a shift in temperature has been observed across a wide range of bacteria. Csps function as nucleic acid chaperones and prevent the formation of secondary structures in mRNA, allowing for transcription and translation to occur at cold temperatures. After an initial cold shock period, the synthesis of Csps decreases and the production of other proteins increases to enable cells to continue to grow at a colder temperature, albeit at a slower rate[198-]. Whether Csps have a role in the regulation of NP production at cold temperatures is unknown and warrants further investigation. The use of transcriptomics at high and low fermentation temperatures may shed light on the mechanisms involved on the regulation of natural products between fermentation temperatures.

CHAPTER 4: CULTURE INDEPENDENT AND DEPENDENT CHARACTERIZATION OF THE FUNGAL DIVERSITY OF SEDIMENT WITHIN FROBISHER BAY

4.1 Introduction

Fungi within the terrestrial environment have been a tremendous resource for the discovery of new and bioactive NPs[199]. In comparison, fungi within the marine environment have been poorly studied and their distribution within this environment remains largely unknown. Within the marine environment, fungi are involved in biogeochemical processes and have been shown to be symbionts or pathogens of marine flora and fauna[32]. To data 1,112 species of fungi have been documented from marine sources[79], although this number needs to be interpreted with caution as many of these isolates are widespread in the terrestrial environment and have not been shown to be able to colonize the marine environment. Many fungi found within the marine environment are of terrestrial origin and are able to persist within the marine environment as dormant propagules or spores. Unlike marine bacteria, marine fungi cannot be classified solely on their ability to grow in seawater, as many osmotolerant terrestrial fungi exist. One leading definition of a true marine fungus (marine *sensu strictu*) is that, "the organism's vegetative state must be shown to colonize and interact with its substratum and that the organism disperse via spores or vegetative propagules back to its substratum to reinitiate its life cycle"[86].

Next generation sequencing of samples from within the marine environment has revealed that diverse assemblages of fungi exist across a wide range of habitats such as the deep sea floor, hydrothermal vents, anoxic environments, pelagic waters and in association with marine macroorganisms including coral, sponges, mangroves and algae[75]. Studies specifically focused on sediment have occurred within the Arabian Sea, South China Sea, Bay of Bengal, Sea of Japan, Indian Ocean, Atlantic Ocean, Pacific Ocean and Arctic Ocean[76]. These studies have revealed divergent marine linages of

yeasts, chytrids, and filamentous fungi within the phyla Ascomycota and Basidiomycota in addition to ubiquitous fungi that are found both within the marine and terrestrial environment.

Biogeographic studies of pelagic and benthic ecosystems have revealed that fungal communities within are shaped by their geographic location and environmental conditions (including temperature, salinity, pressure, pH, etc.)[200]. Within the Arctic Ocean and northern Atlantic Ocean only a handful of NGS studies have looked at fungal diversity and include analysis of sea ice cores, sediment and pelagic seawater from the Beaufort Sea[200-201], benthic sediment samples from the Laptev Sea, coastal sediment samples collected from Kongsfjorden in Svalbard, Norway[202] and analysis of driftwood collected from Svalbard, Norway[203]. These limited studies have revealed the fungal assemblage within to be diverse and host many uncharacterized fungi.

Due to the lack of investigation of Arctic fungi from the marine environment for NP discovery, further investigation of the fungal assemblage of Frobisher Bay was undertaken to determine the fungal diversity within this region. The first aim of this study was to use 454-pyrosquencing to determine the fungal community composition within sediment from intertidal regions of Frobisher Bay. Fungal specific ITS primers were used to generate amplicons from environmental DNA for pyrosequencing analysis in order to obtain deeper sequencing depth compared with standard eukaryotic ITS primers. The second aim of this study was to establish a library of culturable fungi for subsequent NP discovery. The overall fungal diversity of Frobisher Bay is discussed in this chapter from a culture independent and culture dependent standpoint

4.2 Experimental Procedures

4.2.1 Sample Collecting and Processing

Thirteen sediments samples were collected from Frobisher Bay and environmental DNA was isolated as described in Chapter 2.2.2 by Brad Haltli (Kerr Lab, UPEI). Ten of these samples were used for pyrosequencing analysis (AB1, AB2, IH1, IH2, PI1, PI2, QI, TI, WC1 and WC2) and five were used for the culture dependent portion of this study (AB3, PI1, QI, TI2 and TI3). The culture dependent and independent portions of the study were completed in tandem and due to issues with DNA amplification, some of the sites included within the culture dependent portion were unable to be included in the culture independent portion of the study.

4.2.2 ITS Amplicon Pyrosequencing

Culture independent assessment of the fungal diversity of extracted DNA from ten sediment samples was undertaken using a bacterial-tag encoded GS-FLX amplicon pyrosequencing approach (Roche GS-FLX sequencer) performed by Genome Quebec (McGill University, Montreal). Fusion primers were designed for each sample whereby Primer A (forward primer) consisted of a 454 FLX adaptor, a unique identifier barcode and ITS1-F primer[204] and Primer B (reverse primer) consisted of a 454 FLX adaptor and ITS4 primer[205].

Amplicons were generated by polymerase chain reaction (PCR) from template gDNA (25 ng per 50 µl) using the ITS1 and ITS4 fusion primers and AmpliTaq Gold 360 DNA polymerase (Applied Biosystems, Foster City, CA) PCR conditions were as follows; a hot start at 95 °C for 10 min followed by 15 cycles of 94°C for 30 s, 54°C for 40 s and 72°C for 1 min with a final extension of 10 min at 72°C. After purification

using a QIAquick PCR purification kit, amplicons were pooled (three replicate PCR reactions) and DNA concentration was determined using a Quant-iT PicoGreen dsDNA Assay kit (Turner Biosystems, Sunnyvale, CA) according to manufacturer's instructions. Amplicons were sent to Genome Quebec for FLX-pyrosequencing.

Processing of the .sfff files was completed using Mothur v. 1.35.1[119]. Sequences were denoised using Mothur's implementation of PyroNoise[120] (shhh.flows) and filtered for quality. Sequences were removed if they contained homopolymers greater than 8 bp in length, had more than one mismatch to the forward primer sequence or barcode or were shorter than 200 bp. Within QIIME v. 1[206] singletons were identified and removed, OTUs were clustered with a 97% similarity cut-off using UPARSE[207] and chimeric sequences were identified and removed using UCHIME[122] (using the UNITE database as a reference)[208]. Taxonomy was assigned using BLASTn searches in GenBank and OTUs with less than 80% similarity to an identified fungal sequence were excluded. Alpha and beta diversity calculations were performed within Mothur v. 1.35.1 on subsampled datasets.

4.2.3 Fungal Isolation

A portion of the each collected sediment sample (~10 g) was resuspended in sterile filtered seawater (ddH_2O + 18 g/L Instant Ocean™) and separated based on particle size (≥ 104 µm, ≥ 51 µm and < 51 µm) using an adapted particle filtration apparatus. Serial dilutions (1 to 10^{-2}) of three particle sizes (≥ 104 µm, <104 µm to >51 µm and <51 µm) were prepared with sterile ddH_2O + IO (18 g/L). Aliquots (10 µL) of each dilution were plated into each well of a 48 well plate containing one of five different isolation media; yeast malt agar (YM), yeast malt agar with high salt (YMS),

yeast malt agar with cottonseed oil (YMO), colloidal chitin agar (CH)[128] and potato dextrose agar (PDA). Each was supplemented with 50% IO (18 g/L) or in the case of YMS, 100% IO (36 g/L) and chloramphenicol (100 µg/ml) to inhibit the growth of bacteria. Plates were incubated at 22°C and 4°C for 6 months and fungi were subcultured onto YM agar plates until pure. Pure cultures were grown in YM broth for five days and preserved at -80C in 10% (v/v glycerol). Fungi were taxonomically dereplicated based on their micro and macromorphology.

4.2.4 Dereplication of Yeasts using MALDI-TOF

Due to their similarities in morphology, yeast isolates were dereplicated prior to ITS or 28S rRNA sequencing based on their protein fingerprints using Matrix-Assisted Laser Desorption/Ionization-Time of Flight Mass Spectrometry (MALDI-TOF-MS) (Microflex LT, Bruker, Daltonics Mass Spectrometer, Leipzig, Germany). Yeast cells were grown on YM agar for 72 h at 22°C, scraped from the plate and resuspended in 900 µL EtOH. The cells were centrifuged at 10,000 *g* and resuspended in 70% formic acid (10 µL) and 100% CH_3CN (10 µl). After a 10 min incubation period, 1 µL of the yeast supernatant was pipetted onto a target plate and overlaid with 1.5 µl matrix (1 mL saturated solution of α-cyano-4-hydroxy-cinnamic acid in 50% CH_3CN and 2.5% aqueous trifluoroacetic acid) and allowed to dry. Each yeast protein profile was obtained using a MALDI-TOF-MS equipped with a 50.0 Hz nitrogen laser (laser power 50%; up to 400 shots fired, mass range 2,000-12,000 *m/z*). Peak profiles were generated using FlexControl software (Bruker Daltonics). Principal component analysis was used to compare yeast protein spectra based on peak presence and intensity in each spectra. Cluster analysis of the spectra using UPGMA was performed using BioTyper v 2.0

software (Bruker Daltonics). *Saccharomyces cerevisiae* (Lalvin, EC-1118) was used as a control strain in triplicate to determine the cut-off between species. Isolates were deemed different species if they clustered at a difference greater than the control.

4.2.5 Genomic DNA Extraction and PCR Amplification of Fungal Genes

Extraction of genomic DNA of cultured isolates was carried out using a Fungi/Yeast Genomic DNA isolation kit (Norgen Biotek) according to the manufacturer's instructions. PCR amplification of the ITS region was conducted using ITS1 and ITS4 primers[205]. PCR cycling conditions included an initial denaturing period of 3 min at 95°C, followed by 30 cycles of 95°C for 1 min, 54.6°C for 1.5 min and 72°C for 2 min with a final extension of 5 min at 72°C. The presence of the correct PCR amplicon was verified using gel electrophoresis (110 V, 40 min, Biorad, Mississauga, On) using 1.0% agarose gel containing 0.001% ethidium bromide. PCR products were visualized using a UV transilluminator (Biospectrum, OptiChemi HR Camera, Upland, CA). Sequencing was performed by Eurofins MWG Operon (Huntsville, AL) using the ITS4 primer. Additional amplification and sequencing of the 28S rRNA gene (using LR0R, LR3R, LR5 and LR7 primers)[209], 18S rRNA gene (using NS1, NS3, NS5 and NS8 primers)[205], and TEF-1α gene (using 983F and 2218R primers)[210] for putatively new isolates was also undertaken.

Sequences were trimmed and assembled using Contig Express (Vector NTI Advance 10.3.0, Invitrogen, Carlsbad, CA). Similar sequences were grouped into OTUS (97% sequence similarity) and compared to known sequences within the GenBank database using BLASTn[131]. Sequence alignment was completed using Clustal W in MEGA v. 6.06[124]. Phylogenetic trees were inferred using the maximum-likelihood

method in MEGA v. 6.06 and the GTR+G model of DNA substitution (as determined by Modeltest). Bootstrap analysis was performed with 1000 replicates and values less than 60% were collapsed.

4.2.6 Comparison of Cultured Fungi to Culture Independent Analysis

To compare the cultured fungal isolates to the culture independent library, a local BLAST nucleotide database containing all unique culture independent sequences was created in BioEdit version 7.2.5[135]. The cultured fungal ITS sequences were searched against this local database using an Expectation (*E*) value of $1.0E^{-100}$ and the Matrix BLOSUM64. Cultured sequences with high sequence similarity (≥99%) to members of the culture independent library were recorded.

4.3 Results and Discussion

4.3.1 Culture Independent Analysis

4.3.1.1 Fungal Alpha Diversity

Ten sediment samples were collected from various sites within Frobisher Bay including two each from Iqaluit harbour (IH1 and IH2), Apex Bay (AB1 and AB2), White Ledge Channel (WC1 and WC2) and Pugh Island Channel (PI1 and PI2) and a single sample from Tarr Inlet (TI) and Qaummaarviit Island (QI) (Figure 2.1). Pyrosequencing of ITS1-5.8S-ITS2 amplicons from environmental DNA from each of these sites resulted in 52,593 high quality sequence reads. Each sample contained 950 (TI) to 9,987 (AB1) sequence reads. Fungal diversity calculations were performed at the species level (OTU, *D*=0.03) on a data set subsampled to 900 (Table 4.1). Observed fungal richness ranged from 21 OTUs (AB2) to 115 OTUs (QI). The Chao1 estimator was used to calculate the estimated richness at the species level and ranged from 33

OTUs (AB2) to 158 OTUs (PI2). Good's coverage estimator was used to calculate coverage for each sample and ranged from 96.0% (IH2)-99.0% (WC2), indicating the sequencing depth was sufficient to detect most species present within the sample set. Rarefaction analysis showed most of the curves began to reach the plateau of their asymptote, although further sequencing would be required to adequately describe the species level diversity at some sites (Figure 4.1). At the species level, the number of OTUs predicted at some sample sites was much higher than the observed number of OTUs and additional richness at the species level would be observed with further sampling.

The Shannon diversity (H') index ranged from 1.27 (AB2) to 3.66 (QI) and Shannon equitability (E) index from 0.42 (AB2) to 0.79 (QI). The higher index values calculated for some sediment samples indicated a higher level of fungal diversity within these sites, whereas the low Shannon diversity index values for sites AB1, AB2 and WC1 indicated much lower diversity within these sites. The low Shannon evenness values for some sites was explained by the dominance of one or two phylotypes e.g. AB1 (E = 0.45) was dominated by reads corresponding to OTU 1 (64.9% of subsampled reads), AB2 (E = 0.42) was dominated by reads corresponding to OTU 2 (60.0% of subsampled reads) and OTU 16 (20.6%) and site WC1 (E = 0.49) was dominated by reads corresponding to OTU 1 (48.9%) and OTU 2 (23.9%). The Shannon diversity indices were similar to studies of sediment collected from Kongsfjorden, Svalbard[202], seawater collected from the Atlantic, Pacific and Indian Oceans[211], were higher than reported values from the deep sea floor[212] and lower than values reported for intertidal sediments from North Carolina[213] and sediment collected from subtropical Chinese

Seas[214]. Often, sediment samples collected from near shore environments exhibit greater microbial diversity than offshore sediments due to the influx of freshwater, nutrients and other microorganisms from the terrestrial environment. Due to differences in sampling, methodology and analysis accurate comparisons of diversity indices between studies cannot be made with confidence.

Table 4.1. Fungal richness and alpha diversity analysis of Frobisher Bay on a subsampled dataset (950 reads). OTUs were calculated at a distance of 0.03.

Sample	Sample Size	Richness (S_{obs})	Chao1 estimated richness (S_{est})	Good's Coverage *C* (%)	Shannon diversity index (*H'*)	Shannon equitability index (*E*)
AB1	9,987	56	79	98.21	1.81	0.45
AB2	1,769	21	33	98.95	1.27	0.42
IH1	5,755	69	100	97.16	2.77	0.67
IH2	8,612	87	131	96.00	3.19	0.72
PI1	3,511	85	101	97.47	3.36	0.78
PI2	4,824	96	158	95.79	3.12	0.68
QI	5,241	115	132	96.63	3.66	0.79
TI	950	33	39	98.94	2.16	0.62
WC1	9,588	37	104	97.89	1.81	0.49
WC2	2,356	44	49	98.95	2.22	0.59

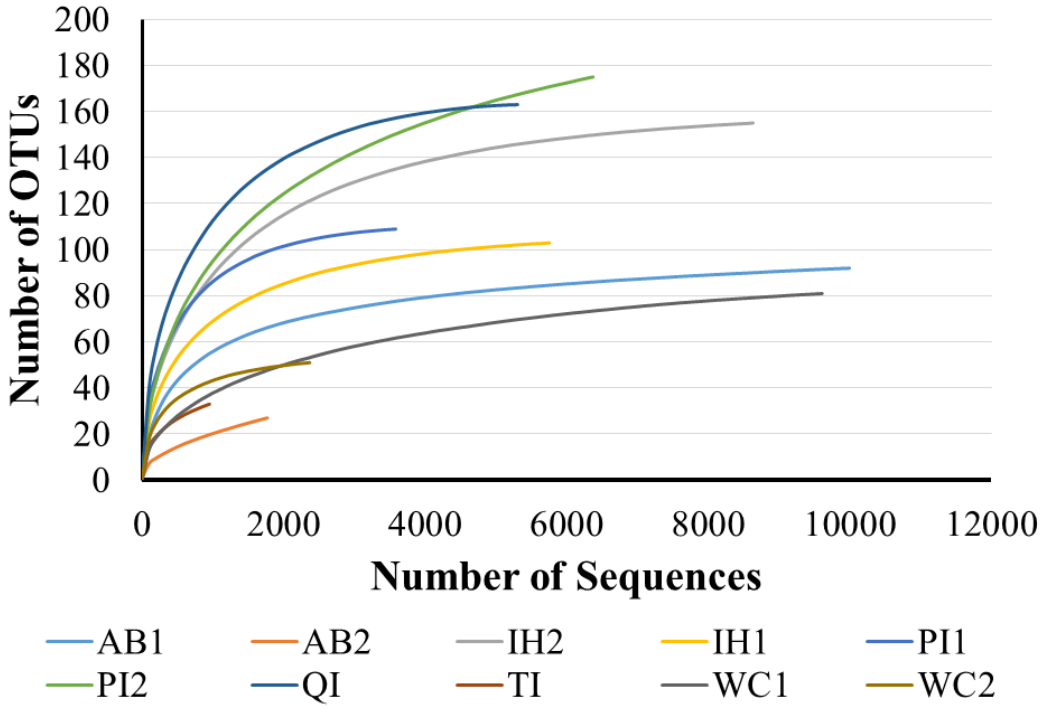

Figure 4.1. Rarefaction curve of sediment samples from Frobisher Bay (*D*=0.03)

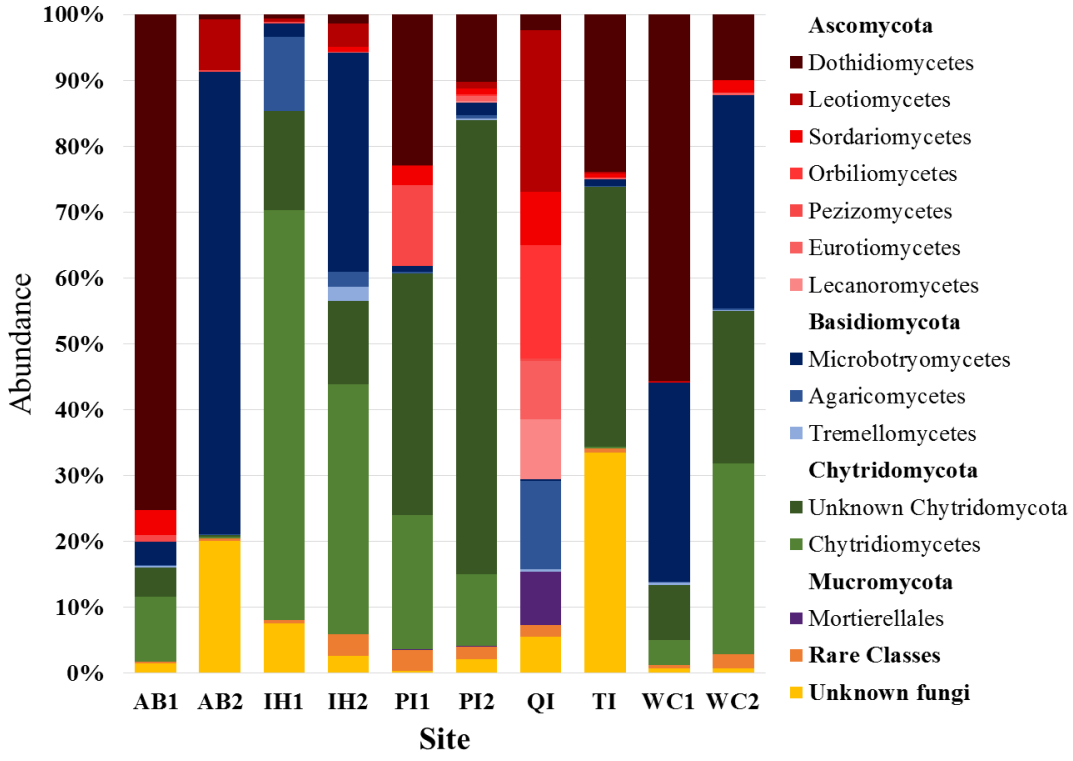

Figure 4.2. Phylum and class level fungal diversity of Frobisher Bay.

4.3.1.2 Fungal Community Composition

BLASTn was used to classify the 52,593 sequence reads with a confidence threshold of 80%. Six phyla were detected across all samples in addition to unknown fungi that could not be classified to a known phylum. Ascomycota made up 8.5% (IH2) to 80.3% (AB1) of reads per site, Basidiomycota made up 1.2% (TI) to 70.3% (AB2) of reads per site and Chytridiomycota made up 0.02% (QI) to 77.1% (IH1) of reads per site (Figure 4.2). Fungi that could not be classified to a phylum made up 0.4% (PI1) to 20.1% (AB2) of the reads per site. Sites AB1, QI, and WC1 were dominated by Ascomycota whereas sites IH2, IH2, PI1, PI2, TI and WC2 were dominated by Chytridiomycota. Only site AB2 was dominated by Basidiomycota.

At a finer taxonomic level, 20 recognized classes and 49 recognized orders were detected across sediment samples in addition to unclassified fungi belonging to Ascomycota, Basidiomycota, Chytridiomycota and unknown fungal phyla. Within the phylum Ascomycota, members within the classes Dothidiomycetes (28.5% of total reads) and Sordariomycetes (2.1%) were present at every site. Within the Basidiomycota, Microbotryomycetes (16.0%), Kriegeriales (15.2%) and Agaricomyctes (3.1%) were detected at every site. Within the Chytridiomycota reads detected at every site were composed of Chytridiomycetes (19.3%) and unknown Chytridiomycota (19.2%).

Ascomycetes made up 39.6% of the total sequence reads obtained. Of these reads, 70.6% corresponded to OTUs within the order Pleosporales. Within Pleosporales, 85.1% of reads corresponded to the genus *Didymella* and 13.8% corresponded to unknown OTUs within Pleosporales. Members within the filamentous fungal genus *Didymella* are commonly isolated in the terrestrial environment and have been mainly

reported as agricultural plant pathogens[215]. Several species within this genus have been described or isolated from the marine environment in association with mangroves[216], sponges[217], seaweed and algae[218]. Within the marine environment *Didymella fucicola*, *D. gloiopeltidis* and *D. magnei* are parasites of algae and cause Black Dots Disease within their algal hosts[219]. The OTUs detected in this study were 98-99% similar to known *Didymella* species and formed their own distinct clade within the genus (Figure 4.3). Due to a lack of sequence data for marine *Didymella* isolates, comparison of sequence similarity to marine strains could not be determined. Within Frobisher Bay, members within these OTUs may serve a role as pathogens of algae and seaweed.

The remaining reads within Ascomycota were either unclassifiable (19.9%) or corresponded to the genera *Cadophora* (4.1%), *Trichoderma* (2.3%), *Tolypocladium* (0.9%) or rare genera having less than 100 sequence reads each (*Penicillium*, *Fusarium*, *Venturia*, *Lachnum*, *Metschnikowia*, *Tetracladium*, *Pseuderotium* and *Erysiphe*). All of the identified genera detected within this study have been previously isolated or detected from both the terrestrial and marine environment except *Venturia* and *Erysiphe*[220,79]. Both *Venturia* and *Erysiphe* are plant pathogenic fungal genera and this is the first detection of these in the marine environment. Due to the low number of detected sequence reads, these isolates may represent dormant members within these sediment samples and be the result of wash off of plant detritus from the terrestrial environment.

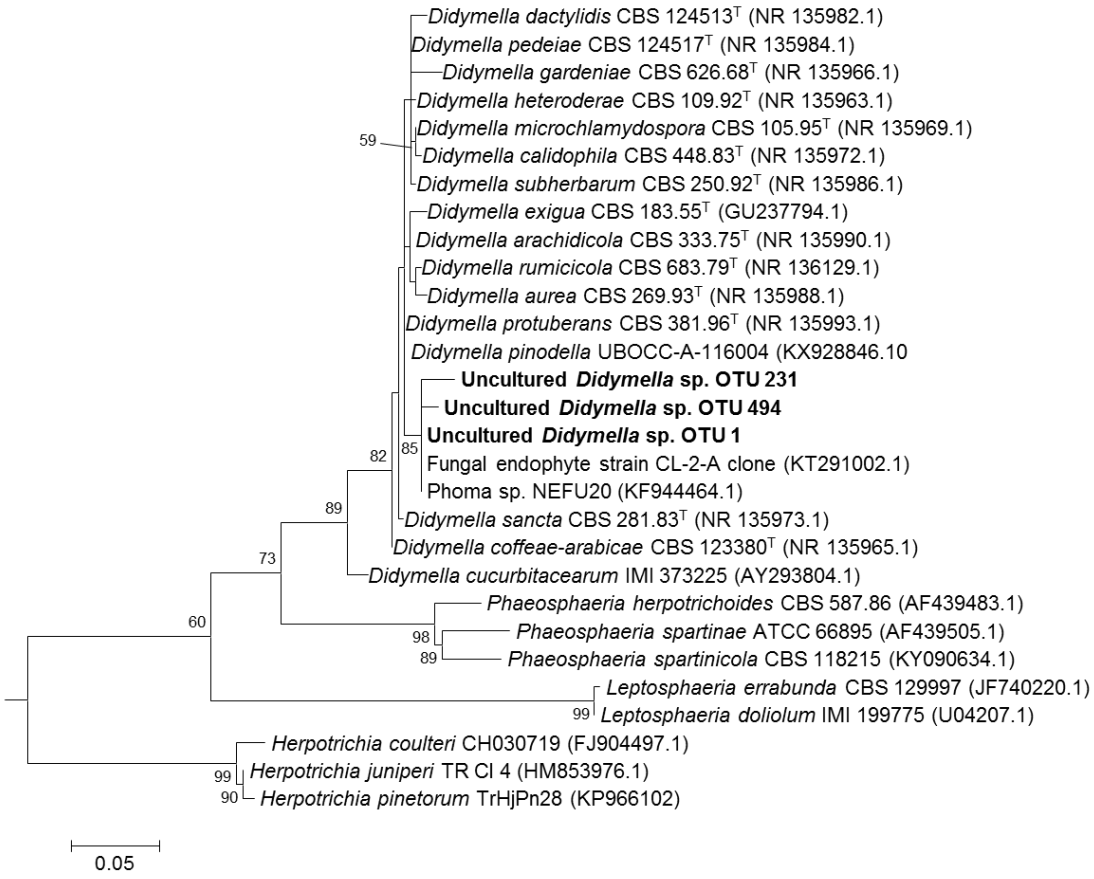

Figure 4.3. Maximum likelihood analysis of ITS region of uncultured fungal OTUs within the genus *Didymella* detected by 454-pyrosequencing. Alignment was based on a total of 264 nucleotide positions. Phylogram was constructed using the GTR+G model of DNA substitution using 1000 bootstrap iterations. Node support below 50% is collapsed.

Basidiomycete and ascomycete yeasts made up 20% of the total sequence reads (19.5% and 0.5% respectively). Within Basidiomycota, 80.7% of total Basidiomycota reads correspond to yeasts belonging to the genera *Glaciozyma* (95.4% of all Basidiomycete yeast reads), *Mrakia* (2.1%), *Cryptococcus* (0.7%) and rare genera having less than 30 reads each (*Leucosporidiella*, *Trichosporon*, *Rhodotorula*, *Dioszegia* and *Guehomyces*). Within Ascomycota, 1.3% of all sequence reads corresponded to yeasts including *Exophiala* (47.4% of total Ascomycota yeast reads), *Metschnikowia* (45.7%), *Candida* (4.9%) and *Kluyveromyces* (3.8%) (Figure 4.4).

Yeasts are frequently reported from many marine habitats and have been shown to be dominant in some deep sea environments through culture independent methods[221,222]. The ability of many genera of yeasts to grow under elevated hydrostatic pressure, low water activity and cold temperatures helps to explain their success in the marine environment[223]. Many genera of yeast are ubiquitous and exist within the marine and terrestrial environment, however several marine *sensu strictu* species have been described within the genera *Candida*, *Rhodosporidium*, *Torulopsis* and *Metschnikowia*[219]. All of the genera detected within this study have previously been detected in the marine environment[79] and several genera detected are known pathogens of marine animals and fish (e.g. *Exophiala*, *Trichosporon*, *Rhodotorula*, *Cryptococcus* and *Candida*)[224,225].

The majority of yeast sequences obtained corresponded to the genus *Glaciozyma*. *Glaciozyma* is a genus of psychrophilic yeasts that have been isolated exclusively from cold environments including Antarctica (soil, subglacial water), the Southern Ocean (seawater), the Arctic Ocean (sediment) and glaciers within the Italian

alps[226,227]. The mechanisms by which *Glaciozyma antarctica* copes with cold temperatures has been investigated. Transcriptomic analysis during cold shock of *G. antarctica* has revealed many over expressed genes encoding antifreeze proteins which help to avoid ice crystallization within the cell at cold temperatures, genes encoding for desaturases to maintain membrane fluidity and genes encoding molecular chaperones to allow for proper protein folding at cold temperatures[228,229,230]. These specialized adaptations may be the reason why *Glaciozyma* was so prevalent within this environment.

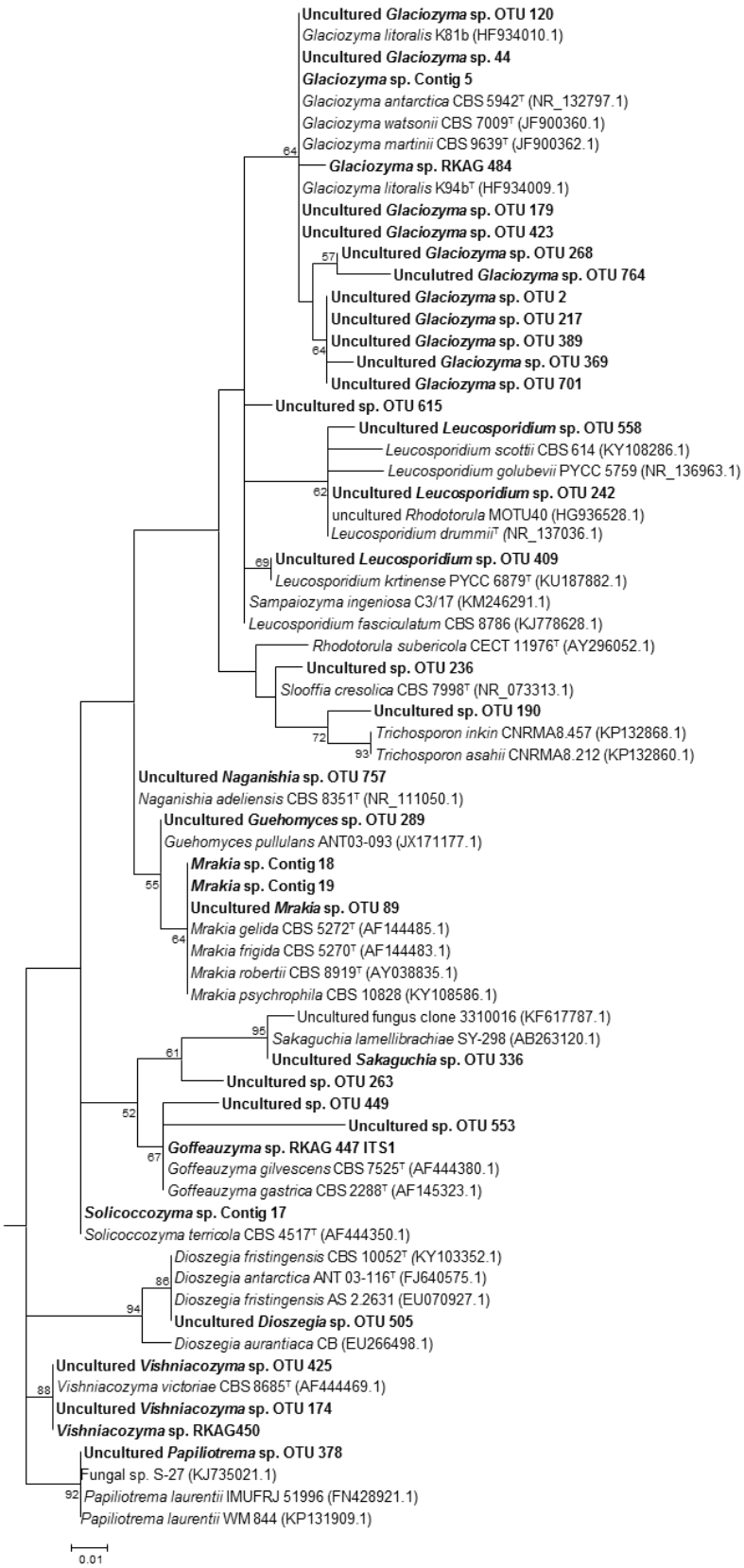
Uncultured Glaciozyma sp. OTU 120
Glaciozyma litoralis K81b (HF934010.1)
Uncultured Glaciozyma sp. 44
Glaciozyma sp. Contig 5
Glaciozyma antarctica CBS 5942T (NR_132797.1)
Glaciozyma watsonii CBS 7009T (JF900360.1)
Glaciozyma martinii CBS 9639T (JF900362.1)
64
Glaciozyma sp. RKAG 484
Glaciozyma litoralis K94bT (HF934009.1)
Uncultured Glaciozyma sp. OTU 179
Uncultured Glaciozyma sp. OTU 423
57
Uncultured Glaciozyma sp. OTU 268
Uncultutred Glaciozyma sp. OTU 764
Uncultured Glaciozyma sp. OTU 2
Uncultured Glaciozyma sp. OTU 217
Uncultured Glaciozyma sp. OTU 389
64
Uncultured Glaciozyma sp. OTU 369
Uncultured Glaciozyma sp. OTU 701
Uncultured sp. OTU 615
Uncultured Leucosporidium sp. OTU 558
Leucosporidium scottii CBS 614 (KY108286.1)
Leucosporidium golubevii PYCC 5759 (NR_136963.1)
62
Uncultured Leucosporidium sp. OTU 242
uncultured Rhodotorula MOTU40 (HG936528.1)
Leucosporidium drummiiT (NR_137036.1)
69
Uncultured Leucosporidium sp. OTU 409
Leucosporidium krtinense PYCC 6879T (KU187882.1)
Sampaiozyma ingeniosa C3/17 (KM246291.1)
Leucosporidium fasciculatum CBS 8786 (KJ778628.1)
Rhodotorula subericola CECT 11976T (AY296052.1)
Uncultured sp. OTU 236
Slooffia cresolica CBS 7998T (NR_073313.1)
Uncultured sp. OTU 190
72
Trichosporon inkin CNRMA8.457 (KP132868.1)
93
Trichosporon asahii CNRMA8.212 (KP132860.1)
Uncultured Naganishia sp. OTU 757
Naganishia adeliensis CBS 8351T (NR_111050.1)
Uncultured Guehomyces sp. OTU 289
Guehomyces pullulans ANT03-093 (JX171177.1)
Mrakia sp. Contig 18
56
Mrakia sp. Contig 19
Uncultured Mrakia sp. OTU 89
64
Mrakia gelida CBS 5272T (AF144485.1)
Mrakia frigida CBS 5270T (AF144483.1)
Mrakia robertii CBS 8919T (AY038835.1)
Mrakia psychrophila CBS 10828 (KY108586.1)
Uncultured fungus clone 3310016 (KF617787.1)
95
Sakaguchia lamellibrachiae SY-298 (AB263120.1)
61
Uncultured Sakaguchia sp. OTU 336
Uncultured sp. OTU 263
Uncultured sp. OTU 449
52
Uncultured sp. OTU 553
Goffeauzyma sp. RKAG 447 ITS1
67
Goffeauzyma gilvescens CBS 7525T (AF444380.1)
Goffeauzyma gastrica CBS 2288T (AF145323.1)
Solicoccozyma sp. Contig 17
Solicoccozyma terricola CBS 4517T (AF444350.1)
Dioszegia fristingensis CBS 10052T (KY103352.1)
86
Dioszegia antarctica ANT 03-116T (FJ640575.1)
Dioszegia fristingensis AS 2.2631 (EU070927.1)
94
Uncultured Dioszegia sp. OTU 505
Dioszegia aurantiaca CB (EU266498.1)
Uncultured Vishniacozyma sp. OTU 425
88
Vishniacozyma victoriae CBS 8685T (AF444469.1)
Uncultured Vishniacozyma sp. OTU 174
Vishniacozyma sp. RKAG450
Uncultured Papiliotrema sp. OTU 378
Fungal sp. S-27 (KJ735021.1)
92
Papiliotrema laurentii IMUFRJ 51996 (FN428921.1)
Papiliotrema laurentii WM 844 (KP131909.1)
0.01

Figure 4.4. Maximum likelihood analysis of ITS region of uncultured yeasts detected by 454-pyrosequencing and cultured yeasts within the Basidiomycota. Alignment was based on a total of 283 nucleotide positions. Phylogram was constructed using 1000 bootstrap iterations. Node support below 50% is collapsed.

Members within the phylum Chytridiomycota (chytrids) made up a large portion of sequence reads (38.5%) and were the dominant phylum at many sites. Chytrids are ubiquitous and occur in the marine[231], aquatic[232] and terrestrial[233] environment. Within the aquatic environment chytrids are parasites of algae[234], zooplankton[235] and larger animals such as amphibians[236]. Within the aquatic environment, chytrids have a free living zoosporic stage where they actively seek out new hosts to parasitize. Once infected, chytrids extract nutrients, mature, and release zoospores into the environment. Zooplankton in turn ingest these zoospores creating what is termed the mycoloop, an important driver of community structure within the aquatic environment[232]. In the Arctic marine environment, chytrids have been shown to parasitize diatoms and increase in concentration during spring algal blooms[237], but due to the limited characterization of chytrids from the marine environment[238,239], their ecological role within the marine environment remains largely unknown.

NGS studies have revealed chytrids are quite rare within deep seawater and deep sea sediment[240,241] and are largely associated with surface waters, near shore sediments and sea ice[231,242], locations where phytoplankton inhabit. The presence of a large number of sequences corresponding to chytrids within this study is logical as these samples were collected in August at a time when sea ice is melting and there is an influx of nutrients into the environment allowing for algal blooms. The chytrid phylotypes detected within this study have very low sequence similarity to known chytrids (<92% to *Clydea vesicula*) and may represent new chytrid lineages (Figure 4.5). Previous NGS sequencing of the 18S rRNA gene from Arctic seawater and ice from different locations throughout the Arctic revealed several new chytrid lineages[231], but due to differences in

the genes sequenced (ITS vs 18S rRNA), it is unknown whether these sequences correspond to those previously discovered taxonomic lineages.

4.3.1.3 Fungal Beta Diversity

A Bray-Curtis dissimilarity analysis was performed between sites revealing a lack of similarity (Figure 4.6). Values for dissimilarity ranged from 0.47-0.98, where 1 means complete dissimilarity and 0 means complete similarity. This dissimilarity can be explained by the large number of OTUs detected at only one or two sites within Frobisher Bay. Of the 559 OTUs detected, 340 were only detected at one site and 135 were detected only at two sites. No OTUs were shared across all ten sites. In terms of similarity, only 27 OTUs were shared by at least five sites (Table 4.2). Those OTUs that were shared consisted mainly of filamentous ascomycetes including members within the genera *Didymella*, *Trichoderma*, *Tolypocladium* and *Thelebolus*, unknown members within the Chytridiomycota and unicellular yeasts within the genera *Glaciozyma*, *Mrakia*, and *Metschnikowia*.

The fungal community structure within Frobisher Bay is largely varied between sites which could be a result of the level of freshwater influx, availability of organic detritus and the effect of wash in from the terrestrial environment at each site. Since DNA based sequencing analysis cannot discriminate between active and dormant members within the environment, it cannot be determined whether the large amounts of OTUs found only at one site are indeed active members within this environment or dormant spores or propagules originating from the terrestrial environment. Transcriptomics would help to shed light on the active members within these communities.

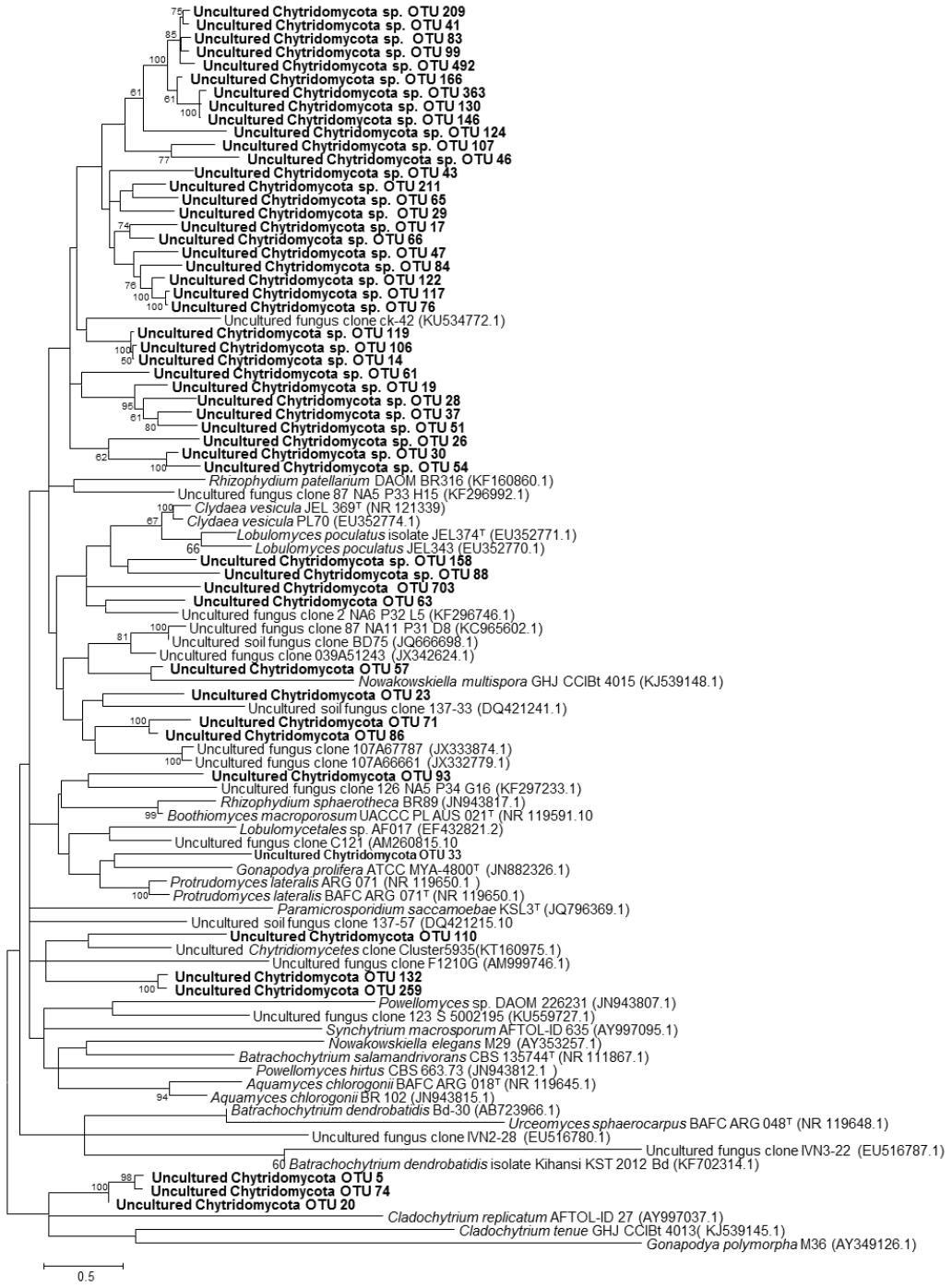

Figure 4.5. Maximum likelihood analysis of the ITS region of uncultured fungal OTUs within the Chytridiomycota detected by 454-pyrosequencing. Alignment was based on a total of 211 nucleotide positions. Phylogram was constructed using 1000 bootstrap iterations. Node support below 50% is collapsed.

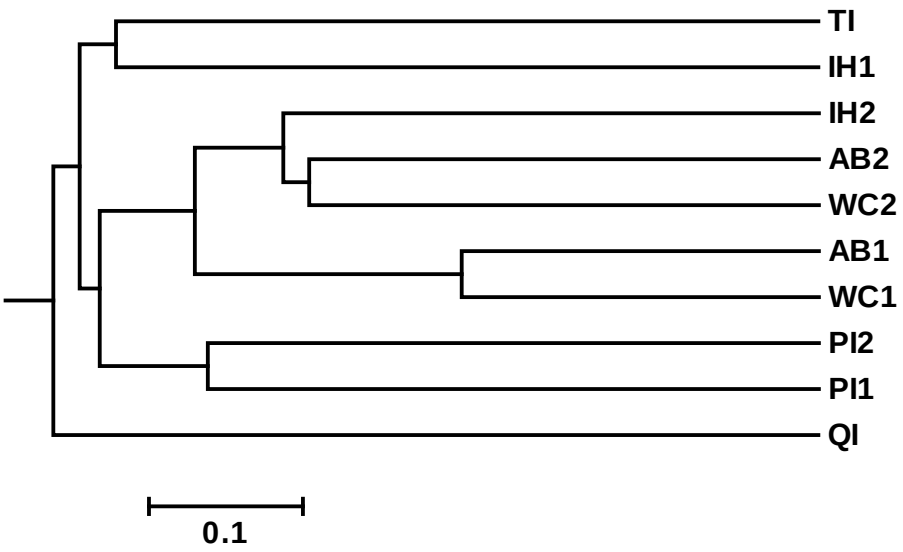

Figure 4.6. Bray-Curtis analysis dissimilarity analysis of sediment samples from Frobisher Bay (D = 0.03). Data was subsampled to 950 reads.

Table 4.2. Shared fungal OTUs across sites detected by 454-pyrosequencing.

Total Read %	# of Shared Sites	% coverage	% identity	Closest accessioned strain
23.5	9	100	99	*Didymella pinodes* K52 (KY703842.1)
12.7	9	90	99	*Glaciozyma litoralis* K94b (HF934009.1)
0.8	9	90	97	*Glaciozyma litoralis* K94b (HF934009.1)
0.5	9	100	98	*Trichoderma crassum* DAOM 164916 (NR_134370.1)
1.5	8	90	97	*Glaciozyma litoralis* K94b (HF934009.1)
0.4	8	100	96	*Didymella pinodes* K52 (KY703842.1)
1.3	7	99	80	*Rhizophydiales* sp. ARG009 (EF585636.1)
0.4	7	100	99	*Trichoderma minutisporum* DAOM 167059 (AY865634.1)
2.2	6	100	98	Uncultured fungus clone ck-133 (KU534847.1)[a]
1.0	6	41	88	*Aquamyces chlorogonii* (NR_119645.1)
0.7	6	40	91	*Rhizophlyctis rosea* KP034 (EU379232.1)
0.6	6	81	97	*Cyathicula microspora* M267 (EU940165.1)
0.6	6	56	87	*Clydaea vesicula* JEL 369 (NR_121339.1)
0.4	6	80	85	*Teratosphaeria ohnowa* CBS 120745 (EF394845.1)
0.3	6	99	99	*Mrakia frigida* CBS 5688 (KY104289.1)
0.3	6	100	100	*Tolypocladium inflatum* NBRC 31669 (AB255606.1)
0.3	6	57	89	*Chytriomyces poculatus* JEL343 (EU352770.1)
0.1	6	91	95	*Glaciozyma litoralis* K94b (HF934009.1)
0.8	6	90	96	*Glaciozyma litoralis* K94b (HF934009.1)
1.8	5	99	80	*Rhizophydiales* sp. ARG009 (EF585636.1)
1.5	5	97	81	Uncultured fungus clone S211T 17 (KU164022.1) [a]
1.2	5	46	99	*Triparticalcar equi* WJD101 (KX019806.1)
0.2	5	100	91	*Metschnikowia vanudenii* CBS 9134 (KY104212.1)
0.1	5	41	91	*Borealophlyctis paxensis* DAOM BR 368 (NR_111314.1)
0.1	5	57	87	*Clydaea vesicula* JEL 369 (NR_121339.1)
0.6	5	89	100	*Thelebolus globosus* CBS 113940 (NR_138367.1)
0.1	5	92	87	*Tettrasphaeria associata* CNS 114165 (EU707858.1)

[a]no similar cultured representatives

4.3.2 Fungal Isolation

To develop a fungal library for subsequent NP discovery, five sediment samples were selected for fungal isolation (AB3, PI1, QI, TI2, and TI3). A portion of each sediment sample was resuspended in ddH_2O and passed through a series of molecular sieves to separate the sediment based on particle size (>104 µM, 54-104 µm, <54 µm). The separation by particle size increases the rate of isolation of fungi originating from vegetative propagules embedded within a matrix as opposed to dormant spores and has proven useful in the isolation of marine fungi[243,86]. Serial dilutions of each sediment size were plated onto 48 well plates containing either YM-IO, YM-IO (high salt), YM-IO with cottonseed oil, PDA-IO and CC-IO supplemented with 200 µg/L chloramphenicol to prevent bacterial growth. Plates were incubated for up to 4 months at 22˚C and 4˚C. Unicellular and filamentous fungi were subcultured onto YM-IO from the 48 well plates resulting in the isolation of 259 filamentous fungi and 95 unicellular yeasts. Due to the similar morphologies observed between yeast isolates, MALDI-TOF MS was used to generate protein fingerprints and group the yeasts according to their protein fingerprint similarity.

Genomic DNA was obtained from each of the filamentous fungi and representatives of the dereplicated yeasts, and the ITS sequence was obtained for each isolate. Isolates were grouped at a conservative 97% sequence similarity cutoff, to delineate species. The consensus ITS1-5.8S-ITS2 OTU sequence was used to identify isolates by comparison to sequences within GenBank using a BLASTn search. Fifty-four unique species were identified consisting of 37 OTUs and 17 singleton sequences

(Table 4.3, Figure 4.7). At a 99% cutoff, 77 strains were identified consisting of 43 OTUS and 34 singleton sequences (data not shown).

The 54 unique species obtained represented 33 genera falling into 17 orders. The largest number of unique isolates fell into the orders Eurotiales (11 species) and Hypocreales (16 species). Of the 354 isolates obtained, almost a third (109 isolates) were isolated at 4˚C. Sixteen species were only isolated at 4˚C and included *Penicillium canescens*, *Penicillium thymicola*, *Mucor hiemalis*, *Mucor zonatus*, *Graphium jumulu*, *Tolypocladium cylindrosporum* (contig 25), *Acremonium alternatum*, *Neocosmospora rubicola* (contig 29), an unknown *Sesquicillium* sp. (RKAG 627), an unknown *Nectriaceae* sp. (RKAG 628), an unknown *Herpotrichiellaceae* sp. (RKAG 672), an unknown *Leotiomycetes* sp. (contig 36) and the previously reported psychrophilic yeasts *Mrakia gelida*, *Mrakia nivalis*, *Glaciozyma litoralis*, *Cryptococcus gilvescens* and *Cryptococcus victoriae*. Eighteen species were isolated at both 4˚C and 22˚C and 20 isolates were obtained at 22˚C. In total 63% of species cultured had a representative isolated at 4˚C.

Thirteen distinct isolates (representing nine species) were obtained with <97% sequence similarity to a recognized accessioned fungal strain within GenBank. Additional taxonomic markers were sequenced including the 28S rRNA gene, the 18S rRNA gene and the TEF1-α gene to aid in further identification. Traditional fungal characterization has been based solely on morphological features and many described fungal species have no sequence information associated with them. This makes the assessment of novelty of a fungus by sequence similarity alone challenging. Therefore

each of the 13 distinct isolates were grown on various media and monitored for sporulation to aid in their identification. Due to a lack of sporulation, isolates RKAG 628 (unknown *Nectriaceae*), 670 (unknown Leotiomycetes), 672 (unknown *Herpotrichiellaceae*), 170 (unknown *Venturia* sp.) and 573 (unknown *Rosellinia* sp.) could not be further characterized. Several isolates sporulated and appeared to be new species based on their phylogenetic novelty and micromorphology. Further characterization of these isolates is described in subsequent chapters (Chapter 5 description of *Mortierella* sp. RKAG 110, Chapter 6 descriptions of *Sesquicillium* sp. RKAG 571 and 627 and Chapter 8 descriptions of *Tolypocladium* sp. RKAG 373, 560, 574, 673 and 677).

4.3.3 Comparison of Cultured Fungi to Culture Independent Library

The ITS sequence of cultured fungal isolates was compared to the culture independent sequences by doing a local BLAST search within BioEdit v. 7.2.5. Thirty-five of the 54 cultured isolates were detected in the culture independent analysis. The lack of detection of all isolates could be due to insufficient sequencing depth as a result of the rarity of these isolates within the environment.

The culture library obtained only represents a very small portion of the total fungal diversity present within Frobisher Bay. Many organisms that are prevalent in the environment as determined by next generation sequencing have not been cultured in the lab due to a lack of understanding of the nutritional and physical conditions required for culture. Further sampling within Frobisher Bay using a larger variety of isolation media and techniques may aid in the isolation of this uncultured diversity.

Table 4.3 Identification of cultured fungi from Frobisher Bay

	# of isolates	Phylogenetic Order	Rep. Isolate	Closest GenBank Relative [Acc. No.]	% ID	Seq. length
4	9	*Capnodiales*	RKAG 104[a,b]	*Cladosporium antarcticum* CBS 690.92 [NR_121332.1]	99%	484
	1	*Chaetothyriales*	RKAG 672[a,b]	*Minimelanolocus curvatus* MFLUCC 15-0259 [KR215605.1]	90%	555
19	2	*Cystofilobasidiales*	RKAG 435[a,b]	*Mrakia gelida* CBS 5272 [AF144485.1]	100%	562
18	4	*Cystofilobasidiales*	RKAG 445[a,b]	*Mrakia nivalis* CBS 5266 [AF144484.1]	100%	562
10	4	*Eurotiales*	RKAG 105[b]	*Aspergillus creber* NRRL 58592 [NR_135442.1]	100%	501
9	2	*Eurotiales*	RKAG 553	*Aspergillus terreus* ATCC 1012 [NR_131276.1]	99%	547
	1	*Eurotiales*	RKAG 638[a]	*Penicillium cansecens* NRRL 910 [NR_121256.1]	100%	526
13	3	*Eurotiales*	RKAG 685[a]	*Penicillium citreonigrum* NRRL 761 [NR_138264.1]	100%	528
15	37	*Eurotiales*	RKAG 325[a,b]	*Penicillium fimorum* CBS 140576 KU904342.1	99%	539
	1	*Eurotiales*	RKAG 221	*Penicillium lemhiflumine* NRRL 35843 [KF932964.1]	100%	511
35	3	*Eurotiales*	RKAG 179[a]	*Penicillium sumatranse* CBS 281.36 [NR_119812.1]	99%	532
6	39	*Eurotiales*	RKAG 410[a]	*Penicillium thymicola* CBS 111225 [KJ834518.1]	99%	540
31	42	*Eurotiales*	RKAG 211[a]	*Penicillium swiecickii* NRRL 918 [NR_121254.1]	99%	536
20	3	*Eurotiales*	RKAG 389[b]	*Penicillium biourgeianum* NRRL 32240 AY484909.1	100%	535
21	8	*Eurotiales*	RKAG 395[b]	*Penicillium wellingtonense* CBS 130375 [NR_121519.1]	100%	532
	1	*Filobasidiales*	RKAG 447[a,b]	*Goffeauzyma gilvescens* CBS 7525 [NR_073228.1]	99%	530
17	4	*Filobasidiales*	RKAG 443[a]	*Solicoccozyma terricola* CBS 4517 [NR_073221.1]	99%	449
	1	*Filobasidiales*	RKAG 450[a,b]	*Vishniacozyma victoriae* CBS 8685 [NR_073260.1]	100%	360
	1	*Helotiales*	RKAG 208[b]	*Botrytis caroliniana* ATCC MYA-4856 [NR_111839.1]	99%	406
	1	*Helotiales*	RKAG 191[b]	*Cadophora luteo-olivacea* CBS 141.41 [NR_111149.1]	99%	576
	1	*Hypocreales*	RKAG 625[a]	*Acremonium alternatum* CBS 407.66 [HE798150.1]	99%	505
	1	*Hypocreales*	RKAG 561	*Beauveria pseudobassiana* ARSEF 3405 [NR_111598.1]	100%	383
38	2	*Hypocreales*	RKAG 133	*Fusarium solani* CBS 2012 [JX435180.1]	99%	510
37	14	*Hypocreales*	RKAG 102[a,b]	*Fusarium torulosum* NRRL 52772 [JF740926.1]	99%	512
30	4	*Hypocreales*	RKAG 558[b]	*Isaria farinosa* ARSEF 4029 [HQ880828.1]	100%	528
24	2	*Hypocreales*	RKAG 186[a,b]	*Sesquicillium microsporum* NRRL 54217 [GU219471.1]	98%	495
	1	*Hypocreales*	RKAG 571[b]	*Sesquicillium microsporum* NRRL 54217 [GU219471.1]	96%	492
	1	*Hypocreales*	RKAG 627[a]	*Sesquicillium microsporum* NRRL 54217 [GU219471.1]	96%	437
1	12	*Hypocreales*	RKAG 557[a]	*Sarocladium strictum* CBS 346.70 [NR_111145.1]	100%	522

	1	*Hypocreales*	RKAG 563[b]	*Simplicillium aogashimaense* JCM 18167 [NR_111026.1]	100%	401
	1	*Hypocreales*	RKAG 628[a]	*Nectria dacryocarpa* CBS 113532 [KM231848.1]	90%	416
29	3	*Hypocreales*	RKAG 356[a]	*Neocosmospora rubicola* CBS 101018 [KM231800.1]	100%	470
8	6	*Hypocreales*	RKAG 578[a,b]	*Paecilomyces lilacinus* ATCC 10114 [AY213665.1]	99%	538
3	5	*Hypocreales*	RKAG 373[a,b]	*Tolypocladium cylindrosporum* CBS 122173 DQ449656.1	95%	507
2	8	*Hypocreales*	RKAG 189[a,b]	*Tolypocladium inflatum* NBRC 31669 [AB255606.1]	100%	497
25	2	*Hypocreales*	RKAG 560[a,b]	*Tolypocladium cylindrosporum* CBS 122173 DQ449656.1	97%	491
5	13	*Kriegeriales*	RKAG 484[a,b]	*Glaciozyma litorales* [HF934009.1]	99%	606
36	2	*Leotiomycetes* incertae sedis	RKAG 165[a,b]	*Leohumicola minima* DAOM 232587 [AY706329.1]	93%	496
26	2	*Leotiomycetes* incertae sedis	RKAG 372[a,b]	*Oidiodendron periconioides* [AF062802.1]	99%	394
33	15	*Leotiomycetes* incertae sedis	RKAG 200[b]	*Geomyces pannorum* ATCC 11501 [FJ545236.1]	100%	512
23	5	*Leotiomycetes* incertae sedis	RKAG 347[a,b]	*Pseudogymnoascus pannorum* NRRL 62968 [KM030298.1]	99%	502
	1	*Microascales*	RKAG 640[a]	*Graphium jumulu* CPC 24639 [KR476722.1]	98%	405
34	2	*Mortierellales*	RKAG 198[b]	*Mortierella parvispora* FSU 10758 [JX976005.1]	100%	580
	1	*Mortierellales*	RKAG 156[b]	*Mortierella horticola* CBS 305.52 [JX975874.1]	99%	482
39	3	*Mortierellales*	RKAG 110[b]	*Mortierella antarctica* CBS 609.70 [HQ630347.1]	95%	482
43	2	*Mortierellales*	RKAG 139[b]	*Mortierella hyalina* CBS 115655 JN943802.1	97%	498
7	4	*Mucorales*	RKAG 607[a]	*Mucor hiemalis* CBS 201.65 [EU484277.1]	99%	581
16	4	*Mucorales*	RKAG 528[a]	*Mucor zonatus* CBS 148.69 [NR_103638.1]	99%	569
	1	*Pleosporales*	RKAG 175	*Ascochyta hordei* NRRL 54518 [HQ882800.1]	98%	478
14	2	*Saccharomycetales*	RKAG 554	*Candida zeylanoides* CBS 619 [NR_131278.1]	99%	570
28	5	*Thelebolales*	RKAG 184[a,b]	*Thelebolus globosus* CBS 113940 [DQ028268.1]	99%	493
32	2	*Venturiales*	RKAG 209	*Venturia populina* CBS 256.38 [EU035467.1]	91%	353
27	2	*Xylariales*	RKAG 368[a,b]	*Hyalotiella spartii* MFLUCC 13-0397 [NR_137972.1]	98%	364
	1	*Xylariales*	RKAG 573	*Rosellinia quercina* ATCC 36702 [AB017661.1]	95%	533

[a]isolated at 4˚C

[b]detected in culture independent analysis

A)

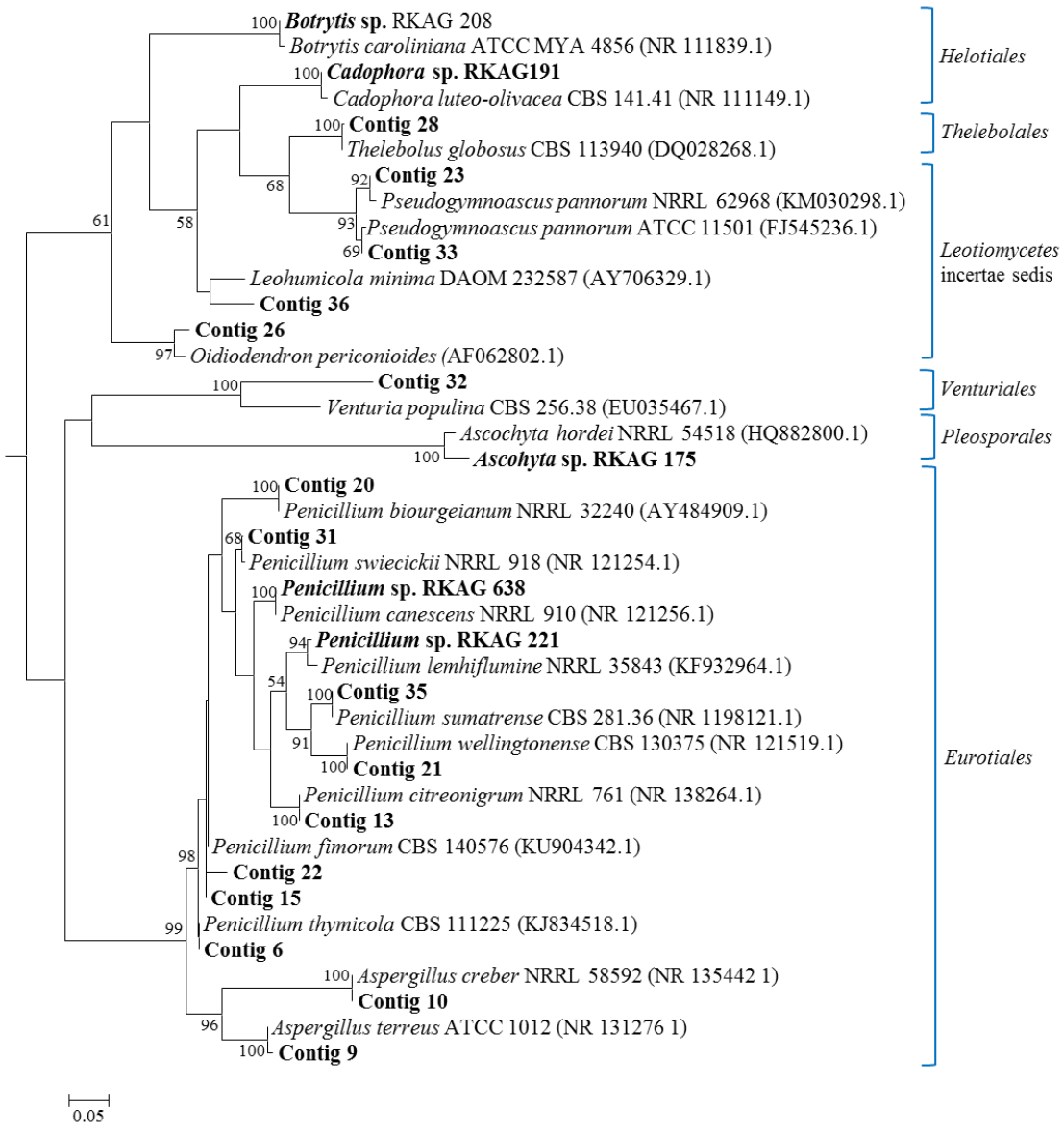

Figure 4.7. Maximum likelihood analysis of the ITS region of cultured fungal isolates within the phylum Ascomycota. Alignment was based on a total of 468 nucleotide positions. Phylogram was constructed using the GTR+G model of nucleotide substitution and 1000 bootstrap iterations. The phylogram was split into two subtrees (**A** and **B**). Node support below 50% is collapsed.

B)

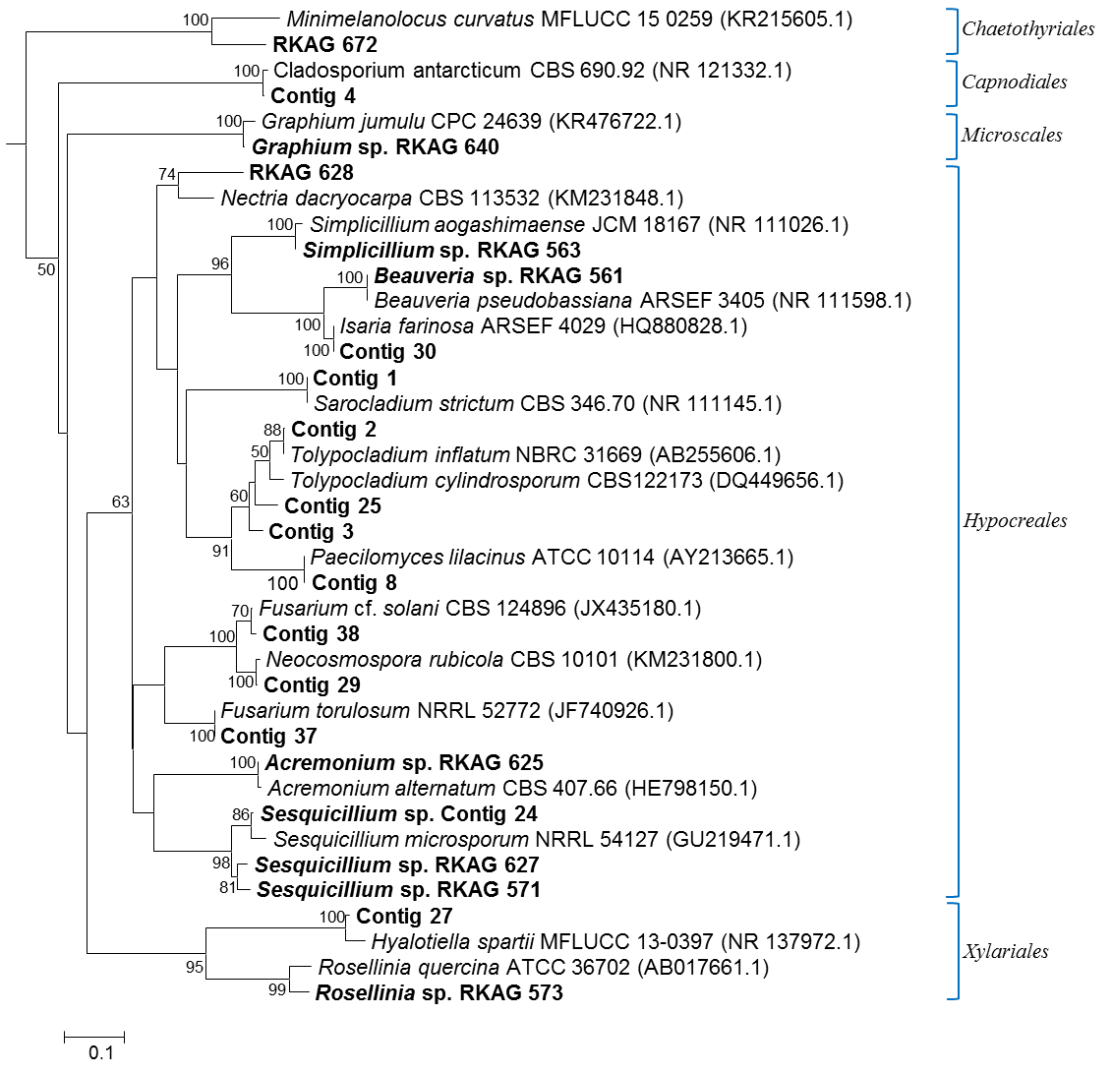

Figure 4.7. Continued from previous page.

4.4 Conclusions

This analysis gives the first overall view of the fungal diversity within sediment from Frobisher Bay and reveals sediment within this region to contain unique, diverse fungal assemblages. Depending on sample site, sediment within this region appears to be dominated by unknown chytrids, basidiomycete yeasts within the genus *Glaciozyma* and filamentous ascomycetes within the genus *Didymella*. A large portion of total reads could not be classified to a phylum, order, class or genus level and may be representative of new fungal taxa. The presence of putatively new and uncharacterized fungal biodiversity makes this region extremely interesting from a NPs standpoint.

The isolation of a large, taxonomically diverse library of fungi containing many putatively new species highlights the utility of Frobisher Bay as a resource for taxonomically distinct fungi. The large metabolic diversity of these organisms will undoubtedly yield a wide range of structurally diverse NPs. The further investigation of the NPs produced by these cultured fungal isolates is discussed in Chapters 5-8.

Chapter 5: Investigation of Natural Products Produced by Sediment-Derived Fungi from Frobisher Bay and Isolation of New Secondary Metabolites

5.1 Introduction

Within the terrestrial environment fungi have proven to be a fruitful source of bioactive NPs including the clinically relevant antibiotics penicillin and griseofulvin, the cholesterol lowering compounds lovastatin and mevastatin, and the immunosuppressant cyclosporin[33]. Despite the large success of fungal NPs, there is a large discrepancy observed between fungal metabolites described from the terrestrial and marine environment, which is largely due to a lack of bioprospecting within the marine realm. The marine environment is predicted to contain upwards of 10,000 (if not more) fungal species[244]. Genome sequencing of marine fungal lineages is beginning to shed light on the potential of these organisms for NP production. The genome of the marine *sensu stricto* fungi *Verruculina enalia, Torpedospora radiata, Lindra thalassiae* and *Corollospora maritima* have recently been sequenced and preliminary AntiSmash analysis indicates the genomes of these isolates encode polyketide synthase genes, non-ribosomal peptide synthetase genes, terpene encoding genes and other NP genes[245]. Characterization of these gene clusters and the NPs produced by them has not yet been reported formally, so it is unknown how these NPs compare structurally to those isolated from the terrestrial environment.

Of the ~2,000 reported fungal NPs from the marine environment, only 190 have been isolated from the cold biosphere, including Earth's polar regions and the deep sea environment[87]. Due to the unique stresses associated with living in the cold biosphere, organisms must be uniquely adapted to live under these conditions. The vast genetic and metabolic diversity of these cold-adapted organisms is largely understudied and may offer a tremendous resource for the isolation of new NPs.

The fungal diversity of Frobisher Bay was determined to be species rich by 454-pyrosequencing and isolation of fungi from this region resulted in the culture of many cold-tolerant isolates and several putatively new species (described in Chapter 4). The isolates obtained are taxonomically diverse and are expected to be a rich resource for NP discovery based on their genetic variation. The aim of this study was to investigate the cultured library of fungi for the production of new NPs. Each isolate was fermented under the OSMAC (One Strain Many Compounds) approach[176] employing a variety of fermentation conditions. Extracts were analyzed using a chemically driven LC-HRMS dereplication approach to prioritize isolates based on chemical novelty. The diversity of NPs detected will be described in addition to the isolation and structural characterization of several new non-ribosomal peptides and polyketides.

5.2 Experimental Procedures

5.2.1 Small-Scale Fermentation

At least one representative from each fungal OTU described in Chapter 4 was fermented on solid Czapek yeast extract agar (CYA)[246], MMK2 agar (mannitol 40 g, yeast extract 5 g, Murashuge & Skoog salts 4.3 g; 1 L ddH_2O), yeast extract sucrose agar (YES)[247] and potato dextrose agar (PDA, Difco), with and without the addition of Instant Ocean™ Sea Salt (36 g/L) and at two different fermentation temperatures (15˚C and 22˚C). For those isolates that had low sequence similarity to accessioned strains within GenBank, additional fermentations on solid rice medium (rice 10 g, yeast nitrogen base 6.7 g, sucrose 5.0 g, 25 mL ddH_2O), corn meal agar (CMA, Sigma), vermiculite solid medium (vermiculite 6.0 g, maltose 0.75 g, yeast extract 0.01 g, glucose 0.25 g, peptone 0.05 g, 25 mL ddH_2O), casamino acid medium agar (casein

hydrosylate 2.5 g, glucose 40.0 g, $MgSO_4$ 0.1 g, KH_2PO_4 1.8 g, 1 L ddH_2O) and glycerol-yeast extract-tryptone medium agar (GYT, glucose 3.5 g, peptone 0.5 g, soluble starch 1.0 g, soybean flour 2.0 g, vegetable extract 0.3 g, yeast extract 0.5 g, KH_2PO_4 0.05 g, 1 L ddH_2O) were undertaken. Glycerol stocks (500 µL) were used to inoculate seed tubes containing 15 mL of YM broth and incubated at 22˚C at 150 rpm for seven days. Seed culture (200 µL) was used to inoculate a Petri plate (60 mm x 15 mm) containing solid fermentation media or a 50 mL flask containing rice or vermiculite medium. Dual fermentations were incubated at 15˚C and 22˚C for 21 days and purity was assessed visually. After 21 days, the solid fermentations were cut up into 1 x 1 cm squares, placed into a 25 x 25 mm borosilicate tube and extracted with EtOAc (30 mL). The EtOAc was retained, dried *in vacuo* and partitioned between 80% CH_3CN and 100% hexane. The CH_3CN layer was retained, dried *in vacuo* and analyzed by LC-HRMS (conditions described in Chapter 3). Chromatograms were assessed visually for metabolite production using Xcalibur.

5.2.2 Large-Scale Fermentation, Extraction and Purification of Natural Products from RKAG 170, 208 and 563

Isolate RKAG 170, RKAG 208 and RKAG 563 were inoculated into 15 mL of YM liquid seed at 22°C and agitated at 200 rpm for five days. Seed culture (200 µL) inoculated onto 50 Petri plates (100 x 15 mm) containing 20 mL of solid agar (MMK2, CYA, PDA for RKAG 170, RKAG 208 and RKAG 563 respectively) and grown for 21 days at 22°C. The solid agar cultures were roughly cut up, pooled and extracted with EtOAc. The extract was evaporated to dryness *in vacuo* and partitioned between 80% CH_3CN and 100% hexane. The CH_3CN layer was collected and dried *in vacuo* to give a crude extract.

The crude extract was fractionated using automated reversed-phase flash chromatography with a linear gradient from 20% aqueous MeOH to 100% MeOH over 20 min on a 15.5 g C_{18} column (High Performance GOLD RediSep Rf) with a flow rate of 30 mL/min. Pure fractions of the compounds of interest were obtained by Combiflash for RKAG 208 (*m/z* 489.3202 $[M+Na]^+$, yield = 26 mg, *m/z* 505.3133 $[M+Na]^+$, yield = 1 mg) and RKAG 170 (*m/z* 353.1025 $[M+H]^+$ yield = 50 mg).

The semi-pure fraction eluting at 18 min was subjected to reversed-phase HPLC using a Gemini 110Å C18 column (5µm 250 x 10 mm, Phenomenex) and flow rate 3.0 mL/min on a Thermo Surveyor HPLC system coupled with an evaporative light scattering detector (Sedex 55) and photodiode array (PDA) detector. Isocratic elution in 55% aqueous MeOH, resulted in the purification of compounds **1** (10.4 mg) and **2** (1.5 mg).

Further RP-HPLC purification of a combiflash fraction containing the compounds of interest from RKAG 563 was performed on a Waters HPLC system coupled with an ELSD (Waters 2424) and PDA detector (Waters 2489) and a flow rate of 3 mL/min. Using a Gemini 110Å C18 column (5µm 250 x 10 mm, Phenomenex) and 20 min isocratic elution with 70% aqueous CH_3CN (0.1% formic acid), hirsutellic acid A (**4**) (4 mg), hirsutellic acid C (**5)** (1.5 mg) and verlamelin (**3**) (3 mg) were purified at 16.9, 14.9 and 24 min respectively. All compounds were tested for their antimicrobial and cytotoxic activity as described in Chapter 3.1.3 and 3.1.7.

Hirsutellic acid C (**5**) White powder; UV (MeOH) λ_{max} 301, 253, 226 nm; IR (film) V_{max} 3401, 3285, 2962, 1652, 1501, 1440, 1372, 1302, 762 cm^{-1}; (+) HRESIMS *m/z* 511.2896 $[M + H]^+$, (calcd. for $C_{28}H_{39}N_4O_5$, 511.2915, Δ 3.72 ppm).

Compound (6) Red powder; UV (MeOH) λ_{max} 382, 348, 328, 252 nm; IR (film) V_{max} 3348, 1625, 1546, 1463, 1387, 1320, 1241, 1027 cm^{-1}; (+) HRESIMS *m/z* 353.1025 $[M + H]^+$, (calcd. for $C_{59}H_{99}O_{13}$, 353.1020, Δ 1.42 ppm).

Cameronic acid B (**7**) White powder; UV (MeOH) λ_{max} 226 nm; IR (film) V_{max} 3395, 3342, 2960, 2929, 2871, 1719, 1565, 1456, 1372, 1071, 1015, 967 cm^{-1}; (+) HRESIMS *m/z* 489.3202 $[M + Na]^+$, (calcd. for $C_{27}H_{45}NaO_6$, 489.3187, Δ 3.07 ppm).

Cameronic acid C (**8**) White powder; UV (MeOH) λ_{max} 226 nm; IR (film) V_{max} 3390, 3339, 2960, 2929, 2869, 1718, 1562, 1450, 1364, 1073, 1010, 967 cm^{-1}; (+) HRESIMS *m/z* 505.3133 $[M + H]^+$, (calcd. for $C_{27}H_{46}NaO_7$, 505.3136, Δ 0.59 ppm).

5.3 Results and Discussion

5.3.1 Small-Scale Fermentation and Isolate Prioritization

Isolates not exhibiting significant ITS sequence similarity to known cultured isolates within GenBank were of great interest for further investigation due to their potential to be new species (RKAG 110, 165, 209, 373, 560, 573, 574, 628, 670, and 672) and being unexplored in terms of their secondary metabolome. In order to stimulate the production of NPs, the OSMAC approach was undertaken by the alteration of fermentation parameters including media composition, fermentation temperature (15˚C and 22˚C) and osmotic stress (presence and absence of sea salts). Fermentations were carried out over 21 days and EtOAc crude extracts were generated for each combination of fermentation conditions. Crude extracts were analyzed by LC-HRMS and strains were prioritized based on chemical novelty as determined by database searches (Antibase 2012 and SciFinder) and relative abundance of the metabolites produced as judged by the ELSD chromatogram.

Several of these putatively new species were of interest due to the production of unknown compounds. *Sesquicillium* sp. RKAG 571, RKAG 186 and RKAG 627 produced several new peptide NPs resulting in the isolation of a new family of cyclic decapeptides and a new family of peptaibols which will be discussed in Chapter 6. *Mortierella* sp. RKAG 110 produced compounds with *m/z* values of 770.5175, 804.5021, 804.5024 and 838.4862 $[M+H]^+$. The structure of these compounds was solved using 1D and 2D NMR analysis and they were determined to be a family of new cyclic heptapeptides. The purification and structural characterization of these new compounds will be discussed in Chapter 7. *Tolypocladium* sp. RKAG 373 produced compounds corresponding to *m/z* 306.1702 and 320.1492 $[M+H]^+$ and *Tolypocladium* sp. RKAG 560 produced compounds corresponding to *m/z* 340.1917, 356.1860 and 374.1907 $[M+H]^+$ which resulted in the isolation and characterization of several new tetramic acid containing compounds which will be discussed in Chapter 8.

Several of the putatively new isolates were deprioritized for further investigation due to a lack of production of metabolites (RKAG 165, 209 and 670) under the fermentation conditions tested or the production of known metabolites. RKAG 672 produced a compound with an *m/z* 1202.8508 $[M+H]^+$ and was tentatively identified as the known metabolite cyclosporin A. Cyclosporin is a cyclic peptide and is clinically approved as an immunosuppressant. Compounds within the cyclosporin family are produced by a large number of fungal genera within the order *Hypocreales* including *Neocosmospora*, *Cylindrocarpon* and *Tolypocladium*[19,248,249]. Although confirmation of this structure by MS/MS analysis was not undertaken, this isolate was deprioritized based on this tentative identity and lack of production of other metabolites. RKAG 573

(tentatively identified to be within the genus *Rosellinia*) produced several metabolites with an *m/z* 456.2596 (unknown), 508.2694 (cytochalasin M), 367.1750 (hyminograndin) and 351.1801 (hymendial) $[M+H]^+$. Due to the complex profile and large number of hits for each of these compounds within Antibase 2012, this isolate was deprioritized. Lastly RKAG 628 produced a compound with an *m/z* corresponding to 365.0786 $[M+H]^+$ which had three hits within Antibase 2012, all chlorinated compounds. A typical chlorinated isotopic signature was evident based on the ratio of the M and M+2 peak in the mass spectrum and under one of the fermentation conditions (MMK2, 22˚C), this compound consisted of 99% of the crude mass. Analysis of the NMR spectra of this extract confirmed the identity of this compound as the known chlorinated compound, radicicol[250].

Isolates displaying significant sequence similarity to accessioned strains within GenBank were also selected for fermentation. At least one representative from each fungal OTU was selected for fermentation and in the case of an OTU containing multiple strains (99% ITS sequence similarity), a representative isolate from each strain was fermented. In total, 75 isolates were fermented in four different fermentation media, with and without the presence of sea salts and at a fermentation temperature of 15˚C and 22˚C. Extracts were analyzed by LC-HRMS and isolates were prioritized based on chemical novelty (as judged by searches within Antibase 2012) and relative abundance of the compound produced as determined by ELSD. Several of these isolates produced compounds which had no corresponding matches within Antibase 2012, but had to be deprioritized due to the low amounts of compound produced, making scale-up fermentations and purification challenging.

Several isolates were deprioritized because they produced known compounds. *Aspergillus terreus* sp. RKAG 556 produced butyrolactone I and III, *N*-α-acetyl-aszonalenin, β-hydroxymevinolin and asterrriquinone SU-5500. *Paecilomyces lilacinus* RKAG 134 produced leucinostatins, *Isaria farinosa* RKAG 576 made militarinone, *Fusarium torulosum* RKAG 130 made enniatins and oxyspiridone, *Beauveria bassiana* RKAG 561 made beauverolide analogs and beauvericin and *Ascochyta hordei* RKAG 175 produced epicoccamide. The *Penicillium* isolates were also deprioritized due to the production of known compounds or limited production of putatively new compounds making purification challenging.

Several isolates were prioritized for further investigation due to the production of compounds in high yields as judged by ELSD, which had no likely matches to compounds within Antibase 2012. This corresponded to the following isolates; *Simplicillium aogashimaense* RKAG 563 (*m/z* 511.2896 $[M+H]^+$), *Cadophora viticola* RKAG 170 (*m/z* 353.1025 $[M+H]^+$), *Hyalotiella sparti* RKAG 368 (*m/z* 439.2104, 441.2258 $[M+H]^+$) and *Botrytis carolina* RKAG 208 (*m/z* 489.3202, 505.2863 $[M+Na]^+$). These isolates were refermented in large scale (1 L solid agar), extracted with organic solvents and fractionated using C18 flash chromatography. Fractions of interest were submitted for NMR if pure or subjected to RP-HPLC with a C18 stationary phase to separate the compounds of interest. Due to a cessation of production of *m/z* 439.2104, 441.2258 $[M+H]^+$ by RKAG 368, work on this isolate was discontinued.

5.3.2 Isolation of New Natural Products

5.3.2.1 Characterization of a New Hirsutellic Acid Analog from RKAG 563

Simplicillium aogashimaense RKAG 563 was of interest for further investigation due to the production of compounds with an *m/z* of 511.2896 and 525.3090 $[M+H]^+$. Searches within Antibase 2012, revealed no matches for 511.2896 and one match within 5 ppm for 525.3090 corresponding to hirsutellic acid A from a *Hirsutella* sp. Due to the differences in taxonomy of the producing organisms (*Simplicillium* vs. *Hirsutella*) and the presence of an unknown compound, further chemical investigation was undertaken. After fractionation by flash chromatography several fractions were subsequently purified using RP-HPLC leading to the purification of verlamelin (**3**), hirsutellic acid A (**4**) and hirsutellic acid C (**5**).

Compound **3** was obtained as a white powder and a molecular formula of $C_{45}H_{71}N_7O_{11}$ (*m/z* 886.5313) was supported by HRESIMS. Analysis of the NMR spectra revealed **3** was a lipodepsipeptide and was identified as the known compound verlamelin A, originally isolated from *Verticillium lamellicola*. Verlamelin A was previously reported to have weak antifungal activity and no antimicrobial activity[251,252].

Compound **4** (Table 5.1) was obtained as a white powder and HRESIMS supported a molecular formula of $C_{29}H_{40}N_4O_5$ (*m/z* 525.3090 $[M + H]^+$) requiring 12 degrees of unsaturation. Careful analysis of the NMR spectra revealed the presence of the amino acid residues; Ile, *N*-Me Phe and Leu. The presence of an anthranilic acid residue was determined by COSY correlations between H3/H4/H5/H6 and HMBC correlations from H-3 (δ_H 7.90) to C-1 (δ_C 139.6), C-5 (δ_C 130.2) and COOH (δ_C 172.1) and H-4 (δ_H 6.97) to C-2 (δ_C 123.7) and C-6 (δ_C 118.2). HMBC and NOESY

correlations confirmed the sequence of the residues to be identical to hirsutellic acid A (Figure 5.1)[253].

Compound **5** (Table 5.1, Appendix Figures A.7 and A.8) was isolated as a white powder and HRESIMS supported a molecular formula of $C_{28}H_{38}N_4O_5$ (*m/z* 511.2896 $[M + H]^+$) requiring 12 degrees of unsaturation. Comparison of the NMR spectra to **4** revealed extensive similarity between both compounds and it was determined **5** differed from **4** by the loss of a methylene group. This loss was found to correspond to the replacement of the terminal Ile residue with a Val residue. The isolation of this compound represents a new analog within the hirsutellic acid family and has been given the name hirsutellic acid C. The absolute configuration for each amino acid was tentatively assigned to be the same as that of hirsutellic acid A (L-allo-isoleucine, *N*-methyl-D-phenylalanine and L-leucine), however Marfey's analysis of the amino acids would be required to confirm this assignment.

Hirsutellic acid A was previously isolated from *Hirsutella* sp. BCC 1528 isolated from an orthopteran-cricket from northern Thailand. It was shown to exhibit activity against *Plasmodium falciparum* (K1, multi drug resistant strain) with an IC_{50} value of 8.0 µM and exhibited no cytotoxic activity against Vero cells (African green monkey kidney fibroblasts) and three cancer cells lines including human epidermoid carcinoma cells (KB10), unspecified human breast cancer cells and human lung cancer cells (NCI-H187)[253]. Both **4** and **5** were tested for antimicrobial activity, cytotoxicity and anticancer activity and demonstrated no activity at the highest concentration tested (128 µg/mL).

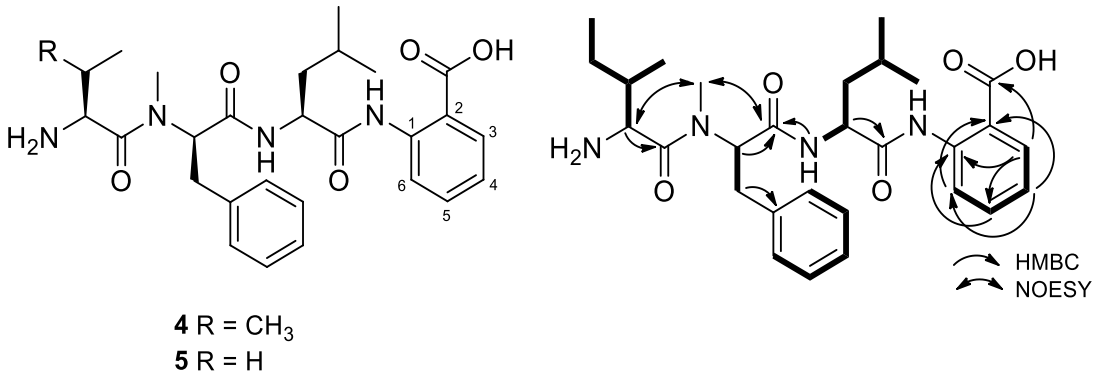

Figure 5.1. Molecular structure of hirsutellic acid A and C and key NMR correlations of hirsutellic acid C.

Table 5.1. ^{1}H (600 MHz) and ^{13}C (150 MHz) NMR data of hirsutellic acid A (4) and hirsutellic acid C (5) in DMSO-*d6*.

Hirsutellic Acid A (4)			Hirsutellic Acid C (5)		
	δ_C	δ_H (*J*/Hz)		δ_C	δ_H (*J*/Hz)
Abz			**Abz**		
NH		13.40, s	NH		13.50, s
1	139.6		1	139.8	
2	123.7		2	123.9	
3	130.6	7.90, dd[a] (7.7, 1.6)	3	130.4	7.90, dd[a] (7.8, 1.3)
4	121.4	6.97, dd[a] (8.4, 7.9, 1.0)	4	121.3	6.97, dd[a] (8., 7.7, 0.9)
5	130.2	7.32, ddd[a] (8.2, 7.9, 1.7)	5	130.0	7.29, ddd[a] (8.9, 7.6, 1.7)
6	118.2	8.54, dd[a] (8.3, 0.7)	6	118.0	8.52, dd[a] (8.3, 0.6)
COOH	172.1		COOH	171.6	
Leu			**Leu**		
CO	170.7		CO	174.0[a]	
NH		8.23, d (7.8)	NH		8.23, d (7.5)
α	52.3	4.32, ddd, (11.3, 7.8, 3.8)	α	52.4	4.28, m
β	39.8	1.67, m	β	39.9	1.64, m
		1.55, m			1.54
γ	23.7	1.45, m	γ	23.8	1.42, m
δ1	22.9	0.85, d (6.6)	δ1	22.9	0.83, d (6.6)
δ2	20.9	0.79, d (6.5)	δ2	20.8	0.77, d (6.5)
Phe			**Phe**		
CO	170.0		CO	169.3	
N-CH3	29.9	2.94, s	N-CH3	29.9	2.95, s
α	54.9	5.62, dd[a] (9.7, 6.6)	α	54.9	5.63, dd (9.6, 6.7)
β	34.2	2.97, m	β	34.2	3.00, dd (14.0, 6.6)
					2.92, dd (14.1, 9.7)
1’	136.6		1’	136.7	
2’	128.9	7.24, m	2’	127.8	7.24, m
3’	127.9	7.24, m	3’	128.7	7.24, m
4’	126.0	7.18, dd (8.6, 4.2)	4’	126.0	7.17, dd (8.4, 4.3)
Ile			**Val**		
CO	169.7		CO	169.8	
NH			NH		
α	52.6	4.01, d (3.5)	α	53.8	3.93, d (3.5)
β	35.1	1.32, m	β	29.1	1.69, m
$\gamma 1_A$	24.7	1.27, m	γ1	18.2	0.74, d (6.9)
$\gamma 1_B$		1.05, m	γ2	16.5	0.61, d (6.7)
γ2	12.9	0.57, d (6.8)			
δ	11.5	0.75, t (8.2, 8.2)			

[a]coupling constant determined in CD_3OD

5.3.2.2 Characterization of a New Reduced Perylene Quinone from RKAG 170

After combiflash fractionation of the crude extract of RKAG 170 (2 g), a relatively pure fraction of the compound of interest was obtained. The compound was obtained as a red powder and a molecular formula of $C_{20}H_{16}O_6$ was supported by HRESIMS (*m/z* 353.1025 $[M+H]^+$) requiring 13 degrees of unsaturation (Figure 5.2, Table 5.2, Appendix Figures A.8 and A.9). The proton and HSQC spectra revealed the presence of two methylene groups, three oxymethine groups and four aromatic protons consisting of two separate ortho coupled protons. HMBC correlations revealed the presence of a ketone and ten quaternary aromatic carbons including two which were consistent with hydroxyl-substituted aromatic carbons. COSY correlations between H-5 (δ_H 2.97) and H-6 (δ_H 3.55) connected the two methylene groups and correlations between H-7 (δ_H 2.53)/H-8(δ_H 3.90)/H-9 (δ_H 5.43) connected the three oxymethines within their own spin system. HMBC correlations from H-2 (δ_H 7.23) and H-5 (δ_H 2.97) to C3a (δ_C 112.3) and H-1 (δ_H 8.83) and H-6 (δ_H 3.55) to C-3b (δ_C 130.1) connected rings A and B together. HMBC correlations from H-9 (δ_H 5.43) to C-9a (115.4) and C-10 (δ_C 156.7) and H-12 (δ_H 8.49) and H-7 (δ_H 5.37) to C-9b (δ_C 128.1) connected the D and E ring. HMBC correlations from H-6 (δ_H 3.55) to C-6a (δ_C 131.6) and C-6b (δ_C 130.8), H-7 (δ_H 5.37) to C-6b, H-1 (δ_H 8.83) to C-12a (δ_C 124.6) and C-12b (δ_C 123.9) and H-12 (δ_H 8.49) to C-12a (δ_C 124.6) and C-12b (δ_C 123.9) connected the rings together and revealed the final structure as a reduced perylene quinone compound. The relative configuration of the stereocentres at C-7, C-8 and C-9 were determined based on vicinal *J*-coupling constants. The large $^3J_{8\text{-}9}$ of 9.0 Hz indicated both H-8 and H-9 had a pseudo-axial orientation. The small $^3J_{7\text{-}8}$ of 3.2 Hz revealed H-7 and H-8 had a pseudo

equatorial/axial configuration with H-7 being pseudo-equatorially configured and H-8 being pseudo-axially configured.

Many compounds within the perylene quinone family are reported phytotoxins and cause damage to the host cell by the generation of free radicals after photo activation[254]. Others have been shown to be mutagenic in bacterial and mammalian cell lines and have gained importance due to their human health risk by causing food and feed contaminations[255,256,257]. These compounds are largely of fungal origin[258,259,260] and the diversity within arises from the levels of reduction and oxidation within the perylene quinone scaffold and the decoration of these compounds with additional carbon substituents. Within this family of compounds, the presence of a non-reduced C ring is quite rare[261] making the isolation of this compound relatively unique to this family.

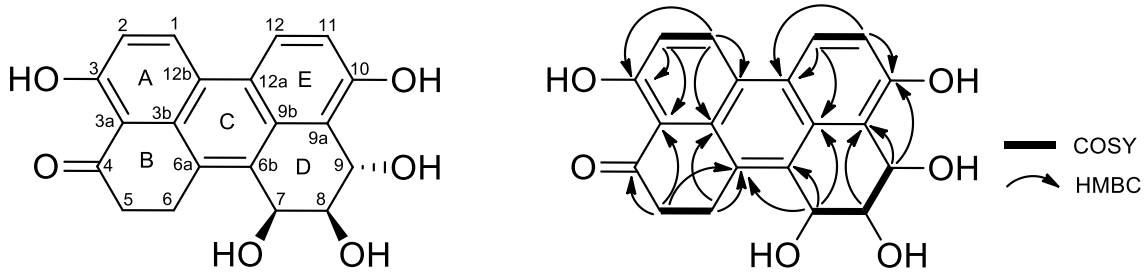

Figure 5.2. Molecular structure and key NMR correlations of compound **6**.

Table 5.2. ^{1}H (600 MHz) and ^{13}C (150 MHz) NMR Data of compound 6 in CD_3OD.

Position	δ_C, type	δ_H (*J*, Hz)	COSY	HMBC
1	133.3, CH	8.83, d (9.3)	2	3, 3b, 12a, 12b
2	119.1, CH	7.23, d (9.3)	1	3a, 12b
3	162.6, C			
3a	112.3, C			
3b	130.1, C			
4	205.5, C			
5	37.5, CH_2	2.97, m	5	3a, 4, 6, 6a
6	24.6, CH_2	3.55, m	4	3b, 4, 5, 6a, 6b
6a	131.6, C			
6b	130.8, C			
7	68.7, CH	5.37, d (3.2)	8	6b, 8, 9, 9b
8	75.3, CH	3.90, dd (3.2, 9.5)	7, 9	9a
9	70.9, CH	5.43, d (9.5)	8	9a, 10
9a	115.4, C			
9b	128.1, C			
10	156.7, C			
11	119.1, CH	7.20 d (9.1)	12	10, 12a
12	124.3, CH	8.49, d (9.1)	11	9b, 12a
12a	124.6, C			
12b	123.9, C			

5.3.2.3 Characterization of New Cameronic Acid Analogs from RKAG 208

After Combiflash fractionation, a pure fraction containing *m/z* 489.3202 $[M+Na]^+$ was obtained and further characterized by NMR (Figure 5.3, Table 5.3, Appendix Figures A.11 and A.12). Compound **7** was obtained as a white powder and HRESIMS supported a molecular formula of $C_{27}H_{46}O_6$ requiring five degrees of unsaturation. The ^{1}H NMR spectrum revealed the presence of six olefinic protons (δ_H 5.45, 5.68, 5.50, 5.63, 5.14 and 5.26), nine methine protons including four oxygenated methines (δ_H 4.14, 3.85, 3.67 and 3.64), one methylene group (δ_H 1.38/1.24) and eight methyl groups including two olefinic methyls (δ_H 1.64 and 1.65). Interpretation of the COSY and TOCSY spectra revealed the presence of three distinct spin systems from H-2 to H-11, H-13 to H-15 and H-17 to H-20. COSY correlations between H-2 (δ_H 2.45)/H-21 (δ_H 1.07), H-6 (δ_H 2.26)/H-22 (δ_H 0.99), H-10 (δ_H 2.33)/H-23 (δ_H 0.85), H-14 (δ_H 2.62)/H-5 (δ_H 5.68) and H-18 (δ_H 2.34)/H-27 (δ_H 0.97) connected the remaining non-olefinic methyl groups within these three spin systems. HMBC correlations from the olefinic methyl group H_3-24 (δ_H 1.65) to C-11 (δ_C 83.9), C-12 (δ_C 137.7), and C-13 (δ_C 133.9) and from the olefinic methyl group H_3-26 (δ_H 1.64) to C-15 (δ_C 84.6), C-16 (δ_C 135.7) and C-17 (δ_C 136.5) established the connectivity of these three fragments. In order to satisfy the molecular formula and the remaining degree of unsaturation, a carboxy group was incorporated and connected at C-2 by HMBC correlations from H-2 (δ_H 2.45) to C-1 (δ_C 179.4).

The configuration of the double bonds at C-4/C-5 and C-8/C-9 was assigned as *E* based on the large $^3J_{H\text{-}4,H\text{-}5}$ and $^3J_{H\text{-}8,H\text{-}9}$ coupling constants (15.5 Hz, 15.4 Hz) observed. The double bond at C-12/C-13 was also assigned as *E* based on NOESY correlations

from H-13 (δ_H 5.26) to H-11 (δ_H 3.67) and H-24 (δ_H 1.65) to H-23 (δ_H 0.85) and H-25 (δ_H 0.79). NOESY correlations from H-17 (δ_H 5.14) to H-15 (δ_H 3.64) and H-26 (δ_H 1.64) to H-25 (δ_H 0.79) and H-27 (δ_H 0.97) confirmed the *E* configuration at C-16/C-17 as well. Due to the linear nature of the compound, the relative stereochemistry could not be assigned to the remaining stereocentres within the molecule. Attempts at preparing benzyl esters (using 2-benzyloxy-1-methylpyridinium triflate according to the method of Poon[262]) to aid in crystallization were unsuccessful and thus only the planar structure is proposed.

Compound **8** was obtained as a white powder and the molecular formula was established as $C_{27}H_{46}O_7$ by HRESIMS (*m/z* 505.5863 $[M+Na]^+$) revealing five degrees of unsaturation (Figure 5.3, Table 5.3, Appendix Figures A.13 and A.14). Analysis of the NMR spectra revealed **2** was an analog of **1** and differed by an additional oxygenation. The loss of a methylene group and gain of an oxymethine localized the substitution to C-19 which was confirmed by COSY correlations between H-18 (δ_H 2.38)/H-19 (δ_H 3.46) and H-19/H-20 (δ_H 1.12). The remainder of the molecule was unchanged and all double bonds were assigned as *E* based on $^3J_{H\text{-}4,H\text{-}5}$ and $^3J_{H\text{-}8,H\text{-}9}$ coupling constants (15.6 Hz, 15.3 Hz) and NOESY correlations between H-13 (δ_H 5.27) to H-11 (δ_H 3.65) and H-24 (δ_H 1.63) to H-23 (δ_H 0.85) and H-25 (δ_H 0.80). NOESY correlations from H-17 (δ_H 5.22) to H-15 (δ_H 3.67) and H-26 (δ_H 1.65) to H-25 (δ_H 0.80) and H-27 (δ_H 1.03).

These two compounds are similar in structure to the linear polyketide cameronic acid from *Xylaria cubensis*[263] and have been named cameronic acid B and C. Compound **7** differs from cameronic acid A by the addition of an olefinic methyl group on C-12 and

8 differs by an additional hydroxyl group on C-19. Only the planar structure of cameronic acid has been proposed and thus no tentative assignments of stereochemistry were made. Cameronic acid A has no reported bioactivity. Due to limited quantities obtained of **8**, only **7** was tested for biological activity. Antimicrobial testing of **7** revealed activity against MRSA 3.10 + 1.76 µM, VRE 5.75 + 2.61 µM and *S. warneri* 5.94 + 2.78 µM. No cytotoxicity was observed against HTB-26 and MCF-7 breast cancer cell lines and HEKa and Vero cell lines (Figure 5.4). The specific antimicrobial activity observed make these molecules interesting for further investigation into their mode of action.

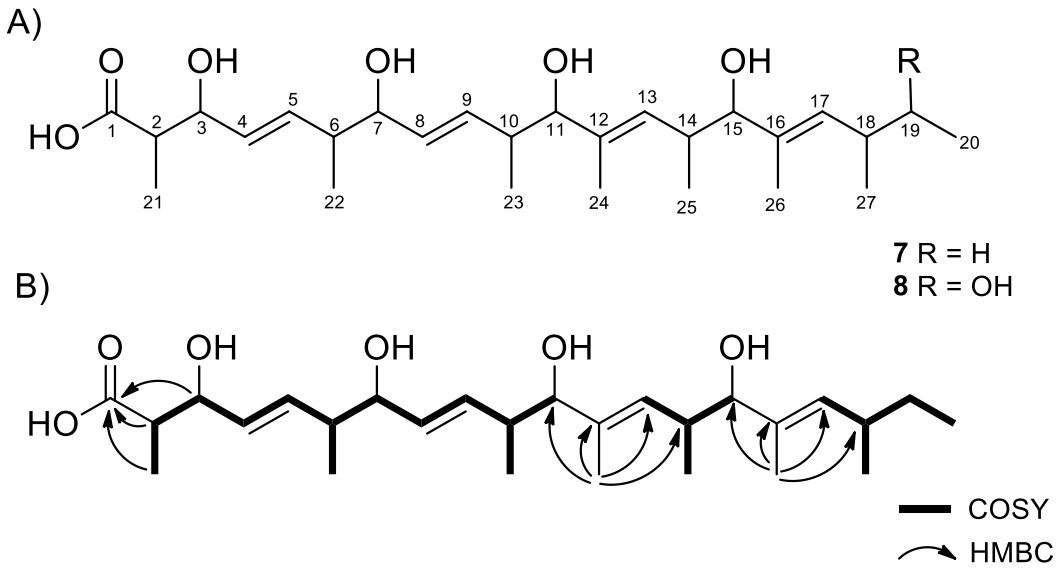

Figure 5.3. A) Molecular structure of cameronic acid B and C. **B)** Key NMR correlations of cameronic acid B.

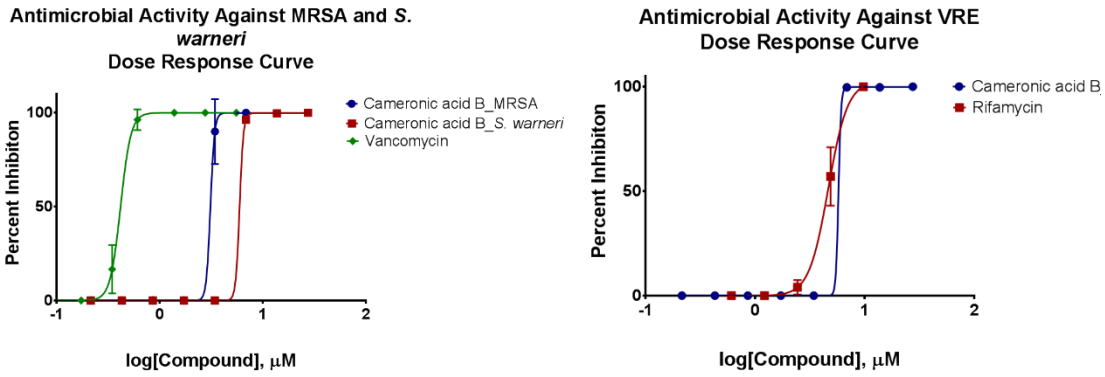

Figure 5.4. Antimicrobial activity of cameronic acid B.

Table 5.3. ^{1}H (600 MHz) and ^{13}C (150 MHz) NMR data of cameronic acid B (7) and cameronic acid C (8) in CD_3OD.

	Cameronic acid B (7)			Cameronic Acid C (8)
Position	δ_C, type	δ_H (J, Hz)	δ_C, type	δ_H (J, Hz)
1	179.4, C		181.6, C	
2	47.5, CH	2.45, m	47.9, CH	2.37, m
3	76.1, CH	4.14, dd (8.0, 8.0)	76.4, CH	4.08, dd (7.7, 7.7)
4	131.9, CH	5.45, dd (15.4, 7.8)	132.5, CH	5.46, dd (15.6, 7.4)
5	137.4, CH	5.68, dd (15.5, 8.1)	136.5, CH	5.68, dd (15.7, 7.8)
6	44.0, CH	2.26, m	43.8, CH	2.26, m
7	78.1, CH	3.85, dd (7.0, 7.0)	77.9, CH	3.86, dd (6.8, 6.8)
8	132.5, CH	5.50, dd (15.4, 7.7)	132.5, CH	5.51, dd (15.3, 7.5)
9	137.6, CH	5.63, dd (15.4, 8.1)	137.3, CH	5.64, dd (15.7, 7.8)
10	41.3, CH	2.33 [a]	41.2, CH	2.33, m
11	83.9, CH	3.67, d,(8.9)	83.9, CH	3.65, m
12	137.7, C		137.9, C	
13	133.9, CH	5.26, d, (9.4)	133.5, CH	5.27, d (9.4)
14	37.0, CH	2.62, m	37.0, CH	2.65, m
15	84.6, CH	3.64, d, (9.2)	83.9, CH	3.67, m
16	135.7, C		136.8, C	
17	136.5, CH	5.14, d, (9.4)	132.7, CH	5.22, d (8.8)
18	35.2, CH	2.34[a]	41.3, CH	2.38, m
19	31.6, CH_2	1.38, m 1.24,	72.8, CH	3.46, m
20	12.6, CH_3	0.87, t (7.4)	21.7, CH_3	1.12, d (6.4)
21	14.3, CH_3	1.07, d (7.1)	14.8, CH_3	1.08, d (7.2)
22	16.9, CH_3	0.99, d (6.9)	16.6, CH_3	0.98, d (7.1)
23	17.9, CH_3	0.85, d (6.7)	17.8, CH_3	0.85, d (6.8)
24	11.5, CH_3	1.65, s	11.4, CH_3	1.63, s
25	18.0, CH_3	0.79, d (6.8)	17.8, CH_3	0.80, d (6.4)
26	11.3, CH_3	1.64, s	11.4, CH_3	1.65, s
27	21.2 CH_3	0.97, d (6.7)	17.1, CH_3	1.03, d (6.4)

[a]overlapping

5.4. Conclusions

The fungal library described in Chapter 4 was investigated for the production of new NPs using an LC-HRMS based chemical dereplication strategy allowing for the rapid prioritization of isolates based on chemical novelty. Compared to traditional bioactivity guided fractionation which relies on the scale up and extensive purification of active fractions and late stage identification of active compounds, the use of LC-HRMS allows for deprioritization of isolates further upstream in the process, saving time and resources. LC-HRMS can also be paired with biological screening to further aid in the prioritization of isolates. In this case, isolates were prioritized solely on chemical novelty which led to the isolation of a new hirsutellic acid analog, two new cameronic acid analogs and a new reduced perylene quinone compound whose structural characterization was discussed within this chapter. The isolation of new decapeptides and peptaibols from new *Sesquicillium* species, cyclic heptapeptides from a new *Mortierella* species and tetramic acids from new *Tolypocladium* species are described in Chapters 6-8. The isolation of a large number of new compounds highlights the utility of chemical based dereplication methods and the tremendous resource Frobisher Bay is for new NPs.

CHAPTER 6: TAXONOMIC CHARACTERIZATION OF *SESQUICILLIUM* SPP. RKAG 186, 571 AND 627 AND ISOLATION OF NEW PEPTIDE NATURAL PRODUCTS

This chapter is a modification of the material submitted for publication as

Grunwald, A.G., Overy, D.P., and Kerr R. G. Tariuqins A-F, eleven residue peptaibols produced by Arctic fungi within the genus *Sesquicillium*. *J. Antibiot.* Submitted 2017.

6.1 Introduction

The fungal genus *Sesquicillium* has undergone numerous revisions over the last 50 years. The genus was originally described in 1968 by Gams, and species within were characterized by the ability to form conidia both from terminal cells of penicilliate conidiophores and from intercalary phialides with short lateral conidiogenous necks[264]. In 1971, additional species were described within *Sesquicillium* which were isolated from soil or Myxomycetes obtained from Canada. Additionally, *Verticillium microsporum* Jaap was transferred into this genus (originally isolated in 1916 from senescent Myxomycete sporangia) and renamed *Sesquicillium microsporum*[265]. In 1983 Bissett transferred *S. microsporum* to the genus *Tolypocladium* due to the similar micromorphology observed between this isolate and those of *Tolypocladium*[266]. In 1989 Samuels reclassified *Tolypocladium microsporum* back to *S. microsporum* and included several new members within the genus[267]. In 2001 Schroers, synonymized all but one member of *Sesquicillium* with *Clonostachys* due to the morphological similarities between both genera and 28S rRNA gene phylogenetic inferences. The remaining member, *S. microsporum* differed from the other *Sesquicillium* species by the size of its phialides and conidia and by having a partly myxomyceticolous lifestyle. Analysis of the 28S rRNA gen supported *S. microsporum* in a clade with two other myxomyceticolous species of *Nectriopsis* and revealed *S. microsporum* is closely related, but not congeneric with *Clonostachys*[268]. Currently *S. microsporum* is the only recognized member of the genus *Sesquicillium* and the recurring reclassification of this isolate based on morphology highlights a large issue in fungal taxonomy; morphological characterization alone is sometimes insufficient to delineate between fungal genera.

Peptides are a large group of NPs exhibiting enormous structural diversity and wide ranging biological activities. They can either be biosynthesized ribosomally and post translationally modified (RiPPs)[6] or synthesized nonribosomally by large multifunctional nonribosomal peptide synthetase (NRPS) enzymes. The immense diversity of nonribosomal peptides (NRPs) arises from the incorporation of non-proteogenic amino acids and through modifications including epimerization, oxygenation, methylation and glycosylation of the peptide scaffold. NRPs can either be linear, cyclic or branched cyclic allowing for even greater structural diversity[269,270].

Cyclic peptides comprise a large portion of NRPs and can cyclize in a variety of ways generating immense diversity. They can cyclize in a typical head to tail fashion between the alpha-amino group of the first residue and the carbonyl group of the final residue forming a peptide bond or by forming amide or ester linkages with amino acid side chains or lipids in a branched chain cyclization[269]. Due to the enormous diversity of cyclic peptides, a wide range of biological activities has been observed. Clinically relevant cyclic peptides include cyclosporin, an immunosuppressant used to prevent graft rejection[19] and the antibiotics tyrocidine, gramicidin and vancomycin[271,272,273].

Peptaibols are a large family of linear nonribosomally synthesized peptides discovered in 1967 from a culture of *Trichoderma virde*[274]. They are linear peptides of 5-21 amino acids, characterized by having an acetylated N-terminus, an amino alcohol on the C-terminus and containing a high proportion of the α,α-dialkylated amino acid α-aminoisobutyric acid (Aib). They are almost exclusively produced by soil-borne, plant pathogenic and fungicolous fungi within the phylum Ascomycota and most commonly produced by species within the genera *Trichoderma*, *Acremonium*, *Paecilomyces* and

Emericelliopsis[275,276]. Peptaibols exhibit wide ranging bioactivities including antifungal, antiviral, cytotoxic and antiparasitic, but are most well known for having potent activity against Gram-positive bacteria. Their range of activities is due to their amphipathic nature and helical secondary structure which allows them to disrupt the cell membrane by self-associating and forming pores within the lipid bilayer[277].

The aim of this work was to further characterize the putatively new *Sesquicillium* species isolated and described in Chapter 4 (RKAG 186, 571 and 627) and to evaluate these isolates for their NP production. The morphological and taxonomic characterization of these isolates will be discussed, in addition to the NPs produced by these isolates including the characterization of four new *N*-methylated cyclic decapeptides from *Sesquicillium* sp. RKAG 186 and six new 11-residue peptaibols from *Sesquicillium* sp. RKAG 186 and 571.

6.2 Experimental Procedures

6.2.1 Morphological Characterization

For morphological characterization, RKAG 571, 186 and 627 were grown on PDA, 2% malt extract agar (MEA), oatmeal agar (OA), 10% corn meal agar (CMA) and water agar plates and incubated at 15˚C and 22˚C. Once sporulating, samples were mounted in lactic acid to observe and measure conidia and conidiophores using either a Leica DME light microscope with phase contrast optics accompanied by a Leica EC3 camera (Leica Microsystems, Switzerland) or a brightfield microscope (Carl Zeiss microscope) with Axio Imager A1m model and a HRc Axiocam digital camera (Carl Zeriss, Heerbrugg, Switzerland). Growth rates were measured for seven days on PDA

and 2% MEA agar on plates and measured in mm from the centre of a point inoculation. Six replicate plates per temperature were incubated at 4˚C, 15˚C, 22˚C, 30˚C and 37˚C.

6.2.2 Phylogenetic Characterization

Sequencing of the ITS region and 28S rRNA gene is described in Chapter 4.2.5. ITS and 28S rRNA gene sequences were retrieved for reference strains from GenBank. Separate alignment of the ITS region and 28S rRNA gene was performed using MAFFT v. 6.822 using the L-INS-I alignment method for the ITS sequence and G-INS-I for the 28S rRNA gene[278] implemented in the CIPRES Science Gateway v. 3.3[279]. Both datasets were imported, trimmed and concatenated in MEGA v 6.06[124]. Maximum likelihood analysis was carried out on the concatenated dataset using RAxML v. 7.2.7[280] implemented within the CIPRES Science Gateway v. 3.3. Using Modeltest, the GTR+G was predicted to be the best model of evolution[133] which was applied separately for each partition. A total of 1000 bootstrap iterations were run.

6.2.3 Large-Scale Fermentation and Purification of Auyuittuqamide A-D and Tariuqin A and B

Sesquicillium sp. (RKAG 186) was inoculated into 15 mL of YM liquid and grown for five days (22°C, agitated at 200 rpm). The seed culture (200 µL) was used to inoculate the producing strain onto 50 Petri plates (100 x 15 mm) containing 20 mL of solid PDA agar and grown for 21 days at 22°C. The solid agar fermentations were pooled and repeatedly extracted with EtOAc. The extract was evaporated to dryness *in vacuo* and partitioned between 80% CH_3CN and 100% hexane. The CH_3CN layer was collected and evaporated to dryness *in vacuo* to give a crude extract (138 mg).

The extract was fractionated using automated reverse-phase flash chromatography (Combiflash Rf) with a linear gradient from 5% aqueous MeOH to 100% MeOH over 20 min with a flow rate of 30 mL/min on a 15.5 g C18 column (High Performance GOLD RediSep Rf) generating 6 fractions. Fraction 5 containing compounds **9-14** eluted between 14.5-15.5 min. RP-HPLC of fraction 5 (23 mg) using a Waters HPLC system coupled with an ELSD (Waters 2424) and PDA detector (Waters 2489), a flow rate of 3 mL/min, a Gemini 110Å C18 column (5 µm 250 x 10 mm, Phenomenex) and a 30 min isocratic elution with 55% aqueous CH_3CN resulted in the purification of **10** (2.1 mg), **11** (1.9 mg), **12** (2.2 mg) and **14** (0.7 mg) at 19, 28, 34 and 38 min respectively. A fraction eluting at 26.0 min contained a mixture of **9** and **13** (10.5 mg). After a successive round of RP-HPLC using a Luna 110 Å phenyl hexyl column (5 µm 250 x 10 mm, Phenomenex) and 30 min isocratic elution with 50% aqueous CH_3CN resulted in the separation of **5** (1.2 mg) and **1** (8 mg) at 17.2 and 27.3 min respectively.

Auyuittuqamide A (**9**) White powder; $[\alpha]_D^{23}$ -3.6 (*c* 0.1, MeOH); UV (MeOH) λ_{max} 222 nm; IR (film) V_{max} 3270, 2965, 1627, 1546, 1418, 1340, 1292, 1112, 1018 cm^{-1}; (+) HRESIMS *m/z* 1015.6201 $[M + H]^+$, (calcd. for $C_{50}H_{83}N_{10}O_{12}$, 1015.6187, Δ 1.38 ppm).

Auyuittuqamide B (**10**) White powder; $[\alpha]_D^{23}$ -4.9 (c 0.1, MeOH); UV (MeOH) λ_{max} 222 nm; IR (film) V_{max} 3282, 2960, 1632, 1547, 1470, 1417, 1386, 1350, 1205, 1138, 1026 cm^{-1}; (+) HRESIMS *m/z* 1001.6013 $[M + H]^+$, (calcd. for $C_{49}H_{81}NO_5$, 1001.6030, Δ 1.70 ppm.

Auyuittuqamide C (**11**) White powder; $[\alpha]_D^{23}$ -1.6 (*c* 0.1, MeOH); UV (MeOH) λ_{max} 222 nm; IR (film) V_{max} 32382, 2964, 1632, 1547, 1467, 1417, 1386, 1209, 1112 cm^{-1}; (+) HRESIMS *m/z* 1029.6342 $[M + H]^+$, (calcd. for $C_{51}H_{85}NO_4$, 1029.6343, Δ 0.01 ppm).

Auyuittuqamide D (**12**) White powder; $[\alpha]_D^{23}$ -1.8 (*c* 0.1, MeOH); UV (MeOH) λ_{max} 222 nm; IR (film) V_{max} 3273, 2963, 1629, 1548, 1465, 1417, 1112, 1016 cm^{-1}; (+) HRESIMS *m/z* 1043.6550 $[M + H]^+$, (calcd. for $C_{52}H_{87}NO_5$, 1043.6500, Δ 4.79 ppm).

Tariuqin A (**13**) White powder; $[\alpha]_D^{23}$ -3.2 (*c* 0.1, MeOH); UV (MeOH) λ_{max} 222, 279 nm; IR (film) V_{max} 3280, 2959, 1642, 1542, 1470, 1016 cm^{-1}; (+) HRESIMS *m/z* 1193.7893 $[M + H]^+$, (calcd. for $C_{58}H_{105}N_{12}O_{14}$, 1193.7868, Δ 2.09 ppm).

Tariuqin B (**14**) White powder; $[\alpha]_D^{23}$ -2.2 (*c* 0.1, MeOH); UV (MeOH) λ_{max} 222, 279 nm; IR (film) V_{max} 3280, 2955, 1640, 1545, 1470, 1014 cm^{-1}; (+) HRESIMS *m/z* 1179.7737 $[M + H]^+$, (calcd. for $C_{57}H_{103}N_{12}O_{14}$, 1179.7712, Δ 2.12 ppm).

6.2.4 Large-Scale Fermentation and Purification of Tariuqin C-F

Sesquicillium sp. RKAG 571 was inoculated into 15 mL of YM liquid seed and grown for five days (22°C, 200 rpm). The seed culture (200 µL) was used to inoculate the producing strain into 40 flasks (250 mL) containing rice medium and grown for 21 days at 22°C. The rice fermentations were repeatedly extracted with EtOAc and pooled. The extract was evaporated *in vacuo* and partitioned between 80% CH_3CN and 100% hexane. The CH_3CN layer was collected and evaporated *in vacuo* to give a crude extract (790 mg).

The crude extract was fractionated using automated reverse-phase flash chromatography (Combiflash Rf) with a linear gradient of 20% aqueous MeOH to 100% MeOH over 20 min on a 15.5 g C18 column (High Performance GOLD RediSep Rf)

with a flow rate of 30 mL/min generating 12 fractions. Fractions 7 and 8 contained almost pure destruxin E and B whose structures were confirmed by NMR. Fraction 10 containing compounds **15-18** eluted at 15 min. RP-HPLC of fraction 10 (40 mg) on a Waters HPLC system coupled with an ELSD (Waters 2424) and PDA detector (Waters 2489), a flow rate of 3 mL/min and using a Gemini 110Å C18 column (5µm 250 x 10 mm, Phenomenex) and a 30 min isocratic elution with 55% aqueous MeOH resulted in the purification of **15** (4.2 mg), **16** (4.5 mg), **17** (3.9 mg) and **18** (4.6 mg) at 19.0, 16.5, 25.0 and 21.1 min.

Tariuqin C (**15**) White powder; $[\alpha]_D^{23}$ -4.0 (*c* 0.1, MeOH); UV (MeOH) λ_{max} 222 nm; IR (film) V_{max} 3321, 2959, 1644, 1599, 1540, 1471, 1386, 1352, 1174, 1087 cm^{-1}; (+) HRESIMS *m/z* 1213.7543 $[M + H]^+$, (calcd. for $C_{60}H_{101}N_{12}O_{14}$, 1213.7555, Δ 0.99 ppm).

Tariuqin D (**16**) White powder; $[\alpha]_D^{23}$ -1.7 (*c* 0.1, MeOH); UV (MeOH) λ_{max} 222 nm; IR (film) V_{max} 3308, 2960, 1646, 1539, 1467, 1386, 1171, 1077 cm^{-1}; (+) HRESIMS *m/z* 1199.7407 $[M + H]^+$, (calcd. for $C_{59}H_{99}N_{12}O_{14}$, 1199.7399, Δ 0.67 ppm).

Tariuqin E (**17**) White powder; $[\alpha]_D^{23}$ -3.2 (c 0.1, MeOH); UV (MeOH) λ_{max} 222 nm; IR (film) V_{max} 3301, 2960, 1645, 1537, 1463, 1385, 1170, 1077 cm^{-1}; (+) HRESIMS *m/z* 1197.7631$[M + H]^+$, (calcd. for $C_{60}H_{101}N_{12}O_{13}$, 1197.7606, Δ 2.09 ppm).

Tariuqin F (**18**) White powder; $[\alpha]_D^{23}$ -2.8 (*c* 0.1, MeOH); UV (MeOH) λ_{max} 222 nm; IR (film) V_{max} 3293, 2960, 1645, 1538, 1456, 1385, 1172, 1044 cm^{-1}; (+) HRESIMS *m/z* 1183.7451 $[M + H]^+$, (calcd. for $C_{59}H_{99}N_{12}O_{13}$, 1183.7450, Δ 0.08 ppm).

6.2.5 Stereochemical Assignment by Marfey's Analysis

The absolute configuration of the amino acids within **9**-**18** was determined using Marfey's method[281]. Briefly, a portion (0.25 mg) of **9**-**18** were dissolved in 70 µL of acetone-H_2O (1:1), treated with 2 N aqueous HCl (60 µL) at 100˚C for 2 h and neutralized with 1 M $NaHCO_3$ solution. *N*-(5-fluoro-2,4,-dinitrophenyl-5)-L-alaninamide (FDAA, 0.4 mg in 380 µL of acetone) was added to the reaction mixture and stirred at 37˚C for 2 h. The reaction was quenched with 1 N aqueous HCl (80 µL), MeOH was added (590 µL) and the sample was analyzed by LC-HRMS using a Hypersil Gold 100 Å column (Thermo, 1.9 µm C_{18} 50 mm × 2.1 mm) and a flow rate of 400 µL/min using the following method: 0-55 min 95% H_2O/0.1% formic acid (solvent A) and 5% CH_3CN/0.1% formic acid (solvent B) to 60% solvent A and 40% solvent B, 55-57 min 60% solvent A:40% solvent B to 100% solvent B, 57-60 min 100% solvent B. Amino acid standards (0.25 mg) were dissolved in acetone-H_2O (1:1) and derivatized with FDAA and analyzed as described above. The retention times were compared with derivatized amino acid standards to determine the configuration of amino acids.

6.3 Results and Discussion

6.3.1 Phylogenetic Analysis

Three isolates (RKAG 186, 571 and 627) were obtained from sediment collected from Frobisher Bay as described in Chapter 4. BLASTn of the ITS region determined these isolates were most similar to *Sesquicillium microsporum* NRRL 54127 (GU219471.1) (RKAG 186 98.4%, RKAG 571 96.5% and RKAG 627 96.4% sequence similarity), *Nectriopsis rexiana* CBS 542.92 (KU382178.1) (RKAG 186 97.0%, RKAG 571 96.5% and RKAG 627 96.1% sequence similarity) and other members within the

Bionectriaceae family. BLASTn of the 28S rRNA gene revealed these isolates were most similar to *S. microsporum* (RKAG 186 99.9%, RKAG 571 98.9% and RKAG 627 98.9% sequence similarity) and other members within the *Bionectriaceae* family. A multigene phylogeny was constructed using the maximum likelihood method with a GTR+G model of nucleotide substitution (Figure 6.1)[134,133]. Due to members within the *Bionectriaceae* family not being well represented in GenBank, only the ITS and 28S rRNA gene were included in the construction of this phylogeny. Maximum likelihood analysis revealed *Sesquicillium microsporum* clustered within the genus *Nectriopsis* and formed a clade with RKAG 186, 571 and 627. Based on the phylogenetic relationship, these isolates are proposed to be new members within the genus *Sesquicillium*.

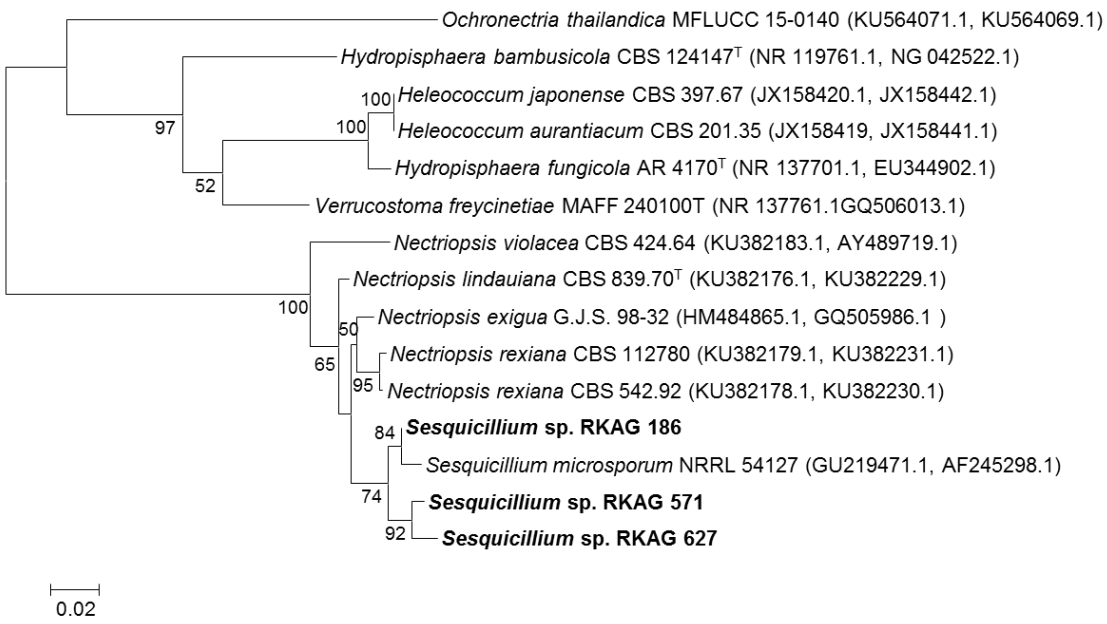

Figure 6.1. Maximum likelihood analysis of the family *Bionectriaceae* using 600 aligned nucleotides of the ITS region and 670 aligned nucleotides of the 28S rRNA gene. The GTR+G model of nucleotide substitution was used and 1,000 bootstrap iterations. Only confidence values above 50% are denoted. The phylogram is midpoint rooted.

6.3.2 Phenotypic Characterization

The genus *Sesquicillium* falls within the order Hypocreales within the phylum Ascomycota and contains only one recognized member, *Sesquicillium microsporum*. *S. microsporum* has previously been isolated from Canada from forest soil collected near Petawawa, ON and from various slime moulds (*Physarum*, *Craterium* and *Didymium*)[266]. *S. microsporum* is described by Bissett as having white colonies that are farinose to densely floccose and a reverse that is white or pale yellow. Colonies reach a diameter of 18-35 mm after 10 days growth at 22˚C. Hyphae are 0.8-2.4 µm wide. Conidiophores are cylindrical, verticilliately branched, 1.8-2.9 µm at the base and up to 120 µm long. Phialides (6.5-15 x 1.4-2.3 µm) can either be terminal or intercalary, are nearly cylindrical or slightly swollen basally and narrow to a neck 0.5 µm wide. Phialides are either solitary or found in verticils of two to five. Conidia are one celled, hyaline, smooth walled, usually asymmetrically flattened 1.8-2.5 x 1.3-1.7 µm (avg. 2.1-1.5 µm) and often have a minute apiculum present[266].

Colonies of *Sesquicillium* sp. RKAG 186 were farinose, white on the front and pale yellow on the reverse (Figure 6.2). After 10 days, colonies were 15-20 mm in diameter at 22˚C and 14-18 mm in diameter at 15˚C on 2% MEA (Figure 6.3). The appearance of conidiophores and conidiospores appeared after several days when grown on PDA. Conidiophores were cylindrical and produced solitary phialides or phialides in verticils of two. Phialides were 9-18 µm in length, 1.1-1.5 µm wide and tapered to a conidiogenous neck with a width of 0.6-1.2 µm. Conidia were one celled, obovoid to globose, measuring 1.9-2.4 µm in length and 1.8-2.4 µm in width with some having the presence of a minute apiculum. The morphology of this isolate was consistent with the

description of *S. microsporum*, although the conidia observed were obovoid as opposed to asymmetrically flattened.

Colonies of *Sesquicillium* sp. RKAG 571 were farinose, white on the front and pale yellow in colour on the reverse. Colonies exhibited slow growth on PDA and 2% MEA, attaining a colony diameter of 23-30 mm after 10 days at 15˚C on 2% MEA. At 22˚C the colony diameter ranged from 12-16 mm after 10 days. Limited growth was observed at 4˚C and no growth was observed at 30˚C. On PDA and CMA medium good mycelial growth was observed and the appearance of conidiophores and conidiospores appeared after a few days. The conidiophores were smooth walled, cylindrical, frequently branched and up to 100 µm in length. Phialides were solitary or in verticils of two and 10-25 µm in length x 1.3x 1.7 µm in width, tapering to a conidiogenous neck about 1.1-1.5 µm wide and producing solitary conidia. Conidia were oblong-elliptical and measured 2.9-3.4 x 1.6-2.4 µm. The main differences between RKAG 571 and *S. microsporum* is the size (3.1 x 2.0 µm vs. 2.1 x 1.5 µm) and shape of the conidia (oblong-elliptical vs. asymmetrically flattened) and the growth rate at 22˚C (12-16 mm vs 18-35 mm).

Colonies of RKAG 627 exhibited slow growth on PDA and 2% MEA, attaining an average colony diameter of 27-33 mm after 10 days at 15˚C on 2% MEA and 11-15 mm on 2% MEA at 22˚C. Limited growth was observed at 4˚C and no growth observed at 30˚C. The colonies were floccose, white to light orange in colour on the front and pale yellow to light orange on the reverse. On PDA and CMA medium good mycelial growth was observed and the appearance of conidiophores and conidiospores appeared after a

few days. The conidiophores were smooth walled, cylindrical and frequently branched up to a length of 75 µm producing phialides that were either solitary or most often in verticils up to three. The phialides were 14-20 µm in length, 1.5-2.2 µm in width, tapering to a conidiogenous neck about 0.7-1.2 µm wide and bearing a single terminal conidium. Conidia were sub globose to broadly obovoid and measured 1.8-2.5 x 1.3-1.7 µm. RKAG 627 differs from *S. microsporum* by the growth rate observed at 22˚C (11-15 mm vs 18-35 mm), phialide length (12-20 µm vs 6.5-15 µm) and size of the conidia (2.2 x 2.0 vs. 2.1 x 1.5 µm).

Based on phylogenetic and morphological considerations, RKAG 571 and 627 may represent new species within the genus *Sesquicillium*. Within GenBank sequence information is only available for *S. microsporum* NRRL 54127 obtained from Hawaii. This isolate does not represent the type strain for *S. microsporum* making phylogenetic inferences from this sequence data challenging. Due to a lack of sequenced genes for the type strain of *S. microsporum* within GenBank, assignment of these isolates as new species is tentative.

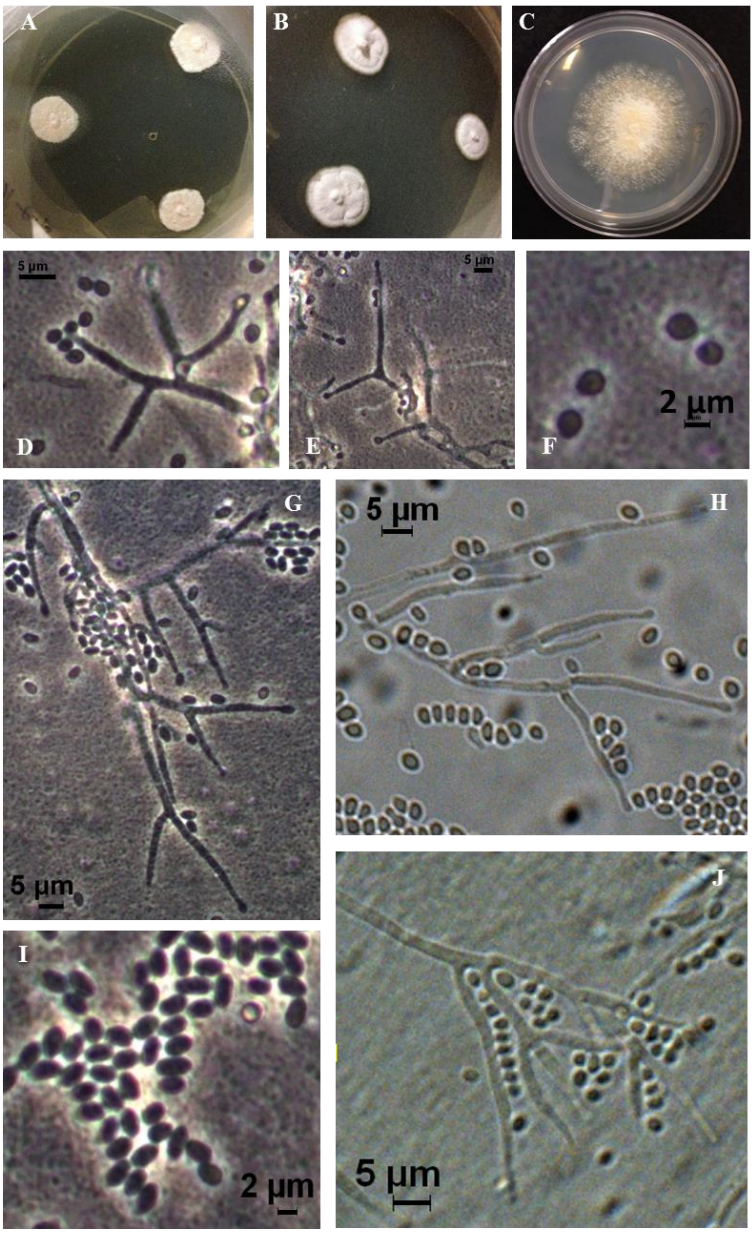

Figure 6.2. Phenotypic observations of RKAG 186, 571 and 627. **A)** Colony morphology of RKAG 571 on PDA medium. **B)** Colony morphology of RKAG 186 on PDA medium. **C)** Colony morphology of RKAG 627 grown on YM medium. **D-F)** Conidiophores, phialides and conidia of RKAG 186 on PDA. **G-I)** Conidiophores, phialides and conidia of RKAG 571 on 10% CMA. **J)** Conidiophores, phialides and conidia of RKAG 627 on 10% CMA.

A)

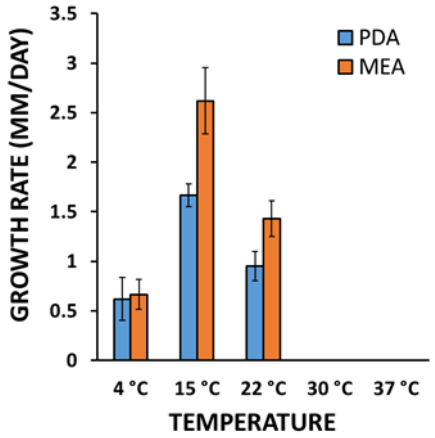

B)

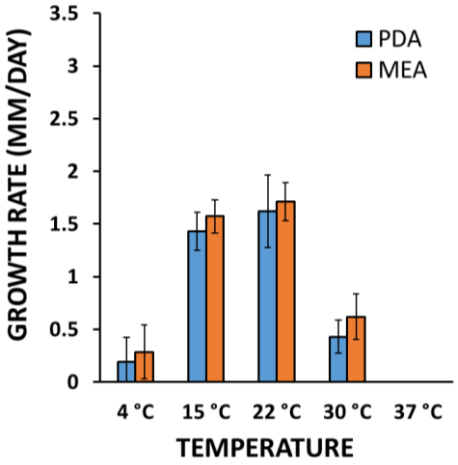

C)

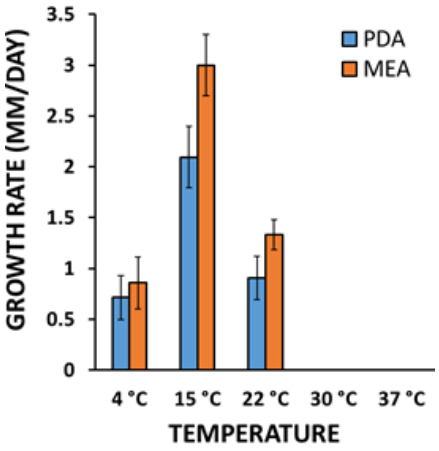

Figure 6.3. Average growth rates for *Sesquicillium* sp. RKAG 571, 186 and 627 on PDA and 2% MEA. **A)** RKAG 186. **B)** RKAG 571. **C)** RKAG 627.

6.3.3 Natural Products Characterization

Due to the potential of these isolates to be new members within the genus *Sesquicillium* and a lack of reported NPs from this genus, further chemical investigation was undertaken. The initial small scale fermentations and LC-HRMS analysis of RKAG 186, 571 and 627 was discussed in Chapter 5. Based on this preliminary analysis, all three isolates were producing putatively new compounds.

6.3.3.1 Structure Elucidation of Auyuittuqamide A-D from *Sesquicillium* sp. RKAG 186

The solid agar fermentation of *Sesquicillium* sp. RKAG 186 was extracted with EtOAc, dried *in vacuo*, and partitioned between 80% CH_3CN and 100% hexane. The CH_3CN soluble portion was subjected to flash chromatography and RP HPLC yielding four new cyclic heptapeptides, auyuittuqamide A (**9**) (4 mg), B (**10**) (1.5 mg), C (**11**) (3 mg) and D (**12**) (2 mg) and two new peptaibols, tariuqin A (**13**) (1.2 mg) and B (**14**) (0.7 mg). Both compounds were named after Inuktitut words whereby auyuittuqamide was named after the Inuktitut word "auyuittuq" (the land that never melts) and tariuqin was named after the Inuktitut word "tariuq" (the sea).

Auyuittuqamide A (**10**) (Figure 6.4, Table 6.1, Appendix Figures A.15 and A.16) was obtained as a white powder and HRESIMS supported a molecular formula of $C_{50}H_{82}N_{10}O_{12}$ (*m/z* 1015.6201 $[M + H]^+$), requiring 15 degrees of unsaturation. The peptidic nature of the compound was determined by analysis of the ^1H NMR spectrum which revealed the presence of seven amide protons and three *N*-methyl amide substituents (2.78, 3.16, 3.24) while the ^{13}C NMR spectrum revealed the presence of 10 amide carbonyls between δ_C 167.6-173.3 ppm and 10 α-amino acid carbon resonances between δ_C 43.0-70.2. Analysis of the COSY, HMBC and TOCSY spectra confirmed

the identity of the amino acid constituents and revealed the presence of two Val, two Gly, one Ser, one Ile, one Leu, one *N*-Me-Phe, one *N*-Me-Val and one *N*-Me-Thr residue within the molecule. In order to account for the remaining degree of unsaturation, it was determined this compound must be cyclic. There were three options for the mechanism of cyclization, either it could cyclize between the *N* and C-terminal amino acids in a peptide bond or cyclize at the *C*-terminal amino acid and the hydroxy of the Thr or Ser side chain in an ester linkage. Due to the presence of free hydroxyl groups for the Ser (δ_H 4.86) and Thr (δ_H 4.67) side chains, it was determined that this molecule cyclized in a peptide bond between the *N*-terminal and *C*-terminal amino acids.

The order of the amino acids was determined using HMBC and ROESY correlations. HMBC correlations from Val1 NH (δ_H 8.70) to *N*-Me-Thr CO (δ_C 169.0), *N*-Me-Thr H_3 (δ_H 3.15) to Leu-CO (δ_C 173.4), Leu NH (δ_H 7.46) to Gly2 CO (δ_C 168.3), and Gly2 NH (δ_H 7.45) to *N*-Me-Val CO (δ_C 169.5) established the five amino acid sequence *N*-Me-Val-Gly2-Leu-*N*-Me-Thr-Val1. HMBC correlations from Ile NH (δ_H 7.44) to Gly1 CO (δ_C 167.7), Gly1 NH (δ_H 7.76) to *N*-Me-Phe CO (δ_C 169.9) established the three amino acid fragment Val2-Gly1-*N*-Me-Phe. A third fragment (Ser-Val2) was established by HMBC correlations from Val2 NH (δ_H 8.91) to Ser CO (δ_C 170.2). Due to the overlapping carbonyl chemical shifts of Val1, Val2 and Ile (δ_C 171.6-171.7), the three fragments could not be definitively connected through HMBC correlations. ROESY correlations from *N*-Me-Val H_3 (δ_H 3.25) to Val2 Hα (δ_H 4.53), Ser NH (δ_H 8.57) to Ile Hα (δ_H 4.42) and *N*-Me-Phe H_3 (δ_H 2.77) to Val1 Hα (δ_H 4.48) connected all three fragments as a cyclic peptide whose final structure was revealed to be cyclo [-*N*-

Me-Thr-Val-*N*-Me-Phe-Gly-Ile-Ser-Val-*N*-Me-Val-Gly-Leu-]. MS/MS analysis confirmed the sequence of the peptide (Appendix Figure A.17).

Auyuittuqamide B (**10**) (Figure 6.1, Table 6.1 and Appendix Figures A.18 and A.19) was obtained as a white powder and HRESIMS supported a molecular formula of $C_{49}H_{80}N_{10}O_{12}$ (*m/z* 1001.6013 $[M + H]^+$), requiring 15 degrees of unsaturation. The ^1H NMR spectrum was very similar to that of **9** and indicated **10** was an analog of **9** that differed by the absence of a methylene group. Analysis of the COSY and TOCSY spectra indicated the Ile residue was replaced by a Val residue. HMBC correlations from Val2 NH (δ_H 7.41) to Gly1 CO (δ_C 167.8) and ROESY correlations from Ser NH (δ_H 8.59) to Val2 Cα (δ_H 4.38) confirmed the new Val residue had replaced the Ile residue in the same position. The identity and sequence of the other amino acids was confirmed by NMR analysis and MS/MS analysis to be identical to **9** (Appendix Figure A.20). Therefore **10** was assigned as cyclo [-*N*-Me-Thr-Val-*N*-Me-Phe-Gly-Val-Ser-Val-*N*-Me-Val-Gly-Leu-].

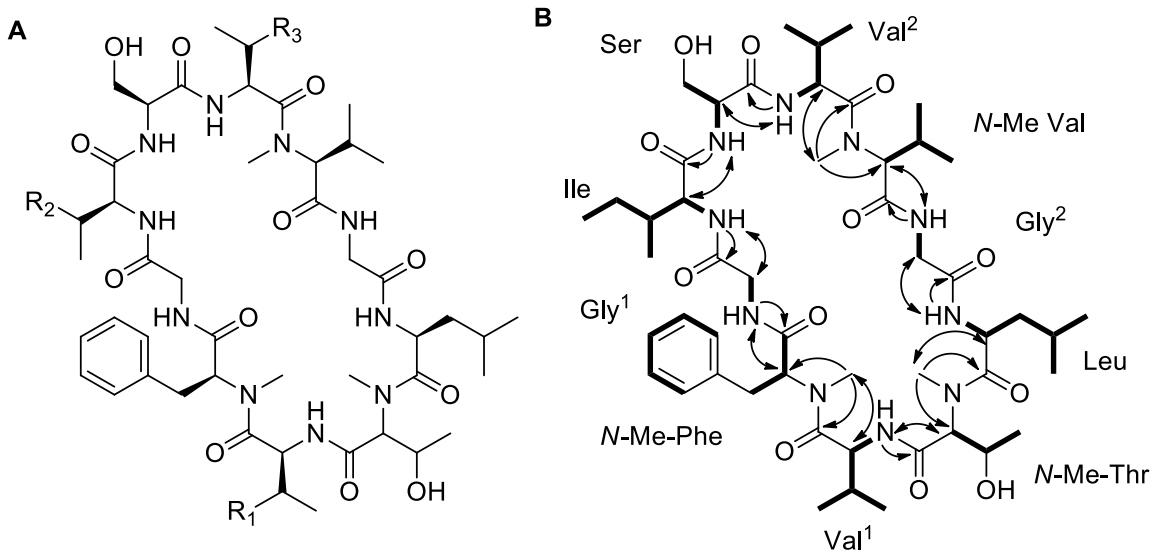

9 R_1 = H R_2 = CH_3 R_3 = H
10 R_1 = H R_2 = H R_3 = H
11 R_1 = H R_2 = CH_3 R_3 = CH_3
12 R_1 = CH_3 R_2 = CH_3 R_3 = CH_3

Figure 6.4. A) Structure of auyuittuqamides A-D. **B)** Key NMR correlations to determine the structure of auyuittuqamide A.

Auyuittuqamide C (**11**) (Figure 6.1, Table 6.2, Appendix Figures A.21 and A.22) was obtained as a white powder and HRESIMS supported a molecular formula of $C_{49}H_{80}N_{10}O_{12}$ (*m/z* 1029.6342 $[M + H]^+$), requiring 15 degrees of unsaturation. The ^1H NMR spectrum was very similar to that of **9** and indicated **11** was an analog of **9** that differed by the presence of a methylene group. Analysis of the COSY and TOCSY spectra indicated that one of the Val residues was replaced by an Ile residue. HMBC correlations from Ile1 NH (δ_H 8.63) to *N*-Me-Thr CO (δ_C 168.8) and ROESY correlations from *N*-Me-Phe (δ_H 2.77) to Ile1 Cα (δ_H 4.59) confirmed the position of the new Ile residue. The identity and sequence of the other amino acids was confirmed by NMR analysis and MS/MS analysis to be identical to **9** (Appendix Figure A.23). Therefore **11** was assigned as cyclo [-*N*-Me-Thr-Ile-*N*-Me-Phe-Gly-Val-Ser-Val-*N*-Me-Val-Gly-Leu-].

Auyuittuqamide D (**12**) (Figure 6.1, Table 6.2 and Appendix Figures A.24 and A.25) was obtained as a white powder and HRESIMS supported a molecular formula of $C_{49}H_{80}N_{10}O_{12}$ (*m/z* 1043.6550 $[M + H]^+$), requiring 15 degrees of unsaturation. The ^1H NMR spectrum was very similar to that of **11** and indicated **12** differed by the presence of a methylene group which corresponded to the replacement of the final Val residue with an Ile residue. HMBC correlations from Ile3 NH (δ_H 8.85) to Ser CO (δ_C 170.0) and ROESY correlations from *N*-Me-Val H_3 (δ_H 3.27) to Ile3 Cα (δ_H 4.69) confirmed the positon of the Ile. The identity and sequence of the remaining amino acids was confirmed by NMR analysis and MS/MS analysis to be identical to **11** (Appendix Figure A.26). Therefore **12** was assigned as cyclo [-*N*-Me-Thr-Ile-*N*-Me-Phe-Gly-Val-Ser-Ile-*N*-Me-Val-Gly-Leu-].

Table 6.1. ^{1}H (600 MHz) and ^{13}C (150 MHz) NMR data of auyuittuqamide A (9) and auyuittuqamide B (10) in DMSO-d_6.

Auyuittuqamide A			**Auyuittuqamide B**		
Position	δ_C, type	δ_H (J/Hz)	Position	δ_C, type	δ_H (J/Hz)
***N*-Me-Thr**			***N*-Me-Thr**		
CO	169.2, C		CO	169.0, C	
N-CH_3	30.4, CH_3	3.16, s	*N*-CH_3	30.6, CH_3	3.15, s
α	61.5, CH	5.03, d (9.8)	α	61.7, CH	5.04, d (9.7)
β	62.6, CH	3.89, m	β	62.9, CH	3.89, m
γ	20.3, CH3	0.89, d (6.0)	γ	20.5, CH_3	0.89, d (6.1)
OH		4.67			4.66
Val			**Val**		
CO	171.5, C		CO	171.6, C	
NH		8.71, d (9.5)	NH		8.70, d (9.4)
α	52.7, CH	4.48, m	α	52.9, CH	4.48, m
B	30.3, CH	1.91, m	β	30.7, CH	1.90, m
γ1	19.2, CH_3	0.79, d (6.6)	γ1	19.3, CH_3	0.78, m
γ2	17.5, CH_3	0.72, d (6.7)	γ2	17.6, CH_3	0.73, d (6.7)
***N*-Me-Phe**			***N*-Me-Phe**		
CO	170.2, C		CO	169.9, C	
N-CH_3	39.1, CH_3	2.78, s	*N*-CH_3	39.2, CH_3	2.77, s
α	66.5, CH	3.93, dd (10.4, 4.1)	α	66.6, CH	3.93, dd (10.3, 4.1)
β_A	33.6, CH_2	3.36, m	β_A	33.9, CH_2	3.33, m
β_B		2.98, dd (10.4, 14.1)	β_B		2.97, dd (14.0, 10.3)
1’	139.0, C		1’	138.9, C	
2’	128.1, CH	7.28, m	2’	128.3, CH	7.28, m
3’	129.0, CH	7.24, m	3’	129.2, CH	7.23, m
4’	126.1, CH	7.21, m	4’	126.3, CH	7.21, m
Gly			**Gly**		
CO	167.8, C		CO	167.7, C	
NH		7.82 t (5.6)	NH		7.76, t 5.5
α	42.6, CH_2	3.80, m	α	42.8, CH_2	3.79, dd (16.9, 4.8)
		3.17, m			3.17, m
Val			**Ile**		
CO	171.5, C		CO	171.7, C	
NH		7.41, d (9.9)	NH		7.44, m
α	56.0, CH	4.38, dd (9.9, 7.9)	α	54.9, CH	4.42, m
β	31.4, CH	1.99 (m)	β	37.4, CH	1.84, m
γ1	18.8, CH_3	0.84 (m)	$\gamma 1_A$	23.6, CH_2	1.46, m
γ2	18.8, CH_3	0.84, m	$\gamma 1_B$		1.20, m
			γ2	15.0, CH_3	0.81, m
			δ	10.5, CH_3	0.77, m
Ser			**Ser**		
CO	170.8, C		CO	170.2, C	
NH		8.59, d (7.1)	NH		8.57, d (7.2)

α	55.0, CH	4.57, m	α	55.2, CH	4.60, m
β1	60.4, CH_2	3.67, m	β	60.7, CH_2	3.67, dd (10.0, 7.4)
β2		3.48, m			3.48, dd (10.0, 7.8)
OH		4.86, s			4.86, s
Val			**Val**		
CO	171.4, C		CO	171.6, C	
NH		8.90, d (9.9)	NH		8.91, d (9.8)
α	53.9, CH	4.54, m	α	54.1, CH	4.53, m
β	29.6, CH	2.02, m	β	30.0, CH	2.01, m
γ1	18.8, CH_3	0.84, m	γ1	19.5, CH_3	0.84, m
γ2	18.8, CH_3	0.84, m	γ2	18.1, CH_3	0.83, m
***N*-Me-Val**			***N*-Me-Val**		
CO	169.6, C		CO	169.5, C	
N-CH_3	40.0, CH_3	3.24, s	*N*-CH_3	40.0, CH_3	3.25, s
α	69.9, CH	3.29, m	α	70.2, CH	3.30, m
β	27.1, CH	2.50, m	β	27.5, CH	2.50, m
γ1	21.6, CH_3	1.04, d (6.6)	γ1	21.8, CH_3	1.04, d (6.6)
γ2	18.8, CH_3	0.84, m	γ2	19.3, CH_3	0.83, m
Gly			**Gly**		
CO	168.5, C		CO	168.3, C	
NH		7.51, dd (6.4, 5.9)	NH		7.45, m
α	42.6, CH_2	3.85, dd (17.0, 6.4)	α	43.0, CH_2	3.84, m
		3.31, m			3.36, m
Leu			**Leu**		
CO	173.2, C		CO	173.4, C	
NH		7.43, d (9.2)	NH		7.46, m
α	45.9, CH	4.92, m	α	46.3, CH	4.91, m
β	40.2, CH_2	1.64, m	β	40.5, CH_2	1.65, m
		1.17, m			1.17, m
γ	23.4, CH	1.62, m	γ	23.8, CH	1.63, m
δ1	21.1, CH_3	0.84, m	δ1	21.3, CH_3	0.84, m
δ2	21.1, CH_3	0.84, m	δ2	23.2, CH_3	0.82, m

Table 6.2. ^{1}H (600 MHz) and ^{13}C (150 MHz) NMR data of auyuittuqamide C (11) and auyuittuqamide D (12) in DMSO-*d*$_6$.

Auyuittuqamide C			**Auyuittuqamide D**		
Position	δ_C, type	δ_H (*J*, Hz)	Position	δ_C, type	δ_H (*J*, Hz)
***N*-Me-Thr**			***N*-Me-Thr**		
CO	168.8, C		CO	168.7, C	
N-CH_3	30.5, CH_3	3.14, s	*N*-CH_3	30.6, CH_3	3.16, s
α	61.4, CH	5.09, d (9.8)	α	61.3, CH	5.16, d (9.8)
β	62.8, CH	3.89, m	β	62.9, CH	3.87, dd (9.7, 6.2)
γ	20.3, CH_3	0.87, m	γ	20.0, CH_3	0.86, m
OH		4.66	OH		4.67
Ile			**Ile**		
CO	171.7, C		CO	171.7, C	
NH		8.63, d (9.5)	NH		8.57, m
α	51.4, CH	4.59, m	α	51.3, CH	4.60, m
β	36.4, CH	1.72, m	β	36.6, CH	1.68, m
γ1$_A$	23.6, CH_2	1.37, m	γ1$_A$	23.2, CH_2	1.37, m
γ1$_B$		0.98, m	γ1$_B$		1.00, m
γ2	15.2, CH_3	0.73, m	γ2	15.3, CH_3	0.73, d (6.6)
δ	9.9, CH_3	0.71, m	δ	10.1, CH_3	0.71, d (7.6)
***N*-Me-Phe**			***N*-Me-Phe**		
CO	169.9		CO	169.9	
N-CH_3	39.2, CH_3	2.82, s	*N*-CH_3	40.0, CH_3	2.79, s
α	66.6, CH	3.97, dd (10.2, 4.1)	α	66.5, CH	3.98, dd (10.3, 4.3)
β$_A$	34.0, CH_2	3.38, dd (14.1, 4.1)	β$_A$	34.0, CH_2	3.38, dd (14.1, 4.1)
β$_B$		2.99, dd (14.1, 10.2)	β$_B$		3.01, dd (14.1, 10.3)
1’	139.0, C		1’	138.9, C	
2’	128.2, CH	7.27, m	2’	128.2, CH	7.27, m
3’	129.2, CH	7.24, m	3’	129.2, CH	7.23, m
4’	126.3, CH	7.21, m	4’	126.3, CH	7.21, m
Gly			**Gly**		
CO	167.6, C		CO	167.7, C	
NH		7.84, t (5.6)	NH		7.90, t (5.6)
α	43.1, CH_2	3.76, dd (16.8, 4.8)	α	43.1, CH_2	3.75, dd (16.9, 4.9)
		3.15, m			3.18, m
Ile			**Ile**		
CO	171.6, C		CO	171.3, C	
NH		7.42, d (9.8)	NH		7.45, d (9.8)
α	54.9, CH	4.42, dd (9.8, 8.5)	α	55.1, CH	4.44, dd (9.8, 8.1)
β	37.4, CH	1.83, m	β	37.6, CH	1.81, m
γ1$_A$	23.8, CH_2	1.47, m	γ1$_A$	23.3, CH_2	1.49, m
γ1$_B$		1.18, m	γ1$_B$		1.16, m
γ2	15.0, CH_3	0.81, d (6.9)	γ2	15.0, CH_3	0.82, m

δ	10.5, CH_3	0.77, m	δ	10.7, CH_3	0.79, m
Ser			**Ser**		
CO	170.2, C		CO	170.0, C	
NH		8.58, d (7.2)	NH		8.57, m
α	55.3, CH	4.63, m	α	54.8, CH	4.79, m
β	60.6, CH_2	3.66, dd (10.3, 6.9)	β	60.8, CH_2	3.61, dd (10.4, 6.7)
		3.48, dd (10.3, 7.9)			3.45, dd (10.3, 8.0)
OH		4.84	OH		4.85
Val			**Ile**		
CO	171.5, C		CO	171 .6, C	
NH		8.91, d (9.8)	NH		8.85, d (9.7)
α	54.1, CH	4.55, m	α	52.2, CH	4.69, m
β	30.0, CH	2.01, m	β	35.9, CH	1.87, m
γ1	19.6, CH_3	0.85, m	$\gamma 1_A$	23.6, CH_2	1.49, m
γ2	18.0, CH_3	0.83, m	$\gamma 1_B$		1.16, m
			γ2	15.5, CH_3	0.82, m
			δ	10.3, CH_3	0.78, m
***N*-Me-Val**			***N*-Me-Val**		
CO	169.5, C		CO	169.4, C	
N-CH_3	40.4, CH_3	3.24, s	*N*-CH_3	40.6, CH_3	3.27, s
α	70.2, CH	3.30, m	α	70.1, CH	3.31, m
β	27.5, CH	2.50, m	β	27.7, CH	2.50, m
γ1	21.8, CH_3	1.04, d (6.6)	γ1	21.8, CH_3	1.03, d (6.7)
γ2	19.3, CH_3	0.84, m	γ2	19.3, CH_3	0.86, m
Gly			**Gly**		
CO	168.4, C		CO	168.3, C	
NH		7.58, m	NH		7.59, m
α	42.8, CH	3.83, dd (17.1, 6.3)	α	42.9, CH	3.82, dd (17.0, 6.1)
		3.32, m			3.31, m
Leu			**Leu**		
CO	173.2, C		CO	173.3, C	
NH		7.46, d (9.1)	NH		7.51, d (9.1)
α	46.3, CH	4.94, m	α	46.2, CH	4.94, m
β	40.5, CH_2	1.69, m	β	40.8, CH_2	1.66, m
		1.13, m			1.23, m
γ	23.7, CH	1.65, m	γ	23.7, CH	1.65, m
δ1	21.2, CH_3	0.85, m	δ1	21.5, CH_3	0.85, m
δ2	23.3, CH_3	0.83, m	δ2	23.2, CH_3	0.84, m

The absolute configuration of the amino acids of **9-12** was determined using Marfey's method. All amino acids were determined to be in the L-configuration (Appendix Figure A.27 and A.28). Due to a lack of availability of *N*-Me-Thr standards, the absolute configuration of this amino acid could not be determined. In an attempt to determine the configuration, a single crystal of **9** was obtained and has been submitted for X-ray crystallography to Dr. A. Decken at the University of New Brunswick.

The isolation of head-to-tail cyclized peptides from fungi is quite common, although the isolation of cyclic decapeptides is quite rare. Only a few cyclic decapeptides from fungal sources have been reported and include antanamide from *Amanita Phalloides* (death-cap fungus)[282] and arborcandins A-F from an unknown plant isolated fungal strain collected in Ube, Japan[283]. The remaining reported decapeptides have been isolated from a marine sponge (phakellistatin[284]), from blue-green algae *Calothrix fusca* (calophycin[285]) from the plant *Leonurus japonicus* (cycloleonuripeptide[286]) and from the bacteria *Bacillus brevis* (gramicidin[272] and tyrocidine A[287]) and *Streptomyces* sp. Tu 6071 (Streptocidins[288]). None of the previously reported decapeptides show structural similarity to auyuittuqamides A-D.

6.3.3.2 Structure Elucidation of Tariuqin A and B from *Sesquicillium* sp. RKAG 186

Tariuqin A (**13**) (Figure 6.5, Table 6.3, Appendix Figures A.30 and A.31) was obtained as a white powder and HRESIMS supported a molecular formula of $C_{57}H_{103}N_{12}O_{14}$ (*m/z* 1193.7893 $[M + H]^+$), requiring 13 degrees of unsaturation. The peptidic nature of the compound was determined by analysis of the ^1H NMR spectrum which revealed the presence of 12 amide protons while the ^{13}C NMR spectrum revealed the presence of 11 amide carbonyls between δ_C 170.8-176.5 ppm and 11 α-amino acid

carbon resonances between δ_C 48.4-60.7. Analysis of the COSY, HMBC, HSQC and TOCSY spectra confirmed the identity of seven proteogenic amino acid constituents and revealed the presence of three Leu, one Ser, one Glu, one Val and one Pro residue. Additionally, a leucine-related coupling spin system was revealed by TOCSY containing an additional hydroxymethylene signal (δ_H 3.26, 3.12) which allowed for the assignment of this residue as leucinol (Leuol).

Analysis of the NH signals revealed five as ^{1}H singlets. Two of the five NH singlets (δ_H 7.23 and 6.77) could be attributed to the amide group on Gln. Another of the singlets (δ_H 7.73) was assigned as an aminoisobutyric (Aib) residue through HMBC correlations from Aib NH (δ_H 7.73) and Aib β-H_3 (δ_H 1.45 and 1.38) to Aib Cα (δ_C 56.0). The remaining two singlets were assigned as isovaline (Iva) residues. COSY correlations established the presence of two ethyl groups containing a characteristic upfield shifted methyl triplet γ-H_3 (δ_H 0.77 and 0.69). These ethyl groups were linked to their respective quaternary Cα through HMBC correlations from γ-H_3 (δ_H 0.77 and 0.69) to Cα (δ_C 58.4 and 58.9). HMBC correlations from the NH singlet signals (δ_H 8.52 and 7.69) and from β-H_3 singlet signals (δ_H 1.29 and 1.36) to Cα (δ_C 58.4 and 58.9) confirmed the identity of the residues as Iva. The presence of an acetyl group was identified by HMBC correlations from Ac H_3 (δ_H 1.93) to CO (δ_C 170.8). HMBC correlations between Ac-H_3 and Iva1 NH (δ_H 8.52) to Ac CO indicated the presence of an acetylated *N*-terminal Iva residue.

The sequential assignment of amino acids within **13** was carried out by HMBC correlations from NH to CO of the adjacent residue and ROESY correlations from NH of one residue to Hα of the adjacent residue. The acetyl group was presumed to be at the

N-terminus and the leucinol at the *C*-terminus, as is the case in known peptaibols. HMBC correlations from Iva1 NH (δ_H 8.52) to Ac CO (δ_C 170.8) and Ser NH (δ_H 8.27) to Iva1 CO (δ_C 176.5) established the sequence Ac-Iva1-Ser. A second sequence was determined by HMBC correlations from Aib NH (δ_H 7.73) to Leu1 CO (δ_C 173.4) to make Leu1-Aib. The third sequence was established by HMBC correlations from Leu2 NH (δ_H 7.86) to Pro CO (δ_C 173.9), Iva2 NH (δ_H 7.69) to Leu2 CO (δ_C 173.8), Gln NH (δ_H 7.32) to Iva2 CO (δ_C 175.9) to make Pro-Leu2-Iva2-Gln. Another two amino acid sequence Leu3-Leuol was revealed by HMBC correlations between Leuol NH (δ_H 6.68) to Leu3 CO (δ_C 171.7). Due to the overlapping carbonyl shifts of Ser, Val and Gln (δ_C 171.4-171.5), HMBC correlations could not be used to definitively connect the established fragments. Instead, ROESY correlations were used to connect the fragments. ROESY correlations from Val NH (δ_H 7.68) to Ser Hα (δ_H 4.02), Leu1 NH (δ_H 7.41) to Val Hα (δ_H 3.85), Leu3 NH (δ_H 7.47) to Gln Hα (δ_H 3.88) and Pro $H\gamma_1$ (δ_H 3.67) to Aib $H_{3\beta1}$ (δ_H 1.45) established the final sequence as Ac-Iva1-Ser-Val-Leu1-Aib-Pro-Leu2-Iva2-Gln-Leu3-Leuol. MS/MS analysis confirmed the final sequence (Appendix Figure A.33).

Tariuqin B (**14**) (Figure 6.5, Table 6.3 and Appendix Figures A.31 and A.32) was obtained as a white powder and HRESIMS supported a molecular formula of $C_{58}H_{105}N_{12}O_{14}$ (*m/z* 1179.7737 $[M + H]^+$), requiring 13 degrees of unsaturation. Careful analysis of the NMR spectra revealed **2** differed from **1** by the loss of a methylene unit. Analysis of COSY, HMBC, HSQC and TOCSY spectra revealed the difference between compounds **13** and **14** was the replacement of an Iva residue by an Aib residue. Through HMBC correlations from Aib1 NH (δ_H 8.92) to Ac CO (δ_C 170.9) and Ser NH (δ_H 8.83)

to Aib1 CO (δ_C 176.5) it was determined the first Iva in the sequence had been replaced. HMBC correlations were used to confirm the remaining portion of the molecule was unchanged. HMBC correlations from Aib1 NH (δ_H 8.92) to Ac CO (δ_C 170.9), Ser NH (δ_H 8.83) to Aib1 CO (δ_C 176.5), Val NH (δ_H 7.72) to Ser CO (δ_C 172.0), Leu1 NH (δ_H 7.51) to Val CO (δ_C 171.6) and Aib2 NH (δ_H 7.80) to Leu1 CO (δ_C 173.5) established the sequence Ac-Aib1-Ser-Val-Leu1-Aib2. A second sequence was established by HMBC correlations from Leu2 NH (δ_H 7.88) to Pro CO (δ_C 173.8), Iva NH (δ_H 7.71) to Leu2 CO (δ_C 173.9) and Gln NH (δ_H 7.33) to Iva CO (δ_C 176.0) resulting in the sequence Pro-Leu2-Iva-Gln. Due to the overlapping carbonyl shifts of Gln and Leu3 (δ_C 171.5), ROESY correlations were used to connect the fragments. ROESY correlations from Leuol NH (δ_H 6.69) to Leu3 Hα (δ_H 4.02), Leu3 NH (δ_H 7.47) to Gln Hα (δ_H 3.89) and Pro Hγ_1 (δ_H 3.67) to Aib2 H$_{3\beta1}$ (δ_H 1.45) confirmed the sequence of amino acids was the same as **13** except for the replacement of Iva1 with Aib. Therefore the final sequence of **14** was confirmed and was established as Ac-Aib1-Ser-Val-Leu1-Aib2-Pro-Leu2-Iva2-Gln-Leu3-Leuol which was confirmed by MS/MS (Appendix Figure A.33). Both **13** and **14** were determined to be new 11 residue peptaibols.

The absolute configuration of the amino acids in **13** and **14** was determined by Marfey's method[281] to be L-Val, L-Leu, L-Pro, L-Ser, L-Ala, L-Gln, L-Leuol and (*R*)-Iva (Appendix Figure A.42).

The isolation of these peptaibols represents the first isolation of this family of compounds from the genus *Sesquicillium*. They are characterized by containing 11 residues and having leucinol at their *C*-terminus. Compound **14** differs from **13** by having an Aib residue in position 1 as opposed to an Iva residue. A search in the

Petabiotics Database revealed these peptaibols are most similar to Hypomurocin A III (Ac-U-Q-V-L-U-P-L-I-U-P-L-OH) isolated from *Hypocrea muroiana*[289] and Trichobrachin B II (Ac-U-N-V-L-U-P-L-U-V-P-L-OH) isolated from *Trichoderma longibrachiatum*[290] as they all share the same resides in positions 1 (U), 3-7 (V-L-U-P-L) and 11 (Leuol).

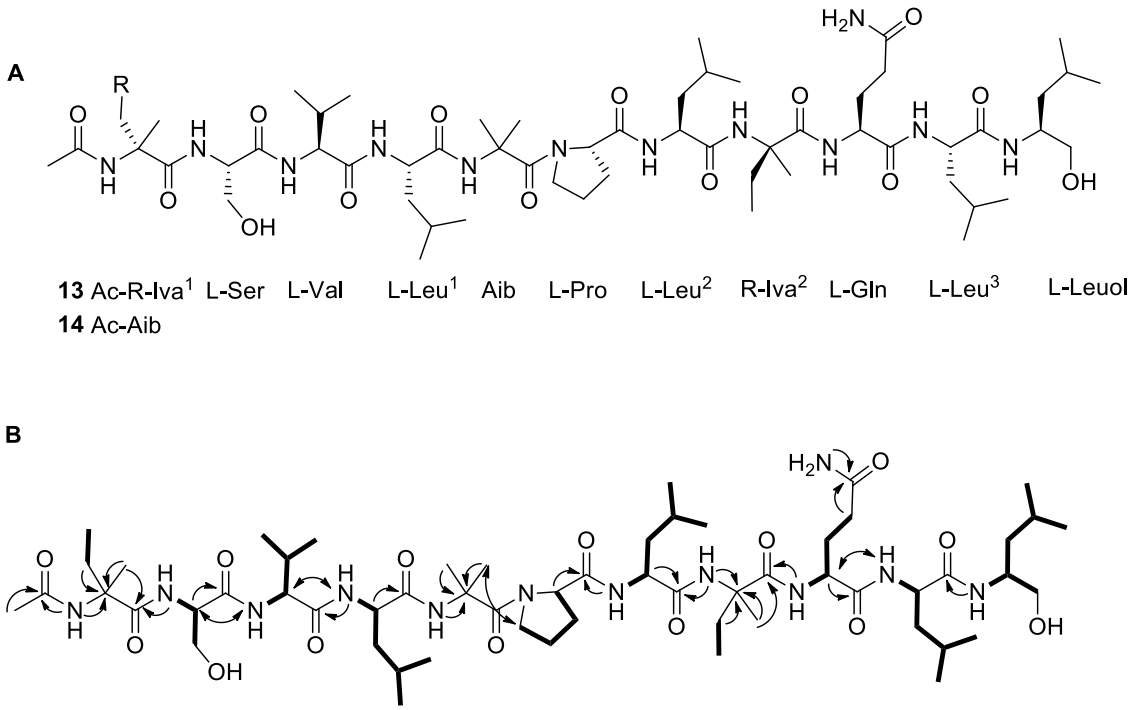

Figure 6.5. A) Molecular structure of tariuqin A and B. **B)** Key NMR correlations to establish the structure of tariuqin A.

Table 6.3. ^{1}H (600 MHz) and ^{13}C (150 MHz) NMR data of tariuqin A (13) and B (14) in DMSO-d_6.

Tariuqin A				**Tariuqin B**			
		δ_C	δ_H (J/Hz)			δ_C	δ_H (J/Hz)
Ac	CH3	23.3	1.90, s	**Ac**	CH3	22.8	1.93, s
	CO	170.9			CO	170.8	
Aib[1]	CO	176.5		**Iva[1]**	CO	176.5	
	NH		8.92, s		NH		8.52, s
	α	55.9			α	58.4	
	β1	25.9	1.36[a]		β_1	22.5	1.29, m
	β2	23.2	1.35[a]		β_2	26.5	2.01, m
							1.85[a]
					γ	7.4	0.77[a]
Ser	CO	172.0		**Ser**	CO	171.5	
	NH		8.83, d, (4.7)		NH		8.27, m
	α	58.3	3.97, m		α	58.5	4.01, m
	β1	60.1	3.71, m		β	60.4	3.71, m
	OH				OH		
Val	CO	171.6		**Val**	CO	171.5	
	NH		7.72, m		NH		7.69, m
	α	60.2	3.84, m		α	60.5	3.85, m
	β	28.7	2.12, m		β	28.9	2.10, m
	γ1	18.6	0.93[a]		γ_1	18.9	0.93[a]
	γ2	18.7	0.90, d (6.8)		γ_2	18.8	0.90, d (6.8)
Leu[1]	CO	173.1		**Leu[1]**	CO	173.4	
	NH		7.51, d (7.9)		NH		7.41, d (7.9)
	α	51.2	4.21, ddd (11.8, 7.9, 4.1)		α	51.3	4.22, ddd (11.7, 7.9, 4.1)
	β	39.3	1.65[a]		β	39.1	1.62[a]
			1.50[a]				1.48[a]
	γ	23.6	1.59, m		γ	24.0	1.60[a]
	δ1	22.6	0.84, m		δ1	23.2	0.85[a]
	δ2	20.1	0.77[a]		δ2	20.2	0.76[a]
Aib[2]	CO	172.7		**Aib**	CO	172.7	
	NH		7.80, s		NH		7.73, s
	α	55.6			α	56.0	
	β1	22.8	1.45 s		β_1	23.0	1.45 s
	β2	25.0	1.39 s		β_2	25.2	1.38[a]
Pro	CO	173.8		**Pro**	CO	173.9	
	A	62.6	4.31, t (8.1)		α	62.8	4.31, t (8.1)
	β1	28.1	2.21[a]		β	28.4	2.22[a]
	β2		1.59[a]				1.59[a]
	$\gamma 1_A$	25.7	1.84[a]		γ	25.7	1.84[a]
	δ	48.3	3.67, m		δ	48.4	3.67, m
	δ		3.39, m				3.37, m

Leu²	CO	173.9		**Leu²**	CO	173.8	
	NH		7.88, d (6.4)		NH		7.86 (d, 6.4)
	α	53.6	3.87[a], m		α	53.8	3.87 [a]
	β	38.4	1.86[a], m		β	38.4	1.85[a]
			1.59[a], m				1.48[a]
	γ	24.3	1.73, m		γ	24.3	1.73, m
	δ1	22.8	0.93, m		δ_1	22.9	0.92[a]
	δ2	20.6	0.82[a], m		δ_2	20.7	0.81[a]
Iva	CO	176.0		**Iva²**	CO	175.8	
	NH		7.71, s		NH		7.69, s
	α	58.9			α	58.9	
	β1	22.5	1.36[a], s		β_1	22.6	1.36[a]
	β2	25.6	2.19[a], m		β_2	25.7	2.19[a]
			1.69, m				1.69, m
	γ1	6.7	0.68, t (7.5)		γ	6.9	0.69, t (7.5)
Gln	CO	171.5		**Gln**	CO	171.5	
	NH		7.33, d (6.0)		NH		7.32, d (6.0)
	α	54.0	3.89[a]		α	54.3	3.88[a]
	β1	31.2	2.23[a]		β	31.5	2.23[a]
			2.17[a]				2.16, m
	γ1	26.3	2.02, m		γ	26.7	2.02, m
			1.85[a]				1.84[a]
	CO	173.5			CO	173.6	
	NH2		7.23, s		NH2		7.23, s
			6.77, s				6.77, s
Leu³	CO	171.5		**Leu³**	CO	171.7	
	NH		7.47, d (7.9)		NH		7.47, d (7.9)
	α	51.8	4.02, m		α	52.1	4.02, m
	β	39.3	1.65[a]		β	39.4	1.65[a]
			1.50[a]				1.51[a]
	γ	24.0	1.65[a]		γ	24.2	1.65[a]
	δ1	22.9	0.88, d (6.4)		δ1	23.1	0.87, d (6.4)
	δ2	20.5	0.78[a]		δ2	20.8	0.79[a]
Leuol	NH	6.69		**Leuol**	NH	6.68	
	α	48.1	3.79, m		α	48.4	3.79, m
	β	39.6	1.36, m		β	39.6	1.36[a]
			1.27, m				1.27, m
	γ	23.7	1.59, m		γ	23.4	1.57, m
	δ1	22.7	0.82[a]		δ1	23.1	0.82[a]
	δ2	21.2	0.78[a]		δ2	21.4	0.80[a]
	β'	63.9	3.27, m		β'	64.2	3.26, dd (9.9, 4.9)
			3.13, m				3.12, t (9.1)
	OH		4.46, brs		OH		4.44, br s

6.3.3.3 Structure Elucidation of Tariuqin C-F from *Sesquicillium* sp. RKAG 571

Fifty flasks of solid rice fermentation media inoculated with *Sesquicillium* sp. RKAG 571 were extracted with EtOAc, dried, and partitioned between 80% CH_3CN and 100% hexane. The CH_3CN soluble portion was subjected to flash chromatography and reversed-phase HPLC yielding four new 11 residue peptaibols, tariuqin A (**15**) (4 mg), tariuqin B (**16**) (1.5 mg), tariuqin C (**17**) (3 mg) and tariuqin D (**18**) (2 mg).

Tariuqin C (**15**) (Figure 6.6, Table 6.4 and Appendix Figures A.34 and A.35) was obtained as a white powder and HRESIMS supported a molecular formula of $C_{60}H_{101}N_{12}O_{14}$ (*m/z* 1213.7543 $[M + H]^+$), requiring 17 degrees of unsaturation. Analysis of the ^1H NMR spectrum revealed the presence of 12 amide protons and analysis of the DEPT-135 and HSQC spectra revealed the presence of 13 carbonyl resonances and 11 α-carbon resonances, whereby four of these α-carbons were quaternary. Analysis of the COSY, HMBC, HSQC and TOCSY spectra confirmed the identity of six amino acid constituents and revealed the presence of two Leu, one Ser, one Glu, one Val, and one Pro residue. The presence of an amino alcohol, corresponding to phenylalaniol (Pheol) was determined by COSY correlations corresponding to two spin systems: Pheol NH (δ_H 6.85)/Hα (δ_H 3.90)/$H_2\beta$ (δ_H 2.89, 2.52) and $H_2\beta$' (δ_H 3.35, 3.26); and H-4' (δ_H 7.13)/H-3' (δ_H 7.21). HMBC correlations from $H_2\beta$ to C-1' (δ_C 139.4) and C-2' (δ_C 127.8); and H-2' (δ_H 7.20) to C-3' (δ_H 129.1) and C-1' connected the two spin systems. The downfield carbon resonance of $H_2\beta$' was consistent with the presence of hydroxyl group.

The remaining four unassigned quaternary Cα resonances corresponded to three Iva and one Aib residue. The Aib residue was assigned by HMBC correlations from Aib

NH (δ_H 7.80) and Aib $H_3\beta_{1,2}$ (δ_H 1.44 and 1.38) to Aib Cα (δ_C 56.0). The three remaining amino acids contained an ethyl group determined by COSY correlations from Iva $H_2\beta_2$ (δ_H 1.67-2.25, 1.58-1.99) to $H_3\gamma$ (δ_H 7.1-7.6) which contained an upfield shifted methyl triplet, characteristic of Iva residues. HMBC correlations from each respective Iva NH (δ_H 7.22-8.67), $CH_3\beta_1$ (δ_H 1.23-1.35) and $CH_2\beta_2$ to their Cα (δ_H 58.6-59.3) confirmed the identity of these three amino acids. Lastly, an acetyl group was identified by HMBC correlations from Ac H_3 (δ_H 1.92) to Ac CO (δ_C 170.9). HMBC correlations from Ac H_3 (δ_H 1.92) and Iva1 NH (δ_H 8.61) to Ac CO (δ_C 170.8) indicated the presence of an acetylated *N*-terminal Iva residue.

The order of the amino acids was resolved by HMBC and ROESY correlations and MS/MS analysis. Three amino acid sequences could be established by HMBC correlations. The first sequence Ac-Iva-Ser-Val-Leu was determined by HMBC correlations from Iva1 NH (δ_H 8.61) to Ac CO (δ_C 170.9), Ser NH (δ_H 8.57) to Iva1 CO (δ_C 176.2), Val NH (δ_H 7.74) to Ser CO (δ_C 171.8) and Leu1 NH (δ_H 7.50) to Val CO (δ_C 171.5). A second sequence (Leu-Iva) was established by correlations from Iva2 NH (δ_H 7.52) to Leu_2 CO (δ_C 173.4). The third sequence was determined to be Iva-Pheol by HMBC correlations from NH Pheol (δ_H 6.85) to Iva_3-CO (δ_C 172.6). ROESY correlations were used to assign a two residue fragment, Aib-Pro by correlations from Aib $H_3\beta_1$ (δ_H 1.44) to Pro $H_2\delta_1$ (δ_H 3.66). Due to the overlapping amide proton shifts of Iva3 NH and Gln NH (δ_H 7.22), Leu2 NH and Aib NH (δ_H 7.80-7.81) and the overlapping carbonyl shifts of Leu1 CO and Gln CO (173.3-173.4), HMBC and ROESY correlations could not be used to definitively assign the location of these amino acids. Tandem mass spectrometry was used to determine the remaining order of amino acids.

Fragmentation of the $[M + Na]^+$ ion generated a series of product ions b_{10}^+ to b_4^+ arising from successive losses of Pheol[11], Iva[10], Gln[9], Iva[8], Leu[7], Pro[6], Aib[5] and Leu[4] confirming the order of the amino acids at the C-terminus (Appendix Figure A.43). The resulting planar structure of **15** was assigned as Ac-Iva-Ser-Val-Leu-Aib-Pro-Leu-Iva-Gln-Iva-Pheol.

Tariuqin D (**16**) (Figure 6.6, Table 6.4 and Appendix Figures A.36 and A.37) was obtained as a white powder and HRESIMS supported a molecular formula of $C_{59}H_{99}N_{12}O_{14}$ (*m/z* 1199.7385 $[M + H]^+$), requiring 17 degrees of unsaturation. The peptidic nature of the compound was established by analysis of the ^1H NMR spectra and revealed **16** was an analog of **15.** Compound **16** differed from **15** by the absence of a methylene group which was attributed to the loss of an Iva residue and the gain of an Aib residue. HMBC correlations from Aib2 NH (δ_H 7.52), $H_3\beta_1$ (δ_H 1.43) and $H_3\beta_2$ (δ_H 1.36) to Cα (δ_C 56.0) confirmed the identity of the Aib residue. HMBC correlations from Aib2 NH (δ_H 7.52) to Leu2 CO (δ_H 173.5) confirmed this residue was located beside Leu2 and had replaced Iva as residue 8. The identity and order of the remaining amino acids was determined to be identical to **15** through NMR analysis and MS/MS analysis. Successive fragmentation of the $[M + Na]^+$ ion generated a series of product ions b_{10}^+ to b_4^+ arising from successive losses of Pheol[11], Iva[10], Gln[9], Aib[8], Leu[7], Pro[6], Aib[5] and Leu[4] and confirmed the position of the new Aib residue (Appendix Figure A.43). HMBC correlations from Iva1 NH (δ_H 8.60) to Ac CO (δ_C 170.9), Ser NH (δ_H 8.53) to Iva1 CO (δ_C 176.6), Val NH (δ_H 7.72) to Ser CO (δ_C 171.8) and Leu1 NH (δ_H 7.50) to Val CO (δ_C 171.5) confirmed the order of the residues at the N-terminus. The

resulting planar structure of **16** was determined to be Ac-Iva-Ser-Val-Leu-Aib-Pro-Leu-Aib-Gln-Iva-Pheol.

Tariuqin E (**17**) (Figure 6.6, Table 6.5 and Appendix Figures A.38 and A.39) was obtained as a white powder and HRESIMS supported a molecular formula of $C_{60}H_{101}N_{12}O_{13}$ (*m/z* 1197.7385 $[M + H]^+$), requiring 17 degrees of unsaturation. The peptidic nature of the compound was determined by analysis of the ^1H NMR spectrum which revealed the presence of 12 amide protons. It was determined **17** differed from **15** by the absence of a hydroxyl group. Comparison of the NMR spectra of **17** to **15** revealed the loss of a hydroxy-methylene group and the appearance of a methyl group (δ_H 1.31) which was attributed to the loss of a Ser residue and the gain of an Ala residue. HMBC correlations from Iva1 NH (δ_H 8.58) to Ac CO (δ_C 170.9), Ala NH (δ_H 8.58) to Iva1 CO (δ_C 176.2), Val NH (δ_H 7.64) to Ala CO (δ_C 174.3) and Leu1 NH (δ_H 7.55) to Val CO (δ_C 171.6) confirmed Ala had replaced Ser as the second residue. The identity and order of the remaining amino acids was determined to be identical to **15** through NMR analysis and MS/MS analysis (Appendix A.43). The planar structure of **17** was determined to be Ac-Iva-Ala-Val-Leu-Aib-Pro-Leu-Iva-Gln-Iva-Pheol.

Tariuqin F (**18**) (Figure 6.6, Table 6.5 and Appendix Figures A.40 and A.41) was obtained as a white powder and HRESIMS supported a molecular formula of $C_{29}H_{99}N_{12}O_{13}$ (*m/z* 1183.7451 $[M + H]^+$), requiring 17 degrees of unsaturation. The peptidic nature of the compound was determined by analysis of the ^1H NMR spectra which revealed the presence of 12 amide protons. It was determined **18** differed from **17** by the absence of a methylene group which was attributed to a loss of an Iva residue and gain of Aib residue. HMBC correlations from Aib2 NH (δ_H 7.52), $H_3\beta_1$ (δ_H 1.43) and

$H_3\beta_2$ (δ_H 1.35) to Cα (δ_C 56.0) confirmed the identity of the Aib residue. Fragmentation of the $[M + Na]^+$ ion resulted in the successive losses of Pheol[11], Iva[10], Gln[9], Iva[8], Leu[7], Pro[6], Aib[5] and Leu[4] confirming Aib had replaced Iva at position 8 (Appendix Figure A43). The order and identity of the remaining amino acids was determined to be identical to **16** by NMR analysis. The resulting planar structure of **18** was determined to be Ac-Iva-Ala-Val-Leu-Aib-Pro-Leu-Aib-Gln-Iva-Pheol.

The absolute configuration of the amino acids of **15-18** was determined using Marfey's method[13] (Appendix Figure A.42). Compounds **15-18** were found to contain L-Leu, L-Val, L-Gln, L-Ser, L-Pro, L-Leuol and both (*R*)-Iva and (*S*)-Iva. Compounds **15** and **17** contain three Iva residues and these were found in a ratio of 2:1 (*R*:*S*). Compounds **16** and **19** contain two Iva residues which were found in a ratio of 1:1 (*R*:*S*). Due to the similarity in structures and chemical shifts of Iva in position 1 and 8 between peptaibols **13** and **14** and **15-18**, the position of the (*R*)-Iva residues was proposed to be the same as that of **13** and **14**. Therefore the remaining Iva residue at position ten was assigned as the *S* configuration. The presence of both (*R*)-Iva and (*S*)-Iva within peptaibols is rare and has been reported for the 11-residue albupeptins[291], the 14-residue peptaibol clonostachin[292] and the 16-residue integramides[293].

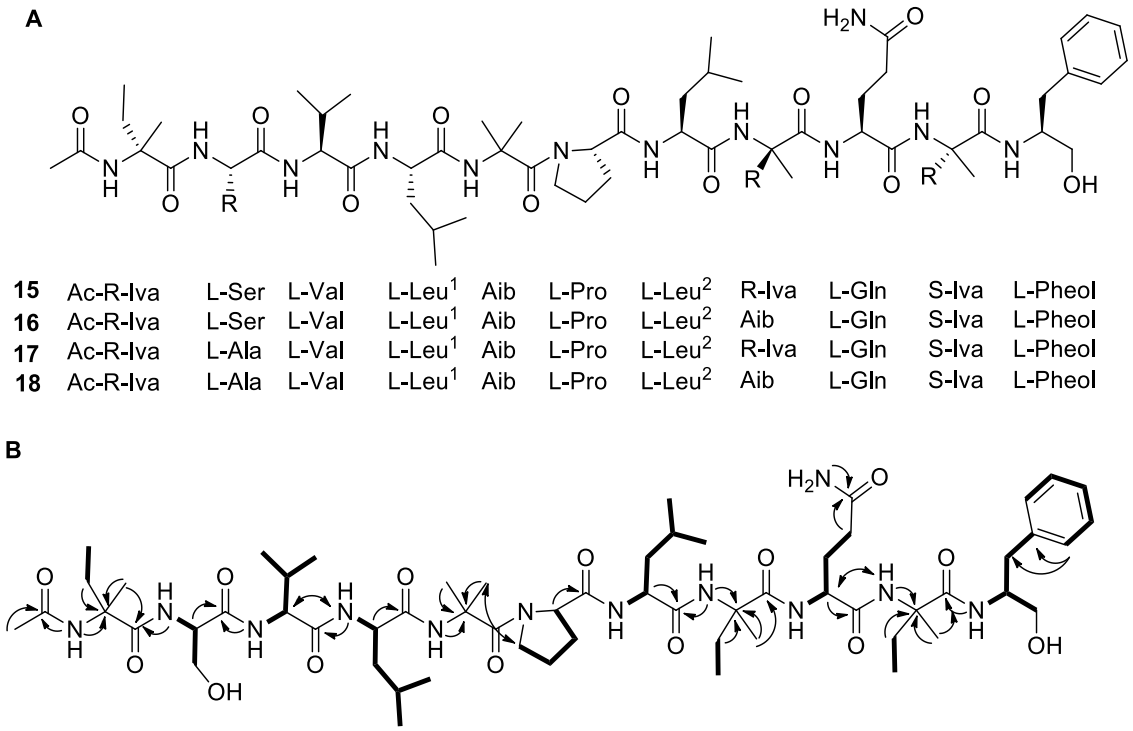

15	Ac-R-Iva	L-Ser	L-Val	L-Leu^1	Aib	L-Pro	L-Leu^2	R-Iva	L-Gln	S-Iva	L-Pheol
16	Ac-R-Iva	L-Ser	L-Val	L-Leu^1	Aib	L-Pro	L-Leu^2	Aib	L-Gln	S-Iva	L-Pheol
17	Ac-R-Iva	L-Ala	L-Val	L-Leu^1	Aib	L-Pro	L-Leu^2	R-Iva	L-Gln	S-Iva	L-Pheol
18	Ac-R-Iva	L-Ala	L-Val	L-Leu^1	Aib	L-Pro	L-Leu^2	Aib	L-Gln	S-Iva	L-Pheol

Figure 6.6. A) Molecular structure of tariuqin C-F. **B)** Key COSY, HMBC and NOESY correlations of tariuqin C.

Table 6.4. ^{1}H (600 MHz) and ^{13}C (150 MHz) NMR data of tariuqin C (15) and D (16) in DMSO-*d6*.

Tariuqin C				**Tariuqin D**			
		δ_C	δ_H, (J/Hz)			δ_C	δ_H, (J/Hz)
Ac	CH_3	22.9	1.92, s	**Ac**	CH_3	22.9	1.92, s
	CO	170.9			CO	170.9	
Iva[1]	CO	176.2		**Iva**[1]	CO	176.6	
	NH		8.61, s		NH		8.60, s
	α	58.6			α	58.6	
	β_1	22.4	1.29, s		β_1	22.4	1.29, s
	β_2	26.7	1.99, m		β_2	26.8	1.99, m
			1.71, m				1.70, m
	γ	7.5	0.78, dd (7.4, 7.4)		γ	7.5	0.78
Ser	CO	171.8		**Ser**	CO	171.8	
	NH		8.57, d (4.2)		NH		8.53, m
	α	58.4	4.01, m		α	58.4	4.01, m
	β	60.4	3.71[a]		β	60.2	3.70[a]
	OH				OH		
Val	CO	171.5		**Val**	CO	171.5	
	NH		7.74, d (6.8)		NH		7.72, d (7.0)
	α	60.5	3.85[a]		α	60.4	3.85[a]
	β	28.9	2.10, m		β	28.9	2.11, m
	γ_1	18.8	0.93[a]		γ_1	18.9	0.93[a]
	γ_2	18.9	0.90, d (6.7)		γ_2	19.0	0.90,
Leu[1]	CO	173.3		**Leu**[1]	CO	173.3	
	NH		7.50, d (7.8)		NH		7.50, m
	α	51.5	4.22, m		α	51.4	4.23, m
	β	39.2	1.62, m		β	39.2	1.62, m
			1.49, m				1.51, m
	γ	24.0	1.63, m		γ	24.0	1.63, m
	δ1	20.9	0.84[a]		δ1	20.9	0.84[a]
	δ2	20.3	0.78[a]		δ2	20.3	0.77[a]
Aib	CO	172.6		**Aib**[1]	CO	172.7	
	NH		7.80, s		NH		7.81, s
	α	56.0			α	56.0	
	β_1	23.0	1.44, s		β_1	23.1	1.44, s
	β_2	25.4	1.38, s		β_2	25.5	1.38, s
Pro	CO	174.0		**Pro**	CO	173.7	
	α	62.7	4.29, dd (7.9, 7.9)		α	62.8	4.28, dd (7.9, 7.9)
	β	28.4	2.20, m		β	28.5	2.21, m
			1.61, m				1.61, m
	γ	26.0	1.83, m		γ	25.7	1.84, m
	δ	48.4	3.66[a]		δ	48.5	3.66[a]
			3.41[a]				3.40[a]
Leu[2]	CO	173.4		**Leu**[2]	CO	173.5	
	NH		7.81[a]		NH		7.80[a]

	α	53.9	3.92[a]		α	53.5	3.99[a]
	β	38.6	1.83, m		β	38.7	1.83, m
			1.54, m				1.54, m
	γ	24.5	1.74, m		γ	24.5	1.72, m
	δ_1	23.1	0.95[a]		δ_1	22.8	0.94[a]
	δ_2	22.8	0.84[a]		δ_2	22.6	0.84[a]
Iva[2]	CO	175.4		**Aib[2]**	CO	175.5	
	NH		7.52, s		NH		7.52, s
	α	58.8			α	56.0	
	β_1	22.6	1.35, s		β_1	26.2	1.43, s
	β_2	25.7	2.25		β_2	22.6	1.36, s
			1.70				
	γ	7.1	0.70				
Gln	CO	171.2		**Gln**	CO	171.2	
	NH		7.22, s		NH		7.22[a]
	α	54.7	3.84[a]		α	54.9	3.84[a]
	β	26.8	1.94, m		β	26.8	1.93, m
			1.83, m				1.83, m
	γ	31.5	2.18, m		γ	31.5	2.17, m
			2.11, m				2.10, m
	CO	173.4			CO		
	NH2				NH2		
Iva[3]	CO	172.6		**Iva[2]**	CO	172.7	
	NH		7.22, s		NH		7.22[a]
	α	59.3			α	59.3	
	β1	20.3	1.23, s		β1	20.2	1.23, s
	β2	30.6	1.67, m		β2	30.6	1.67, m
			1.58, m				1.59, m
	γ	7.6	0.50, dd (7.3, 7.3)		γ	7.6	0.50, dd (7.3, 7.3)
Pheol	NH		6.85, d (9.2)	**Pheol**	NH		6.86, d (9.2)
	α	52.6	3.90, d (9.4)		α	52.7	3.89[a]
	β	36.5	2.89, dd (13.6, 3.7)		B	36.5	2.89, dd (13.6, 3.5)
			2.52				2.52, m
	1’	139.4			1’	139.5	
	2’	127.8	7.20[a]		2’	127.8	7.19[a]
	3’	129.1	7.21[a]		3’	129.1	7.21[a]
	4’	125.7	7.13, m		4’	125.7	7.13, m
	β'	63.4	3.35[a]		β'	63.4	3.35[a]
			3.26, m				3.27, m
	OH				OH		

Table 6.5. ^{1}H (600 MHz) and ^{13}C (150 MHz) NMR data of tariuqin E (17) and F (18) in DMSO-*d6*.

	Tariuqin E				Tariuqin F		
		δ_C	$\delta_{H,}$ (J/Hz)			δ_C	$\delta_{H,}$ (J/Hz)
Ac	CH_3	22.9	1.92, s	**Ac**	CH_3	22.9	1.92, s
	CO	170.7			CO	170.7	
Iva[1]	CO	176.2		**Iva[1]**	CO	176.2	
	NH		8.58[a]		NH		8.58[a]
	α	58.4			α	58.4	
	β_1	22.4	1.28, s		β_1	22.4	1.28, s
	β_2	26.6	1.95, m		β_2	26.5	1.96, m
			1.70, m				1.69, m
	γ	7.5	0.77[a]		γ	7.5	0.77[a]
Ala	CO	174.3		**Ala**	CO	174.3	
	NH		8.58[a]		NH		8.55[a]
	α	51.2	4.00, m		α	51.2	4.01[a]
	β	16.9	1.31, d (7.3)		β	16.9	1.31[a]
Val	CO	171.6		**Val**	CO	171.6	
	NH		7.64, d (7.3)		NH		7.63, d (6.7)
	α	60.3	3.82[a]		α	60.3	3.82[a]
	β	29.0	2.10, m		β	29.1	2.10, m
	γ1	18.9	0.94, d (6.8)		γ_1	18.9	0.94, d (6.9)
	γ2	19.0	0.90, d (6.8)		γ_2	19.0	0.90, d (6.4)
Leu[1]	CO	173.3		**Leu[1]**	CO	173.3	
	NH		7.55, d (7.6)		NH		7.55[a]
	α	51.4	4.23, m		α	51.4	4.23, m
	β	39.1	1.62[a]		β	39.1	1.62[a]
			1.49, m				1.50, m
	γ	24.0	1.63[a]		γ	23..7	1.63[a]
	δ1	20.9	0.84[a]		δ1	20.9	0.84[a]
	δ2	20.3	0.78[a]		δ2	20.3	0.78[a]
Aib	CO	172.6		**Aib[1]**	CO	172.7	
	NH		7.88, s		NH		7.87, s
	α	56.0			α	56.0	
	β1	23.0	1.44, s		β_1	23.0	1.44, s
	β2	25.3	1.38, s		β_2	25.3	1.38, s
Pro	CO	173.9		**Pro**	CO	173.5	
	A	62.7	4.29, dd (7.9, 7.9)		α	62.7	4.28, m
	β1	28.4	2.20, m		β	28.5	2.21, m
	β2		1.61[a]				1.61[a]
	$\gamma 1_A$	25.7	1.86, m		γ	25.7	1.86, [m]
	δ	48.4	3.66, m		δ	48.4	3.66, m
	δ		3.40[a]				3.40[a]
Leu[2]	CO	173.4		**Leu[2]**	CO	173.5	
	NH		7.82, d (6.4)		NH		7.82[a]
	α	53.8	3.92[a]		α	53.5	3.99, m
	β	38.8	1.86, m		β	38.8	1.84, m
			1.53, m				1.54, m
	γ	24.5	1.73, m		γ	24.5	1.71, m
	δ1	23.1	0.94, d (6.9)		δ_1	22.8	0.94, d (6.8)
	δ2	22.8	0.84[a]		δ_2	22.6	0.84[a]
Iva[2]	CO	175.4		**Aib[2]**	CO	175.5	

	NH		7.53, s		NH		7.52[a]
	α	58.8			α	56.0	
	β1	22.6	1.35, s		β_1	26.2	1.43, s
	β2	26.1	2.25, m		β_2	22.6	1.35, s
			1.70, m				
	γ1	7.1	0.70, dd (7.5, 7.5)				
Gln	CO	171.2		**Gln**	CO	171.2	
	NH		7.22[a]		NH		7.22[a]
	α	54.7	3.85[a]		α	54.7	3.84[a]
	β1	26.9	1.93, m		β	26.9	1.93, m
			1.83, m				1.83, m
	γ1	31.5	2.18, m		γ	31.5	2.17, m
			2.11, m				2.20, m
	CO	173.4			CO	173.5	
	NH2		7.23[a]		NH2		
			6.75, s				
Iva[3]	CO	172.6		**Iva[2]**	CO	172.6	
	NH		7.22[a]		NH		7.22[a]
	α	59.3			α	59.4	
	β1	20.4	1.23, s		β1	20.4	1.23, s
	β2	30.6	1.67, m		β2	30.6	1.68, m
			1.58, m				1.59, m
	γ	7.6	0.50, dd (7.5, 7.5)		γ	7.6	0.49, dd (7.3, 7.3)
Pheol	NH		6.84 (d, 9.1)	**Pheol**	NH	6.85	
	α	52.6	3.90[a]		α	52.7	3.90[a]
	β	36.5	2.90, dd (13.7, 4.1)		B	36.5	2.89, dd (13.5, 3.5)
			2.51[a]				2.52[a]
	1’	139.4			1’	139.4	
	2’	127.8	7.19[a]		2’	127.8	7.19[a]
	3’	129.1	7.20[a]		3’	129.1	7.21[a]
	4’	125.7	7.13[a]		4’	125.7	7.13, m
	β'	63.4	3.35[a]		β'	63.5	3.35[a]
			3.26, m				3.26, m
	OH		(br s)		OH		

Compounds **15-18** represent new 11 residue members within the peptaibol family. They are similar to **13** and **14** in sequence and differ in position 10 (Iva vs. Leu) and 11 (Pheol vs Leuol). The presence of Pheol at the *C*-terminus is common in larger peptaibols above 15 residues and this appears to be the first report of an 11 residue peptaibol containing Pheol at the *C*-terminus. Due to the close taxonomic relationship between RKAG 186 and 571 it is unsurprising they are producing similar peptaibols. The other cultured *Sesquicillium* isolate (RKAG 627) also appears to be producing a series of peptaibols corresponding to an *m/z* of 1149.7648, 1163.7813, 1177.7958 and 1191.8118 $[M+H]^+$. These masses could correspond to a peptaibol which is similar in structure to **14** by replacing residue 2 with an Ala residue as opposed to a Ser residue (m/z 1177.7958, $C_{57}H_{103}N_{12}O_{13}$). Successive changes of Aib residues and Iva residues would explain the remaining masses observed. The structure of these compounds have not been confirmed.

6.3.3.4 Bioactivity Testing

Compounds **9-18** were assayed for biological activity against methicillin resistant *Staphylococcus aureus* (ATCC 33591), vancomycin resistant *Enterococcus faecium* (EF379), *Staphylococcus warneri* (ATCC 17917), *Pseudomonas aeruginosa* (ATCC 14210), and *Candida albicans* (ATCC 14035) and for their cytotoxic activity against keratinocyte and fibroblast cell lines, and HTB-26 and MCF-7 breast cancer cell lines.

The auyuittuqamides (**9-12**) exhibited no antimicrobial activity and had weak cytotoxic activity against both MCF7 (IC_{50} 26.2 ± 2.6 to 39.1 ± 3.3 µM) and HTB26 breast cancer cell lines (IC_{50} 28.3 ± 1.4 to 37.4 ± 2.1 µM), a Vero cell line (only **10** and

11 exhibited activity, 43.9 ± 3.9 and 49.5 ± 6.4 µM) and a HEKa cell line (IC_{50} 17.3 ± 1.0 to 30.2 ± 2.6 µM) (Figure 6.7). The tariuqins (**13-18**) had antimicrobial activity against MRSA, VRE and *S. warneri* (Figure 6.8). No growth inhibition was observed against *P. aeruginosa*, *P. vulgaris* or *C. albicans*. All of the peptaibols exhibited similar levels of antimicrobial activity. Compound **16** had the most potent antimicrobial activity against MRSA with an IC_{50} value of 6.0 ± 0.8 µM, an IC_{50} value of 11.7 ± 2.0 µM against VRE and an IC_{50} value of 6.3 ± 1.6 µM against *S. warneri*. The cytotoxic activity of the peptaibols was wide ranging against MCF-7 (IC_{50} 16.5 ± 1.2 to 54.2 ± 7.1 µM), HTB-26 (IC_{50} 12.3 ± 4.1 to 51.2 ± 9.6 µM), Vero (IC_{50} 30.9 ± 6.1 to 114.5 ± 10.1 µM) and HEKa cell lines (IC_{50} 6.3 ± 0.2 to 15.4 ± 2.1 µM).

The antimicrobial and cytotoxic activity observed for these peptaibols is not unexpected as the majority of reported peptaibols have antimicrobial and/or cytotoxic activity. The ability of peptaibols to form helices and insert themselves within phospholipid bilayers to form pores causing disruptions in cellular processes is the main reason for the activity observed for these peptides[277]

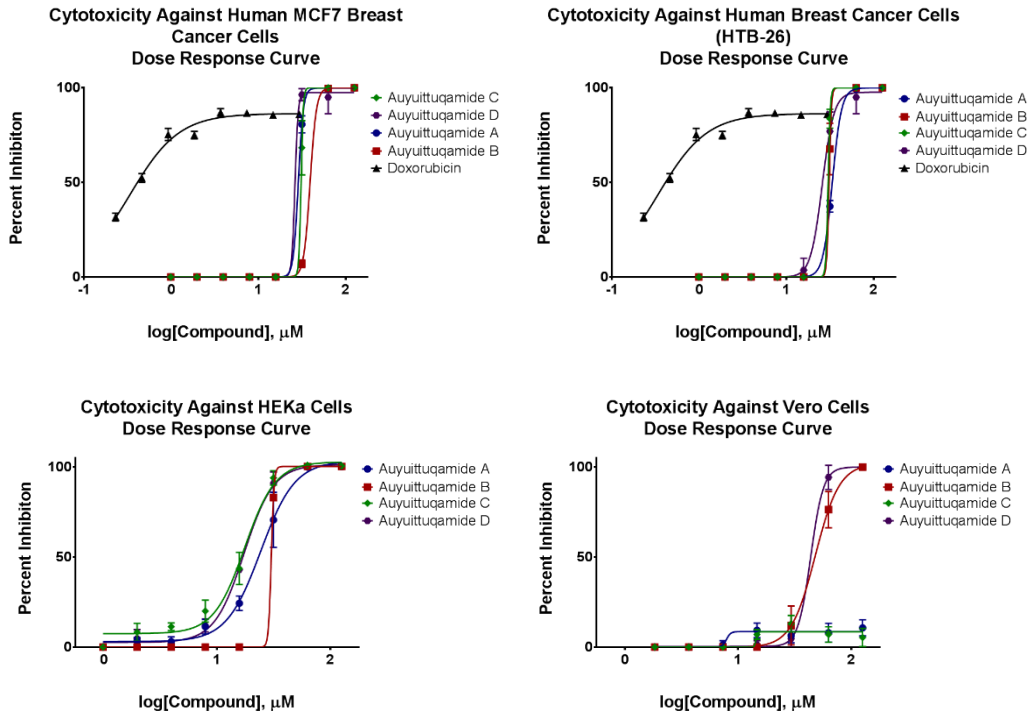

Figure 6.7. Cytotoxic activity of auyuittuqamides A-D

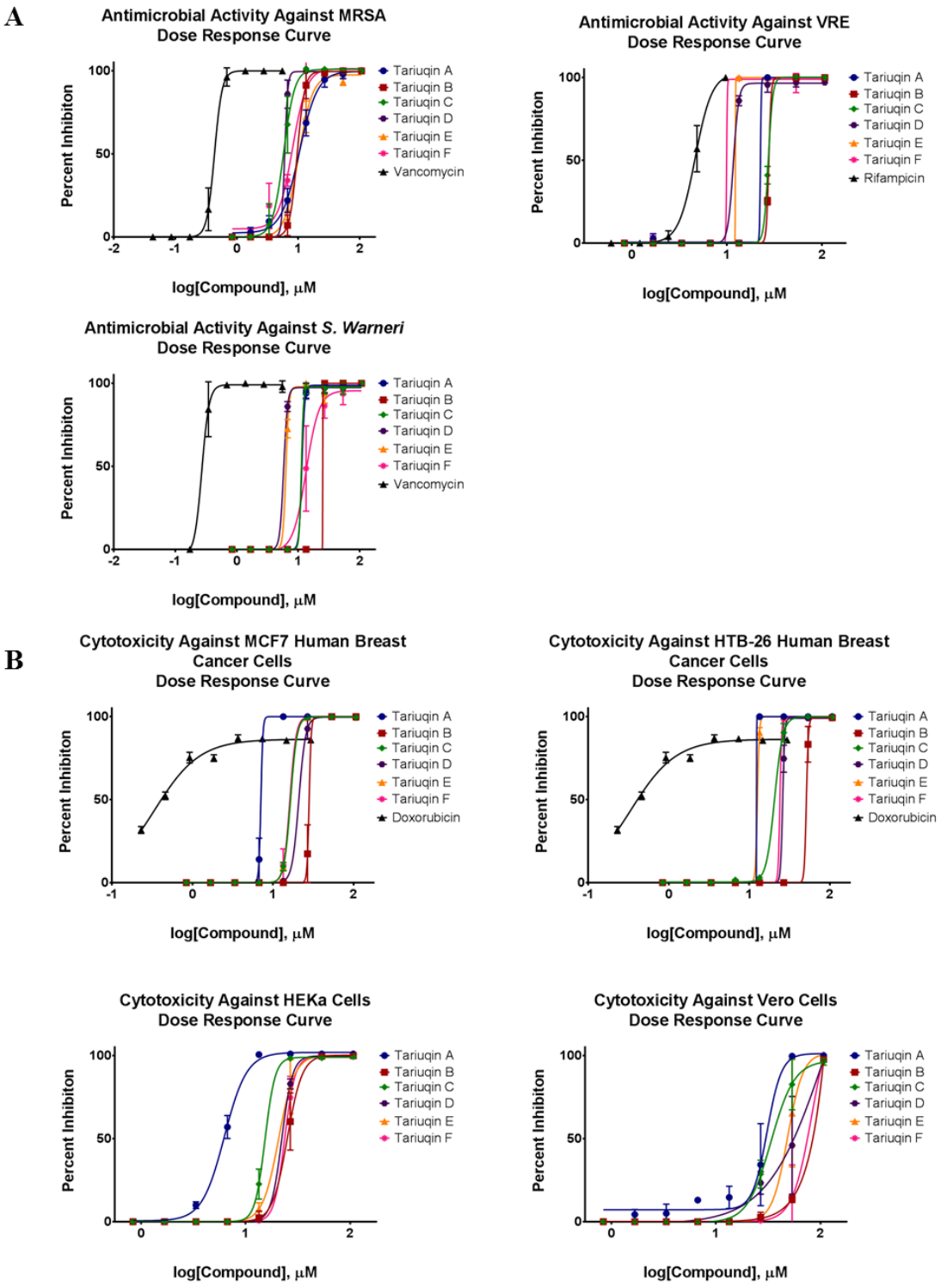

Figure 6.8. Cytotoxicity and antimicrobial testing of tariuqin A-F.

6.4 Conclusions

Three *Sesquicillium* isolates (RKAG 186, 571 and 627) were cultured from Frobisher Bay and were distinct from each other based on their ITS and 28S rRNA gene sequences. Of these isolates, two appeared to be putatively new members within the genus *Sesquicillium* and were determined to by morphologically and phylogenetically distinct from *S. microsporum* NRRL 54127. Due to a lack of sequence data of the type strain of *S. microsporum* within GenBank, further phylogenetic characterization of these isolates is ongoing.

Chemical investigation of *Sesquicillium* sp. RKAG 186 and 571 led to the isolation and structural characterization of four new *N*-methylated cyclic decapeptides and to the isolation of six new 11-residue peptaibols. The remaining isolate *Sesquicillium* sp. RKAG 627 also appears to be producing a series of 11-residue peptaibols, although the structure of these was not confirmed. The peptaibols obtained from RKAG 571 are extremely interesting as they contain both (*R*)-Iva and (*S*)-Iva within their structure. The presence of both diastereomers of Iva within peptaibols is exceptionally rare, making these compounds unique members within the peptaibol family.

The isolation of putatively new species and new compounds from these species highlights that bioprospecting in unexplored areas is a useful tool for NP discovery.

CHAPTER 7: TAXONOMIC CHARACTERIZATION OF A *MORTIERELLA* SP. RKAG 110 AND ISOLATION OF NEW CYCLIC HEPTAPEPTIDES

This chapter is a modification of the material published as

Grunwald, A.G., Berrue, F., Robertson, A.W., Overy, D.P., and Kerr R. G. Mortiamides A-D, Cyclic Heptapeptides from a Novel *Mortierella* sp. Obtained from Frobisher Bay. *J. Nat. Prod.* **2017**, Advanced online publication (10.1021/acs.jnatprod.7b00383).

7.1 Introduction

The order Mortierellales is one of the largest basal fungal lineages. In 1863 Coemans described the type genus within this order, *Mortierella polycephala* isolated from a mushroom. Since this time, six genera have been formally recognized within the order and over 100 species are described amongst these genera. Members within this order are soil inhabiting, saprobic organisms which decay organic matter and have a worldwide distribution. Species within *Mortierella* are commonly isolated and described from cold environments including *M. antarctica* and *M. alpina*[294,295]. Most notably, species within this genus are known for the production of large quantities of polyunsaturated fatty acids (PUFAs) including arachidonic acid and γ-linolenic acid[296]. *M. alpina* is currently used as an industrial source of arachidonic acid as up to 50% of its biomass is composed of various PUFAs[297,298]. Although there are many members of the genus *Mortierella*, very few NPs have been reported[299].

Nonribosomal peptides comprise a large class of diverse NPs with wide ranging bioactivity. Often NRPs undergo extensive modifications including hydroxylation, glycosylation and epimerization. The ability to epimerize amino acids from the L to the non-natural D-configuration occurs largely by epimerization domains within the NRPS enzyme. The activation (A) domain of the NRPS assembly line accepts L-amino acids for activation which are installed as amino-acyl or peptidyl-S-PCP intermediates and subsequently epimerized by epimerization domains within the NRPS module[300]. Alternatively, as in the case of cyclosporine, a racemase enzyme epimerizes an amino acid and provides the D-configured amino acid as a substrate to the NRPS enzyme[301].

The presence of D-amino acids within a peptide NP often enhances the stability of the corresponding compound by making it more resistant to degradation by peptidases[302].

The aim of this chapter was to taxonomically and chemically characterize a newly isolated *Mortierella* species from Frobisher Bay. This isolate (RKAG 110) was found in Chapter 4 to be phylogenetically distinct from all ITS sequenced *Mortierella* species. Preliminary screening of this isolate for NP production in Chapter 5 revealed it to be producing a series of new compounds. Within this chapter the phylogenetic and morphological characterization of this isolate will be discussed in addition to the purification and structure elucidation of four new cyclic heptapeptides, mortiamides A-D (**19**-**22**) which contain an unusually high proportion of D-amino acids.

7.2 Experimental Procedures

7.2.1 Morphological and Phylogenetic Characterization of RKAG 110

The initial isolation of RKAG 110 is described in Chapter 4. Determination of growth rates and morphological characterization was conducted in the same manner as for *Sesquicillium* isolates described in Chapter 6.2.1.

Sequencing of the ITS region and 28S rRNA gene was performed as described in Chapter 4.2.5 Reference ITS and 28S rRNA gene sequences were retrieved from GenBank and separate alignment of the ITS region and 28S rRNA gene was performed using MAFFT v. 7.058 using the L-INS-I alignment method for the ITS sequence and G-INS-I for the 28S rRNA gene [278] implemented in the CIPRES Science Gateway v. 3.3[279]. Both datasets were imported, trimmed and concatenated in MEGA v 6.06. Maximum likelihood analysis was carried out on the concatenated dataset using RAxML v. 7.2.7[280] implemented within CIPRES Science Gateway v. 3.3. RAxML was

run under default settings using the GTR+G model of nucleotide substitution[133] and 1000 bootstrap iterations.

7.2.2 Fermentation, Extraction and Purification of Mortiamides A-D

The initial chemical screening of RKAG 110 is described in Chapter 5. For large-scale fermentation RKAG 110 was inoculated into 15 mL of YM liquid seed and grown for five days (22°C, 200 rpm). The seed culture (200 µL) was used to inoculate the isolate onto 150, Petri plates (100 x 15 mm) containing 20 mL of solid PDA agar and grown for 21 days at 22°C. The solid agar cultures were roughly cut up, pooled and extracted with EtOAc. The extract was evaporated *in vacuo* and partitioned between 80% CH_3CN and 100% hexane. The CH_3CN layer was collected and evaporated *in vacuo* to give a crude extract (820 mg).

The crude extract was fractionated using automated reversed-phase flash chromatography (Combiflash Rf) with a linear gradient from 20% aqueous MeOH to 100% MeOH over 20 min on a 15.5 g C_{18} column (High Performance GOLD RediSep Rf) with a flow rate of 30 mL/min. The semipure fraction eluting at 16-17 min was subjected to reversed-phase HPLC on a Waters HPLC system coupled with an ELSD (Waters 2424) and PDA detector (Waters 2489) and a flow rate of 3 mL/min. Using a Gemini 110Å C18 column (5µm 250 x 10 mm, Phenomenex) and 20 min isocratic elution with 65% aqueous CH_3CN (0.1% formic acid) compounds **19** (4 mg), **20** (1.5 mg), **21** (3 mg) and **22** (2 mg) eluted at 16.9, 14.9, 24 and 25.5 min respectively. These compounds were tested for their antimicrobial and cytotoxic activity as described in Chapter 3.1.3 and 3.1.7.

7.2.3 Synthesis of Dipeptide Standards

All dipeptide standards were synthesized by Andrew Robertson (Department of Chemistry, UPEI). Benzylation of amino acids was accomplished according to literature precedent[303,304]. All dipeptide coupling reactions were carried out using benzyl ester protected amino acids and purchased *N*-Boc-protected amino acids according to modified literature precedent[305]. Deprotection of all dipeptides was accomplished first by hydrogenolysis with ~20% w/w of 10% Pd/C in DCM under an H_2 atmosphere for 24-48 h at room temperature, to produce the corresponding free carboxylic acid. Reactions were filtered through a celite plug and dried *in vacuo*, and used without further purification. Boc removal was accomplished by treatment with a 5 mL mixture of DCM:TFA (1:1) for 1 h at room temperature with stirring. Residual DCM and TFA were removed *in vacuo*. To ensure TFA removal, samples were dried, reconstituted in DCM and dried again. This process was repeated several times (4×) to ensure complete TFA removal, yielding the fully deprotected trifluoroacetic acid salt of the corresponding dipeptide. Reaction progress was monitored by TLC analysis. Deprotected dipeptides were used without further purification or extensive characterization.

7.2.4. Stereochemical Assignment by Marfey's Analysis

Mortiamides A-D (0.25 mg) were hydrolyzed with stirring in 6 N HCl (60 µL) at 80°C for 6 h and neutralized with 1 M $NaHCO_3$. *N*-(5-fluoro-2,4-dinitrophenyl-5)-L-alaninamide (FDAA, 0.4 mg in 380 µL of acetone) was added to the reaction mixture and stirred at 37 °C for 2 h. The reaction was quenched with 1 N aqueous HCl (80 µL)[281]. MeOH was added and the sample was analyzed by LC-HRMS using a Hypersil Gold 100 Å column (Thermo, 1.9 µm C_{18} 50 mm × 2.1 mm) and a flow rate of 400

μL/min. The following method was used: 0-55 min 95% H_2O/0.1% formic acid (solvent A) and 5% CH_3CN/0.1% formic acid (solvent B) to 60% solvent A and 40% solvent B, 55-57 min 60% solvent A: 40% solvent B to 100% solvent B, 57-60 min 100% solvent B. Retention times were compared to derivatized amino acid standards to determine the amino acid configurations. Partial hydrolysis of the mortiamides occurred with 6 N HCL at 80°C for 2 h and derivatized in the same manner as above. The derivatized partial hydrolysis of the compound was monitored by LC-HRMS for the mass of the required derivatized hydrosylate products.

Mortiamide A **(19)** White powder; $[\alpha]^{25}_{D}$ +26.0 (*c* = 0.1, MeOH); IR (film) ν_{max} 3309, 2962, 2934, 2875, 1652, 1533, 1456, 1386, 1027 cm^{-1}; HRESIMS *m/z* 804.5024 $[M+H]^+$, (calcd for $C_{44}H_{65}N_7O_7$, 804.5019).

Mortiamide B **(20)** White powder; $[\alpha]^{25}_{D}$ +11.0 (*c* = 0.1, MeOH); IR (film) ν_{max} 3329, 2963, 1651, 1592, 1531, 1456, 1385, 1352, 1026 cm^{-1}; HRESIMS *m/z* 838.4851 $[M+H]^+$, (calcd for $C_{47}H_{63}N_7O_7$, 838.4862).

Mortiamide C **(21)** White powder; $[\alpha]^{25}_{D}$ +11.0 (*c* = 0.1, MeOH); IR (film) ν_{max} 3330, 2963, 2936, 2875, 1646, 1531, 1468, 1392, 1029 cm^{-1}; HRESIMS *m/z* 770.5189 $[M+H]^+$, (calcd for $C_{41}H_{67}N_7O_7$, 770.5175).

Mortiamide D **(22)** White powder; $[\alpha]^{25}_{D}$ +20.0 (*c* = 0.1, MeOH); IR (film) ν_{max} 3329, 2962, 2931, 1652, 1603, 1531, 1465, 1392, 1027 cm^{-1}; (+) HRESIMS *m/z* 804.5021 $[M+H]^+$, (calcd for $C_{44}H_{65}N_7O_7$, 804.5019).

7.3 Results and Discussion

7.3.1 Phylogenetic Analysis

NCBI BLASTn of the ITS region of RKAG 110 showed greatest sequence similarity to *Mortierella antarctica* CBS 609.70 [NR111580.1] (96.4% similarity) and BLASTn of the 28S rRNA gene showed greatest similarity to *M. antarctica* CBS 609.70 [NG042563.1] (99.5%) and *M. alpina* CBS 210.32 [JN940866.1] (99.8%). A phylogeny of the Mortierellales was previously constructed by Wagner and used as a phylogenetic framework for this study[306]. Construction of a 28S rRNA phylogenetic tree confirmed RKAG 110 fell into Group 6 (*M. alpina* and *M. polycephala*) within the genus *Mortierella* as defined by Wagner (tree not shown). A multigene phylogeny was constructed using the maximum likelihood method and GTR+G model of nucleotide substitution (Figure 7.1). The tree was constructed using the ITS region and the D1/D2 domain of the 28S rRNA gene with members of group 6 used as reference sequences. Within this tree, all species formed well supported nodes, except for isolates within *M alpina* which formed a heterogeneous cluster. Initially these isolates were all described based on morphological similarity, however with DNA sequencing of reference genes, some of these isolates now appear to be genetically distinct from one another. Wagner described *M. alpina* as a species complex requiring reclassification of some isolates of *M. alpina* within this complex based on gene sequence data. RKAG 110 formed a well-supported clade with *M. alpina* FSU 6524, *M. alpina* CBS 219.35, *M. antarctica* CBS 194.89 and *M. antarctica* CBS 609.70. Due to the sequence dissimilarity between these isolates, *Mortierella* sp. RKAG 110 is proposed to be a new species within the genus *Mortierella*.

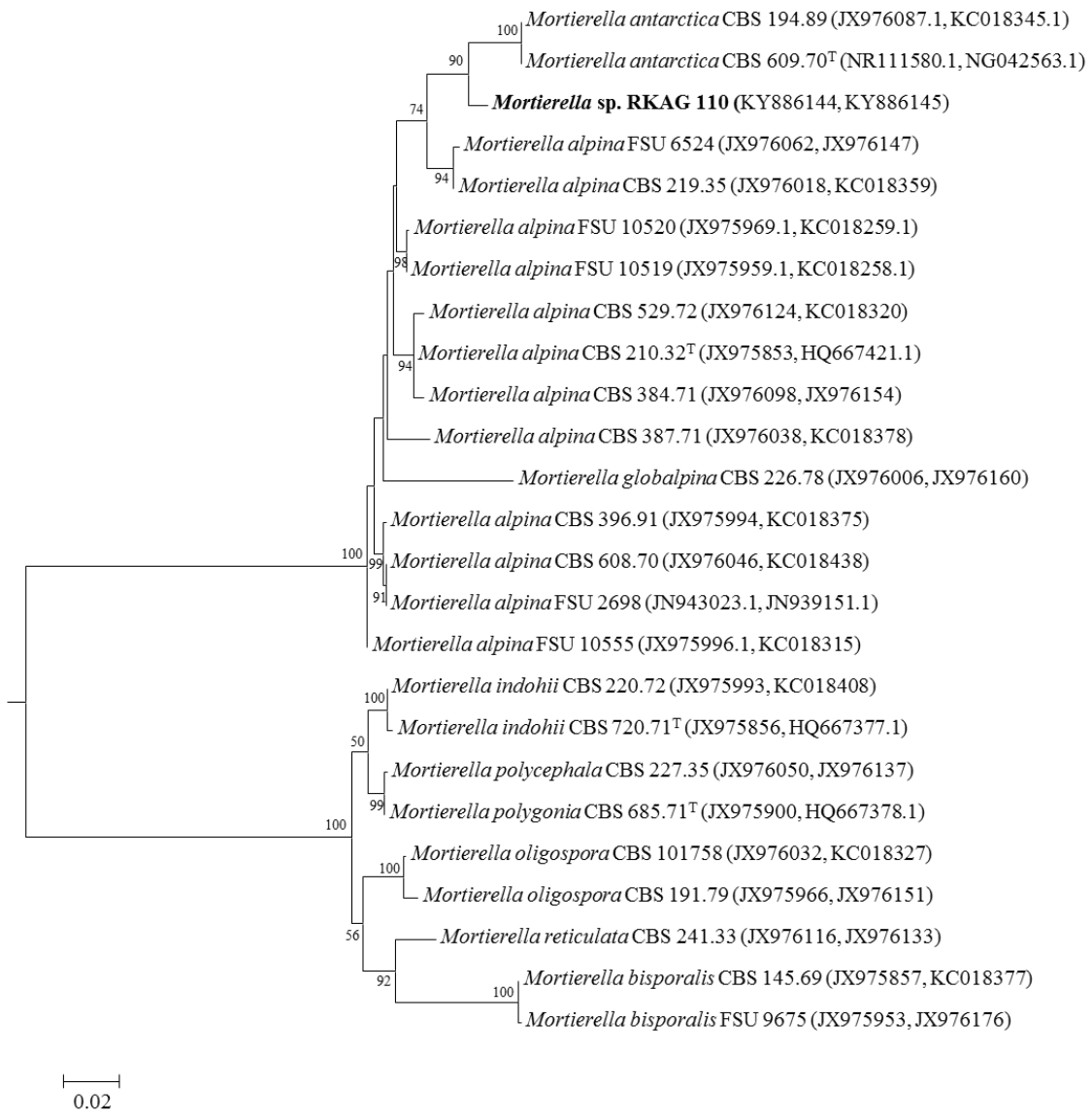

Figure 7.1. Maximum likelihood analysis of the D1/D2 domain of the 28S rRNA gene and ITS region from 24 taxa within the genus *Mortierella*. The phylogram is based on the multigene alignment of 640 nucleotides of the D1/D2 domain of the 28S rRNA gene and 480 nucleotides of the ITS1-5.8S-ITS2 region using the GTR+G model of nucleotide substitution. Node supports above 50% are given. The phylogram is midpoint rooted.

7.3.2 Morphological Characterization

Based on phylogenetic analysis, RKAG 110 was most similar to *M. antarctica*. Further efforts to characterize this isolate were undertaken by examining the macro and micro morphology (Figure 7.2). Colonies of RKAG 110 exhibited fast growth on PDA and 2% MEA, attaining an average colony radius of 22.5 ± 2.7 mm after 7 days at 22˚C on 2% MEA. The growth optima was between 15-22˚C with no growth observed at 37˚C and little growth at 4˚C and 30˚C (Figure 7.3). The colonies were white in colour, becoming off-white with age, broadly zonate and producing a concentric pattern. On PDA and CMA agar, good mycelial growth was observed and typical sporangia and sporangiospores appeared. The sporangiphores were unbranched and 26-40 µm in length containing a terminal sporangium. Sporangiophores exhibited a distinctly widening base (3-5 µm) and tapered (1-2 µm) toward the terminal sporangia. Sporangia were multispored, hyaline and globose and measured 10-15 µm in diameter. The sporangiospores were cylindrical and measured 3-5 µm x 2-3 µm (average 4 µm x 2 µm). After spore liberation, a 3-4 µm dome shaped collarette remained.

M. alpina and *M. antarctica* are described as having colonies that are white and cottony with unbranched sporangiophores that are less than 150 µm in length, have a distinctly widening base and have a terminal sporangia that contain many spores. The sporangiospores of *M. antarctica* are globose and 3-10 µm in diameter whereas those of *M. alpina* are 5-7 µm in length, cylindrical and sometimes curved to irregularly shaped[307].

RKAG 110 is similar to both *M. alpina* and *M. antarctica* by having a white, cottony appearance and unbranched sporangiophores with a widening base culminating

in a mutli-spored terminal sporangia. RKAG 110 differs from *M. antarctica* by having cylindrical spores measuring 3-5 µm x 2-3 µm, as opposed to globose spores measuring 3-10 µm in diameter. RKAG 110 differs from *M. alpina* by having smaller cylindrical sporangiospores, (avg. 4 µm in length vs. 5-7 µm) and shorter sporangiophores (26-40 µm vs. 60-150 µm). Due to the morphological and phylogenetic differences observed between *Mortierella* sp. RKAG 110 and *M. antarctica*, it is proposed RKAG 110 is a new species within the *Mortierella* and has tentatively been given the name *Mortierella arctica*.

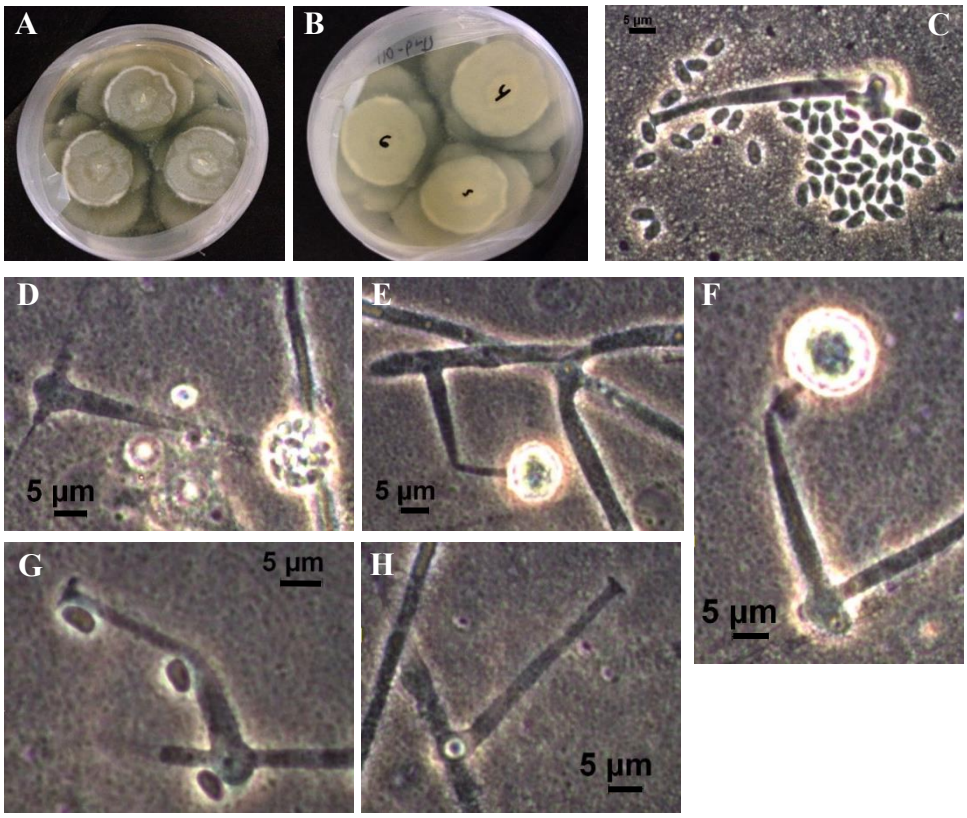

Figure 7.2. Phenotypic observations of RKAG 110. **A-B)** Colony morphology of RKAG 110 on PDA medium. **C)** Sporangiospores on 10% CMA. **D-F)** Sporangia and sporangiophores on 10% CMA. **G-H)** Sporangiophores with collarette after sporangia liberation on 10% CMA.

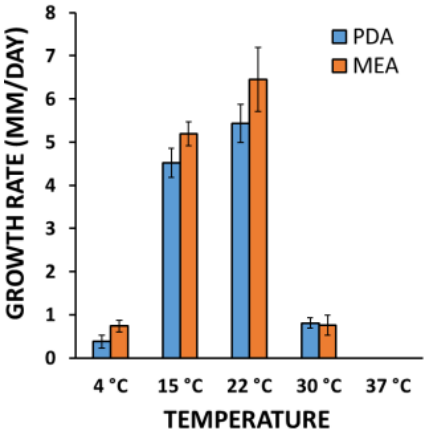

Figure 7.3. Average growth rate of RKAG 110 on PDA and MEA medium.

7.3.3 Natural Products of *Sesquicillium*

7.3.3.1 Preliminary Chemical Screening

An initial small-scale fermentation study of *Mortierella arctica* RKAG 110 was carried out using ten different fermentation media as per the OSMAC approach[176] as described in Chapter 3.1.1. EtOAc crude extracts were generated for each culture condition and partitioned between 80% CH_3CN and 100% hexane. In most fermentation media a family of compounds with an *m/z* 770.5175-838.4891 $[M+H]^+$ were observed in addition to two compounds with an *m/z* 629.4141 and 645.4091 $[M+H]^+$. The latter two compounds had hits within Antibase 2012 corresponding to the cyclic pentapeptides Plactin A and C which contain three D-amino acids and were isolated from an unknown *Agronomycete* fungus[308]. Due to the trace amount of these compounds produced, further confirmation of their structure could not be determined. The other compounds had no likely hits within Antibase 2012 and were produced in purifiable amounts as judged by ELSD detection during LC-HRMS analysis. A large-scale fermentation was undertaken in order to obtain enough material to structurally characterize these compounds.

7.3.3.2 Structure Elucidation of Mortiamides A-D

The solid agar fermentation of isolate RKAG 110 was extracted with EtOAc, dried *in vacuo*, and partitioned between 80% CH_3CN and 100% hexane. The CH_3CN soluble portion was subjected to flash chromatography and reversed-phase HPLC yielding four new cyclic heptapeptides, mortiamide A (**19**) (4.1 mg), B (**20**) (1.5 mg), C (**21**) (3.2 mg) and D (**22**) (2.4 mg) (Figure 7.4).

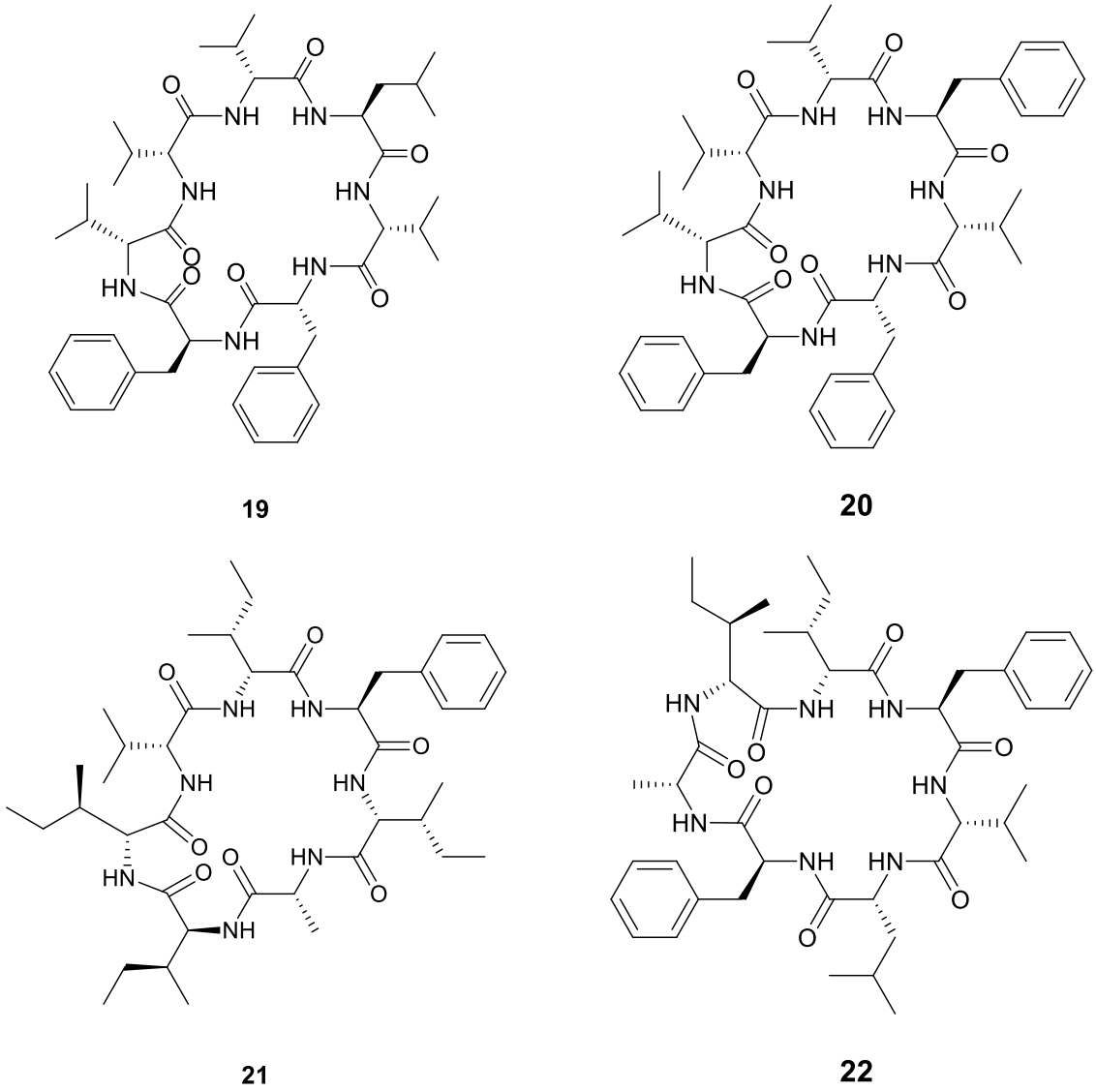

Figure 7.4. Molecular structure of mortiamides A-D.

Mortiamide A (**19**) (Figure 7.4, Table 7.1 and Appendix Figures A.45 and A.46) was obtained as a white powder and HRESIMS supported a molecular formula of $C_{44}H_{65}N_7O_7$ (*m/z* 804.5024 $[M + H]^+$) requiring 16 degrees of unsaturation. The peptidic nature of the compound was determined by the presence of seven amide protons within the ^1H NMR spectrum while the ^{13}C NMR spectrum revealed the presence of seven amide carbonyls between δ170.5 and 173.3 and seven α-amino acid carbon resonances between δ_C 53.4 and 60.3. Additionally TOCSY experiments revealed the presence of seven ^1H spin systems corresponding to seven amino acid side chains consisting of one Leu, two Phe, and four Val residues. Amino acid side chains were assigned using COSY, HMBC, and TOCSY NMR spectra whereby connectivity was determined using HMBC, ROESY and MS/MS analysis (Figure 7.5). HMBC correlations from Val^1-NH (δ_H 8.20) to Phe^2-C=O (δ_C 171.4) and Val^2-NH (δ_H 7.86) to Val^1-C=O (δ_C 172.4) established the three amino acid sequence Phe^2-Val^1-Val^2. HMBC correlations between Val^4-NH (δ_H 7.64) and Leu-C=O (δ_C 171.6) established the two amino acid sequence Leu-Val^4. ROESY correlations from Val^2-Hα (δ_H 4.01) to Val^3-NH (δ_H 8.29) and Val^3-Hα (δ_H 4.03) to Leu-NH (δ_H 7.38) connected both fragments via a Val residue resulting in the six amino acid sequence Phe^2-Val^1-Val^2-Val^3-Leu-Val^4. ROESY correlations from Val^4-Hα (δ_H 4.12) to Phe^1-NH (δ_H 7.72) and Phe^1-Hα (δ_H 4.63) to Phe^2-NH (δ_H 7.64) resulted in the final sequence of the heptapeptide being assigned as [cyclo-(Phe^1-Phe^2-Val^1-Val^2-Val^3-Leu-Val^4)] which was subsequently confirmed using MS/MS experiments (Appendix Figure A.46).

Using Marfey's method[309], **19** was found to contain L-Leu, D-Val and both L-Phe and D-Phe (Appendix Figures A.56-A.58). There are many reports of peptides

containing both L and D configurations of an amino acid within their structure. Several methods have been reported to enable the localization of L and D amino acids within the same molecule including total synthesis[308], single crystal X-ray diffraction[310] and comparison of partial hydrosylate products to synthesized standards[311-312]. Due to the small amounts of peptide obtained and challenging nature of crystallization, this was not a viable option. Total synthesis was also not a viable option due to the large number of compounds that would have to be synthesized, particularly in regards to compounds **20** and **21**. Therefore partial hydrolysis was deemed to be the best option.

A partial hydrolysis of **19** was undertaken to generate dipeptide fragments which were derivatized with *N*-(5-fluoro-2,4-dinitrophenyl-5)-L-alaninamide (FDAA) and analyzed by LC-HRMS.[14] A derivatized Phe-Phe fragment was detected after partial hydrolysis and was used to determine the position of L and D-Phe within the molecule. The retention time of the partial hydrosylate product (FDAA-Phe-Phe) was compared to synthesized dipeptide standards that were derivitized in the same manner (FDAA-L-Phe-D-Phe and FDAA-D-Phe-L-Phe) and revealed the retention time of the partial hydrosylate fragment was consistent with the retention time of the synthesized FDAA-D-Phe-L-Phe standard (figure 2). Therefore the final structure of **19** was assigned as [cyclo-(D-Phe-L-Phe-D-Val-D-Val-D-Val-L-Leu-D-Val)].

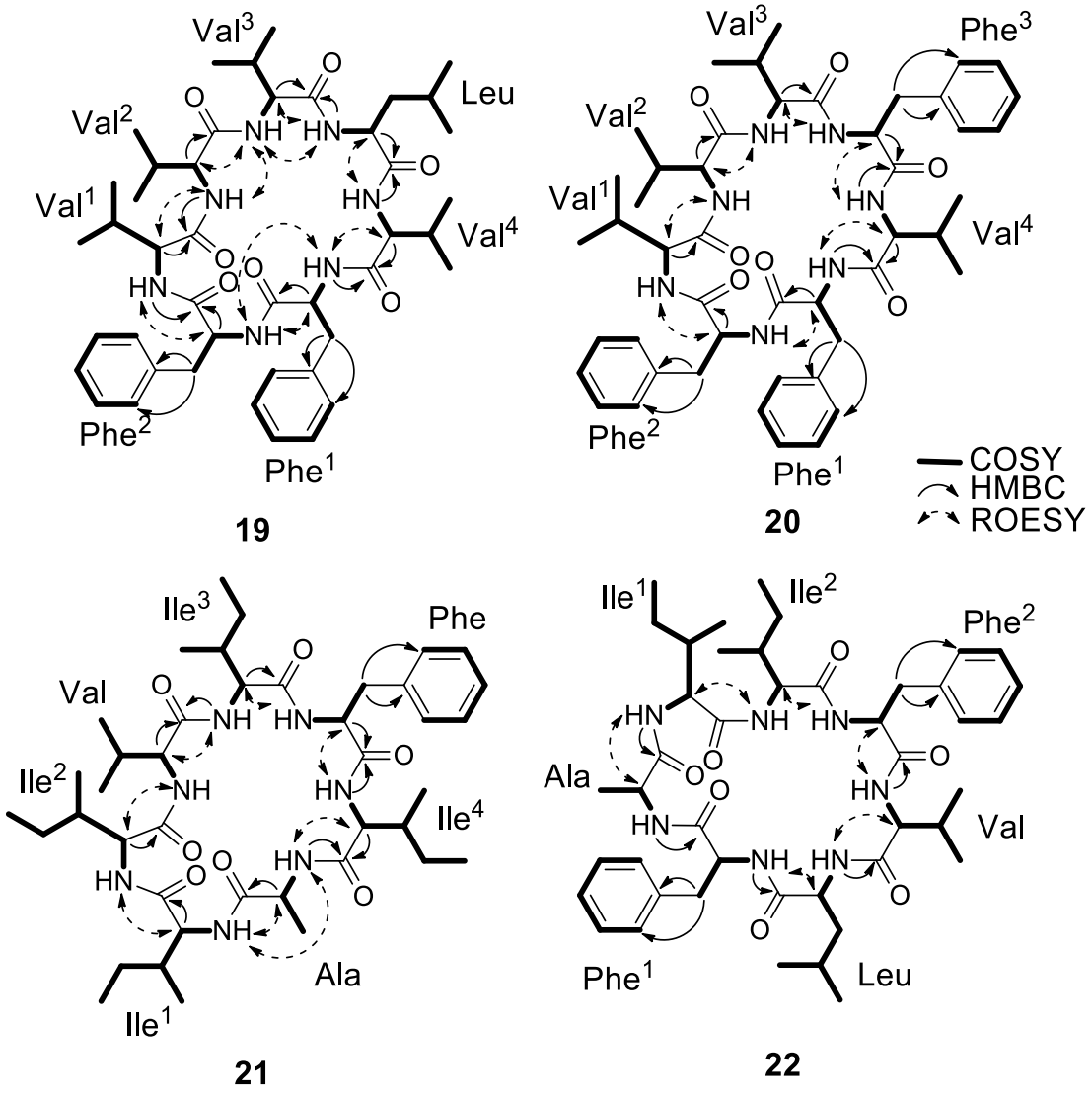

Figure 7.5. Key NMR correlations for structure elucidation of mortiamides A-D.

Mortiamide B (**20**) (Figure 7.4, Table 7.1 and Appendix Figures A.47 and A.48) was obtained as a white powder and HRESIMS supported a molecular formula of $C_{47}H_{63}N_7O_7$ (*m/z* 838.4851 $[M + H]^+$) requiring 20 degrees of unsaturation. TOCSY experiments revealed the presence of seven ^1H spin systems corresponding to three Phe and four Val residues. HMBC correlations from Phe^1-NH (δ_H 7.81) to Val^4-C=O (δ_C 170.7) and Val^4-NH (δ_H 7.56) to Phe^3-C=O (δ_C 170.5) established the three amino acid sequence Phe^3-Val^4-Phe^1. ROESY correlations from Phe^3-NH (δ_H 7.70) to Val^3-Hβ (δ_H 2.06), Val^3-NH (δ_H 8.00) to Val^2- Hβ (δ_H 2.29), Val^2-NH (δ_H 7.78) to Val^1- Hα (δ_H 4.07), Val^1-NH (δ_H 8.24) to Phe^2- Hα (δ_H 4.49) and Phe^2-NH (δ_H 8.19) to Phe^1- Hα (δ_H 4.61) established the final sequence as cyclo-Phe^1-Phe^2-Val^1-Val^2-Val^3-Phe^3-Val^4 (Figure 7.5). The order of the amino acids was confirmed by MS/MS analysis (Appendix Figure A.49). Peptide **20** differed from **19** by the replacement of the Leu residue with a Phe residue in position six. Marfey's analysis[281] of the total hydrosylate of **20** revealed the presence of D-Val, L-Phe and D-Phe in a 2:1 ratio respectively. After partial hydrolysis and derivatization, the retention time of the FDAA-Phe-Phe (RT 48.55 min) fragment was consistent with the retention time of the synthesized FDAA-D-Phe-L-Phe dipeptide (RT 48.40 min). The remaining Phe residue was assigned as L and the final structure of **20** was assigned as [cyclo-(D-Phe-L-Phe-D-Val-D-Val-D-Val-L-Phe-D-Val)] (Appendix Figures A.56-A.58).

Table 7.1. ^{1}H (600 MHz) and ^{13}C (150 MHz) NMR data of mortiamide A (19) and B (20) in DMSO-*d_6*.

Mortiamide A			**Mortiamide B**		
	δ_C, type	δ_H (*J*, Hz)		δ_C, type	δ_H (*J*, Hz)
D-Phe[1]			**D-Phe[1]**		
CO	171.1, C		CO	171.1, C	
NH		7.72, d (8.1)	NH		7.81, d (7.8)
α	53.4, CH	4.63, m	α	53.3, CH	4.61, m
β_1	36.8, CH_2	2.98, dd (13.7, 7.3)	β_A	36.8, CH_2	2.97, dd (6.2, 13.5)
β_2		2.76, dd (13.7, 7.5)	β_B		2.77, dd (8.1, 13.5)
1’	137.5, C		1’	137.7, C	
2’	129.1, CH	7.10, m	2’	128.9, CH	7.09, m
3’	128.2, CH	7.21, m	3’	129.0, CH	7.21, m
4’	126.4, CH	7.18, m	4’	126.2, CH	7.17, m
L-Phe[2]			**L-Phe[2]**		
CO	171.4, C		CO	171.4, C	
NH		8.29 [a]	NH		8.19, d (5.7)
α	55.2, CH	4.47, m	α	55.2, CH	4.49, m
β_1	36.3, CH_2	2.88, dd (13.6, 7.6)	β_A	36.3, CH_2	2.91[a]
β_2		2.81, dd (13.6, 8.0)	β_B		2.83, dd (13.6, 8.2)
1’	137.2, C		1’	137.4, C	
2’	129.1, CH	7.19, m	2’	129.0, CH	7.21, m
3’	128.2, CH	7.23, m	3’	128.0, CH	7.24, m
4’	126.5, CH	7.23, m	4’	126.2, CH	7.17, m
D-Val[1]			**D-Val[1]**		
CO	172.4, C		CO	171.8, C	
NH		8.20, d (7.0)	NH		8.24[b]
α	58.4, CH	4.06, m	α	58.5, CH	4.07[a]
β	29.3, CH	2.10, m	β	29.3, CH	2.10, m
γ1	17.0, CH3	0.73, d (6.9)	γ1	17.1, CH3	0.75, d (6.9)
γ2	19.1, CH3	0.62, d (6.9)	γ2	18.8, CH3	0.65, d (6.9)
D-Val[2]			**D-Val[2]**		
CO	173.3, C		CO	171.4, C	
NH		7.86, d (5.3)	NH		7.78, d (7.8)
α	60.3, CH	4.01, m	α	59.7, CH	4.03[a]
β	28.3, CH	2.34, m	β	28.3, CH	2.29, m
γ1	19.4, CH3	1.03, d (6.6)	γ1	19.0, CH3	0.99, d (6.7)
γ2	18.9, CH3	0.91[a]	γ2	18.8, CH3	0.89, d (6.7)
D-Val[3]			**D-Val[3]**		
CO	170.5, C		CO	172.4, C	
NH		8.29[a]	NH		8.00, d (5.2)
α	59.0, CH	4.03, m	α	58.5, CH	4.03[a]
β	29.1, CH	2.22, m	β	29.3, CH	2.06, m
γ1	18.9, CH3	0.91[a]	γ1	18.7, CH3	0.76, d (6.9)
γ2	16.8, CH3	0.84, d (6.9)	γ2	16.5, CH3	0.63, d (6.9)
L-Leu			**L-Phe[3]**		
CO	171.6, C		CO	170.5, C	
NH		7.38, d (4.4)	NH		7.70[b]
α	58.8, CH	4.09, m	α	55.4, CH	4.39, m

β	38.8, CH2	1.55, m	β_A	35.8, CH_2	3.08, dd (13.8, 6.2)
γ	24.0, CH_3	1.65, m	β_B		2.90, m
δ1	22.7, CH3	0.90[a]	1’	137.9, C	
δ2	21.1, CH3	0.82, d (6.6)	2’	128.9, CH	7.29, m
			3’	128.0, CH	7.24, m
			4’	126.2, CH	7.17, m
D-Val			**D-Val**		
CO	170.5, C		CO	170.7, C	
NH		7.64, d (9.3)	NH		7.56, d (7.8)
α	58.8, CH	4.12, m	α	58.5, CH	4.06[a]
β	30.7, CH	1.91, m	β	29.7, CH	1.88, m
γ1	17.7, CH3	0.69, d (6.8)	γ1	17.2, CH3	0.51[a]
γ2	19.0, CH3	0.64, d (6.8)	γ2	18.7, CH3	0.50[a]

[a]overlapping signals
[b]broad signals

Mortiamide C (**21**) (Figure 7.4, Table 7.2 and Appendix Figures A.50 and A.51) was obtained as a white powder and HRESIMS supported a molecular formula of $C_{41}H_{67}N_7O_7$ (*m/z* 770.5175 $[M + H]^+$) requiring 12 degrees of unsaturation. TOCSY experiments revealed the presence of seven ^1H spin systems corresponding to one Phe, one Ala, one Val and four Ile residues. HMBC correlations from Ala-NH (δ_H 7.54) to Ile^4-C=O (δ_C 170.8) and Ile^4-NH (δ_H 7.80) to Phe-C=O (δ_C 170.6) established the three amino acid sequence Phe-Ile^4-Ala. ROESY correlations from Phe-NH (δ_H 7.61) to Ile^3-Hα (δ_H 4.00), Ile^3-NH (δ_H 7.89) to Val-Hα (δ_H 4.03), Val-NH (δ_H 7.67) to Ile2-Hα (δ_H 4.31), Ile^2-NH (δ_H 8.44) to Ile^1-Hα (δ_H 4.27) and Ile^1-NH (δ_H 7.93) to Ala-Hα (δ_H 4.42) established the final sequence as [cyclo-(Ala-Ile^1-Ile^2-Val-Ile^3-Phe-Ile^4)] (Figure 7.5) which was confirmed by MS/MS experiments (Appendix Figure A.52). The absolute configuration of the amino acid residues was determined to be D-Ala, D-Val, L-Phe L-Ile and D-Ile whereby D-Ile and L-Ile were in in a 3:1 ratio. By comparison of the FDAA-Ile-Ala (RT 37.41 min) and FDAA-Ile-Ile (RT 42.56 min) partial hydrosylate products of **3** to synthesized dipeptide standards it was determined the retention times by LC-HRMS corresponded to FDAA-D-Ile-D-Ala (RT 37.03 min) and FDAA-L-Ile-D-Ile (RT 41.85). Since L-Ile had been localized, the remaining Ile was assigned as D resulting in the final structure being assigned as [cyclo-(D-Ala-L-Ile-D-Ile-D-Val-D-Ile-L-Phe-D-Ile)] (Appendix Figures A.56, A.57 and A.59).

Mortiamide D (**22**) (Figure 4.4, Table 7.2 and Appendix Figures A.53 and A.54) was obtained as a white powder and HRESIMS supported a molecular formula of $C_{44}H_{65}N_7O_7$ (*m/z* 804.5021 $[M + H]^+$) requiring 16 degrees of unsaturation. TOCSY experiments revealed the presence of seven ^1H spin systems corresponding to one Ala,

one Leu, one Val, two Phe and two Ile residues. HMBC correlations from Leu-NH (δ_H 8.32) to Val-C=O (δ_C 171.3) and Val-NH (δ_H 7.35) to Phe^2-C=O (δ_C 170.9) established the three amino acid sequence Phe^2-Val-Leu. HMBC correlations between Ile^1-NH (δ_H 7.44) to Ala-C=O (δ_C 171.9) established a two amino acid sequence of Ala-Ile^1. Fragment 1 was connected to fragment 2 by an Ile residue supported by ROESY correlations from Phe2-NH (δ_H 8.13) to Ile2-Hα (δ_H 3.98) and Ile^2-NH (δ_H 8.38) to Ile^1-Hα (δ_H 4.28) resulting in the six amino acid fragment Ala-Ile^1-Ile^2-Phe^2-Val-Leu. Due to overlapping ^{1}H signals from Ala-NH (δ_H 8.22) and Phe^1-NH (δ_H 8.22), placement of Phe^1 could not be definitively assigned using ROESY or HMBC correlations. In order to support the molecular formula and requirement for unsaturation, the remaining Phe residue was used to cyclize the peptide sequence by peptide bonds between the Ala and Leu residues resulting in the final sequence as [cyclo-(Leu-Phe^1-Ala-Ile^1-Ile^2-Phe^1-Val-)] (Figure 7.5). The final sequence of the peptide was confirmed by MS/MS experiments (Appendix Figure A.55). The absolute configuration of the amino acids within the peptide was definitively assigned using the advanced Marfey's method and consisted of D-Ala, D-Val, L-Phe, D-Leu and D-Ile allowing the final structure to be assigned as [cyclo-(D-Leu-L-Phe D-Ala-D-Ile-D-Ile-L-Phe-D-Val)] (Appendix Figures A.56, A.57 and A.59).

Table 7.2. ^{1}H (600 MHz) and ^{13}C (150 MHz) NMR data of mortiamide C (21) and D (22) in DMSO-*d6*.

Mortiamide C			**Mortiamide D**		
	δ_C, type	δ_H, (*J*, Hz)		δ_C, type	δ_H, (*J*, Hz)
D-Ala			**D-Leu**		
CO	172.9, C		CO	171.8, C	
NH		7.54, d (7.4)	NH		8.32[b]
α	47.9, CH	4.42, m	α	51.9, CH	4.01, m
β	17.3, CH_3	1.18, d (6.8)	β	39.1, CH_2	1.42, m
			γ	23.9, CH	1.22, m
			δ1	22.6, CH_3	0.78, d (6.6)
			δ2	22.1, CH_3	0.72[a]
L-Ile[1]			**L-Phe[1]**		
CO	172.2, C		CO	170.5, C	
NH		7.93, d (7.6)	NH		8.22, d (7.0)
α	57.4, CH	4.27, m	α	55.4, CH	4.26, m
β	35.1, CH	1.71, m	β_A	36.4, CH_2	3.16, m
$\gamma 1_A$	24.3, CH_2	1.49, m	β_B		2.78, dd (13.7, 10.9)
$\gamma 1_B$		1.11, m	1’	138.2, C	
γ2	14.7, CH_3	0.81[a]	2’	129.0, CH	7.24, m
δ	10.6, CH_3	0.83[a]	3’	128.1, CH	7.23, m
			4’	126.2, CH	7.19, m
D-Ile[2]			**D-Ala**		
CO	172.2, C		CO	171.9, C	
NH		8.44[b]	NH		8.22, d (7.1)
α	56.0, CH	4.31, m	α	48.5, CH	4.31, m
β	35.5, C	2.00, m	β	17.5, CH_3	1.20, d (7.2)
$\gamma 1_A$	25.6, CH_2	1.28, m			
$\gamma 1_B$		1.22, m			
γ2	14.3, CH_3	0.87, d (7.0)			
δ	11.2, CH_3	0.81[a]			
D-Val			**D-Ile[1]**		
CO	173.5, C		CO	172.4, C	
NH		7.67[b]	NH		7.44, d (6.9)
α	59.5, CH	4.03, m	α	57.3, CH	4.28, m
β	28.2, CH_2	2.25, m	β	36.1, CH	1.92, m
γ1	18.7	0.94, d (6.7)	$\gamma 1_A$	25.4, CH_2	1.34, m
γ2	18.8, C	0.85, d (7.1)	$\gamma 1_B$		1.09, m
			γ2	15.0, CH_3	0.85[a]
			δ	11.4, CH_3	0.86[a]
D-Ile[3]			**D-Ile[2]**		
CO	170.7, C		CO	171.5, C	
NH		7.89, d (8.8)	NH		8.38[b]
α	57.8, CH	4.00, m	α	58.6, CH	3.98, m
β	35.9, C	1.78, m	β	35.8, C	1.72, m
$\gamma 1_A$	23.5, CH_2	1.10, m	γ1	23.6, CH_2	1.02, m
$\gamma 1_B$		1.02, m	γ2	15.3, CH_3	0.63, d (6.7)
γ2	15.1, CH_3	0.72, m	δ	11.2, CH_3	0.66[a]
δ	11.1, CH_3	0.68, t (7.4)			

L-Phe			**L-Phe[2]**		
CO	170.6, C		CO	170.9, C	
NH		7.61[b]	NH		8.13[b]
α	55.4	4.40, m	α	55.2, CH	4.44, m
β_A	35.9, CH_2	3.03, dd (13.8, 6.2)	β_A	36.5, CH_2	3.13, m
β_B		2.85, dd (13.8, 9.2)	β_B		2.94, dd (10.1, 13.7)
1’	137.5, C		1’	138.0, C	
2’	129.0, CH	7.30, m	2’	129.0, CH	7.25, m
3’	128.1, CH	7.25, m	3’	128.1, CH	7.27, m
4’	126.3, CH	7.19, m	4’	126.2, CH	7.19, m
D-Ile[4]			**D-Val**		
CO	170.8		CO	171.3, C	
NH		7.80, d(8.5)	NH		7.35, d (6.7)
α	56.0, CH	4.30, m	α	58.4, CH	4.00, m
β	36.6, CH	1.81, m	β	29.5, CH	2.02, m
$\gamma1_A$	25.1, CH_2	0.99, m	γ1	18.2, CH_3	0.73[a]
$\gamma1_B$		0.86, m	γ2	18.8, CH_3	0.68[a]
γ2	14.0, CH_3	0.64, d (6.9)			
δ	11.3, CH_3	0.74[a]			

[a]overlapping signals
[b]broad signals

Mortiamides A-D represent four new members within the cyclic peptide family. Cyclic heptapeptides have previously been reported from many microorganisms including fungi and bacteria[310,313,314] as well as macro organisms including tunicates, sponges and plants[315,316] and exhibit a wide range of activities[313,314,317]. Mortiamides A-D are characterized by the presence of seven hydrophobic amino acids, whereby five of these residues are in the D-configuration. The asymmetry of these molecules is conserved across each of the peptides whereby site two and six always contain amino acids in the L-configuration and sites one, three, four, five and seven contain amino acids in the D-configuration. The occurrence of a large number of D amino acids is relatively rare for cyclic peptides and makes the Mortiamides intriguing members within the cyclic peptide family.

7.3.3.3 Bioactivity Testing

Compounds **19**-**22** were assayed for biological activity against methicillin resistant *Staphylococcus aureus* (ATCC 33591), vancomycin resistant *Enterococcus faecium* (EF379), *Staphylococcus warneri* (ATCC 17917), *Pseudomonas aeruginosa* (ATCC 14210), and *Candida albicans* (ATCC 14035). No significant activity was observed for any compound tested at a concentration of 128 µg/mL. Compounds **19**-**22** were also tested for cytotoxicity against keratinocyte, fibroblast, HTB-26 and MCF-7 breast cancer cell lines. None of the tested compounds exhibited activity against these cell lines at 128 µg/mL.

7.4 Conclusions

A new species of *Mortierella* was isolated from Frobisher Bay and was determined to be phylogenetically and morphologically distinct from other described

Mortierella species. Chemical investigation of this isolate led to the isolation of four new cyclic heptaptides, mortiamides A-D. These heptapeptides are unique as they contain five D-amino acids within their structure. These compounds exhibited no antimicrobial or cytotoxic activity. Further investigation into the determination of the molecular target of these compounds may prove useful, as these compounds showed no cytotoxic activity against healthy human cell lines. The isolation of a new species from Frobisher Bay producing new NPs reinforces the idea that bioprospecting in unexplored regions is a useful tool for the discovery of new NPs.

CHAPTER 8: TAXONOMIC CHARACTERIZATION OF NEW TOLYPOCLADIUM SPECIES FROM FROBISHER BAY AND CHARACTERIZATION OF NEW TETRAMIC ACID CONTAINING NATURAL PRODUCTS

This chapter is a modification of the material published as

Grunwald, A.G., Berrue, F., Overy, D.P., and Kerr R. G. Isolation of iqalisetin A and B from a *Tolypocladium* sp. isolated from marine sediment from Frobisher Bay in Canada's Arctic. *Can. J. Chem.* **2016**, *94(4)*, 444-448.

8.1 Introduction

The genus *Tolypocladium* was erected in 1971 by Gams to accommodate the isolation of its first member, *T. inflatum* from a Norwegian soil sample[318]. Since the erection of this genus, 42 additional species have been described. Members within *Tolypocladium* are commonly found in cold and temperate environments and have been isolated from soils[266] and as parasites and pathogens of insects and rotifers[319, 320,321]. Anamorphic states of the genus *Tolypocladium* are currently characterized by conidiophore morphologies as being either verticillium-like or presenting swollen and tapering phialides. Under the "one fungus, one name" initiative[322] taxa of the genera *Elaphocordyceps* and *Chaunopycnis* have been reclassified as taxa of the genus *Tolypocladium* based on phylogenetic congruence and morphological similarity[323].

The genus *Tolypocladium* rose to prominence in the field of fungal NPs after the discovery of the immunosuppressant drug, cyclosporin A[19], from an isolate of *T. inflatum*. Since then, tremendous effort has been expended in exploring the chemical diversity of members of the genus *Tolypocladium* and has resulted in the isolation of a diverse range of NPs including the efrapeptins[324], the elvapeptins[325], the cyclic tetrapeptide 1-alaninechlahmydocin[326], the peptaibols LP237-F8, LP237-F7 and LP237-F5[327] and the diketopiperazines Sch 54796 and Sch 54794[328].

NPs containing a tetramic acid (2,4-pyrrolidinedione) ring system are produced by many terrestrial and marine organisms including bacteria[329], cyanobacteria[330], fungi[331] and sponges[332]. These compounds are synthesized via a polyketide synthase-non-ribosomal peptide synthetase (PKS-NRPS) hybrid enzyme which catalyzes the condensation of amino acids and activated polyketide moieties and releases them via an R-domain catalyzed Dieckmann cyclization as a 3-acyltetramic acid[333,334]. Enormous

structural diversity is observed within family of compounds by the incorporation of different amino acids within the tetramic acid core, the polyketide substrate incorporated and the level of decoration (e.g. glycosylations, methylations, hydroxylations.)[335]. These molecules are of increasing interest due to their wide range of potent biological activities including antimicrobial[336], antitumor[337] and antiviral[338] which arises from their incredible structural diversity. There have been several instances of the isolation of tetramic acid containing compounds from the genus *Tolypocladium* including ophiosetin from *T. ophioglossoides*[331] (syn. *Elaphocordyceps ophioglossoides*), tolypoalbin and F-14329 from *T. album*[339] (syn. *Chaunopycnis alba*), and the chaunolidines from an unknown *Tolypocladium* sp.[340] (at the time cited as an unknown *Chaunopycnis* sp.).

Due to the isolation of putatively new species of *Tolypocladium* (Chapter 4), the detection of putatively new metabolites from these species (Chapter 5) and the known ability of the genus *Tolypocladium* to produce a wide range of bioactive NPs, further taxonomic and chemical investigation of several isolated *Tolypocladium* species were undertaken. The aim of this study was to taxonomically characterize T*olypocladium* species isolated from Frobisher Bay (RKAG 373, 560, 574, 673 and 677) and characterize the metabolites produced by these isolates. The structure elucidation of new tetramic acid compounds from *Tolypocladium* sp. RKAG 373 is described within, in addition to the isolation of a new (at the time of isolation) tetramic acid containing compound from *Tolypocladium* sp. RKAG 560.

8.2 Experimental Procedures

8.2.1 Morphological and Taxonomic Characterization

The initial isolation of *Tolypocladium* sp. RKAG 373, 560, 574, 673 and 677 is described in Chapter 4. Determination of growth rates and morphological characterization was carried out in the same manner as for *Sesquicillium* isolates described in Chapter 6.2.1.

Sequencing of the ITS region, 28S rRNA gene, 18S rRNA gene and TEF 1-α gene was performed as described in Chapter 4.2.5. Reference sequences were retrieved from GenBank and separate alignment of each individual gene was performed using MAFFT v. 7.058 using the L-INS-I alignment method for the ITS sequence and G-INS-I for the 28S rRNA, 18S rRNA and TEF-1α genes[278] implemented in the CIPRES Science Gateway v 3.3[279]. The datasets were imported, trimmed and concatenated in MEGA v 6.06. Maximum likelihood analysis was carried out on the concatenated dataset using RAxML v. 7.2.7[280] implemented within CIPRES Science Gateway. RAxML was run using the GTR+G model of nucleotide substitution[133] and 1000 bootstrap iterations.

8.2.2 Fermentation, Extraction and Purification of Iqalisetin A and B

Tolypocladium sp. (RKAG 373) was inoculated into 15 mL of YM liquid and grown for five days (22°C, 200 rpm). The seed culture (200 µL) was used to inoculate the producing strain onto 50 Petri plates (100 x 15 mm) containing 20 mL of solid CYA agar and grown for 21 days at 22°C. The solid agar cultures were roughly cut up, pooled and repeatedly extracted with EtOAc. The extract was evaporated to dryness and partitioned between 80% CH_3CN and 100% hexane. The CH_3CN layer was collected and evaporated to dryness *in vacuo* to give a crude extract (117 mg).

The crude extract was fractionated using automated reversed-phase flash chromatography with a linear gradient from 20% aqueous methanol to 100% methanol over 15 min on a 15.5 g C_{18} column (High Performance GOLD RediSep Rf) with a flow rate of 30 mL/min. The semipure fraction eluting at 9.5 min was subjected to RP-HPLC on a Thermo Surveyor HPLC system coupled with an ELSD (Sedex 55) and PDA detector using a Gemini 110Å C18 column (5µm 250 x 10 mm, Phenomenex) and 20 min isocratic elution with 70% aqueous MeOH (0.1% formic acid) resulting in the purification of **23** (34.2 mg) at 10 min and **24** (1.15 mg) at 13 min. The antimicrobial and cytotoxic activity of these compounds was determined as described in Chapter 3.1.3 and 3.1.7.

8.2.3 Stereochemical Assignment by Marfey's Method

A portion (0.25 mg) of compounds **23** and **24** were dissolved in 70 µL of acetone-H_2O (1:1) and treated with $NaIO_4$ (2.0 mg) and $KMnO_4$ (1.0 mg) at 5°C for 30 min. Subsequently the mixture was treated with 2 N aqueous HCl (60 µL) at 100˚C for 2 h and neutralized with 1 M $NaHCO_3$[17]. *N*-(5-fluoro-2,4,-dinitrophenyl-5)-L-alaninamide (FDAA, 0.4 mg in 380 µL of acetone) was added to the reaction mixture and stirred at 37˚C for 2 h. The reaction was quenched with 1 N aqueous HCl (80 µL)[281], MeOH was added and the sample was analyzed by LC-MS using a Hypersil Gold 100 Å column (Thermo, 1.9 µm C_{18} 50 mm × 2.1 mm) and a flow rate of 400 µL/min. The following method was used: 0-55 min 95% H_2O/0.1% formic acid (solvent A) and 5% CH_3CN/0.1% formic acid (solvent B) to 60% solvent A and 40% solvent B, 55-57 min 60% solvent A:40% solvent B to 100% solvent B, 57-60 min 100% solvent B. L-alanine

(0.25 mg) and DL-alanine (0.25 mg) were dissolved in acetone-H_2O (1:1) and derivatized with FDAA and analyzed as described above.

Iqalisetin A (**23**) Red oil; $[\alpha]_D^{23}$ +50.0 (*c* 1.0, MeOH); UV (MeOH) λ_{max} 222, 279 nm; IR (film) V_{max} 3334, 2962, 2928, 2876, 1666, 1607, 1506, 1458, 1372, 1227, 1093, 1026, 909, 887, 857, 830, 787, 747, 730, 705 cm^{-1}; (+) HRESIMS *m/z* 306.1702 $[M + H]^+$, (calcd. for $C_{17}H_{24}NO_4$, 306.1705).

Iqalisetin B (**24**) Red oil; $[\alpha]_D^{23}$ +39.74 (*c* 0.87, MeOH); UV (MeOH) λ_{max} 222, 279 nm; IR (film) V_{max} 3310, 2961, 2930, 2876, 1712, 1665, 1606, 1506, 1459, 1404, 1372, 1227, 1093, 1026, 909, 887, 858, 829, 787, 747, 729, 704 cm^{-1}; (+) HRESIMS *m/z* 320.1492 $[M + H]^+$, (calcd. for $C_{17}H_{22}NO_5$, 320.1498).

8.2.4 Fermentation, Extraction and Purification of Tolypoalbin, Trichodin A and F-14329

Tolypocladium sp. RKAG 560 was inoculated into 15 mL of YM liquid seed at 22°C and agitated at 200 rpm for five days. The seed culture (200 µL) was used to inoculate the producing strain onto 50 Petri plates (100 x 15 mm) containing 20 mL of solid PDA agar and grown for 21 days at 22°C. The solid agar fermentations were pooled and repeatedly extracted with EtOAc. The extract was evaporated to dryness i*n vacuo* and partitioned between 80% CH_3CN and 100% hexane. The CH_3CN layer was collected and evaporated to dryness *in vacuo* to give a crude extract (117 mg).

The crude extract was fractionated using automated reverse-phase flash chromatography with a linear gradient from 5% aqueous MeOH to 100% MeOH over 10 min on a 15.5 g C_{18} column (High Performance GOLD RediSep Rf) followed by a 5 min wash step with 100% MeOH with a flow rate of 30 mL/min generating 12 fractions. Fraction 4 eluting from 9-10 min and fraction 5 eluting between 10-11 min were further

purified by RP-HPLC on a Thermo Surveyor HPLC system coupled with an ELSD (Sedex 55) and PDA detector using a Gemini 110A C18 column (5µm 250 x 10 mm, Phenomenex) and a 30 min isocratic elution with 70% aqueous CH_3CN (0.1% formic acid) with a flow rate of 3 ml/min. This resulted in the purification of **25** (2.8 mg) at 21 min, **26** (4.5 mg) at 12.14 min and **27** (0.7 mg) at 11 min. The antimicrobial and cytotoxic activity of these compounds was determined as described in Chapter 3.1.3 and 3.1.7.

8.3 Results and Discussion

8.3.1 Phylogenetic Characterization

Five *Tolypocladium* isolates (RKAG 373, 560, 574, 673, and 677) were obtained from Frobisher Bay as described in Chapter 4.2.3. BLASTn of their ITS nucleotide sequences confirmed them as members within the genus *Tolypocladium* as the closest match of the ITS nucleotide sequence to an accessioned strain in a recognized culture collection was with that of *Tolypocladium cylindrosporum* strain CBS 122173 (DQ449656.1), with less than 97% sequence similarity. Based on ITS sequence data, these isolates fell within the genus *Tolypocladium* and formed their own clade with 57% confidence (Figure 8.1). Construction of a multigene phylogeny (28S rRNA, 18S rRNA and TEF-1α) using the maximum likelihood model and GTR+G model of nucleotide substitution showed these isolates clustered into two distinct clades (Figure 8.2). The first clade contained RKAG 560, 574 and 677 with bootstrap support of 94%. The second clade contained RKAG 373 and 673 with 93% bootstrap support. Due to the sequence divergence within *Tolypocladium*, low internal bootstrap values were observed making definitive phylogenetic placement of these isolates within the genus challenging.

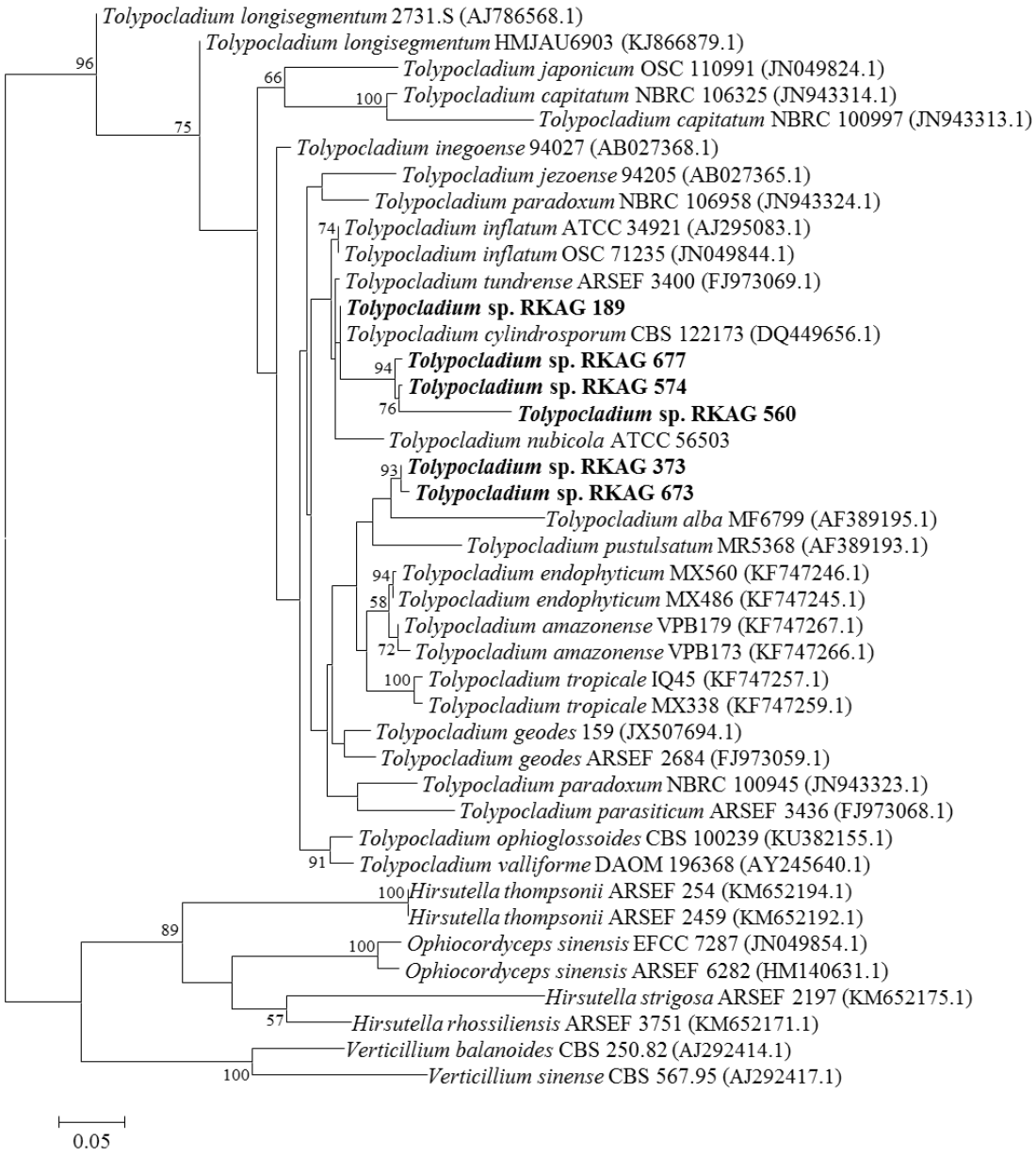

Figure 8.1. Maximum likelihood analysis of the genus *Tolypocladium* using 450 aligned nucleotides of the ITS region. The GTR+G model of nucleotide substitution was used and 1,000 bootstrap iterations. Only confidence values above 50% are denoted. The phylogram is mid-point rooted.

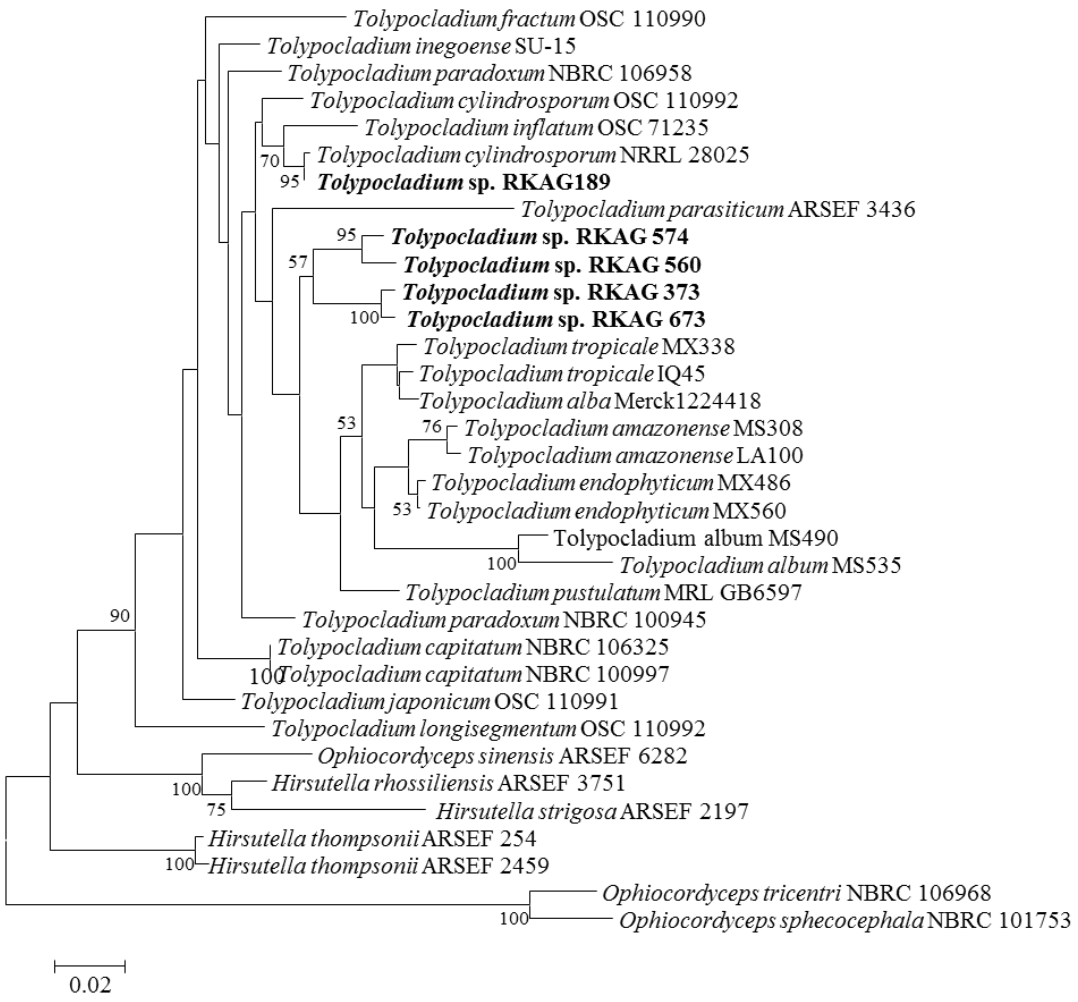

Figure 8.2. Maximum likelihood analysis of the genus *Tolypocladium* using 825 aligned nucleotides of the 18S rRNA gene, 670 aligned nucleotides of the 28S rRNA gene and 936 aligned nucleotides of the TEF-1α gene. The GTR+G model of nucleotide substitution was used and 1,000 bootstrap iterations. Only confidence values above 50% are denoted. *Ophiocordyceps tricentri* NBRC 106968 and *O. specocephala* NBRC 101753 are used as outgroups.

8.3.2 Morphological Characterization

The genus *Tolypocladium* is characterized by slow growing, white, floccose colonies with conidiophores arising from aerial hyphae terminally and laterally. Phialides are verticilliate and have a swollen base which tapers to a narrow neck producing terminal conidia in slimy heads[318]. Within the genus *Tolypocladium*, 42 members are described.

Due to a lack of sporulation of RKAG 560, 574, 673 and 677, only RKAG 373 could be described in further detail. RKAG 373 grew as floccose, white colonies with a pale yellow to orange reverse (Figure 8.3). After 10 days at 15˚C colonies obtained a diameter of 22-26 mm on PDA and a diameter of 15-23 mm at 22˚C (Figure 8.4). Microscopic examination of RKAG 373 revealed the isolate produced phialides that were solitary or in verticils of two which were present on undifferentiated hyphae or on sparingly branched conidiophores. Phialides were largely cylindrical (3.8-18 µm in length), although some were slightly swollen and tapered toward a neck (0.8-1.1 µm wide) bearing a terminal single celled, globose conidia measuring 1.6-2.2 µm in diameter. RKAG 373 was most similar to *Tolypocladium geodes* based on morphology as determined by the taxonomic key by Bissett[266]. *T. geodes* is described as forming white, floccose colonies with a pale yellow or dark brown reverse which are slow growing (10-15 mm after 10 days at 22˚C). Phialides are solitary or in verticils of 2 to 4, cylindrical (5.6-12.4 x 1.4-2.8 µm) at the base and gradually narrow toward the neck bearing conidia that are subglobose to obovoid (less than 2.4 µm in length). Colonies of *T. geodes* are characterized by a pungent earthy odor which was lacking from RKAG 373. RKAG 373 is morphologically similar *to T. geodes* in terms of phialide and conidia

shape and size, but is taxonomically distinct based on ITS sequence similarity to *T. geodes* ARSEF 2684 (FJ973059.1) with 96.6% sequence similarity. Due to a lack of sequenced genes within GenBank of the type strain of *T. geodes* CBS 723.70, the phylogenetic similarities between RKAG 373 and *T. geodes* cannot be confirmed.

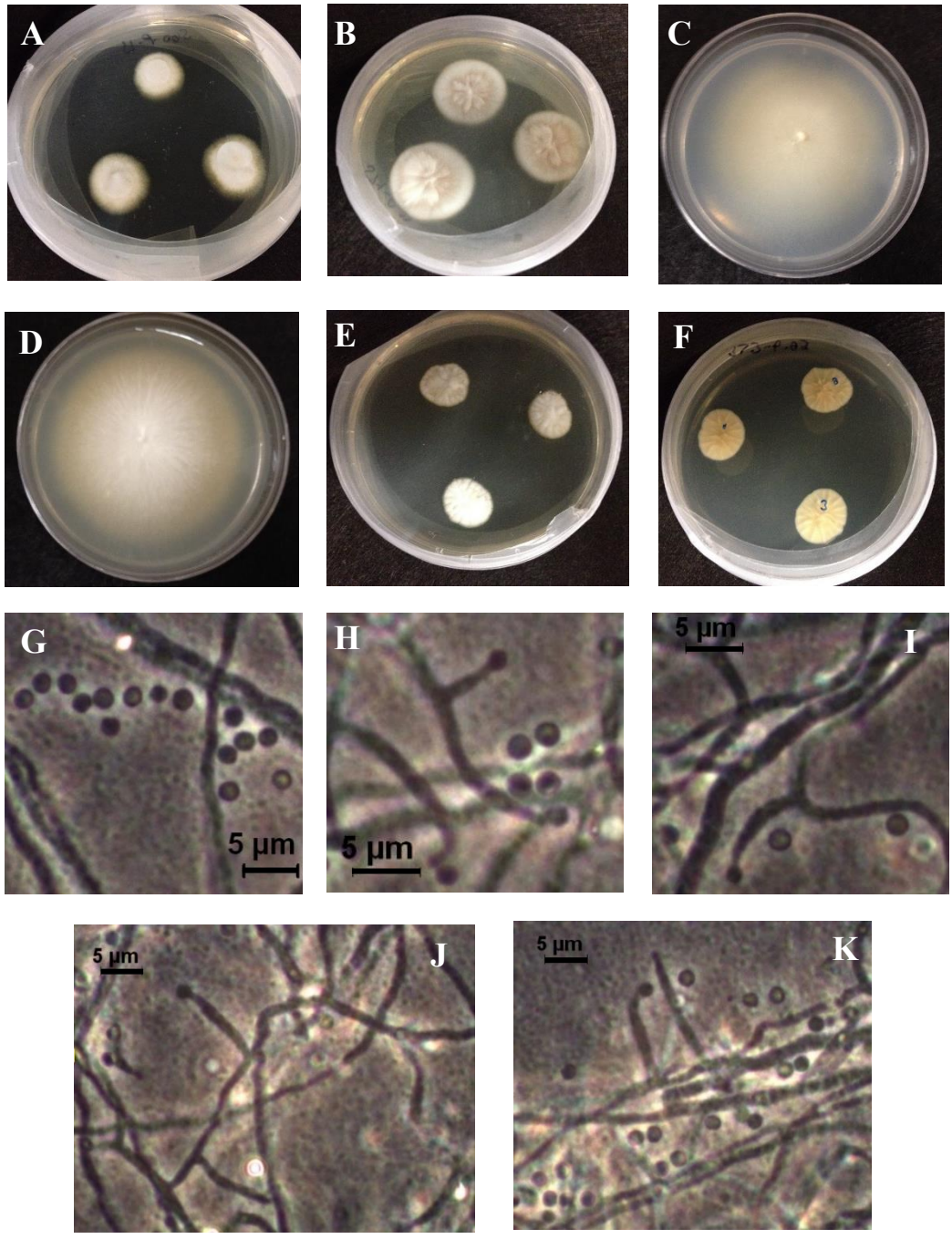

Figure 8.3. Phenotypic observations of *Tolypocladium*. **A)** Colony morphology of RKAG 560 on PDA medium. **B)** RKAG 574 on PDA medium. **C)** RKAG 673 on YM medium. **D)** RKAG 677 on YM medium. **E-F)** RKAG 373 on PDA medium. **G)** Conidia on 10% CMA. **H-K)** Phialides with terminal conidia on 10% CMA.

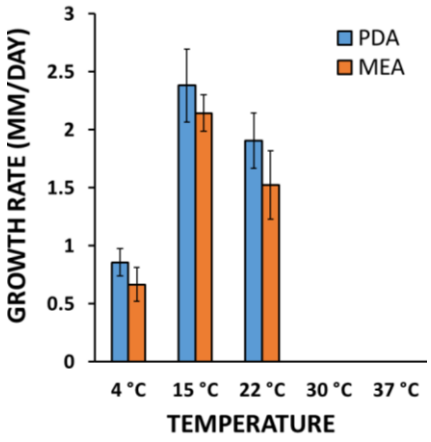

Figure 8.4. Average growth rate of RKAG 373 on PDA and 2% MEA.

8.3.3 Natural Products from *Tolypocladium*

Due to the likelihood of these isolates being new members within the genus *Tolypocladium* and the reputation of this genus to produce a wide range of bioactive NPs, further chemical investigation of these isolates was undertaken. The small-scale fermentations and LC-HRMS analysis of RKAG 373, 560, 574, 673 and 677 are discussed in Chapter 5. Based on this preliminary analysis, RKAG 373 and 560 were prioritized for further chemical investigation due to the production of compounds that had no likely hits within NPs databases.

8.3.3.1 Structure Elucidation of Iqalisetin A and B

A 1.5 L solid agar fermentation of *Tolypocladium* sp. RKAG 373 was extracted with EtOAc, dried *in vacuo* and partitioned between 80% CH_3CN and 100% hexane. The CH_3CN soluble portion was subjected to RP-HPLC resulting in the isolation of two new compounds, iqalisetin A (**23**) (32.5 mg) and B (**24**) (1.2 mg) (Figure 8.5) and the known compound nalanthalide whose structure was confirmed by NMR analysis.

The molecular formula of compound **23** was assigned as $C_{17}H_{23}NO_4$ (*m/z* 306.1702 $[M + H]^{+)}$ by HRESIMS indicating seven degrees of unsaturation (Figure 8.5, Table 8.1 and Appendix Figures A.60 and A.61). The ^{13}C NMR spectrum showed 17 carbon signals and the ^{1}H NMR and HSQC spectra indicated the presence of two olefinic, three methylene, two methyl and six methine protons. The TOCSY spectrum indicated the presence of two distinct spin systems consisting of H-2 to H_3-12 and H-5' to H_3-6'. Analysis of the ^{13}C and HMBC spectra revealed four signals at δ_C 198.3 (C-4'), δ_C 193.9 (C-1), δ_C 176.3 (C-2'), and δ_C 102.6 (C-3') consistent with the presence of a tetramic acid moiety[341]. COSY correlations between H-5' (δ_H 3.90) and H_3-6' (δ_H

1.30) and HMBC correlations between H_3-6' (δ_H 1.30) and C-4' (δ_C 199.1) revealed an Ala residue was incorporated within the tetramic acid.

Due to the absence of quaternary carbons in the decalin backbone, interpretation by COSY correlations readily led to the assignment of the spin system H-2 to H-11 (Figure 2). The location of the methyl group on the decalin skeleton was deduced from COSY correlations between H-3 (δ_H 2.69) and H_3-12 (δ_H 1.61) and HMBC correlations from H_3-12 (δ_H 0.94), to C-2 (δ_C 48.2), C-3 (δ_C 34.2) and C-4 (δ_C 132.6). The position of the hydroxyl group at C-8 was assigned based on COSY correlations from H-8 (δ_H 4.08) to H-7a (δ_H 1.84), H-7b (δ_H 1.33), H-9a (δ_H 1.81) and H-9b (δ_H 1.58) and HMBC correlations from H-7a (δ_H 1.84), H-9a (δ_H 1.81), H-10a (δ_H 1.66) and H-6 (δ_H 2.29) to C-8 (δ_C 66.8). The olefinic protons at C-4 and C-5 were assigned based on COSY correlations between H-3 (δ_H 2.56) and H-4 (δ_H 5.62), H-4 (δ_H 5.62) and H-5 (δ_H 5.38) and H-5 (δ_H 5.38) and H-6 (δ_H 2.29). HMBC correlations from H-2 (δ_H 3.77), H-3 (δ_H 2.56) and H-6 (δ_H 2.29) to C-4 (δ_C 132.6) and H-7a (δ_H 1.84) and H-6 (δ_H 2.29) to C-5 (δ_C 131.4) confirmed this assignment. HMBC correlations between H-2 (δ_H 3.77) and C-1 (δ_C 193.9) allowed for the incorporation a keto/enol group at C-1. In order to satisfy the remaining requirement for unsaturation for the molecule, C-1 (δ_C 193.9) was linked to the tetramic acid at C-3' (δ_C 102.6) to give the planar structure of **23**.

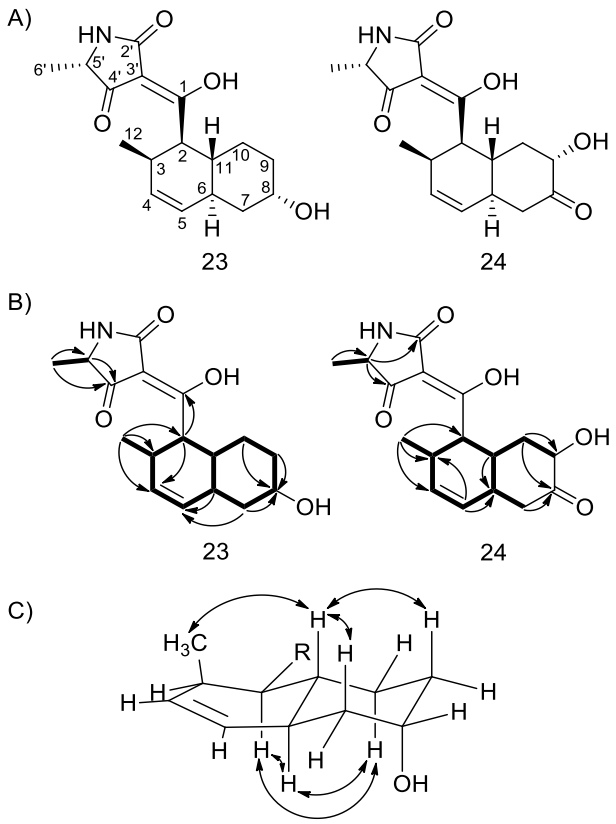

Figure 8.5. A) Molecular structure of iqalisetin A and B. **B)** Key NMR correlations for structure elucidation of iqalisetin A and B**. C)** Key NOESY correlations to determine the relative stereochemistry of the decalin ring system.

Table 8.1. ^{1}H (600 MHz) and ^{13}C (150 MHz) NMR data of iqalisetin A (23) and B (24) in CD_3OD.

	Iqalisetin A		**Iqalisetin B**	
	δ_C, type	δ_H (J/*Hz*)	δ_C, type	δ_H (J/*Hz*)
1	193.9[a], C		-	
2	48.2, CH	3.77, m	49.4, CH	4.02, dd (10.9, 5.7)
3	34.2, CH	2.56, m	31.5, CH	2.69, m
4	132.6, CH	5.62, ddd (10.0, 4.4, 2.8)	134.0, CH	5.70, m
5	131.4, CH	5.38, br d (10.0)	126.9, CH	5.35, br d (10.0)
6	36.4, CH	2.29, br dd (11.3, 11.3)	42.8, CH	2.11, m
7a	40.5, CH_2	1.84, ddd (14.0, 4.8, 4.1)	45.1, CH_2	2.43, m
7b		1.33, m		2.29, m
8	66.8, CH	4.08, b	211.0, C	
9a	33.9, CH_2	1.81, ddd (14.5,2.8, 2.8)	75.1, CH	4.25, dd (11.7, 6.7)
9b		1.58, m		
10a	25.2, CH_2	1.66, m	38.8, CH_2	2.65, m
10b		1.32, m		1.11, m
11	37.0, CH	1.61, m	33.0, CH	2.10, m
12	18.4, CH_3	0.94, d (7.1)	16.6, CH_3	0.89, d (7.2)
2'	176.3[a], C		177.4, C	
3'	102.6[a], C		-	
4'	199.1[a], C		198.3, C	
5'	58.4, CH	3.90, m	54.9, CH	3.55, q (6.6)
6'	17.7, CH_3	1.30, d (6.9)	17.1, CH_3	1.23, d (6.6)

[a]Broad signal. [b]Signal not observed.

The molecular formula of compound **24** was assigned as $C_{17}H_{21}NO_5$ (*m/z* 320.1492 $[M + H]^+$) by HRESIMS indicating eight degrees of unsaturation (Figure 8.5, Table 8.1 and Appendix Figures A.62 and A.63). The ^1H NMR and HSQC spectra indicated the presence of two olefinic, two methylene, two methyl and six methine protons. Comparison of the HSQC and HMBC data showed compound **24** was an analog of **23** and differed by the absence of a methylene group which was replaced by a ketone within the decalin core. The decalin substructure was confirmed through COSY and HMBC correlations as shown in figure 2. Due to similar chemical shifts for H-6 (δ_H 2.11) and H-11 (δ_H 2.10), HMBC correlations between H-11 (δ_H 2.10) and C-6 (δ_C 42.8) were used to close the cyclohexene ring of the decalin skeleton. HMBC correlations between H_3-12 (δ_H 0.90) and C-2 (δ_C 49.4), C-3 (δ_C 3.15) and C-4 (δ_H 134.0) and COSY correlations between H_3-12 (δ_H 0.90) and H-3 (δ_H 2.69) confirmed the location of the methyl group within the cyclohexene ring. The second ring of the decalin skeleton was closed via a ketone group at C-8 (δ_C 211.0) which was confirmed by HMBC correlations from H-10a (δ_H 2.65) and H-7a (δ_H 2.43). The chemical shift of the ketone within the decalin skeleton was consistent with reported values for a similar compound, streptosetin A[341]. The hydroxyl group at C-9 was determined through COSY correlations between H-10ab (δ_H 2.65, 1.11) and H-9 (δ_H 4.25) and HMBC correlations from H-10ab (δ_H 2.65, 1.11) to C-9 (δ_C 75.1). The presence of an alanine within the tetramic acid was deduced by COSY correlations between H-5' (δ_H 3.55) and H_3-6' (δ_H 1.23) and by HMBC correlations between H-5' (δ_H 3.55) and C-4' (δ_C 198.3) and C-2' (δ_C 177.4).

Dynamic tautomerization within the tetramic acid from the keto to enol form often causes signal broadening and makes it difficult to observe all carbon signals within the tetramic acid moiety as has been previously reported[341,342]. Due to tautomerization and the limited amount of compound obtained, the signals at C-1 and C-3' were not observed in any NMR experiment. Obtaining NMR at low temperature has been observed to decrease broadening of these signals and increase their resolution[337]. Attempts at obtaining HMBC data at low temperature (-25°C) to observe HMBC cross peaks for C-3' and C-1 proved unsuccessful. The planar structure of **24** is proposed despite these missing signals.

8.3.3.2 Determination of the Relative Configuration of Iqalisetin A and B

The relative stereochemistry of the decalin skeleton of **23** was determined by NOESY experiments (Figure 8.5). Correlations between H-11 (δ_H 1.61) and H-7b (δ_H 1.33) and CH_3-12 (δ_H 0.94) indicated a *syn* relationship. Correlations between H-6 (δ_H 2.29) and H-10b (δ_H 1.32) and H-2 (δ_H 3.77) and a correlation between H-10b (δ_H 1.32) and H-2 (δ_H 3.77) indicated a *syn* relationship amongst these protons but on the opposite face of the molecule. The large coupling constant between H-6 and H-11 ($^3J_{6,11}$ = 11.3 Hz) supported the trans fusion of the decalin skeleton. On the basis of these data, the relative configuration of **23** was established.

The relative stereochemistry of the decalin ring system of **24** was solved through evaluation of NOESY correlations. Correlations from H-11 (δ_H 2.10) to H-7a (δ_H 2.43), H-9 (δ_H 4.25) and H_3-12 (δ_H 0.89) demonstrated a *syn* relationship amongst these protons. Correlations from H-6 (δ_H 2.11) to H-2 (δ_H 4.02), and H-10b (δ_H 1.11) showed

a *syn* relationship for these protons, but on the opposite face of the molecule. Thus a trans fused decalin structure was proposed.

8.3.3.3 Stereochemical Assignment by Marfey's Method

The absolute configuration at C-5' was determined using Marfey's method[281,332] after oxidative bond cleavage of the tetramic acid followed by acid hydrolysis. Iqalisetin A was oxidized with $NaIO_4$ and $KMnO_4$, followed by hydrolysis with HCl and subsequent derivatization with *N*-(2,4-dinitro-5-fluorophenyl)-L-alaninamide (L-FDAA). LC-HRMS analysis was carried out and the retention time of FDAA-Ala was compared to that of derivatized L-Ala and D-Ala standards. The retention time of derivatized Ala most closely matched the retention time of derivitized L-Ala for compound **23** (Appendix Figure A.61).

Determination of the absolute stereochemistry of the decalin skeleton was attempted by performing a Mosher derivatization to generate MPTA chloride esters or MPA esters of **23**. Compound **23** was treated with (*R*)- and (*S*)-MPTA chloride as described previously[343] or with (*R*)- and (*S*)-MPA as described previously[344] and analyzed by LC-HRMS and ^{1}H NMR. Derivatization using both methods repeatedly resulted in a mixture of products with the expected Mosher-ester product not being observed. Similarly, this result has previously been reported for the related compound streptosetin A[341] where the Mosher's ester could not be detected after derivatization. Thus the absolute stereochemistry of the decalin skeleton was not determined.

Iqalisetins A and B are new members of the 3-decalinoyltetramic acid family of compounds. Compound **23** differs from **24** by the replacement of the methylene group at C-9 with a hydroxyl group and the oxidation of the hydroxyl group at C-8 to a keto

group. The presence of a hydroxyl group within the decalin skeleton is rare within this metabolite class and has only been reported for pallidorosetin A[345], neopestalotin A and C[346], integramycin[347] and signamycin[348]. Even rarer is the presence of a ketone at C-8, which to the best of our knowledge has not been previously reported for this family of compounds**.** Compound **23** is most similar to TA-289[349] and differs by the presence of a hydroxyl group at C-8 as opposed to a methylene group.

8.3.3.4 Structure Elucidation of Tolypoalbin, F-14329 and Trichodin A

A 1.5 L solid PDA agar fermentation of *Tolypocladium* sp. RKAG 560 was extracted with EtOAc, dried *in vacuo* and partitioned between 80% CH_3CN and 100% hexane. The CH_3CN soluble portion was subjected to RP-HPLC resulting in the purification of a new compound (at the time of isolation), tolypoalbin (**25**) (2.5 mg) and the known compounds F-14329 (**26**) (4.5 mg), trichodin A (**27**) (0.8 mg) and ergokonin B (**27**) (Figure 8.6).

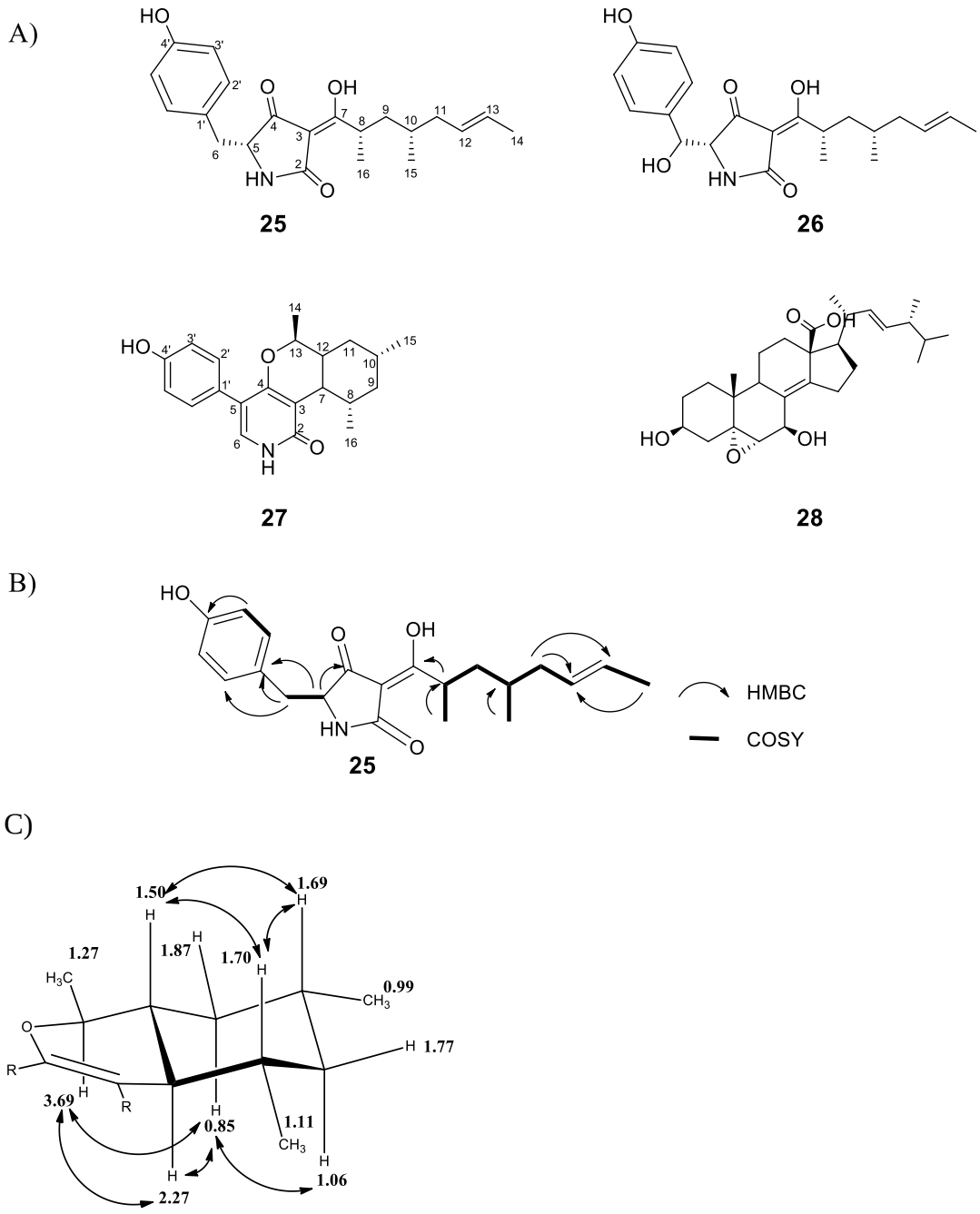

Figure 8.6 A) Structures of Tolypoalbin, F-14329 and Trichodin A. **B)** Key COSY and HMBC correlations of tolypoalbin. **C)** Key NOESY correlations of trichodin A to determine relative stereochemistry of the decalin ring system

The molecular formula of compound **25** was assigned as $C_{21}H_{27}NO_4$ (*m/z* 358.1997 $[M + H]^+$) by HRESIMS indicating nine degrees of unsaturation (Figure 8.6, Table 8.2 and Appendix Figures A.65 and A.66). The ^1H spectrum and HSQC indicated the presence of two olefinic, four aromatic, three sp^3 methine, three sp^3 methylene and three sp^3 methyl groups. The HMBC spectra revealed the presence of five quaternary carbon resonances representing two carbonyls and three sp^2 carbons. Only 20 of the 21 carbons predicted in the molecular formula could be observed within the NMR spectra, and thus a signal for a quaternary carbon was presumed to be missing. Analysis of the HMBC spectrum revealed four signals at C-4 (δ_C 194.4), C-2 (δ_C 176.5), C-7 (δ_C 197.7) and C-5 (δ_C 59.6) consistent with the presence of a tetramic acid moiety[341]. HMBC correlations from H-5 (δ_H 3.49) to C-2 (δ_C 176.5) and C-4 (δ_C 194.4) further supported the connectivity of the tetramic acid moiety. The missing quaternary carbon signal was presumed to be at C-3 and should have an expected shift of δ_C 100.0-105.0. This signal is often difficult to observe due to signal broadening caused by tautomerization of the tetramic acid and the lack of neighbouring protons[341,342].

The presence of doublets at H-2'and H-3' in the ^1H spectrum was consistent with the presence of an AA'BB' spin coupling system of a para disubstituted phenyl group which was fully assigned through HMBC and COSY correlations. HMBC correlations connected the equivalent protons H-2' and H-6' (δ_H 6.96) to C-6 (δ_C 37.4) and C-5 (δ_C 59.6) indicating a methylene bridge connects the *p*-hydroxyphenyl ring with the tetramic acid at position C-5.

The presence of an unsaturated aliphatic side chain was revealed by the appearance of a large number of high field protons in the ^1H spectrum and was

established by analysis of the COSY and TOCSY spectra. Analysis of the COSY and TOCSY spectra revealed a spin system from H-8 to H-14. COSY correlations from H-8 (δ_H 4.03) to H-16 (δ_H 0.82) and H10 (δ_H 1.34) to H-15 (δ_H 0.75) indicated the positions of the remaining two methyl groups. Connectivity of the side chain to C-7 was determined through HMBC correlations between H-8 (δ_H 4.03) to C-7 (δ_C 197.7).

The absolute configuration at C-5' was determined in the same way as iqalisetin A. After oxidative bond cleavage of the tetramic acid followed by acid hydrolysis and derivatization with FDAA, the configuration at this centre corresponded to L-Tyr. The structure of **25** was elucidated and shown to be a new tetramic acid derivative at the time of isolation. Shortly after, the structure of this compound was published by Fukuda *et al* and named tolypoalbin isolated from *Tolypocladium album* TAMA 479 from a soil sample from Machida, Tokyo, Japan[339].

Compound **26** was found to have the molecular formula $C_{21}H_{27}NO_5$ (*m/z* 374.1970 $[M + H]^+$) by HRESIMS (Figure 8.6, Table 8.2 and Appendix Figure A.67 and A.68). Analysis of the NMR spectra indicated portions of the molecule were identical to **26** including the aliphatic side chain, tetramic acid moiety and *p*-hydroxyphenyl moiety. Compound **26** differed from **25** by the presence of a hydroxy methine group at C-6 instead of a methylene bridge and was determined to be the known patented metabolite F-14329. This compound was previously isolated from *Chaunopycnis alba* and patented in 2007 for its ability to lower murine postprandial blood triglyceride levels. Within this patent, only the planar structure was reported and in 2015, the full structural characterization was published[340].

Compound **27** was assigned as $C_{21}H_{25}NO_3$ (*m/z* 340.1910 $[M + H]^+$) by HRESIMS (Figure 8.6, Table 8.2 and Appendix Figures A.69 and A.70). Analysis of the NMR spectra led to the identification of **27** as the known pyridone containing compound trichodin A, initially isolated in 2014 from *Trichoderma* sp. MF 106 isolated from the Arctic waters of the Fram Strait[96]. The relative configuration of **27** was determined using NOESY correlations and revealed the configuration was the same as trichodin A. Due to the presumed shared biosynthesis of all three compounds, the relative stereochemistry of **25** and **26** was assigned based on **27**[350,351].

Compound **28** was assigned as $C_{26}H_{41}NO_5$ (*m/z* 459.3092 $[M + H]^+$) by HRESIMS. Careful interpretation of the NMR data led to the assignment of this compound as the steroid ergokonin B which has previously been isolated from *Trichoderma koningii* and *Tolypocladium inflatum*[352,353].

Table 8.2. ^{1}H (600 MHz) and ^{13}C (150 MHz) NMR data of tolypoalbin (25), F-14329 (26) and trichodin (27) in CD_3OD.

	Tolypoalbin		**F-14329**		**Trichodin**	
	δ_C, type	δ_H (J/Hz)	δ_C, type	δ_H (J/Hz)	δ_C, type	δ_H (J/Hz)
1	NH		NH		NH	
2	177.6, C		177.6, C		165.8, C	
3	---[a]		---[a]		112.7, C	
4	197.1, C		196.4, C		165.9, C	
5	61.8, CH	3.80, dd (6.9, 4.0)	66.7, CH	4.04, d (4.4)	117.8, C	
6a	37.8, CH	3.00, dd (13.8, 3.8)	75.3, CH	4.90, d (4.4)	130.8, CH	7.10, s
6b		2.72, dd (13.8, 6.9)				
7	199.8, C		198.4, C		45.1, CH	2.27, dd (10.0, 10.0)
8	37.4, CH	3.93, dd (14.7, 6.5)	36.8, CH	3.76, m	41.5, CH	1.70, m
9a	41.5, CH_2	1.72, m	41.4, CH_2	1.69, m	46.8, CH_2	1.77, m
9b		0.97, m		0.96, m		1.06, m
10	31.7, CH_3	1.34, m	32.1, CH_3	1.25, m	33.8, CH	1.69, m
11a	41.1, CH_2	1.97, m	41.4, CH_2	1.92, m	38.3, CH_2	1.87, m
11b		1.73, m		1.76, m		0.85, m
12	130.6, CH	5.37[b]	130.7, CH	5.36[b]	50.9, CH	1.50, m
13	126.1, CH	5.37[b]	126.7, CH	5.37[b]	79.5, CH	3.69, dq (10.0, 6.3)
14	17.6, CH_3	1.62, d (3.3)	17.9, CH_3	1.63, d (4.5)	18.6, CH_3	1.27, d (6.3)
15	19.5, CH_3	0.80, d (6.6)	19.7, CH_3	0.78, d (8.9)	22.4, CH_3	0.99, d (6.5)
16	18.4, CH_3	0.96, d[c] (6.7)	18.6 CH_3	0.91, d (8.9)	23.0, CH_3	1.11, d (6.8)
1'	128.3, C		130.6, C		126.5, C	
2'	131.0, CH	7.01, d (8.4)	129.4, CH	7.14, d (8.1)	131.1, C	7.21, d (8.7)
3'	115.4, CH	6.65, d (8.4)	115.4, CH	6.66, d (8.1)	115.5, C	6.78, d (8.7)
4'	155.9, C		157.9, C		157.8, C	

[a]Signal not observed

[b]Overlapping

[c]Multiplicity determined in DMSO-d_6

8.3.3.5 Bioactivity Testing

Compounds within the tetramic and pyridone family of secondary metabolites exhibit a wide range of biological activities including antimicrobial, antiviral and neurotrophic activity[335]. Trichodin A (**27**) has previously been reported to exhibit moderate antibiotic activity against *Bacillus subtilis* (IC_{50} 27.05 ± 0.53 µM), *Staphylococcus epidermis* (IC_{50} 24.28 ± 3.90 µM) and *Candida albicans* (IC_{50} 25.38 ± 0.41 µM)[96]. Determination of the antimicrobial activity of F-14329 (**26**) and tolypoalbin (**25**) has never been reported but both have adipogenic activity[339].

Compounds **23-27** were assayed for biological activity against methicillin resistant *Staphylococcus aureus* (ATCC 33591), vancomycin resistant *Enterococcus faecium* (EF379), *Staphylococcus warneri* (ATCC 17917), *Pseudomonas aeruginosa* (ATCC 14210), and *Candida albicans* (ATCC 14035). No significant activity was observed for any of the compounds tested at a concentration up to 128 µg/mL. Hydroxylation at the C-8 position has previously been shown to be detrimental for *S. aureus* activity as is reported for pallidorosetin A, which bears a hydroxyl group at C-8 versus a methyl group as in the case of the bioactive derivative equisetin[345]. Hydroxylation of the decalin skeleton in **23** and **27** may thus be responsible for the lack of observed activity. Compounds **23-27** were also tested for cytotoxicity against keratinocyte, fibroblast, and HTB-26 breast cancer cell lines. Neither compounds exhibited activity against these cell lines when tested at 128 µg/mL.

8.4 Conclusions

Several putatively new species of *Tolypocladium* were isolated from sediment in Frobisher Bay and determined to be phylogenetically distinct from other sequenced

Tolypocladium species. Due to a lack of sporulation of most of these isolates, further morphological characterization could not be undertaken. Chemical investigation of *Tolypocladium* sp. RKAG 373 led to the isolation of two new 3-decalinoyltetramic acids which were named iqalisetin A and B. Investigation of *Tolypocladium* sp. RKAG 560 resulted in the characterization of a new tetramic acid containing compound, which shortly after isolation was published by Fukuda *et al* as tolypoalbin from a *Tolypocladium* sp.[339]. The previously patented compound, F-14329 and the known pyridone containing compound, trichodin A were also characterized from this isolate. The isolation of these new compounds from putatively new species within *Tolypocladium* enforces the notion that Canada's Arctic is a prosperous resource for the discovery of new microbial and chemical diversity.

CHAPTER 9: CONCLUSIONS

9.1 Summary

9.1.1 Microbial Diversity of Frobisher Bay (Chapters 2 and 4)

Within sediment from Frobisher Bay the fungal and bacterial assemblages were found to be very diverse as determined by 454-pyrosequencing. Sites within Frobisher Bay were found to be dominated by members within the phyla Proteobacteria and Bacteroidetes, whereas Actinobacteria made up a small, but significant portion of the diversity within this region (7.1% total abundance). The use of Actinobacteria-specific primers resulted in greater sequencing depth within the Actinobacteria and revealed the presence of rare phylotypes that were not detected using universal 16S rRNA primers. Within the Actinobacteria, members within the genus *Ilumatobacter* were the dominant members found within Frobisher Bay. The fungal diversity of Frobisher Bay was largely dominated by unknown Chytridiomycota, basidiomycete yeasts within the genus *Glaciozyma* and filamentous ascomycetes within the genus *Didymella*.

The bacterial and fungal assemblages were largely variable across sites within Frobisher Bay. The differences in microbial diversity between sites may be the result of many factors including anthropogenic influences from Iqaluit, differences in freshwater and nutrient input from the terrestrial environment and various other physical and chemical influences from the marine environment. The large microbial taxonomic diversity uncovered and the presence of a large number of unclassified bacterial and fungal sequences within this dataset makes Frobisher Bay a promising resource for taxonomically distinct microorganisms for NP discovery.

Actinobacteria are prolific producers of NPs[25] and made up a small, but significant proportion of sequences reads with Frobisher Bay (7.1 % of total reads). In

order to further study the ability of these Actinobacteria to produce NPs, a library of Actinobacteria was constructed using a selective pre-treatment (dry stamp) in addition to dilution of wet sediment and Actinobacteria-specific isolation media. Ninety actinomycete isolates were cultured consisting of 25 species representing six genera (*Streptomyces*, *Actinomadura*, *Amycolatopsis*, *Kribella*, *Rhodococcus* and *Streptosporangium*). Several of these actinomycetes were isolated at 4˚C highlighting their ability to grow and survive under cold temperatures.

Fungi are also well known producers of NPs and within Frobisher Bay, were shown to consist of site-specific fungal communities by 454-pyrosequencing. Using a particle filtration method and a range of isolation media, 354 fungi were isolated from sediment samples representing 54 species. Almost two thirds of these fungi were isolated at 4˚C demonstrating their ability to grow at cold temperatures. Of these species, nine appeared to be putatively novel based on their ITS gene sequence. Further phylogenetic and morphological characterization of these putatively new species was undertake and included isolates within the genera *Mortierella*, *Tolypocladium* and *Sesquicillium*. The isolation of these novel microorganisms represents an extremely promising source for new NPs due to the unstudied nature of their metabolome.

9.1.2 Effect of Fermentation Temperature on the Production of Microbial Natural Products (Chapter 3)

The library of actinomycetes isolated from Frobisher Bay was fermented and screened for the production of NPs. Due to the unique environment from which they were isolated, fermentations were carried out at both 30°C (standard lab fermentation temperature) and a more ecologically relevant 15°C to determine if fermentation

temperature had an effect on NP production within these isolates. The use of an LC-HRMS metabolomics based approach allowed for the quick comparison of metabolite production at 30°C and at 15°C in order to look for the upregulation or induction of NPs at each fermentation temperature. Changes in fermentation temperature were shown to affect the metabolome of each of these actinomycetes to a varying degree. The *de novo* induction of actinomycin was observed in fermentations at 15°C by *Streptomyces* sp. RKAG 337. This colder fermentation temperature also resulted in the upregulated production of two new landomycin analogs in *Streptomyces* sp. RKAG 290 and allowed for the purification and characterization of these compounds. These new landomycin analogs are unique to the landomycin family as they contain an ethyl substituent at C-3 (instead of a methyl) within the landomycin core, presumably as a result of a propionate starter unit, instead of acetyl-CoA. Additionally they contain the longest sugar chain (9 sugars) of any of the landomycins reported to date. Landomycins have previously been shown to exhibit potent anticancer activity and activity has been shown to increase with increasing sugar length[190]. Biological testing of landomycin AA and AB resulted in potent activity against MCF-7 and HTB-26 breast cancer cell lines down to the lowest concentration tested (1 µg/mL).

The mechanism by which the production of secondary metabolites is affected by cold temperature is unknown. Bacteria have envolved many mechanisms for deal with cold temepratures including alterations in membrane fluidity and the production of cold shock proteins (Csp) in response to a shift in temperature to allowing for transcription and translation to occur at cold temperatures[198]. Whether Csps have a role in the

regulation of NP production at cold temperatures is unknown and warrants further investigation.

This study demonstrates that fermentation temperature can have a wide ranging impact on NP production within actinomycetes and is a useful tool for the induction or upregulation of NPs. When paired with chemical metabolomics, differences between fermentation temperatures can be rapidly observed and allow for quick prioritization of chemical extracts for further investigation. Changes in fermentation temperature were shown to be a way to access silent NP gene clusters (as demonstrated by the *de novo* induction of actinomycin at 15˚C) within *Streptomyces* sp. RKAG 337 and to upregulate the production of NPs (as demonstrated by the upregulation of landomycin AA and AB) within *Streptomyces* sp. RKAG 290. Investigation into the thermo-regulation of actinomycin and landomycin production through genome sequencing and transcriptomic analysis is warranted in these two isolates as alteration of fermentation temperature is a promising tool to access silent or under expressed metabolites. Although these were only two examples described of induction or upregulation of NPs by fermentation temperature, many other examples of this phenomenon were observed within the library. The continued investigation of these isolates will surely lead to further examples of temperature dependent induction of NPs.

9.1.3 Characterization of New Fungal Natural Products (Chapters 5-8)

The isolation of new microorganisms represents an extremely promising source for new NPs due to the unstudied nature of their metabolome. Several putatively new species of fungi were isolated from Frobisher Bay and fermentation of these isolates led to the characterization of many new NPs. Fermentation of a new *Mortierella* species led

to the isolation of four new cyclic heptapeptides, mortiamides A-D. These compounds are extremely interesting due to the high proportion of non-proteogenic D amino acids found within. The isolation of several new 3-decalinoyltetramic acids from a *Tolypocladium* species and new 11 residue peptaibols from a *Sesquicillium* species also highlights the utility of new species as a resource for NP discovery.

The isolation of known fungi from Frobisher Bay also proved to be an excellent resource for new NP discovery. A family of new *N*-methylated decapeptides and 11 residue peptaibols were characterized from *Sesquicillium microsporum* RKAG 186, two new linear polyketide cameronic acid analogs were characterized from *Botrytis carolina* RKAG 208, a new hirsutellic acid analog was characterized from *Simplicillium aogashimaense* RKAG 563 and a new perylene quinone compound was characterized from *Cadophora viticola* RKAG 170.

The isolation of 20 new NPs, representing 7 NP families from Frobisher Bay highlights this area as an excellent resource for NP discovery. The detection of many other putatively new NPs from this library, which were not characterized, will enable future NP discovery from this library.

9.2 Future Directions

With the advancement in metagenomic sequencing technologies, the microbial diversity of the marine environment from cold environments is only beginning to be revealed. This thesis offers a snapshot of the microbial diversity within sediment isolated from Frobisher Bay and reveals a large number of unclassified bacteria and fungi whose role and identity within the marine environment is unknown. The detection of a large number of microbial phylotypes by 454-pyrosequencing and the limited

laboratory culture of these phylotypes within this thesis highlights a large issue when culturing environmental microorganisms, that many of them are "unculturable". The inability to culture most microorganisms within a lab is often due to their fastidious growth requirements and/or the requirement of metabolic cooperation of other microorganisms[169,170].

The development of innovative culture techniques, such as the isolation chip (iCHIP) may assist in the culture of these "unculturables". The iCHIP is an *in situ* cultivation method and consists of a miniature chip containing hundreds of diffusion chambers which when loaded, allow microorganisms on the iCHIP to receive nutrients and environmental cues from their surroundings[354]. The utility of this method is highlighted by the culture of a new species, *Elefitheria terrae* using the iCHIP and the subsequent isolation of the NP, teixobactin from this newly described species. Teixobactin is a promising antibiotic candidate due to its potent activity against multi-drug resistant Gram positive pathogens and *Mycobacterium tuberculosis*[355]. The use of the iCHIP technology within Frobisher Bay may increase access to these uncultured microorganisms for NP discovery.

This thesis offers a preliminary investigation into the NPs produced by fungi and Actinobacteria isolated from Frobisher Bay. The detection of a large number of putatively new metabolites by LC-HRMS that were not further investigated further demonstrates the novelty of this library for NP discovery. It is known that Actinobacteria and fungi can harbour upwards of 50 NP biosynthetic gene clusters and many of these are silent under standard laboratory cultivation[174,356]. Within this library only a handful of NPs were detected from each of these isolates, although they have the

genetic potential to produce many more. The use of co-culture, epigenetic modifiers and stressors has been shown to activate silent gene clusters or upregulate gene clusters[357] and the use of these methods within this library will undoubtedly lead to detection of greater chemical diversity.

The sequencing of microbial genomes has given insight into the potential of these organisms for NP production. The clustered organization of bacterial and fungal gene clusters on the genome can enable the heterologous production of these gene clusters within the lab albeit often with challenges. Recently the use of fungal artificial chromosomes (FACs) for the capture of fungal NP biosynthetic gene clusters and heterologous production of these FACs within *Aspergillus nidulans* has been reported. When paired with the use of untargeted LCMS chemical metabolomics, it has allowed for the high throughput screening of captured fungal biosynthetic gene clusters within these FACs. The proof of concept of this method has resulted in the detection of 15 novel secondary metabolites from captured biosynthetic gene clusters of *Aspergillus terreus*, *A. aceuleatus* and *A. wenti*[358]. The continued development of this technique will undoubtedly be a useful resource for accessing silent fungal biosynthetic gene clusters in a high throughput screen.

9.3 Concluding Remarks

This thesis gives the first account of the microbial diversity of sediment within Frobisher Bay. The use of actinobacterial and fungal specific primers allowed for greater sequencing depth by 454-pyrosequencing within these prolific NP producing organisms and showed this region to be extremely biodiverse and host to many uncultured lineages of fungi and bacteria. The isolation of a large number of new NPs

from only a small proportion of these cultured organisms reveals the immense potential still left within this library. This thesis highlights that bioprospecting in overlooked regions is a tremendous opportunity to uncover taxonomic and chemical novelty.

The diversity of fungi and bacteria on Earth is great and corresponds to enormous metabolic potential. Only a small fraction of microorganisms on Earth have been utilized for NP discovery. NPs have evolved over billions of years to be specific for a biological target and have provided us with most of our modern day pharmaceuticals. With the rise in antimicrobial and anticancer drug resistance, the need for new bioactives is great. Bioprospecting in inhospitable environments which have long been overlooked by NP researchers, may hold the key to finding the next generation of life-saving remedies. This thesis offers a small glimpse into the diversity and NP capabilities of microorganisms within Canada's Arctic and the continued investigation of this vast region will undoubtedly provide a rich resource for future NP discovery.

References

(1) Stone, M.; Williams, D. *Mol. Microbiol.* **1992**, *6*, 29-34.
(2) Dias, D. A.; Urban, S.; Roessner, U. *Metabolites* **2012**, *2*, 303-336.
(3) Osbourn, A. E.; Lanzotti, V. *Plant-derived natural products*; Springer, 2009.
(4) Kutchan, T. M. *The Plant Cell* **1995**, *7*, 1059.
(5) Oldfield, E.; Lin, F. Y. *Angew. Chem. Int. Ed.* **2012**, *51*, 1124-1137.
(6) Arnison, P. G.; Bibb, M. J.; Bierbaum, G.; Bowers, A. A.; Bugni, T. S.; Bulaj, G.; Camarero, J. A.; Campopiano, D. J.; Challis, G. L.; Clardy, J. *Nat. Prod. Rep.* **2013**, *30*, 108-160.
(7) Fischbach, M. A.; Walsh, C. T. *Chem. Rev.* **2006**, *106*, 3468-3496.
(8) Fleming, A. *Brit. J. Exp. Pathol.* **1929**, *10*, 226.
(9) Silver, L. L. *Clin. Microbiol. Rev.* **2011**, *24*, 71-109.
(10) Neuss, N.; Gorman, M.; Hargrove, W.; Cone, N. J.; Biemann, K.; Buchi, G.; Manning, R. *J. Am. Chem. Soc.* **1964**, *86*, 1440-1442.
(11) Kumar, A.; Patil, D.; Rajamohanan, P. R.; Ahmad, A. *PloS One* **2013**, *8*, e71805.
(12) Wani, M. C.; Taylor, H. L.; Wall, M. E.; Coggon, P.; McPhail, A. T. *J. Am. Chem. Soc.* **1971**, *93*, 2325-2327.
(13) Stierle, A.; Strobel, G.; Stierle, D. *Science.* **1993**, *260*, 214-214.
(14) Da Rocha, A. B.; Lopes, R. M.; Schwartsmann, G. *Curr. Opin. Pharmacol.* **2001**, *1*, 364-369.
(15) Endo, A.; Kuroda, M.; Tsujita, Y. *J. Antibiot.* **1976**, *29*, 1346-1348.
(16) Negishi, S.; Huang, Z.; Hasumi, K.; Murakawa, S.; Endo, A.; Soc. Ferm. Bioeng. **1986**, *64*, 509-512.
(17) Heinrich, M. *Pharm. J.* **2004**, *273*, 905-906.
(18) Tu, Y. *Nat. Med.* **2011**, *17*, 1217-1220.
(19) Dreyfuss, M.; Härri, E.; Hofmann, H. e. a.; Kobel, H.; Pache, W.; Tscherter, H. *Appl. Microbiol. Biotechnol.* **1976**, *3*, 125-133.
(20) Van Dongen, P. W.; de Groot, A. N. *Eur. J.Obstet. Gynecol. Reprod. Biol.* **1995**, *60*, 109-116.
(21) Goetz, M.; Lopez, M.; Monaghan, R.; Chang, R.; Lotti, V.; Chen, T. *J. Antibiot.* **1985**, *38*, 1633-1637.
(22) Campbell, W.; Fisher, M.; Stapley, E.; Albers-Schonberg, G.; Jacob, T. *Science* **1983**, *221*, 823-828.
(23) Patridge, E.; Gareiss, P.; Kinch, M. S.; Hoyer, D. *Drug Discov. Today.* **2016**, *21*, 204-207.
(24) Newman, D. J.; Cragg, G. M. *J. Nat. Prod.* **2016**, *79*, 629-661.
(25) Bérdy, J. *J. Antibiot.* **2012**, *65*, 385-395.
(26) Harvey, A. *Drug Discov. Today.* **2000**, *5*, 294-300.
(27) Rodríguez-Valera, F. *FEMS Microbiol. Lett.* **2004**, *231*, 153-158.
(28) Ventura, M.; Canchaya, C.; Tauch, A.; Chandra, G.; Fitzgerald, G. F.; Chater, K. F.; van Sinderen, D. *Microbiol. Mol. Biol. Rev.* **2007**, *71*, 495-548.
(29) Goodfellow, M.; Williams, S. *Annual Reviews in Microbiology* **1983**, *37*, 189-216.
(30) Demain, A. L. *Med. Res. Rev.* **2009**, *29*, 821-842.
(31) Mueller, G. M.; Schmit, J. P. *Biodivers. Conserv.* **2007**, *16*, 1-5.

(32) Hyde, K. D.; Jones, E. G.; Leaño, E.; Pointing, S. B.; Poonyth, A. D.; Vrijmoed, L. L. *Biodivers. Conserv.* **1998**, *7*, 1147-1161.
(33) Aly, A. H.; Debbab, A.; Proksch, P. *Fungal Divers.* **2011**, *50*, 3.
(34) Rutledge, P. J.; Challis, G. L. *Nat. Rev. Microbiol.* **2015**, *13*, 509.
(35) Bachmann, B. O.; Van Lanen, S. G.; Baltz, R. H. *J. Indust. Microbiol. Biotechnol.* **2014**, *41*, 175-184.
(36) Blunt, J. W.; Copp, B. R.; Keyzers, R. A.; Munro, M. H.; Prinsep, M. R. *Nat. Prod. Rep.* **2017**.
(37) Jaspars, M.; De Pascale, D.; Andersen, J. H.; Reyes, F.; Crawford, A. D.; Ianora, A. *J. Mar. Biol. Assoc.U.K.* **2016**, *96*, 151-158.
(38) Bergmann, W.; Feeney, R. J. *J. Am. Chem. Soc.* **1950**, *72*, 2809-2810.
(39) Schöffski, P.; Dumez, H.; Wolter, P.; Stefan, C.; Wozniak, A.; Jimeno, J.; Van Oosterom, A. T. *Exp. Opin. Pharmacother.* **2008**, *9*, 1609-1618.
(40) Hirata, Y.; Uemura, D. *Pure Appl. Chem.* **1986**, *58*, 701-710.
(41) Menis, J.; Twelves, C. *Breast Cancer.* **2011**, *3*, 101.
(42) Katz, J.; Janik, J. E.; Younes, A. *Clin. Cancer Res.* **2011**, *17*, 6428-6436.
(43) Bergmann, W.; Feeney, R. J. *J. Org. Chem.* **1951**, *16*, 981-987.
(44) Klotz, U. *Int. J. Clin. Pharmacol. Ther.* **2006**, *44*.
(45) Koski, R. R. *Pharmacol. Ther.* **2008**, *33*, 271.
(46) Hu, G.-P.; Yuan, J.; Sun, L.; She, Z.-G.; Wu, J.-H.; Lan, X.-J.; Zhu, X.; Lin, Y.-C.; Chen, S.-P. *Mar. Drugs* **2011**, *9*, 514-525.
(47) Simmons, T. L.; Coates, R. C.; Clark, B. R.; Engene, N.; Gonzalez, D.; Esquenazi, E.; Dorrestein, P. C.; Gerwick, W. H. *PNAS.* **2008**, *105*, 4587-4594.
(48) Blunt, J. W.; Copp, B. R.; Keyzers, R. A.; Munro, M. H.; Prinsep, M. R. *Nat. Prod Rep.* **2016**, *33*, 382-431.
(49) Fenical, W.; Jensen, P. R. *Nat. Chem. Biol.* **2006**, *2*, 666-673.
(50) Weyland, H. *Nature* **1969**, *223*, 858.
(51) Helmke, E.; Weyland, H. *Int. J. Syst. Evol. Microbiol.* **1984**, *34*, 127-138.
(52) Maldonado, L. A.; Fenical, W.; Jensen, P. R.; Kauffman, C. A.; Mincer, T. J.; Ward, A. C.; Bull, A. T.; Goodfellow, M. *Int. J. Syst. Evol. Microbiol.* **2005**, *55*, 1759-1766.
(53) Matsumoto, A.; Kasai, H.; Matsuo, Y.; Ōmura, S.; Shizuri, Y.; Takahashi, Y. *J. Gen. Appl. Microbiol.* **2009**, *55*, 201-205.
(54) Tian, X.-P.; Zhi, X.-Y.; Qiu, Y.-Q.; Zhang, Y.-Q.; Tang, S.-K.; Xu, L.-H.; Zhang, S.; Li, W.-J. *Int. J. Syst. Evol. Microbiol.* **2009**, *59*, 222-228.
(55) Han, S. K.; Nedashkovskaya, O. I.; Mikhailov, V. V.; Kim, S. B.; Bae, K. S. *Int. J. Syst. Evol. Microbiol.* **2003**, *53*, 2061-2066.
(56) Feling, R. H.; Buchanan, G. O.; Mincer, T. J.; Kauffman, C. A.; Jensen, P. R.; Fenical, W. *Angew. Chem. Int. Ed.* **2003**, *42*, 355-357.
(57) Buchanan, G. O.; Williams, P. G.; Feling, R. H.; Kauffman, C. A.; Jensen, P. R.; Fenical, W. *Org. Lett.* **2005**, *7*, 2731-2734.
(58) Udwary, D. W.; Zeigler, L.; Asolkar, R. N.; Singan, V.; Lapidus, A.; Fenical, W.; Jensen, P. R.; Moore, B. S. *PNAS.* **2007**, *104*, 10376-10381.
(59) Williams, P. G.; Asolkar, R. N.; Kondratyuk, T.; Pezzuto, J. M.; Jensen, P. R.; Fenical, W. *J. Nat. Prod.* **2007**, *70*, 83-88.

(60) Williams, P. G.; Miller, E. D.; Asolkar, R. N.; Jensen, P. R.; Fenical, W. *J. Org. Chem.* **2007**, *72*, 5025-5034.
(61) Oh, D.-C.; Williams, P. G.; Kauffman, C. A.; Jensen, P. R.; Fenical, W. *Org. Lett.* **2006**, *8*, 1021-1024.
(62) Oh, D.-C.; Gontang, E. A.; Kauffman, C. A.; Jensen, P. R.; Fenical, W. *J. Nat. Prod.* **2008**, *71*, 570-575.
(63) Veyisoglu, A.; Cetin, D.; Bektas, K. I.; Guven, K.; Sahin, N. *Int. J. Syst. Evol. Microbiol.* **2016**, *66*, 4856-4863.
(64) Phongsopitanun, W.; Kudo, T.; Ohkuma, M.; Pittayakhajonwut, P.; Suwanborirux, K.; Tanasupawat, S. *Int. J. Syst. Evol. Microbiol.* **2016**, *66*, 3607-3613.
(65) Huang, X.; Zhou, S.; Huang, D.; Chen, J.; Zhu, W. *Int. J. Syst. Evol. Microbiol.* **2015**.
(66) Khan, S. T.; Tamura, T.; Takagi, M.; Shin-ya, K. *Int. J. Syst. Evol. Microbiol.* **2010**, *60*, 2775-2779.
(67) Hughes, C. C.; Prieto-Davo, A.; Jensen, P. R.; Fenical, W. *Org. Lett.* **2008**, *10*, 629-631.
(68) Nam, S.-J.; Kauffman, C. A.; Paul, L. A.; Jensen, P. R.; Fenical, W. *Org. Lett.* **2013**, *15*, 5400-5403.
(69) He, H.; Williamson, R. T.; Shen, B.; Graziani, E. I.; Yang, H. Y.; Sakya, S. M.; Petersen, P. J.; Carter, G. T. *J. Am. Chem. Soc.* **2002**, *124*, 9729-9736.
(70) Kwon, H. C.; Kauffman, C. A.; Jensen, P. R.; Fenical, W. *J. Am. Chem. Soc.* **2006**, *128*, 1622-1632.
(71) Kwon, H. C.; Kauffman, C. A.; Jensen, P. R.; Fenical, W. *J. Org. Chem.* **2008**, *74*, 675-684.
(72) Nam, S.-J.; Kauffman, C. A.; Jensen, P. R.; Fenical, W. *Tetrahedron* **2011**, *67*, 6707-6712.
(73) Pathirana, C.; Jensen, P. R.; Fenical, W. *Tetrahedron Lett.* **1992**, *33*, 7663-7666.
(74) Asolkar, R. N.; Singh, A.; Jensen, P. R.; Aalbersberg, W.; Carté, B. K.; Feussner, K.-D.; Subramani, R.; DiPasquale, A.; Rheingold, A. L.; Fenical, W. *Tetrahedron* **2017**, *73*, 2234-2241.
(75) Richards, T. A.; Jones, M. D.; Leonard, G.; Bass, D. *Ann. Rev. Mar. Sci.* **2012**, *4*, 495-522.
(76) Manohar, C. S.; Raghukumar, C. *FEMS Microbiol. Lett.* **2013**, *341*, 69-78.
(77) Sutherland, G. *New Phytol.* **1915**, *14*, 33-42.
(78) Sutherland, G. K.; Eastwood, A. *Ann. Bot.* **1916**, *30*, 333-351.
(79) Jones, E. G.; Suetrong, S.; Sakayaroj, J.; Bahkali, A. H.; Abdel-Wahab, M. A.; Boekhout, T.; Pang, K.-L. *Fungal Divers.* **2015**, *73*, 1-72.
(80) Saleem, M.; Ali, M. S.; Hussain, S.; Jabbar, A.; Ashraf, M.; Lee, Y. S. *Nat. Prod. Rep.* **2007**, *24*, 1142-1152.
(81) Bugni, T. S.; Ireland, C. M. *Nat. Prod. Rep.* **2004**, *21*, 143-163.
(82) Rateb, M. E.; Ebel, R. *Nat. Prod. Rep.* **2011**, *28*, 290-344.
(83) Newton, G.; Abraham, E. *Biochem. J* **1956**, *62*, 651.
(84) Fenical, W.; Jensen, P. R.; Cheng, X. C.; Google Patents: 2000.
(85) Mita, A.; Heist, R.; Aren, O.; Mainwaring, P.; Bazhenova, L.; Gadgeel, S.; Blum, R.; Polikoff, J.; Biswas, J.; Spear, M. *J. Clin. Oncol.* **2010**, *28*, 7592-7592.

(86) Overy, D. P.; Bayman, P.; Kerr, R. G.; Bills, G. F. *Mycology* **2014**, *5*, 145-167.
(87) Soldatou, S.; Baker, B. J. *Nat. Prod. Rep.* **2017**.
(88) Margesin, R.; Neuner, G.; Storey, K. *Naturwissenschaften* **2007**, *94*, 77-99.
(89) Zhang, H. L.; Hua, H. M.; Pei, Y. H.; Yao, X. S. *Chem. Pharm. Bull.* **2004**, *52*, 1029-1030.
(90) Al-Zereini, W.; Schuhmann, I.; Laatsch, H.; Helmke, E.; Anke, H. *J. Antibiot.* **2007**, *60*, 301.
(91) Shin, H. J.; Mondol, M. M.; Yu, T. K.; Lee, H.-S.; Lee, Y.-J.; Jung, H. J.; Kim, J. H.; Kwon, H. J. *Phytochem. Lett.* **2010**, *3*, 194-197.
(92) Gao, X.; Lu, Y.; Xing, Y.; Ma, Y.; Lu, J.; Bao, W.; Wang, Y.; Xi, T. *Microbiol. Res.* **2012**, *167*, 616-622.
(93) Yang, A.; Si, L.; Shi, Z.; Tian, L.; Liu, D.; Zhou, D.; Proksch, P.; Lin, W. *Org. Lett.* **2013**, *15*, 5366-5369.
(94) Moon, K.; Ahn, C.-H.; Shin, Y.; Won, T. H.; Ko, K.; Lee, S. K.; Oh, K.-B.; Shin, J.; Nam, S.-I.; Oh, D.-C. *Mar. Drugs* **2014**, *12*, 2526-2538.
(95) Macherla, V. R.; Liu, J.; Bellows, C.; Teisan, S.; Nicholson, B.; Lam, K. S.; Potts, B. C. *J. Nat. Prod.* **2005**, *68*, 780-783.
(96) Wu, B.; Oesker, V.; Wiese, J.; Schmaljohann, R.; Imhoff, J. F. *Mar. Drugs* **2014**, *12*, 1208-1219.
(97) Stach, J. E.; Maldonado, L. A.; Ward, A. C.; Goodfellow, M.; Bull, A. T. *Environ. Microbiol.* **2003**, *5*, 828-841.
(98) Berdy, J. *J. Antibiot.* **2005**, *58*, 1.
(99) Gosink, J. J.; Woese, C. R.; Staley, J. T. *Int. J. Syst. Evol. Microbiol.* **1998**, *48*, 223-235.
(100) Knoblauch, C.; Sahm, K.; Jørgensen, B. B. *Int. J. Syst. Evol. Microbiol.* **1999**, *49*, 1631-1643.
(101) Dupont, C. L.; Rusch, D. B.; Yooseph, S.; Lombardo, M.-J.; Richter, R. A.; Valas, R.; Novotny, M.; Yee-Greenbaum, J.; Selengut, J. D.; Haft, D. H. *Int. J. Syst. Evol. Microbiol.* **2012**, *6*, 1186-1199.
(102) Ghai, R.; Mizuno, C. M.; Picazo, A.; Camacho, A.; Rodriguez-Valera, F. *Sci. Rep.* **2013**, *3*, 2471.
(103) Pedrós-Alió, C.; Potvin, M.; Lovejoy, C. *Prog. Oceanogr.* **2015**, *139*, 233-243.
(104) Ghiglione, J.-F.; Galand, P. E.; Pommier, T.; Pedrós-Alió, C.; Maas, E. W.; Bakker, K.; Bertilson, S.; Kirchman, D. L.; Lovejoy, C.; Yager, P. L. *PNAS.* **2012**, *109*, 17633-17638.
(105) Mamaeva, E.; Galach'yants, Y. P.; Khabudaev, K.; Petrova, D.; Pogodaeva, T.; Khodzher, T.; Zemskaya, T. *Microbiol.* **2016**, *85*, 220-230.
(106) Zeng, Y.; Zou, Y.; Chen, B.; Grebmeier, J. M.; Li, H.; Yu, Y.; Zheng, T. *Polar Biol.* **2011**, *34*, 907-919.
(107) Jacob, M.; Soltwedel, T.; Boetius, A.; Ramette, A. *PLoS One*. **2013**, *8*, e72779.
(108) Park, S. J.; Park, B. J.; Jung, M. Y.; Kim, S.-J.; Chae, J. C.; Roh, Y.; Forwick, M.; Yoon, H. I.; Rhee, S. K. *Microb. Ecol.* **2011**, *62*, 537-548.
(109) Teske, A.; Durbin, A.; Ziervogel, K.; Cox, C.; Arnosti, C. *Appl. Environ. Microbiol.* **2011**, *77*, 2008-2018.
(110) Algora, C.; Vasileiadis, S.; Wasmund, K.; Trevisan, M.; Krüger, M.; Puglisi, E.; Adrian, L. *FEMS Microbiol. Ecol.* **2015**, *91*, fiv056.

(111) Li, H.; Yu, Y.; Luo, W.; Zeng, Y.; Chen, B. *Extremophiles.* **2009**, *13*, 233-246.
(112) Junge, K.; Eicken, H.; Deming, J. W. *Appl. Environ. Microbiol.* **2004**, *70*, 550-557.
(113) Brown, M. V.; Bowman, J. P. *FEMS Microbiol. Ecol.* **2001**, *35*, 267-275.
(114) Ortega-Retuerta, E.; Joux, F.; Jeffrey, W. H.; Ghiglione, J.-F. *Biogeosciences.* **2013**, *10*, 2747-2759.
(115) Comeau, A. M.; Li, W. K.; Tremblay, J.-É.; Carmack, E. C.; Lovejoy, C. *PLoS One.* **2011**, *6*, e27492.
(116) Sogin, M. L.; Morrison, H. G.; Huber, J. A.; Welch, D. M.; Huse, S. M.; Neal, P. R.; Arrieta, J. M.; Herndl, G. J. *PNAS.* **2006**, *103*, 12115-12120.
(117) Bienhold, C.; Zinger, L.; Boetius, A.; Ramette, A. *PloS One.* **2016**, *11*, e0148016.
(118) Lane, D.; John Wiley and Sons: Chichester, UK: 1991.
(119) Schloss, P. D.; Westcott, S. L.; Ryabin, T.; Hall, J. R.; Hartmann, M.; Hollister, E. B.; Lesniewski, R. A.; Oakley, B. B.; Parks, D. H.; Robinson, C. J. *Appl. Environn Microbiol.* **2009**, *75*, 7537-7541.
(120) Quince, C.; Lanzen, A.; Davenport, R. J.; Turnbaugh, P. J. *BMC Bioinform.* **2011**, *12*, 38.
(121) Pruesse, E.; Quast, C.; Knittel, K.; Fuchs, B. M.; Ludwig, W.; Peplies, J.; Glöckner, F. O. *Nucleic Acid. Res.* **2007**, *35*, 7188-7196.
(122) Edgar, R. C.; Haas, B. J.; Clemente, J. C.; Quince, C.; Knight, R. *Bioinformatics.* **2011**, *27*, 2194-2200.
(123) Bray, J. R.; Curtis, J. T. *Ecol. Mono.* **1957**, *27*, 325-349.
(124) Kumar, S.; Nei, M.; Dudley, J.; Tamura, K. *Brief. Bioinform.* **2008**, *9*, 299-306.
(125) Jensen, P. R.; Gontang, E.; Mafnas, C.; Mincer, T. J.; Fenical, W. *Environ. Microbiol.* **2005**, *7*, 1039-1048.
(126) Vickers, J.; Williams, S.; Ross, G. *Biological, Biochemical and Biomedical Aspects of Actinomycetes.* **1984**, 553-561.
(127) Küster, E.; Williams, S. *Nature.* **1964**, *202*, 928-929.
(128) Mincer, T. J.; Jensen, P. R.; Kauffman, C. A.; Fenical, W. *Appl. Environ. Microbiol.*. **2002**, *68*, 5005-5011.
(129) D'costa, V. M.; McGrann, K. M.; Hughes, D. W.; Wright, G. D. *Science.* **2006**, *311*, 374-377.
(130) Kieser, T. *Practical streptomyces genetics*; John Innes Foundation, 2000.
(131) Altschul, S. F.; Madden, T. L.; Schäffer, A. A.; Zhang, J.; Zhang, Z.; Miller, W.; Lipman, D. J. *Nucleic Acids Res.* **1997**, *25*, 3389-3402.
(132) Posada, D.; Crandall, K. A. *Bioinform.* **1998**, *14*, 817-818.
(133) Waddell, P. J.; Steel, M. *Mol. Phylogen. Evol.* **1997**, *8*, 398-414.
(134) Felsenstein, J. *J. Mol. Evolv.* **1981**, *17*, 368-376.
(135) Hall, T. *Department of Microbiology, North Carolina State University* **2005**.
(136) Chao, A. *Scand. Stat, Theory. Appl.* **1984**, 265-270.
(137) Good, I. J. *Biometrika*. **1953**, *40*, 237-264.
(138) Shannon, C. E. *Bell Syst. Tech. J.* **1948**, *27*, 623-656.
(139) Li, Y.; Liu, Q.; Li, C.; Dong, Y.; Zhang, W.; Zhang, W.; Xiao, T. *Acta Oceanologica Sinica* **2015**, *34*, 93.
(140) Duncan, K.; Haltli, B.; Gill, K. A.; Kerr, R. G. *Mar. Drugs.* **2014**, *12*, 899-925.

(141) Duncan, K.; Haltli, B.; Gill, K.; Correa, H.; Berrué, F.; Kerr, R. *J. Ind. Microbiol. Biotech.* **2015**, *42*, 57-72..
(142) Zinger, L.; Amaral-Zettler, L. A.; Fuhrman, J. A.; Horner-Devine, M. C.; Huse, S. M.; Welch, D. B. M.; Martiny, J. B.; Sogin, M.; Boetius, A.; Ramette, A. *PLoS One.* **2011**, *6*, e24570.
(143) Romanenko, L. A.; Tanaka, N.; Frolova, G. M.; Mikhailov, V. V. *Int. J. Syst. Evol. Microbiol.* **2010**, *60*, 1613-1619.
(144) Du, Z.-J.; Wang, Z.-J.; Zhao, J.-X.; Chen, G.-J. *Int. J. Syst. Evol. Microbiol.* **2016**, *66*, 107-112.
(145) Mußmann, M.; Pjevac, P.; Krüger, K.; Dyksma, S. *Int. J. Syst. Evol. Microbiol.* **2017**.
(146) Kirchman, D. L.; Cottrell, M. T.; Lovejoy, C. *Environ. Microbiol.* **2010**, *12*, 1132-1143.
(147) Matsumoto, A.; Kasai, H.; Matsuo, Y.; Shizuri, Y.; Ichikawa, N.; Fujita, N.; Ōmura, S.; Takahashi, Y. *Int. J. Syst. Evol. Microbiol.* **2013**, *63*, 3404-3408.
(148) Fujinami, S.; Takarada, H.; Kasai, H.; Sekine, M.; Omata, S.; Harada, T.; Fukai, R.; Hosoyama, A.; Horikawa, H.; Kato, Y. *Stand. Genomic Sci.* **2013**, *8*, 430.
(149) Maldonado, L. A.; Fragoso-Yáñez, D.; Pérez-García, A.; Rosellón-Druker, J.; Quintana, E. T. *Antonie Van Leeuwenhoek* **2009**, *95*, 111-120.
(150) Das, S.; Lyla, P.; Khan, S. A. *Curr. Sci.* **2006**, *90*, 1325-1335.
(151) Hill, J. E.; Town, J. R.; Hemmingsen, S. M. *Environ. Microbiol.* **2006**, *8*, 741-` 746.
(152) Farris, M.; Olson, J. *Lett. Appl. Microbiol.* **2007**, *45*, 376-381.
(153) Kurahashi, M.; Fukunaga, Y.; Sakiyama, Y.; Harayama, S.; Yokota, A. *Int. J. Syst. Evol. Microbiol.* **2009**, *59*, 869-873.
(154) Yoon, J.-H.; Lee, C.-H.; Oh, T.-K. *Int. J. Syst. Evol. Microbiol.* **2005**, *55*, 2171-2175.
(155) Bruns, A.; Philipp, H.; Cypionka, H.; Brinkhoff, T. *Int. J. Syst. Evol. Microbiol.* **2003**, *53*, 1917-1923.
(156) Yokota, A.; Tamura, T.; Nishii, T.; Hasegawa, T. *Int. J. Syst. Evol. Microbiol.* **1993**, *43*, 52-57.
(157) Lee, S. D. *Int. J. Syst. Evol. Microbiol.* **2006**, *56*, 1279-1283.
(158) Prauser, H. *Int. J. Syst. Evol. Microbiol.* **1976**, *26*, 58-65.
(159) Choi, D. H.; Kim, H. M.; Noh, J.-H.; Cho, B. C. *Int. J. Syst. Evol. Microbiol.* **2007**, *57*, 775-779.
(160) Kämpfer, P.; Terenius, O.; Lindh, J. M.; Faye, I. *Int. J. Syst. Evol. Microbiol.* **2006**, *56*, 389-392.
(161) Kageyama, A.; Takahashi, Y.; Yasumoto-Hirose, M.; Kasai, H.; Shizuri, Y.; Omura, S. *J. Gen. Appl. Microbiol.* **2007**, *53*, 185-189.
(162) Dastager, S. G.; Lee, J.-C.; Ju, Y.-J.; Park, D.-J.; Kim, C.-J. *Int. J. Syst. Evol. Microbiol.* **2008**, *58*, 1060-1063.
(163) Lee, S. D. *Int. J. Syst. Evol. Microbiol.* **2007**, *57*, 1391-1395.
(164) He, L.; Li, W.; Huang, Y.; Wang, L.; Liu, Z.; Lanoot, B.; Vancanneyt, M.; Swings, J. *Int. J. Syst. Evol. Microbiol.* **2005**, *55*, 1939-1944.
(165) Busse, H.-J. *Int. J. Syst. Evol. Microbiol.* **2016**, *66*, 9-37.

(166) Cui, Y.-S.; Im, W.-T.; Yin, C.-R.; Yang, D.-C.; Lee, S.-T. *Int. J. Syst. Evol. Microbiol.* **2007**, *57*, 713-716.
(167) Yuan, M.; Yu, Y.; Li, H.-R.; Dong, N.; Zhang, X.-H. *Mar. Drugs.* **2014**, *12*, 1281-1297.
(168) Li, J.; Tian, X.-P.; Zhu, T.-J.; Yang, L.-L.; Li, W.-J. *Antonie Van Leeuwenhoek* **2011**, *100*, 537.
(169) D'Onofrio, A.; Crawford, J. M.; Stewart, E. J.; Witt, K.; Gavrish, E.; Epstein, S.; Clardy, J.; Lewis, K. *Chem. Biol.* **2010**, *17*, 254-264.
(170) Lewis, K.; Epstein, S.; D'onofrio, A.; Ling, L. L. *J. Antibiot.* **2010**, *63*, 468-476.
(171) Nelson, M. L.; Levy, S. B. *Ann. N. Y. Acad. Sci.* **2011**, *1241*, 17-32.
(172) Waksman, S. A. *Nature and practical applications.* **1949**.
(173) Sauermann, R.; Rothenburger, M.; Graninger, W.; Joukhadar, C. *Pharmacology.* **2007**, *81*, 79-91.
(174) Bentley, S. D.; Chater, K. F.; Cerdeno-Tarraga, A.-M.; Challis, G. L.; Thomson, N.; James, K. D.; Harris, D. E.; Quail, M. A.; Kieser, H.; Harper, D. *Nature.* **2002**, *417*, 141-147.
(175) Ōmura, S.; Ikeda, H.; Ishikawa, J.; Hanamoto, A.; Takahashi, C.; Shinose, M.; Takahashi, Y.; Horikawa, H.; Nakazawa, H.; Osonoe, T. *PNAS.* **2001**, *98*, 12215-12220.
(176) Bode, H. B.; Bethe, B.; Höfs, R.; Zeeck, A. *Chembiochem.* **2002**, *3*, 619-627.
(177) Rateb, M. E.; Houssen, W. E.; Harrison, W. T.; Deng, H.; Okoro, C. K.; Asenjo, J. A.; Andrews, B. A.; Bull, A. T.; Goodfellow, M.; Ebel, R. *J. Nat. Prod.* **2011**, *74*, 1965-1971.
(178) Yoshida, N.; Tani, Y.; Ogata, K. *J. Antibiot.* **1972**, *25*, 653-659.
(179) Yoshida, N.; Hayashi, S.; Tani, Y.; Ogata, K. *J. Antibiot.* **1974**, *27*, 128-132.
(180) Liao, Y.; Wei, Z.-H.; Bai, L.; Deng, Z.; Zhong, J.J. *J. Biotechnol.* **2009**, *142*, 271-274.
(181) Wu, H.; Qu, S.; Lu, C.; Zheng, H.; Zhou, X.; Bai, L.; Deng, Z. *BMC Genomics.* **2012**, *13*, 337.
(182) Forner, D.; Berrué, F.; Correa, H.; Duncan, K.; Kerr, R. G. *Anal. Chim. Acta* **2013**, *805*, 70-79.
(183) Gill, K. A.; Berrué, F.; Arens, J. C.; Kerr, R. G. *J. Nat. Prod.* **2014**, *77*, 1372-1376.
(184) Bertrand, S.; Azzollini, A.; Schumpp, O.; Bohni, N.; Schrenzel, J.; Monod, M.; Gindro, K.; Wolfender, J. L. *Mol. Biosys.* **2014**, *10*, 2289-2298.
(185) Sproule, A. T., University of Prince Edward Island, 2016.
(186) Overy, D. P.; Berrue, F.; Correa, H.; Hanif, N.; Hay, K.; Lanteigne, M.; McQuilian, K.; Duffy, S.; Boland, P.; Jagannathan, R.; Carr, G. S.; Vansteeland, M.; Kerr, R. G. *Mycology.* **2014**, *5*, 130-144.
(187) Waksman, S. A.; Woodruff, H. B. *Exp. Biol. Med.* **1940**, *45*, 609-614.
(188) Newman, D. J.; Cragg, G. M. *J. Nat. Prod.* **2007**, *70*, 461-477.
(189) Henkel, T.; Rohr, J.; Beale, J. M.; Schwenen, L. *J. Antibiot.* **1990**, *43*, 492-503.
(190) Shaaban, K. A.; Stamatkin, C.; Damodaran, C.; Rohr, J. *J. Antibiot.* **2011**, *64*, 141-150.

(191) Ostash, B.; Rix, U.; Rix, L. L.; Liu, T.; Lombo, F.; Luzhetskyy, A.; Gromyko, O.; Wang, C.; Brana, A. F.; Mendez, C.; Salas, J. A.; Fedorenko, V.; Rohr, J. *Chem. Biol.* **2004**, *11*, 547-555.
(192) Ostash, B.; Rix, U.; Rix, L. L.; Liu, T.; Lombo, F.; Luzhetskyy, A.; Gromyko, O.; Wang, C.; Brana, A. F.; Mendez, C.; Salas, J. A.; Fedorenko, V.; Rohr, J. *Chem. Biol.* **2004**, *11*, 547-555.
(193) Zhu, L.; Luzhetskyy, A.; Luzhetska, M.; Mattingly, C.; Adams, V.; Bechthold, A.; Rohr, J. *Chembiochem.* **2007**, *8*, 83-88.
(194) Erb, A.; Krauth, C.; Luzhetskyy, A.; Bechthold, A. *Appl. Microbiol. Biotech.* **2009**, *83*, 1067-1076.
(195) Shaaban, K. A.; Srinivasan, S.; Kumar, R.; Damodaran, C.; Rohr, J. R. *J. Nat. Prod.* **2010**, *74*, 2-11.
(196) Kharel, M. K.; Rohr, J. *Curr. Opin. Chem. Biol.* **2012**, *16*, 150-161.
(197) Rohr, J.; Thiericke, R. *Nat. Prod. Rep.* **1992**, *9*, 103-137.
(198) Keto-Timonen, R.; Hietala, N.; Palonen, E.; Hakakorpi, A.; Lindström, M.; Korkeala, H. *Front. Microbiol.* **2016**, *7*.
(199) Alberti, F.; Foster, G. D.; Bailey, A. M. *Appl. Microbiol. Biotechnol.* **2017**, *101*, 493-500.
(200) Tisthammer, K. H.; Cobian, G. M.; Amend, A. S. *Fungal Ecol.* **2016**, *19*, 39-46.
(201) Hassett, B. T.; Ducluzeau, A. L. L.; Collins, R. E.; Gradinger, R. *Environ. Microbiol.* **2017**, *19*, 475-484.
(202) Zhang, T.; Wang, N. F.; Zhang, Y. Q.; Liu, H. Y.; Yu, L. Y. *Sci. Rep.* **2015**, *5*, 14524.
(203) Rämä, T.; Davey, M. L.; Nordén, J.; Halvorsen, R.; Blaalid, R.; Mathiassen, G. H.; Alsos, I. G.; Kauserud, H. *Microb. Ecol.* **2016**, *72*, 295-304.
(204) Gardes, M.; Bruns, T. D. *Mol. Ecol.* **1993**, *2*, 113-118.
(205) White, T. J.; Bruns, T.; Lee, S.; Taylor, J. *PCR protocols: a guide to methods and applications.* **1990**, *18*, 315-322.
(206) Caporaso, J. G.; Kuczynski, J.; Stombaugh, J.; Bittinger, K.; Bushman, F. D.; Costello, E. K.; Fierer, N.; Peña, A. G.; Goodrich, J. K.; Gordon, J. I. *Nature Methods*. **2010**, *7*, 335-336.
(207) Edgar, R. C. *Nature Methods.* **2013**, *10*, 996-998.
(208) Kõljalg, U.; Larsson, K. H.; Abarenkov, K.; Nilsson, R. H.; Alexander, I. J.; Eberhardt, U.; Erland, S.; Høiland, K.; Kjøller, R.; Larsson, E. *New Phytol.* **2005**, *166*, 1063-1068.
(209) Vilgalys, R.; Hester, M. *J. Bacteriol.* **1990**, *172*, 4238-4246.
(210) Rehner, S. A.; Buckley, E. *Mycologia.* **2005**, *97*, 84-98.
(211) Pernice, M. C.; Giner, C. R.; Logares, R.; Perera-Bel, J.; Acinas, S. G.; Duarte, C. M.; Gasol, J. M.; Massana, R. *The ISME Journal*. **2016**, *10*, 945-958.
(212) Rédou, V.; Navarri, M.; Meslet-Cladière, L.; Barbier, G.; Burgaud, G. *Appl. Environ. Microbiol.* **2015**, *81*, 3571-3583.
(213) Picard, K. T. *Fungal Ecol.* **2017**, *25*, 1-13.
(214) Li, W.; Wang, M. M.; Wang, X. G.; Cheng, X. L.; Guo, J. J.; Bian, X. M.; Cai, L. *Sci. Rep.* **2016**, *6*.
(215) Navas-Cortés, J.; Perez-Artes, E.; Jimenez-Diaz, R.; Llobell, A.; Bainbridge, B.; Heale, J. *Phytoparasitica.* **1998**, *26*, 199-212.

(216) Patil, S.; Borse, B. *Mycol. Soc. Jpn.* **1985**, *26*, 271-276.
(217) Li, Q.; Wang, G. *Microbiol. Res.* **2009**, *164*, 233-241.
(218) Wilson, I. M.; Knoyle, J. M. *Fungal Biol.* **1961**, *44*, 55-71.
(219) Kohlmeyer, J.; Kohlmeyer, E. *Marine mycology: the higher fungi*; Elsevier, 2013.
(220) Landy, E. T.; Jones, G. M. *Mycologist.* **2006**, *20*, 15-21.
(221) Bass, D.; Howe, A.; Brown, N.; Barton, H.; Demidova, M.; Michelle, H.; Li, L.; Sanders, H.; Watkinson, S. C.; Willcock, S. *Proc. R. Soc. Lond. B. Bio. Sci.* **2007**, *274*, 3069-3077.
(222) Takishita, K.; Tsuchiya, M.; Reimer, J. D.; Maruyama, T. *Extremophiles.* **2006**, *10*, 165-169.
(223) Singh, P.; Raghukumar, C. *Kavaka.* **2014**, *43*, 50-63.
(224) Gaskins, J.; Cheung, P. *Mycopathologia.* **1986**, *93*, 173-184.
(225) Higgins, R. *Can. Vet. J.* **2000**, *41*, 105.
(226) Turchetti, B.; Hall, S. R. T.; Connell, L. B.; Branda, E.; Buzzini, P.; Theelen, B.; Müller, W. H.; Boekhout, T. *Extremophiles.* **2011**, *15*, 573.
(227) Kachalkin, A. *Antonie Van Leeuwenhoek.* **2014**, *105*, 1073-1083.
(228) Boo, S. Y.; Wong, C. M. V. L.; Rodrigues, K. F.; Najimudin, N.; Murad, A. M. A.; Mahadi, N. M. *Pol. Biol.* **2013**, *36*, 381-389.
(229) Izwan, B.; Najad-Zamirah, Z.; Farah-Diba, A.; Nor-Muhammad, M.; Mohd-Nazalan, M.; Rosli, M.; Abdul-Munir, A. *Malays. Appl. Biol.* **2014**, *43*, 71-79.
(230) Yusof, N. A.; Hashim, N. H. F.; Beddoe, T.; Mahadi, N. M.; Illias, R. M.; Bakar, F. D. A.; Murad, A. M. A. *Cell Stress and Chaperones.* **2016**, *21*, 707-715.
(231) Comeau, A. M.; Vincent, W. F.; Bernier, L.; Lovejoy, C. *Sci. Rep.* **2016**, *6*.
(232) Kagami, M.; Miki, T.; Takimoto, G. *Roles and Mechanisms of Parasitism in Aquatic Microbial Communities, Frontiers Media SA, Switzerland.* **2015**, 36-44.
(233) Freeman, K.; Martin, A.; Karki, D.; Lynch, R.; Mitter, M.; Meyer, A.; Longcore, J.; Simmons, D.; Schmidt, S. *PNAS.* **2009**, *106*, 18315-18320.
(234) Sime-Ngando, T. *Front. Microbiol.* **2012**, *3*, 361.
(235) Redfield, G.; Vincent, W. *Freshwater Biol.* **1979**, *9*, 503-510.
(236) Berger, L.; Roberts, A. A.; Voyles, J.; Longcore, J. E.; Murray, K. A.; Skerratt, L. F. *Fungal Ecol.* **2016**, *19*, 89-99.
(237) Hassett, B.; Gradinger, R. *Environ. Microbiol.* **2016**.
(238) Gleason, F. H.; Küpper, F. C.; Amon, J. P.; Picard, K.; Gachon, C. M.; Marano, A. V.; Sime-Ngando, T.; Lilje, O. *Marine and Freshwater Res.* **2011**, *62*, 383-393.
(239) Lepelletier, F.; Karpov, S. A.; Alacid, E.; Le Panse, S.; Bigeard, E.; Garcés, E.; Jeanthon, C.; Guillou, L. *Protist.* **2014**, *165*, 230-244.
(240) Singh, P.; Raghukumar, C.; Meena, R. M.; Verma, P.; Shouche, Y. *Fungal Ecol.* **2012**, *5*, 543-553.
(241) Pachiadaki, M. G.; Rédou, V.; Beaudoin, D. J.; Burgaud, G.; Edgcomb, V. P. *Front. Microbiol.* **2016**, *7*.
(242) Jeffries, T. C.; Curlevski, N. J.; Brown, M. V.; Harrison, D. P.; Doblin, M. A.; Petrou, K.; Ralph, P. J.; Seymour, J. R. *Environ. Microbiol. Rep.* **2016**.
(243) Bills, G. F.; Foster, M. S.; Mueller, G. M. *Biodiversity of Fungi: Inventory and Monitoring Methods*; Academic Press, **2004**.

(244) Jones, E. G. *Fungal Divers.* **2011**, *50*, 73.
(245) Pang, K.-L.; Overy, D. P.; Jones, E. G.; da Luz Calado, M.; Burgaud, G.; Walker, A. K.; Johnson, J. A.; Kerr, R. G.; Cha, H.-J.; Bills, G. F. *Fungal Biol. Rev.* **2016**, *30*, 163-175.
(246) Pitt, J. I. *The genus Penicillium and its teleomorphic states Eupenicillium and Talaromyces.* **1979**.
(247) van Reenen-Hoekstra, E. S.; Samson, R. A. *Introduction to food-borne fungi*; Centraalbureau voor Schimmelcultures, 1988.
(248) Palacios, R.; Möller, G. *Nature*. **1981**. *290*, 792-794.
(249) Nakajima, H.; Hamasaki, T.; Tanaka, K.; Kimura, Y.; Udagawa, S.; Horie, Y. *Agric. Biol. Chem.* **1989**, *53*, 2291-2292.
(250) Kwon, H. J.; Yoshida, M.; Abe, K.; Horinouchi, S.; Beppu, T. *Biosci. Biotechnol. Biochem.* **1992**, *56*, 538-539.
(251) Rowin, G. L.; Miller, J. E.; Albers-Schonberg, G.; Onishi, J. C.; Davis, D.; Dulaney, E. L. *J. Antibiot.* **1986**, *39*, 1772-1775.
(252) Ishidoh, K.-i.; Kinoshita, H.; Igarashi, Y.; Ihara, F.; Nihira, T. *J. Antibiot.* **2014**, *67*, 459-463.
(253) Thongtan, J.; Saenboonrueng, J.; Rachtawee, P.; Isaka, M. *J. Nat. Prod.* **2006**, *69*, 713-714.
(254) Daub, M. E.; Herrero, S.; Chung, K.R. *FEMS Microbiol. Lett.* **2005**, *252*, 197-206.
(255) Fleck, S. C.; Burkhardt, B.; Pfeiffer, E.; Metzler, M. *Tetrahedron Lett.* **2012**, *214*, 27-32.
(256) Stack, M. E.; Mazzola, E. P.; Page, S. W.; Pohland, A. E.; Highet, R. J.; Tempesta, M. S.; Corley, D. G. *J. Nat. Prod.* **1986**, *49*, 866-871.
(257) Tiessen, C.; Gehrke, H.; Kropat, C.; Schwarz, C.; Baechler, S.; Fehr, M.; Pahlke, G.; Marko, D. *World Mycotoxin J.* **2013**, *6*, 233-244.
(258) Lou, J.; Fu, L.; Peng, Y.; Zhou, L. *Molecules.* **2013**, *18*, 5891-5935.
(259) Gao, S. S.; Li, X.-M.; Wang, B. G. *Nat. Prod. Comm.* **2009**, *4*, 1477-1480.
(260) Kishi, T.; Tahara, S.; Taniguchi, N.; Tsuda, M.; Tanaka, C.; Takahashi, S. *Planta Med.* **1991**, *57*, 376-379.
(261) Chagas, F. O.; Dias, L. G.; Pupo, M. T. *Tetrahedron Lett.* **2016**, *57*, 3185-3189.
(262) Poon, K. W.; Albiniak, P. A.; Dudley, G. B. *Org. Synth.* **2007**, 295-305.
(263) Adeboya, M.; Edwards, R.; Laessoe, T.; Maitland, D. *J. Chem. Res. Syn.* **1995**, 356-357.
(264) Gams, K. *Plant Biol.* **1968**, *17*, 455-460.
(265) Veenbaas-Rijks, J. *Plant Biol.* **1970**, *19*, 323-325.
(266) Bissett, J. *Can. J. Bot.* **1983**, *61*, 1311-1329.
(267) Samuels, G. *N.Y. Bot. Gard.* **1989**, *49*, 266-285.
(268) Schroers, H.-J. *A Monograph of Bionectria (Ascomycota, Hypocreales, Bionectriaceae) and its Clonostachys anamorphs*; Centraalbureau voor Schimmelcultures, **2001**.
(269) Mootz, H. D.; Schwarzer, D.; Marahiel, M. A. *Chembiochem.* **2002**, *3*, 490-504.
(270) Marahiel, M. A.; Stachelhaus, T.; Mootz, H. D. *Chem. Rev.* **1997**, *97*, 2651-2674.
(271) Hotchkiss, R. D. *J. Biol. Chem.* **1941**, *141*, 171-185.

(272) Erlanger, B. F.; Goode, L. *Nature.* **1954**, *174*, 840-841.
(273) Levine, D. P. *Clin. Infect. Dis.* **2006**, *42*, 5-12.
(274) Meyer, C.; Reusser, F. *Cell. Mol. Life Sci.* **1967**, *23*, 85-86.
(275) Degenkolb, T.; Kirschbaum, J.; Brückner, H. *Chem. Biodivers.* **2007**, *4*, 1052-1067.
(276) Szekeres, A.; Leitgeb, B.; Kredics, L.; Antal, Z.; Hatvani, L.; Manczinger, L.; Vágvölgyi, C. *Acta Microbiol. Immun. Hung.* **2005**, *52*, 137-168.
(277) Duclohier, H. *Chem. Biodivers.* **2007**, *4*, 1023-1026.
(278) Katoh, K.; Toh, H. *Brief. Bioinform.* **2008**, *9*, 286-298.
(279) Miller, M. A.; Pfeiffer, W.; Schwartz, T. In *Gateway Computing Environments Workshop (GCE)*. **2010**, 1-8.
(280) Stamatakis, A. *Bioinform.* **2006**, *22*, 2688-2690.
(281) Marfey, P. *Carlsberg Res. Comm.* **1984**, *49*, 591-596.
(282) Wieland, T.; Rohr, G.; Faulstich, H.; Zobeley, S.; Trischmann, H. *Justus Liebigs Ann. Chem.* **1977**, 381-386.
(283) Ohyama, T.; Kurihara, Y.; Ono, Y.; Ishikawa, T.; Miyakoshi, S.; Hamano, K.; Araei, M.; Suzuki, T.; Igari, H.; Suzuki, Y. *J. Antibiot.* **2000**, *53*, 1108-1116.
(284) Herald, D. L.; Cascarano, G. L.; Pettit, G. R.; Srirangam, J. K. *J. Am. Chem. Soc.* **1997**, *119*, 6962-6973.
(285) Moon, S. S.; Jian, L. C.; Moore, R. E.; Patterson, G. M. *J. Org. Chem.* **1992**, *57*, 1097-1103.
(286) Morita, H.; Gonda, A.; Takeya, K.; Itokawa, H.; Iitaka, Y. *Tetrahedron.* **1997**, *53*, 1617-1626.
(287) Qin, C.; Bu, X.; Wu, X.; Guo, Z. *J. Comb. Chem.* **2003**, *5*, 353-355.
(288) Holtzel, A.; Jack, R. W.; Nicholson, G. J.; Jung, G.; Gebhardt, K.; Fiedler, H.-P.; Sussmuth, R. D. *J. Antibiot.* **2001**, *54*, 434-440.
(289) Becker, D.; Kiess, M.; Brückner, H. *Liebigs Ann.* **1997**, *1997*, 767-772.
(290) Mohamed-Benkada, M.; Montagu, M.; Biard, J. F.; Mondeguer, F.; Verite, P.; Dalgalarrondo, M.; Bissett, J.; Pouchus, Y. F. *Rapid Commun. Mass Spectrom.* **2006**, *20*, 1176-1180.
(291) Otto, A.; Laub, A.; Porzel, A.; Schmidt, J.; Wessjohann, L.; Westermann, B.; Arnold, N. *Eur. J. Org. Chem.* **2015**, *2015*, 7449-7459.
(292) Chikanishi, T.; Hasumi, K.; Harada, T.; Kawasaki, N.; Endo, A. *J. Antibiot.* **1997**, *50*, 105-110.
(293) Singh, S. B.; Herath, K.; Guan, Z.; Zink, D. L.; Dombrowski, A. W.; Polishook, J. D.; Silverman, K. C.; Lingham, R. B.; Felock, P. J.; Hazuda, D. J. *Org. Lett.* **2002**, *4*, 1431-1434.
(294) Gonçalves, V. N.; Vaz, A.; Rosa, C. A.; Rosa, L. H. *FEMS Microbiol. Ecol.* **2012**, *82*, 459-471.
(295) Zycha, H.; Siepmann, R.; Linnemann, G. *Mucorales: eine Beschreibung aller Gattungen und Arten dieser Pilzgruppe; mit einem Beitrag zur Gattung Mortierella von G. Linnemann*; Cramer, **1969**.
(296) Dyal, S. D.; Narine, S. S. *Food Res. Int.* **2005**, *38*, 445-467.
(297) Ratledge, C. *Biochimie.* **2004**, *86*, 807-815.
(298) Streekstra, H. *J. Biotechnol.* **1997**, *56*, 153-165.
(299) Soman, A. G.; Gloer, J. B.; Wicklow, D. T. *J. Nat. Prod.* **1999**, *62*, 386-388.

(300) Walsh, C. T.; Chen, H.; Keating, T. A.; Hubbard, B. K.; Losey, H. C.; Luo, L.; Marshall, C. G.; Miller, D. A.; Patel, H. M. *Curr. Opin. Chem. Biol.* **2001**, *5*, 525-534.
(301) Hoffmann, K.; Schneider-Scherzer, E.; Kleinkauf, H.; Zocher, R. *J. Biol. Chem.* **1994**, *269*, 12710-12714.
(302) Gentilucci, L.; De Marco, R.; Cerisoli, L. *Curr. Pharm. Des.* **2010**, *16*, 3185-3203.
(303) Zervas, L.; Winitz, M.; Greenstein, J. P. *J. Org. Chem.* **1957**, *22*, 1515-1521.
(304) Soicke, A.; Reuter, C.; Winter, M.; Neudörfl, J. M.; Schloerer, N.; Kühne, R.; Schmalz, H. G. *Eur. J. Org. Chem.* **2014**, *2014*, 6467-6480.
(305) Peterson, Q. P.; Goode, D. R.; West, D. C.; Botham, R. C.; Hergenrother, P. J. *Nat. Protoc.* **2010**, *5*, 294-302.
(306) Wagner, L.; Stielow, B.; Hoffmann, K.; Petkovits, T.; Papp, T.; Vágvölgyi, C.; De Hoog, G.; Verkley, G.; Voigt, K. *Persoonia.* **2013**, *30*, 77-93.
(307) Gams, W. *Persoonia.* **1977**, *9*, 381-391.
(308) Inoue, T.; Hasumi, K.; Kuniyasu, T.; Endo, A. *J. Antibiot.* **1996**, *49*, 45-49.
(309) Harada, K.-i.; Fujii, K.; Mayumi, T.; Hibino, Y.; Suzuki, M.; Ikai, Y.; Oka, H. *Tetrahedron Lett.* **1995**, *36*, 1515-1518.
(310) Chen, Z.; Song, Y.; Chen, Y.; Huang, H.; Zhang, W.; Ju, J. *J. Nat. Prod.* **2012**, *75*, 1215-1219.
(311) Pesic, A.; Baumann, H. I.; Kleinschmidt, K.; Ensle, P.; Wiese, J.; Süssmuth, R. D.; Imhoff, J. F. *Mar. Drugs* **2013**, *11*, 4834-4857.
(312) Takada, K.; Ninomiya, A.; Naruse, M.; Sun, Y.; Miyazaki, M.; Nogi, Y.; Okada, S.; Matsunaga, S. *J. Org. Chem.* **2013**, *78*, 6746-6750.
(313) Tan, L. T.; Cheng, X. C.; Jensen, P. R.; Fenical, W. *J. Org. Chem.* **2003**, *68*, 8767-8773.
(314) Renner, M. K.; Shen, Y.-C.; Cheng, X.-C.; Jensen, P. R.; Frankmoelle, W.; Kauffman, C. A.; Fenical, W.; Lobkovsky, E.; Clardy, J. *J. Am. Chem. Soc.* **1999**, *121*, 11273-11276.
(315) Williams, D. E.; Yu, K.; Behrisch, H. W.; Van Soest, R.; Andersen, R. J. *J. Nat. Prod.* **2009**, *72*, 1253-1257.
(316) Toske, S. G.; Fenical, W. *Tetrahedron Lett.* **1995**, *36*, 8355-8358.
(317) Morita, H.; Enomoto, M.; Hirasawa, Y.; Iizuka, T.; Ogawa, K.; Kawahara, N.; Goda, Y.; Matsumoto, T.; Takeya, K. *Bioorg. Med. Chem. Lett.* **2007**, *17*, 5410-5413.
(318) Gams, W. *Persoonia*, **1971**, *6*, 185-191.
(319) Weiser, J.; Matha, V.; Jegorov, A. *Folia Parasitologica* **1990**, *38*, 363-369.
(320) Barron, G. *Can. J. Bot.* **1983**, *61*, 2566-2569.
(321) Hodge, K. T.; Krasnoff, S. B.; Humber, R. A. *Mycologia* **1996**, 715-719.
(322) McNeill, J.; Barrie, F.; Buck, W.; Demoulin, V.; Greuter, W.; Hawksworth, D.; Herendeen, P.; Knapp, S.; Marhold, K.; Prado, J. *Regnum Veg.* **2012**, *154*.
(323) Quandt, C. A.; Kepler, R. M.; Gams, W.; Araújo, J. P.; Ban, S.; Evans, H. C.; Hughes, D.; Humber, R.; Hywel-Jones, N.; Li, Z. *IMA Fungus.* **2014**, *5*, 121-134.
(324) Jackson, C. G.; Linnett, P. E.; Beechey, R. B.; Henderson, P. J. *Biochem. Soc. Trans* **1979**, *7*, 224-226.

(325) Bullough, D. A.; Jackson, C. G.; Henderson, P. J.; Beechey, R. B.; Linnett, P. E. *FEBS Lett.* **1982**, *145*, 258-262.
(326) Du, L.; Risinger, A. L.; King, J. B.; Powell, D. R.; Cichewicz, R. H. *J. Nat. Prod.* **2014**, *77*, 1753-1757.
(327) Tsantrizos, Y. S.; Pischos, S.; Sauriol, F. *J. Org. Chem.* **1996**, *61*, 2118-2121.
(328) Chu, M.; Mierzwa, R.; Truumees, I.; Gentile, F.; Patel, M.; Gullo, V.; Chan, T.-M.; Puar, M. S. *Tetrahedron Lett.* **1993**, *34*, 7537-7540.
(329) Höltzel, A.; Gänzle, M. G.; Nicholson, G. J.; Hammes, W. P.; Jung, G. *Angew. Chem. Int. Ed.* **2000**, *39*, 2766-2768.
(330) Luesch, H.; Yoshida, W. Y.; Moore, R. E.; Paul, V. J. *Tetrahedron.* **2002**, *58*, 7959-7966.
(331) Putri, S. P.; Kinoshita, H.; Ihara, F.; Igarashi, Y.; Nihira, T. *J. Antibiot.* **2010**, *63*, 195.
(332) Wang, C.-Y.; Wang, B.-G.; Wiryowidagdo, S.; Wray, V.; van Soest, R.; Steube, K. G.; Guan, H.-S.; Proksch, P.; Ebel, R. *J. Nat. Prod.* **2003**, *66*, 51-56.
(333) Gui, C.; Li, Q.; Mo, X.; Qin, X.; Ma, J.; Ju, J. *Org. Lett.* **2015**, *17*, 628-631.
(334) Xu, W.; Cai, X.; Jung, M. E.; Tang, Y. *J. Am. Chem. Soc.* **2010**, *132*, 13604-13607.
(335) Schobert, R.; Schlenk, A. *Biorg. Med. Chem.* **2008**, *16*, 4203-4221.
(336) Segeth, M. P.; Bonnefoy, A.; Broenstrup, M.; Knauf, M.; Schummer, D.; Toti, L.; Vertesy, L.; Wetzel-Raynal, M.C.; Wink, J.; Seibert, G. *J. Antibiot.* **2003**, *56*, 114-122.
(337) Lang, G.; Blunt, J. W.; Cummings, N. J.; Cole, A. L.; Munro, M. H. *J. Nat. Prod.* **2005**, *68*, 810-811.
(338) Yang, S.-W.; Mierzwa, R.; Terracciano, J.; Patel, M.; Gullo, V.; Wagner, N.; Baroudy, B.; Puar, M.; Chan, T.-M.; McPhail, A. T. *J. Nat. Prod.* **2006**, *69*, 1025-1028.
(339) Fukuda, T.; Sudoh, Y.; Tsuchiya, Y.; Okuda, T.; Matsuura, N.; Motojima, A.; Oikawa, T.; Igarashi, Y. *J. Antibiot.* **2015**, *68*, 399.
(340) Shang, Z.; Li, L.; Espósito, B. P.; Salim, A. A.; Khalil, Z. G.; Quezada, M.; Bernhardt, P. V.; Capon, R. J. *Org. Biomol. Chem.* **2015**, *13*, 7795-7802.
(341) Amagata, T.; Xiao, J.; Chen, Y.-P.; Holsopple, N.; Oliver, A. G.; Gokey, T.; Guliaev, A. B.; Minoura, K. *J. Nat. Prod.* **2012**, *75*, 2193-2199.
(342) Ondeyka, J.; Harris, G.; Zink, D.; Basilio, A.; Vicente, F.; Bills, G.; Platas, G.; Collado, J.; González, A.; Cruz, M. d. l. *J. Nat. Prod.* **2008**, *72*, 136-141.
(343) Ohtani, I.; Kusumi, T.; Kashman, Y.; Kakisawa, H. *J. Am. Chem. Soc.* **1991**, *113*, 4092-4096.
(344) Marchbank, D. H.; Berrue, F.; Kerr, R. G. *J. Nat. Prod.* **2012**, *75*, 1289-1293.
(345) Whitt, J.; Shipley, S. M.; Newman, D. J.; Zuck, K. M. *J. Nat. Prod.* **2014**, *77*, 173-177.
(346) Zhao, S.; Chen, S.; Wang, B.; Niu, S.; Wu, W.; Guo, L.; Che, Y. *Fitoterapia.* **2015**, *103*, 106-112.
(347) Singh, S. B.; Zink, D. L.; Heimbach, B.; Genilloud, O.; Teran, A.; Silverman, K. C.; Lingham, R. B.; Felock, P.; Hazuda, D. J. *Org. Lett.* **2002**, *4*, 1123-1126.

(348) Watanabe, T.; Igarashi, M.; Okajima, T.; Ishii, E.; Kino, H.; Hatano, M.; Sawa, R.; Umekita, M.; Kimura, T.; Okamoto, S. *Antimicrob. Agents Chemother.* **2012**, *56*, 3657-3663.
(349) Quek, N. C.; Matthews, J. H.; Bloor, S. J.; Jones, D. A.; Bircham, P. W.; Heathcott, R. W.; Atkinson, P. H. *Mol. BioSystems.* **2013**, *9*, 2125-2133
(350) Halo, L. M.; Heneghan, M. N.; Yakasai, A. A.; Song, Z.; Williams, K.; Bailey, A. M.; Cox, R. J.; Lazarus, C. M.; Simpson, T. J. *J. Am. Chem. Soc.* **2008**, *130*, 17988-17996.
(351) Fujita, Y.; Oguri, H.; Oikawa, H. *Tetrahedron Lett.* **2005**, *46*, 5885-5888.
(352) Gräfe, U.; Ihn, W.; Schlegel, B.; HOFLE, G.; Augustiniak, H.; Sandor, P. *Pharmazie.* **1991**, *46*, 613-614.
(353) Augustiniak, H.; Forche, E.; Reichenbach, H.; Wray, V.; Gräfe, U.; Höfle, G. *Eur. J. Org. Chem.* **1991**, *1991*, 361-366.
(354) Nichols, D.; Cahoon, N.; Trakhtenberg, E.; Pham, L.; Mehta, A.; Belanger, A.; Kanigan, T.; Lewis, K.; Epstein, S. *Appl. Environ. Microbiol.* **2010**, *76*, 2445-2450.
(355) Piddock, L. J. *J. Antimicrob. Chemother.* **2015**, *70*, 2679-2680.
(356) Keller, N. P.; Turner, G.; Bennett, J. W. *Nat. Rev.* **2005**, *3*, 937.
(357) Brakhage, A. A.; Schroeckh, V. *Fungal Genet. Biol.* **2011**, *48*, 15-22.
(358) Clevenger, K. D.; Bok, J. W.; Ye, R.; Miley, G. P.; Verdan, M. H.; Velk, T.; Chen, C.; Yang, K.; Gao, P.; Robey, M. *The FASEB Journal* **2017**, *31*, 766.

APPENDIX

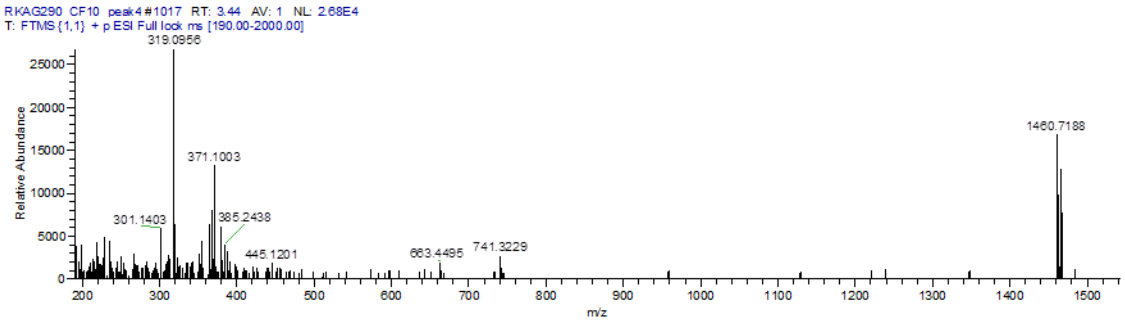

Figure A.1. +ESI HRMS of landomycin AA *m/z* 1460.7188 $[M+NH_4]^+$.

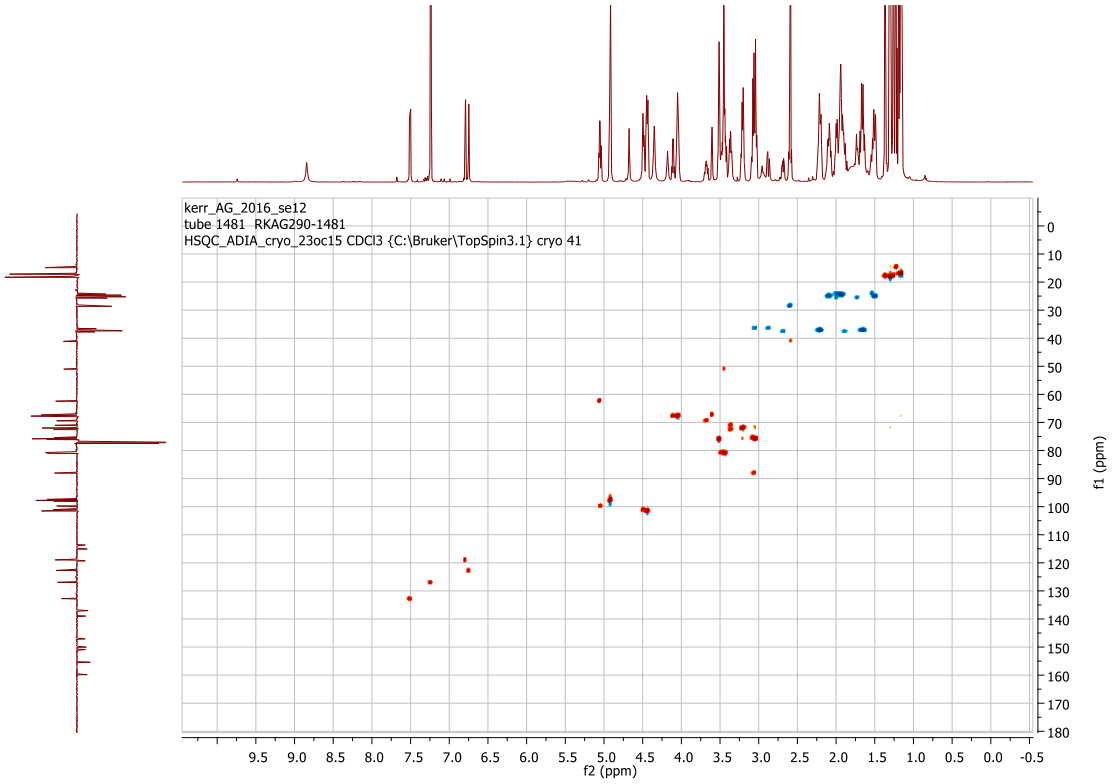

Figure A.2. HSQC spectrum of landomycin AA in $CDCl_3$.

A

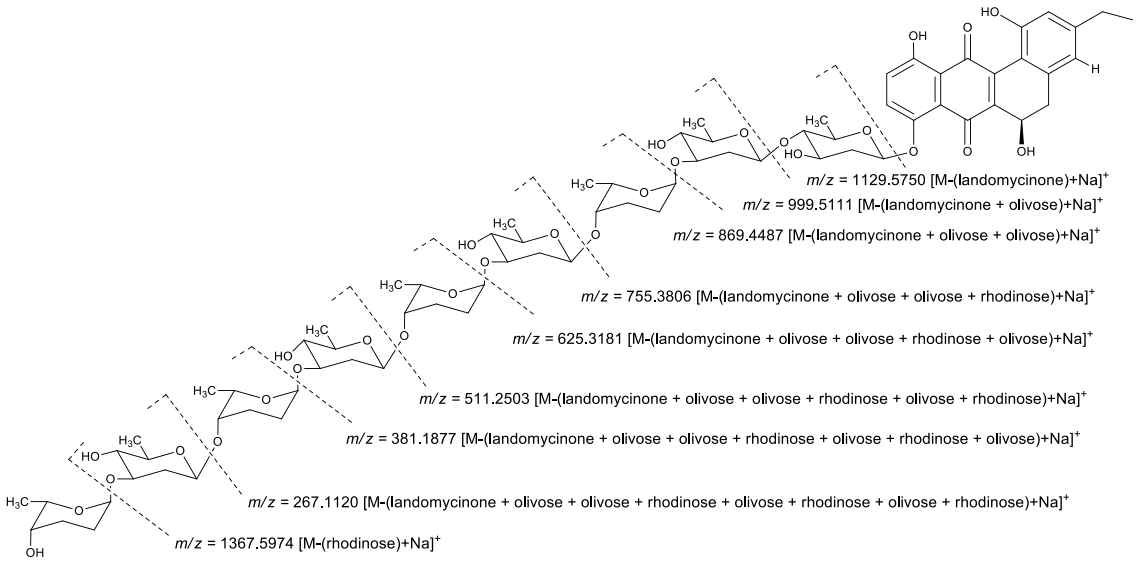

B

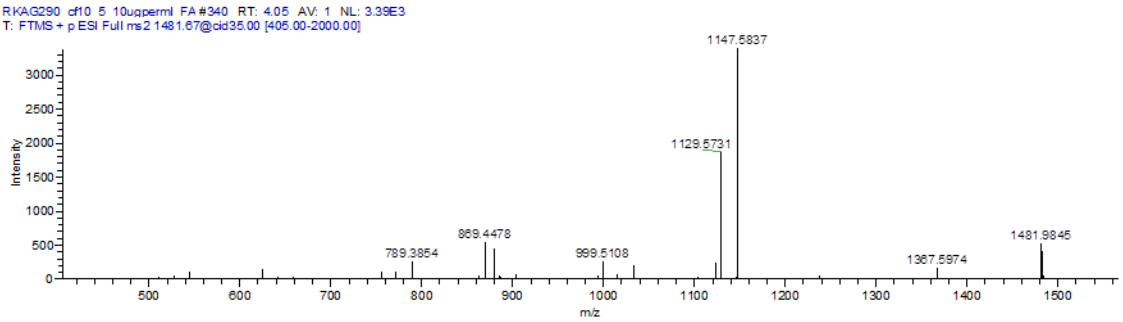

C

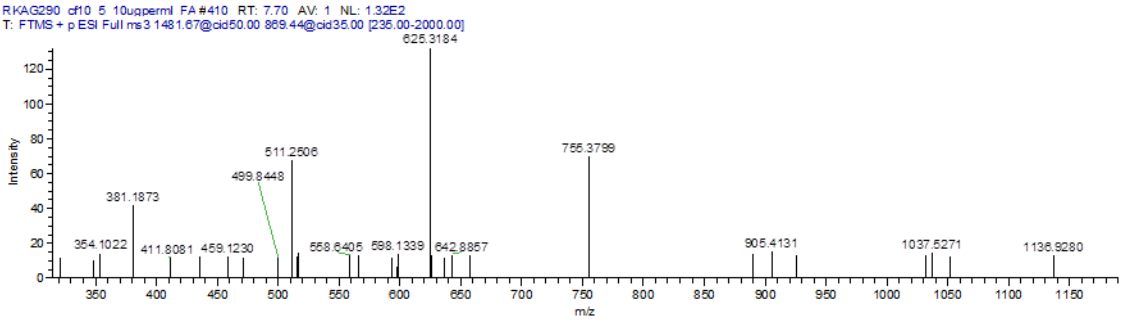

Figure A.3. A. MS^n fragments used to determine the structure of landomycin AA. **B**. MS^2 spectrum of *m/z* 1481.67 $[M+Na]^+$. **C**. MS^3 spectrum of *m/z* 869.44 $[M+Na]^+$.

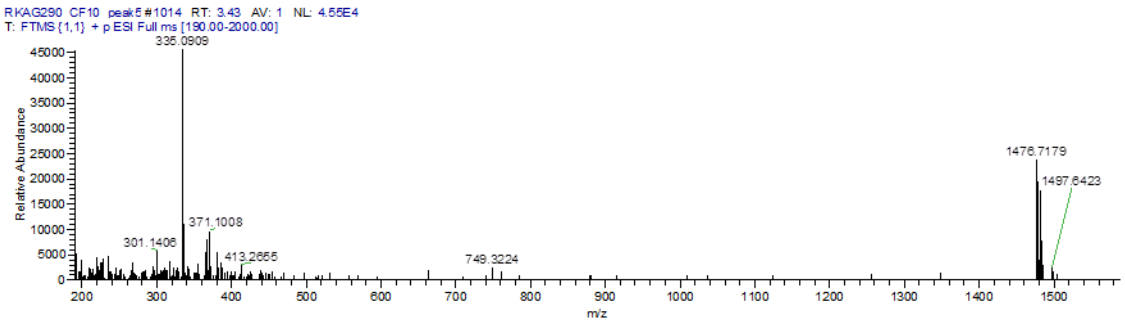

Figure A.4. +ESI HRMS of landomycin AB *m/z* 1476.7179 $[M+NH_4]^+$.

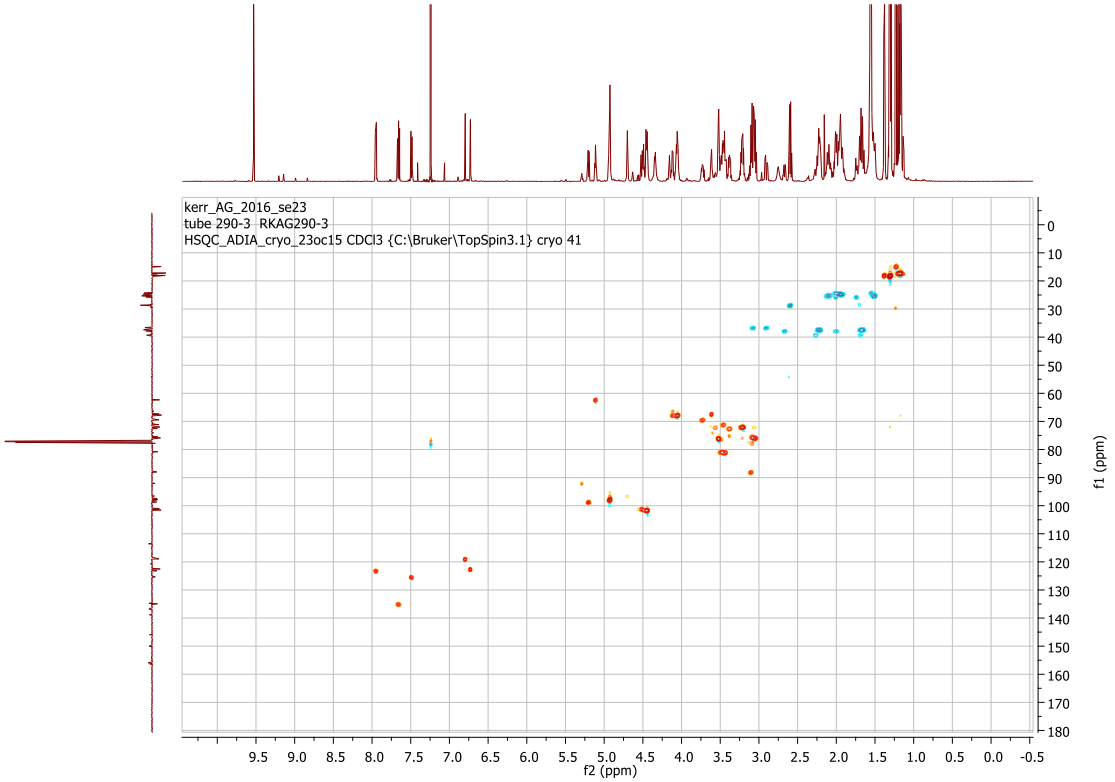

Figure A.5. HSQC spectrum of landomycin AB in $CDCl_3$.

A

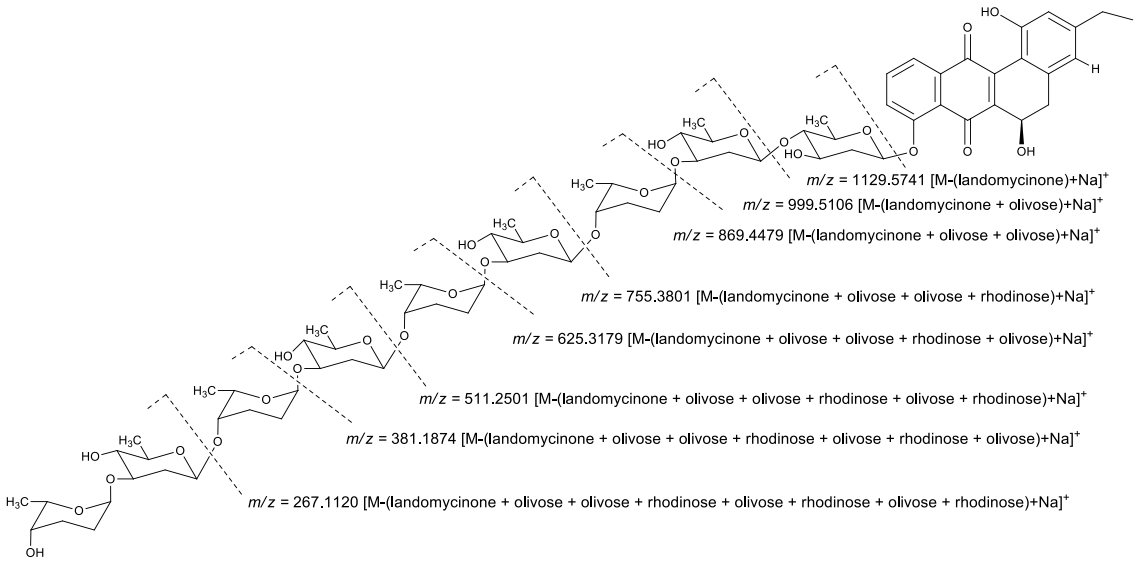

B

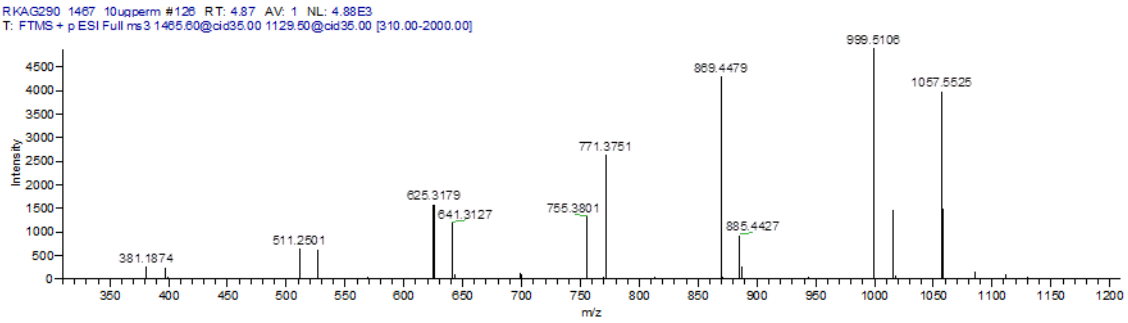

Figure A.6. A. MS^n fragments used to determine the structure of landomycin AB. **B**. MS^3 spectrum of *m/z* 1129.50 $[M+Na]^+$.

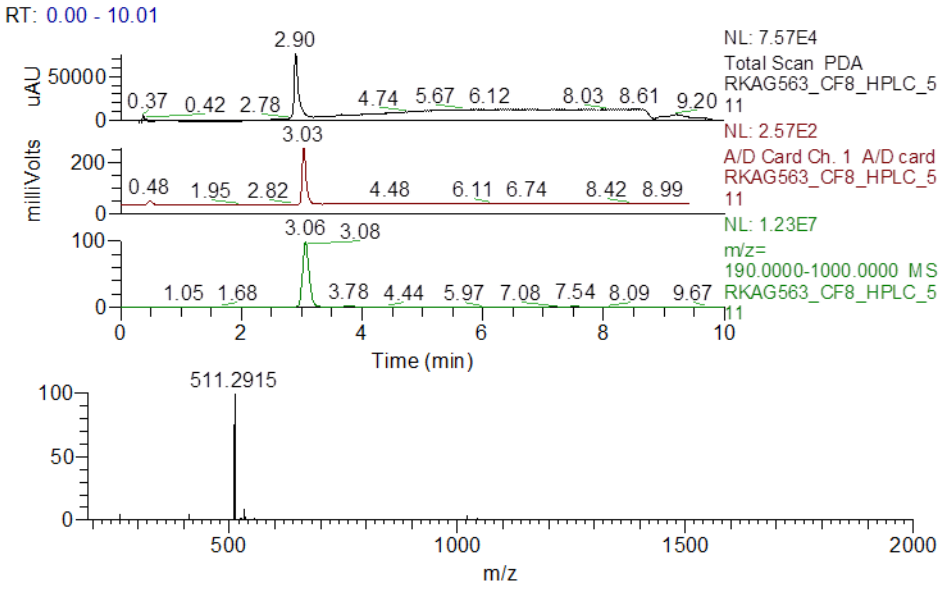

Figure A.7. ESI HRMS of hirsutellic acid C *m/z* 511.2915 $[M+H]^+$.

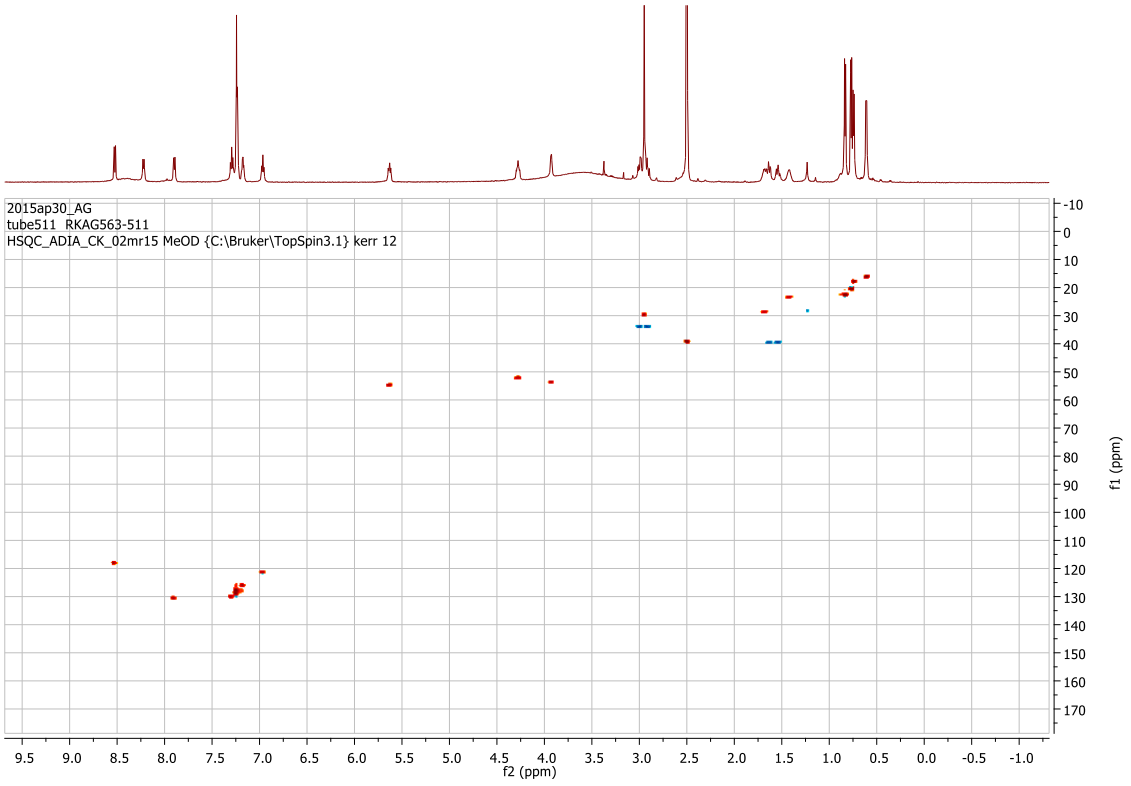

Figure A.8. HSQC spectrum of hirsutellic acid C in DMSO-d_6.

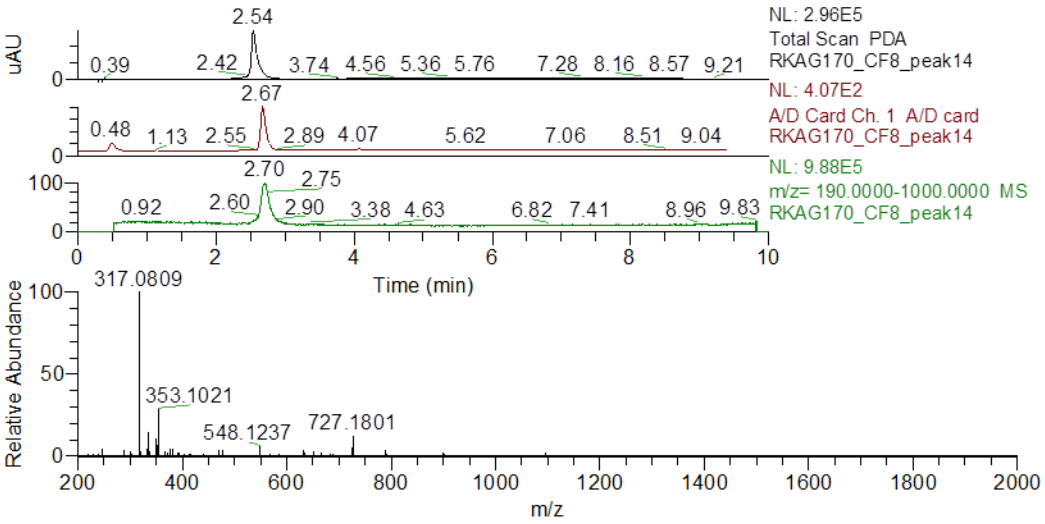

Figure A.9. +ESI HRMS of compound **6** *m/z* 353.1021 $[M+H]^+$.

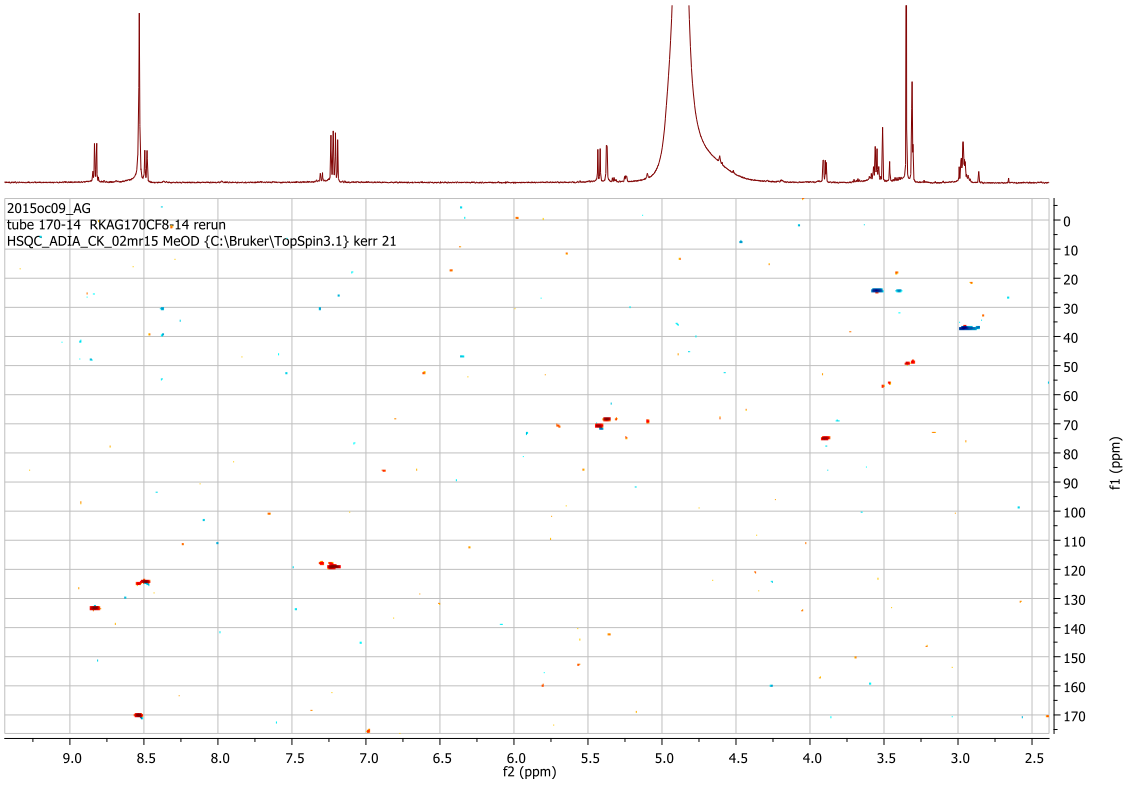

Figure A.10. HSQC spectrum of compound **6** in CD_3OD.

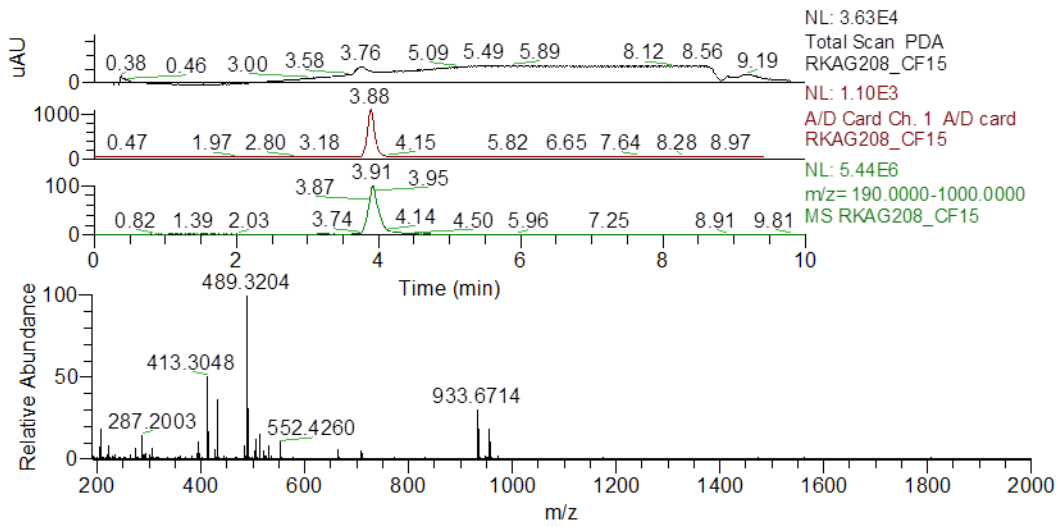

Figure A.11. +ESI HRMS of cameronic acid B *m/z* 489.3204 $[M+Na]^+$.

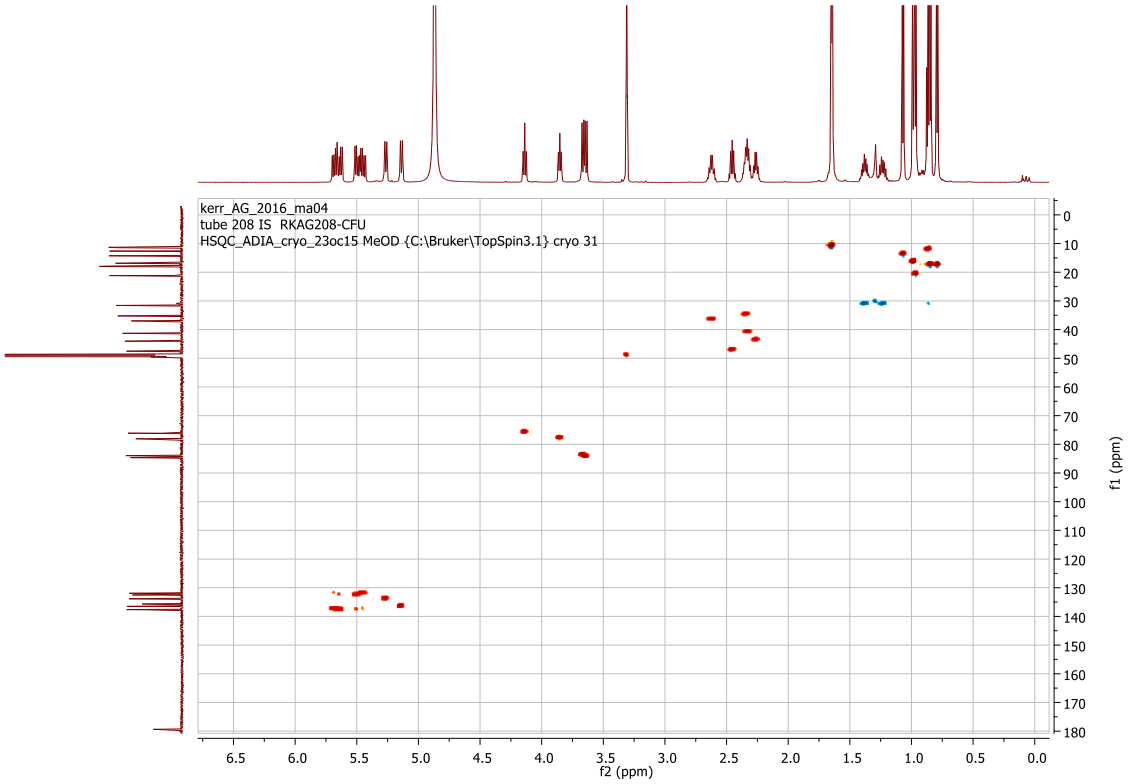

Figure A.12. HSQC spectrum of cameronic acid B in CD_3OD.

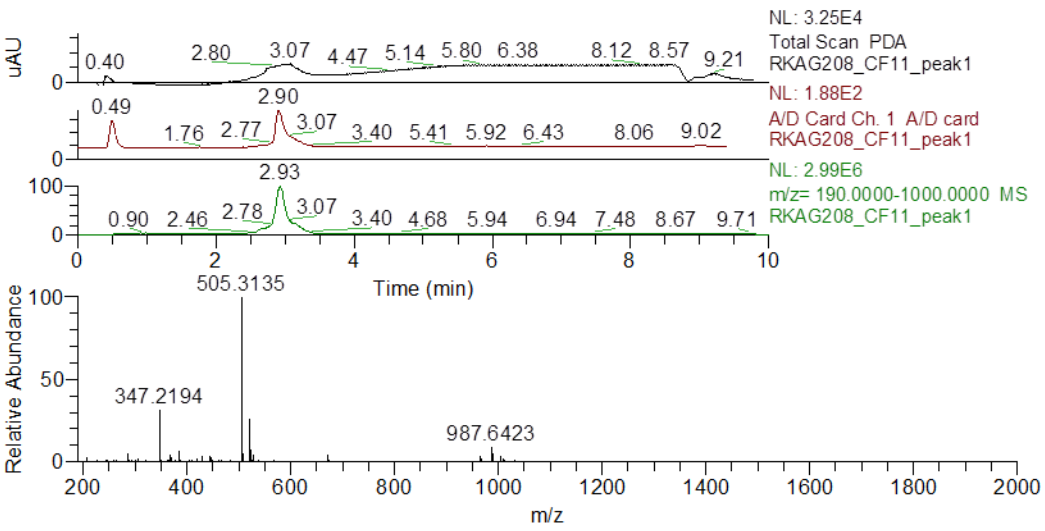

Figure A.13. +ESI HRMS of cameronic acid B *m/z* 505.3135 $[M+Na]^+$.

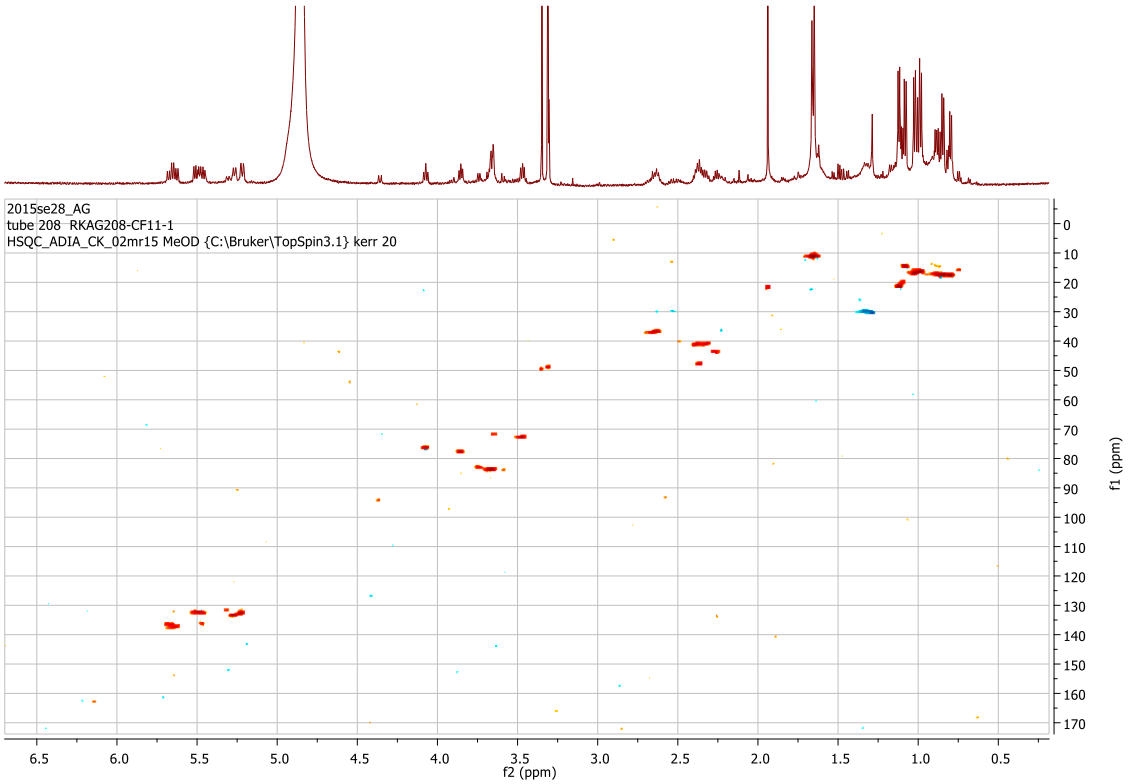

Figure A.14. HSQC spectrum of cameronic acid C in CD_3OD.

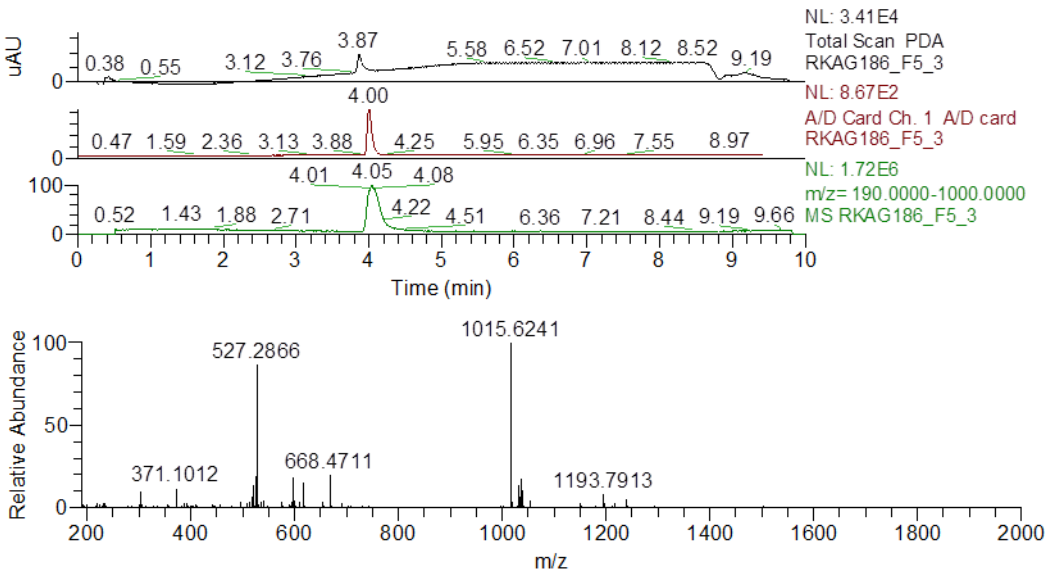

Figure A.15. +ESI HRMS of auyuittuqamide A *m/z* 1015.6241 $[M+H]^+$.

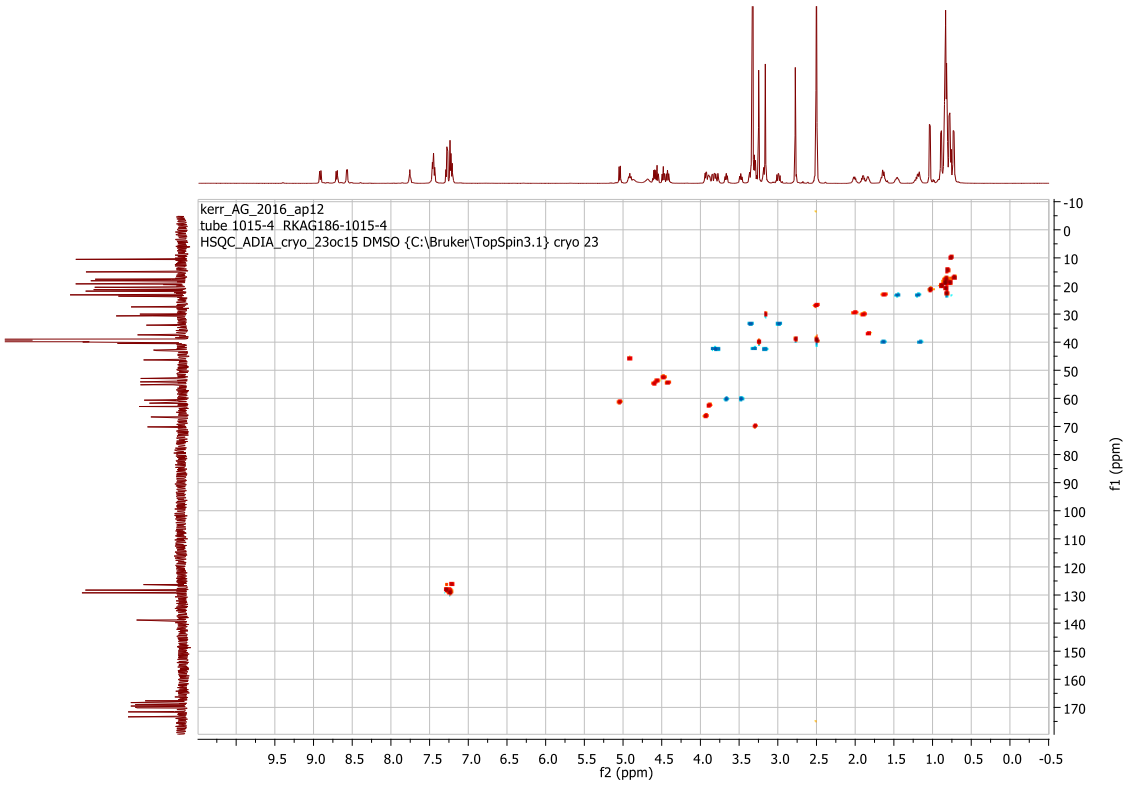

Figure A.16. HSQC spectrum of auyuittuqamide A DMSO-d_6.

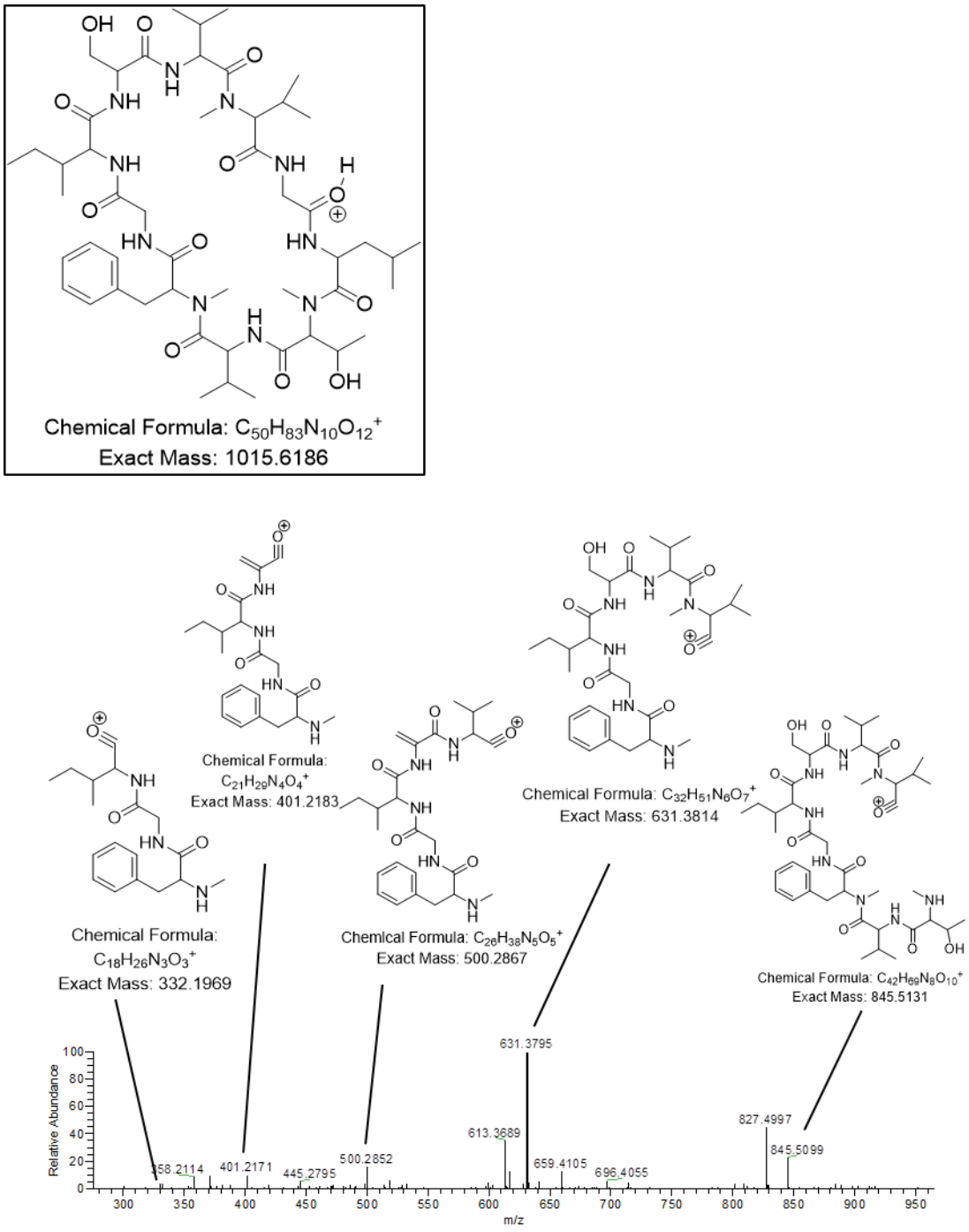

Figure A.17. MS^n fragments used to determine the structure of auyuittuqamide A.

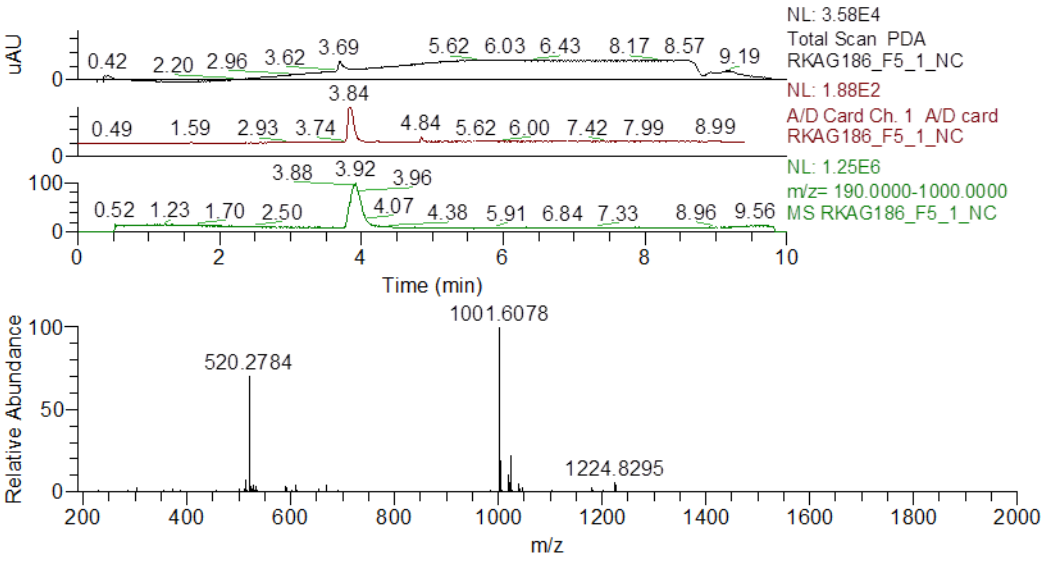

Figure A.18. +ESI HRMS of frobiamide B *m/z* 1001.6078 $[M+H]^+$.

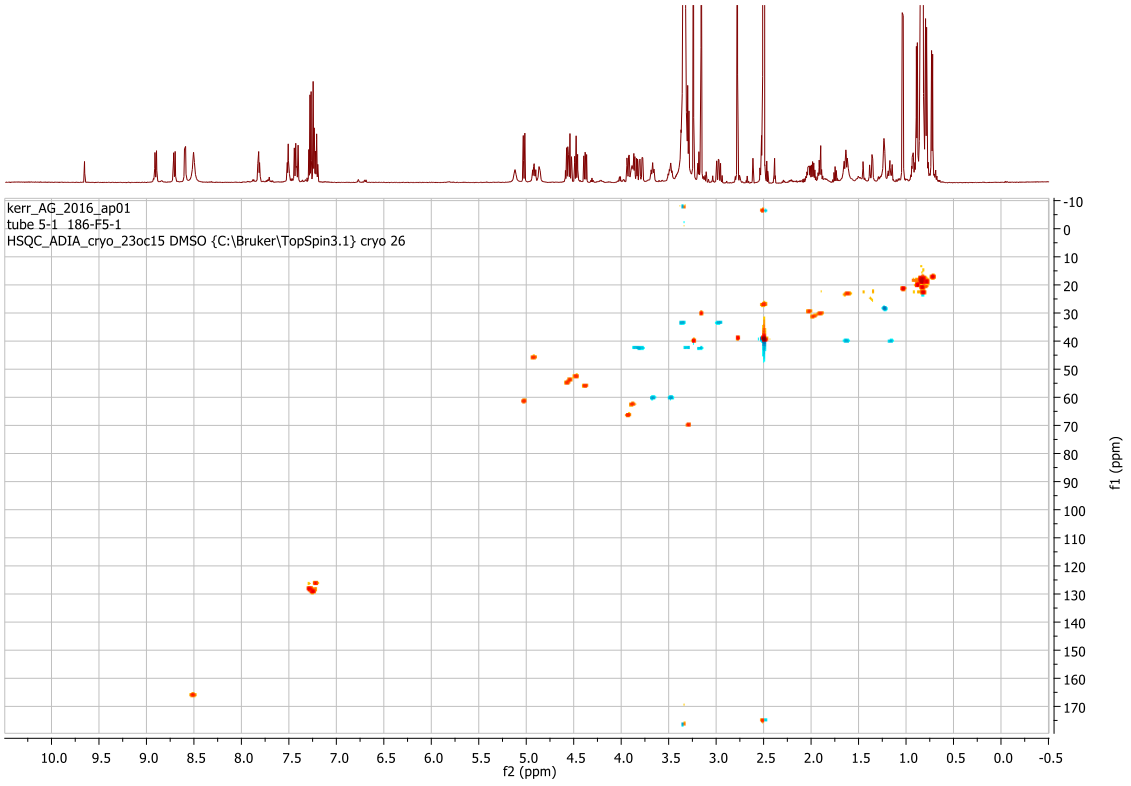

Figure A.19. HSQC spectrum of auyuittuqamide B DMSO-d_6.

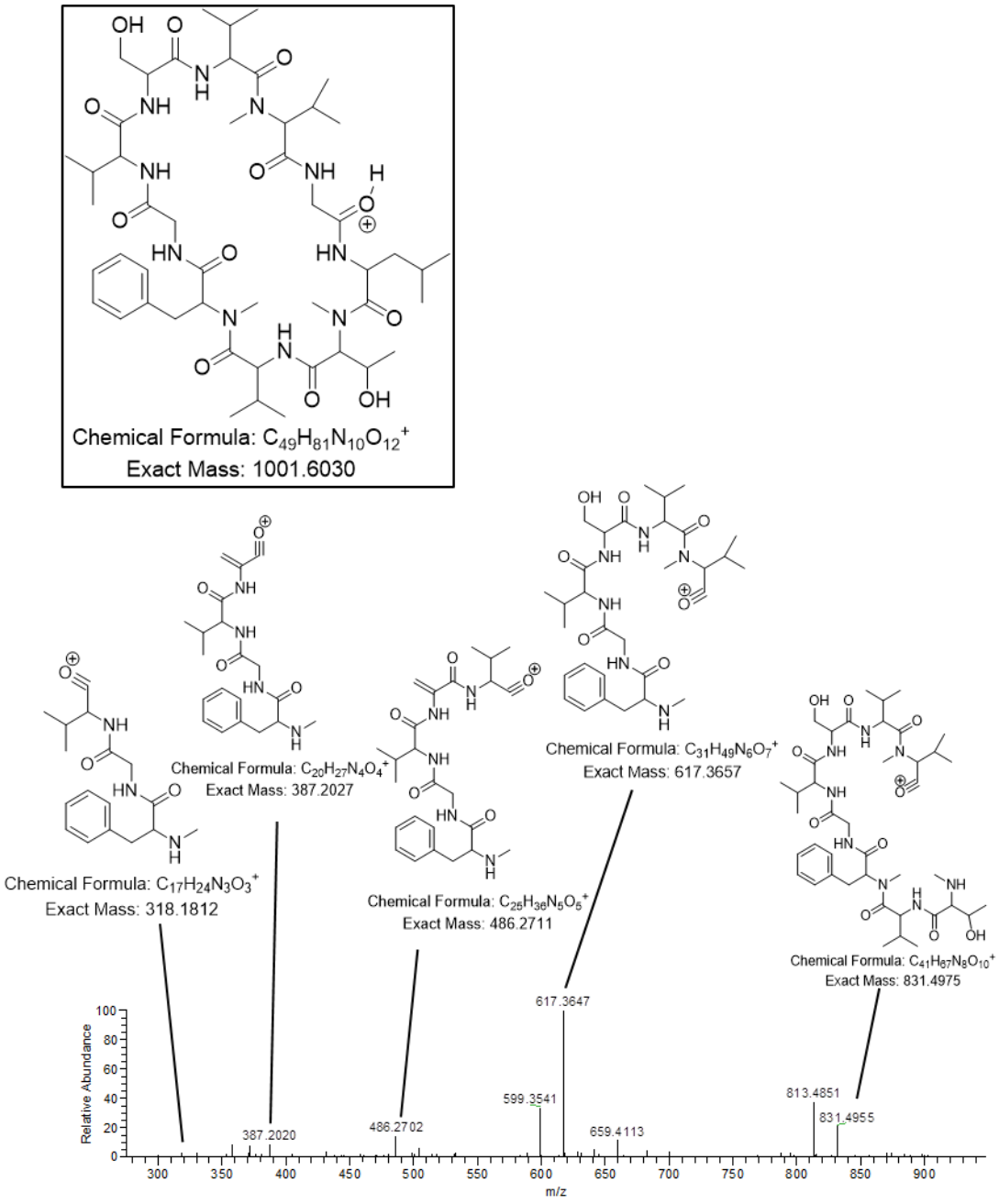

Figure A.20. MS^n fragments used to determine the structure of auyuittuqamide B.

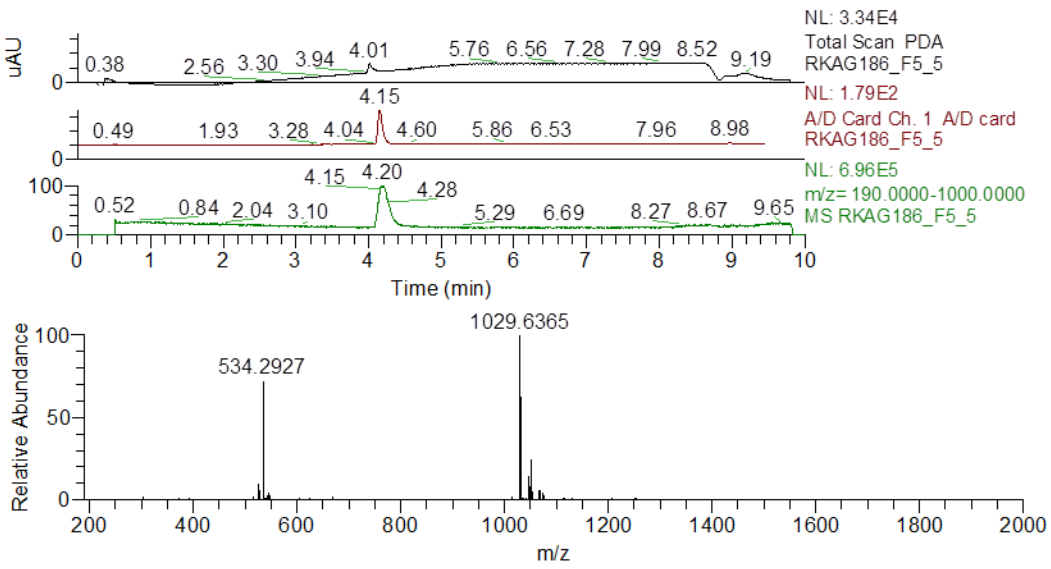

Figure A.21. +ESI HRMS of auyuittuqamide C *m/z* 1029.6365 $[M+H]^+$.

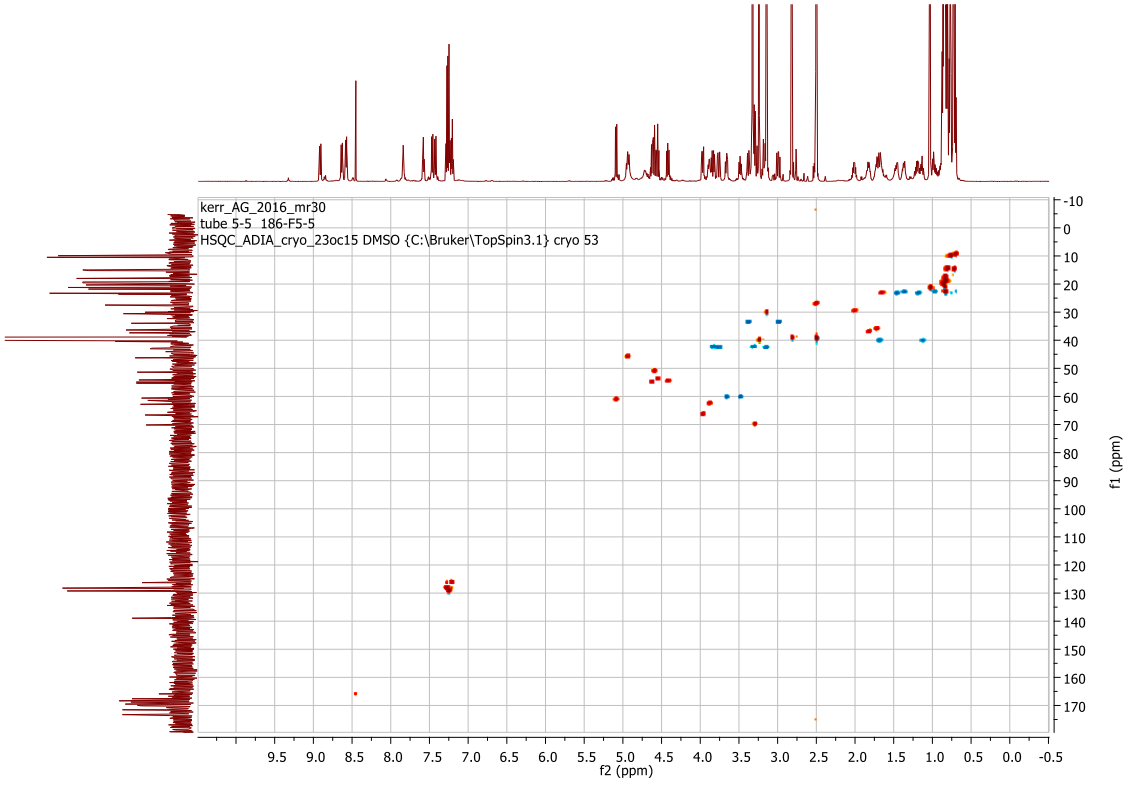

Figure A.22. HSQC spectrum of auyuittuqamide C in DMSO-d_6.

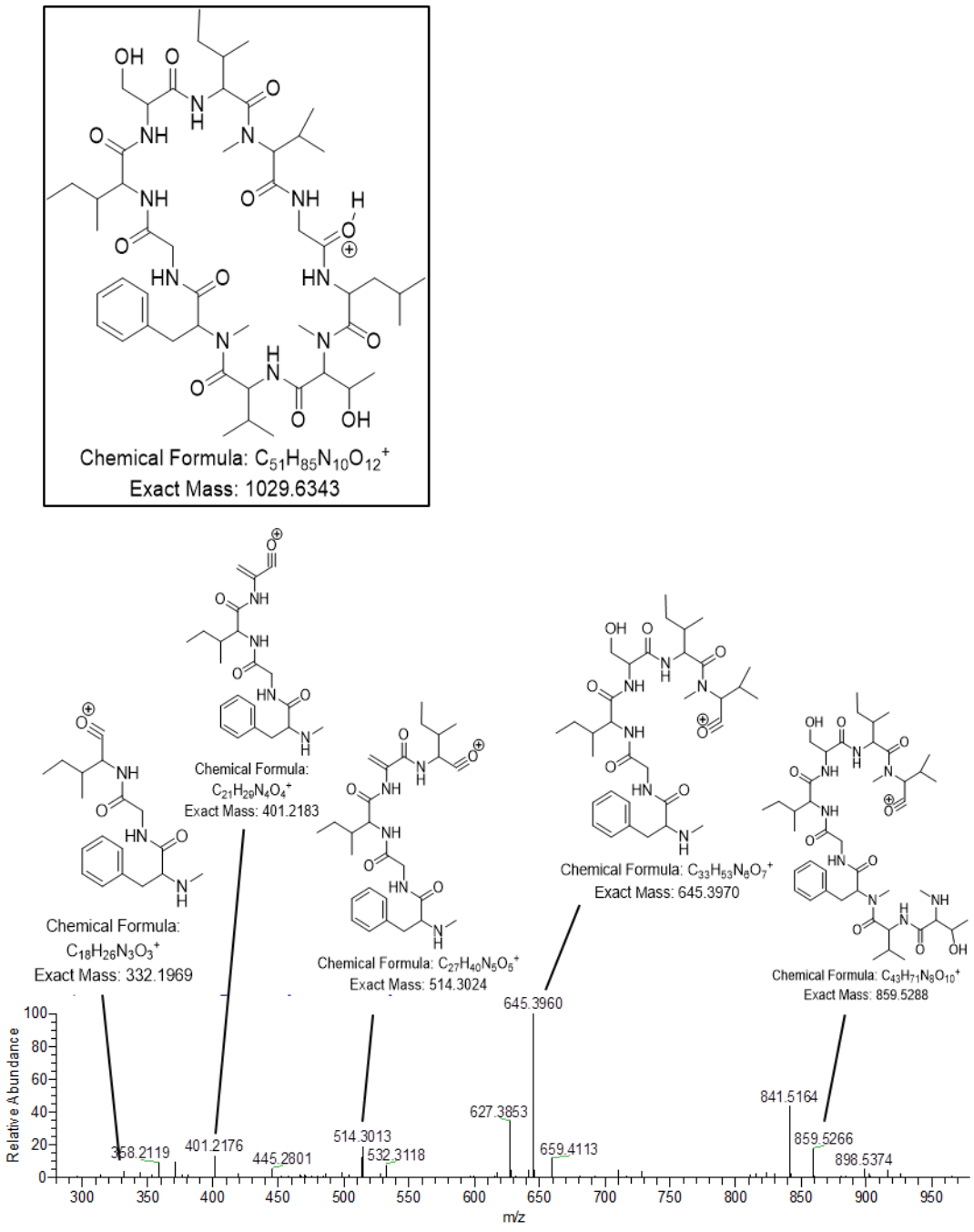

Figure A.23. MS^n fragments used to determine the structure of auyuittuqamide C.

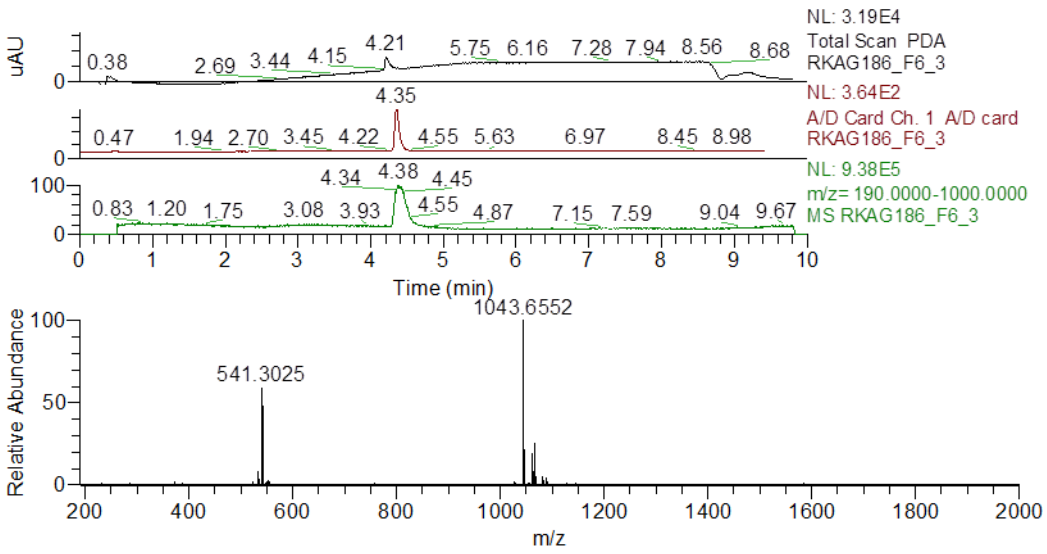

Figure A.24. +ESI HRMS of auyuittuqamide D *m/z* 1043.6552 $[M+H]^+$.

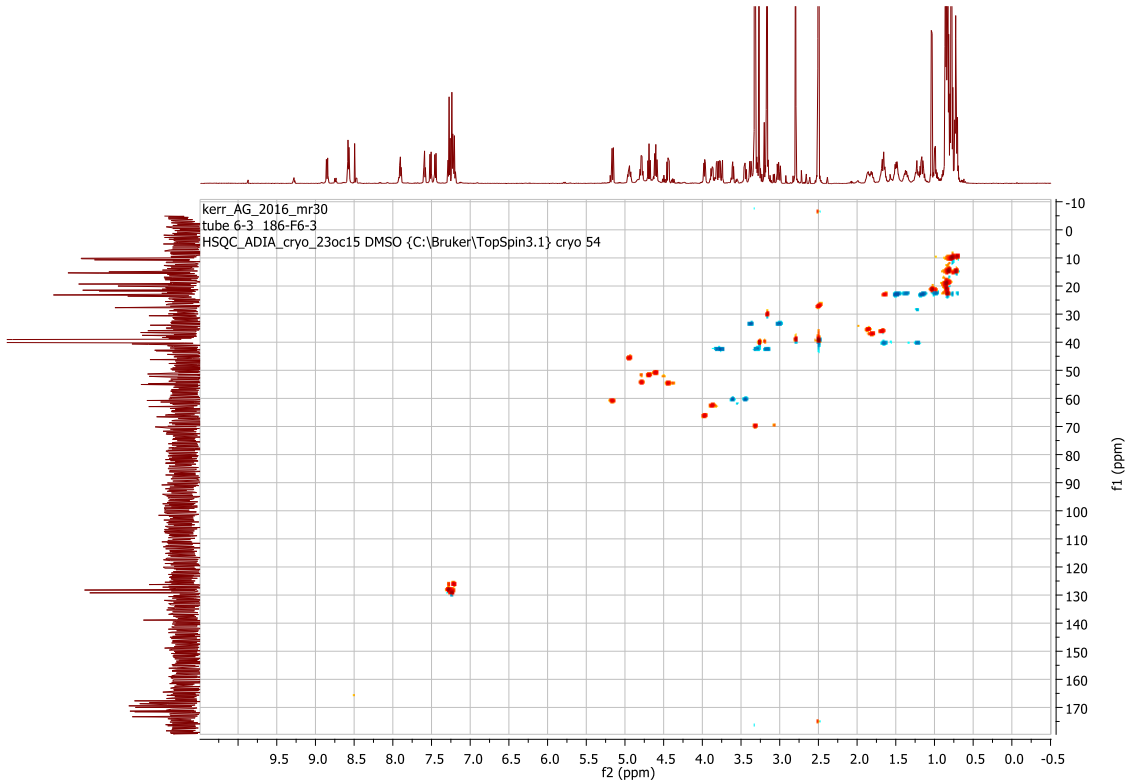

Figure A.25. HSQC spectrum of auyuittuqamide D in DMSO-d_6.

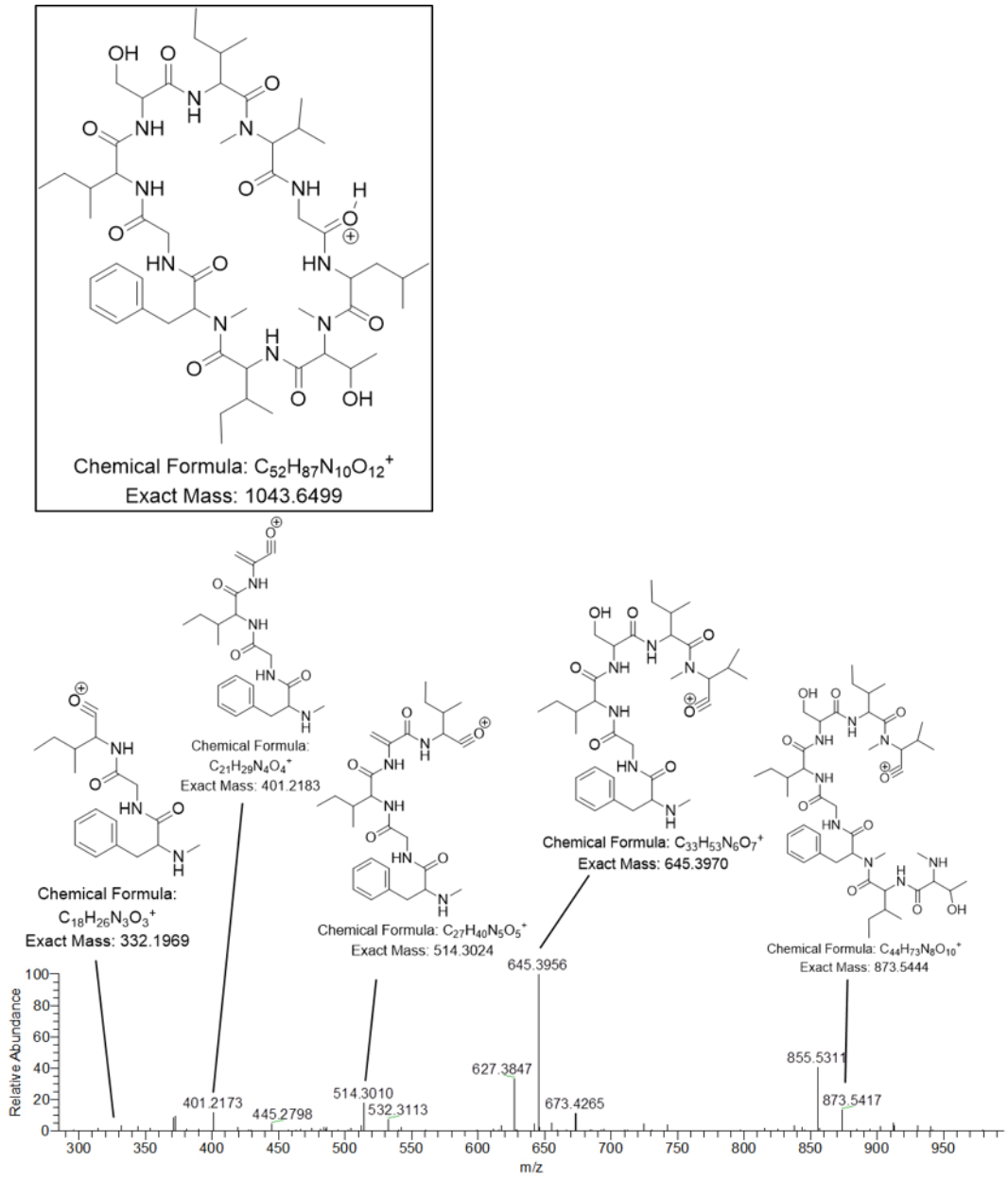

Figure A.26. MS^n fragments used to determine the structure of auyuittuqamide D.

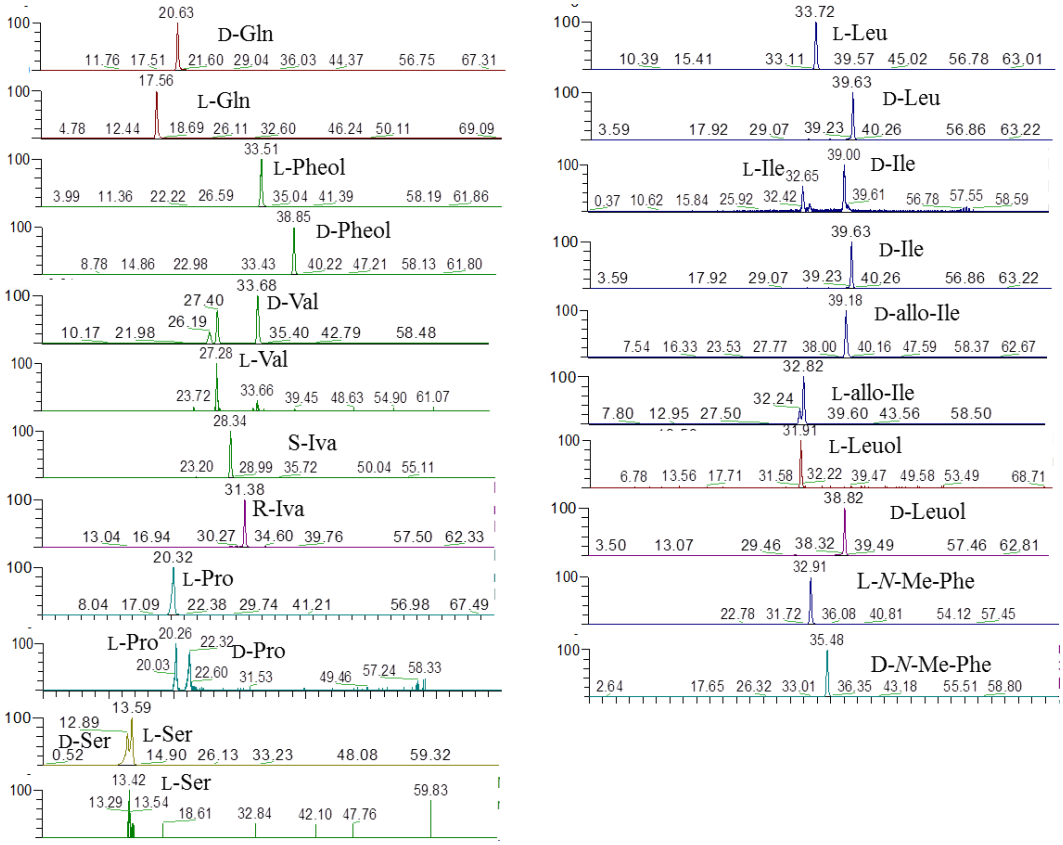

Figure A.27. Marfey's analysis of amino acid standards.

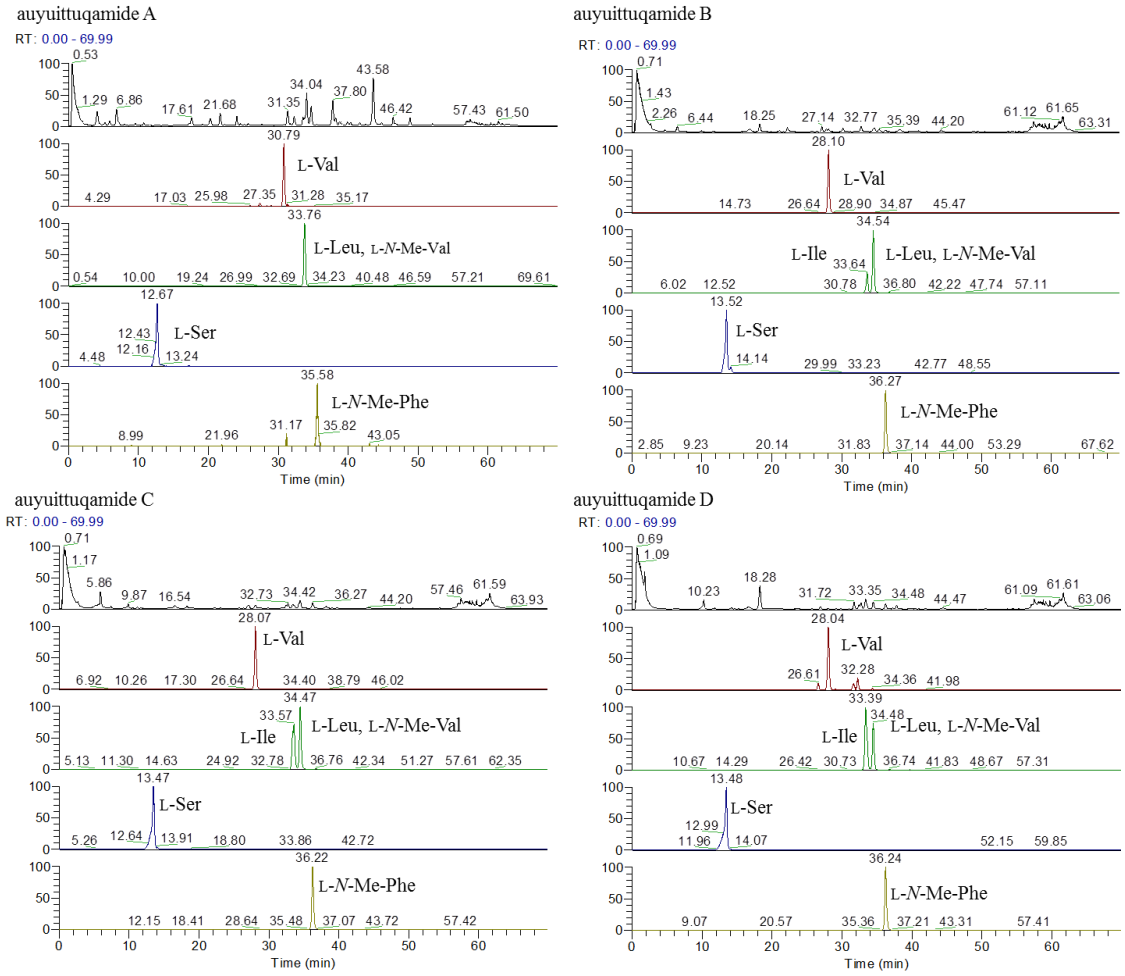

Figure A.28. Marfey's analysis of auyuittuqamide A-D.

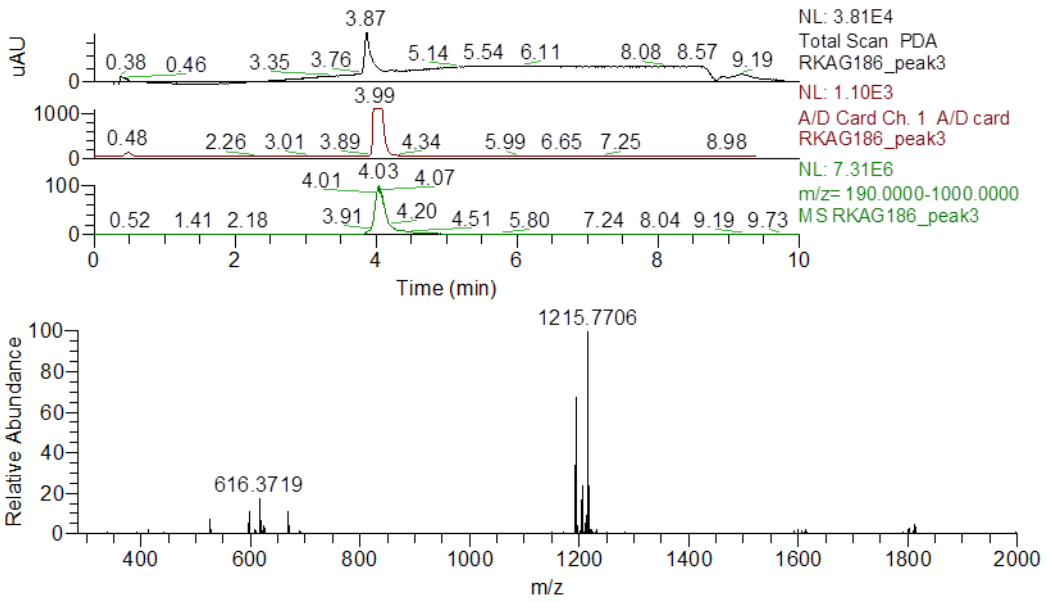

Figure A.29. +ESI HRMS of tariuqin A *m/z* 1215.7706 $[M+Na]^+$.

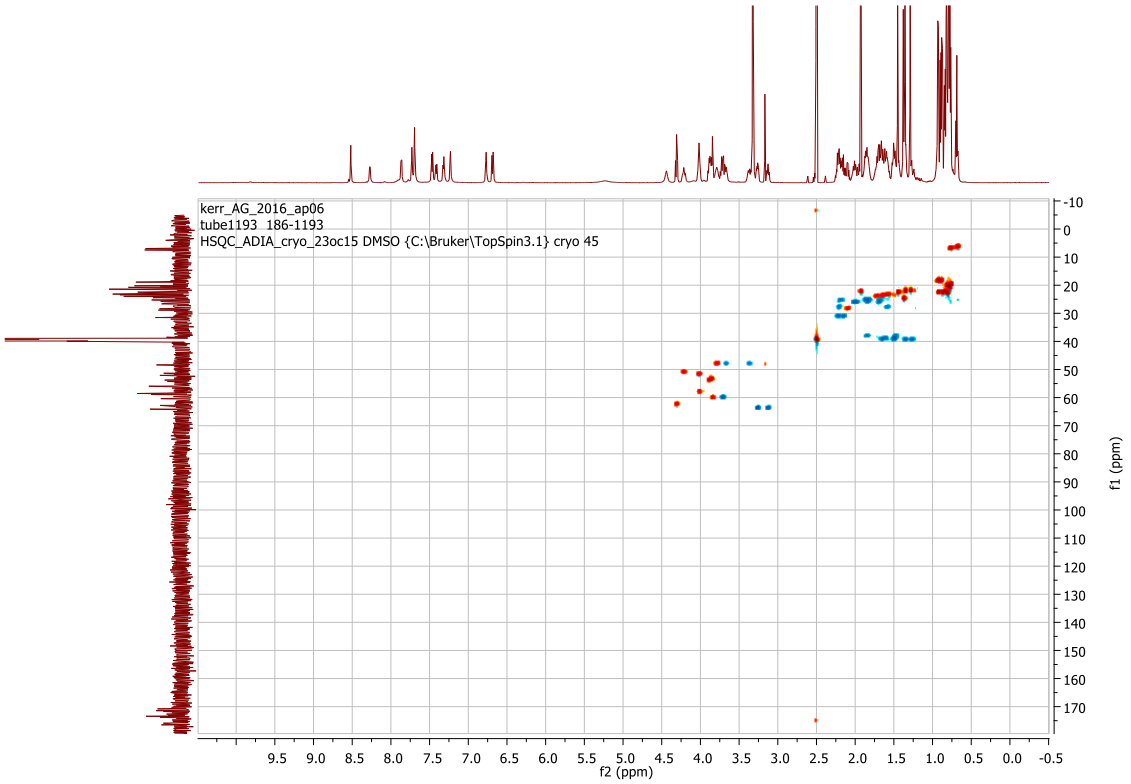

Figure A.30. HSQC spectrum of tariuqin A in DMSO-d_6.

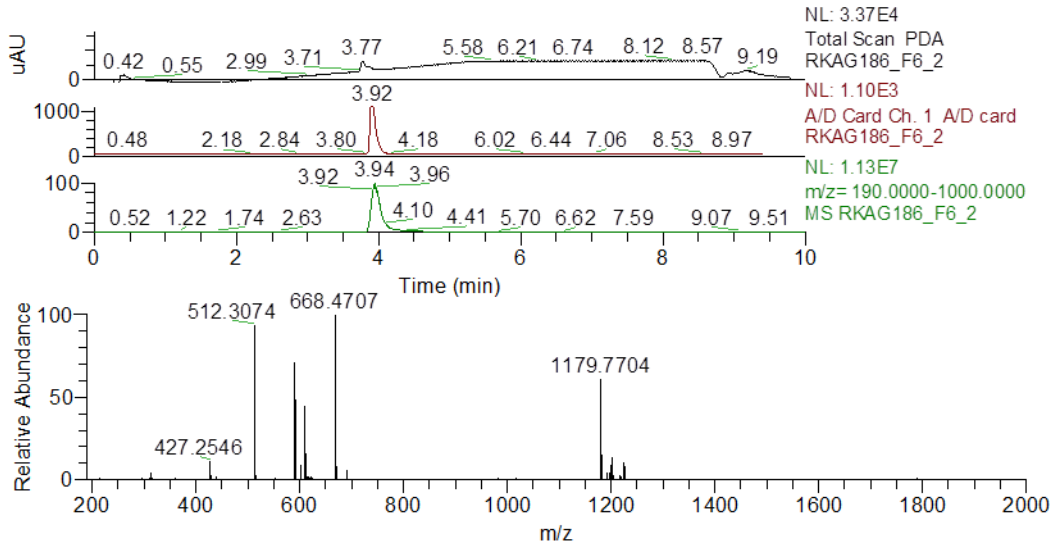

Figure A.31. +ESI HRMS of B *m/z* 1179.7704 $[M+H]^+$.

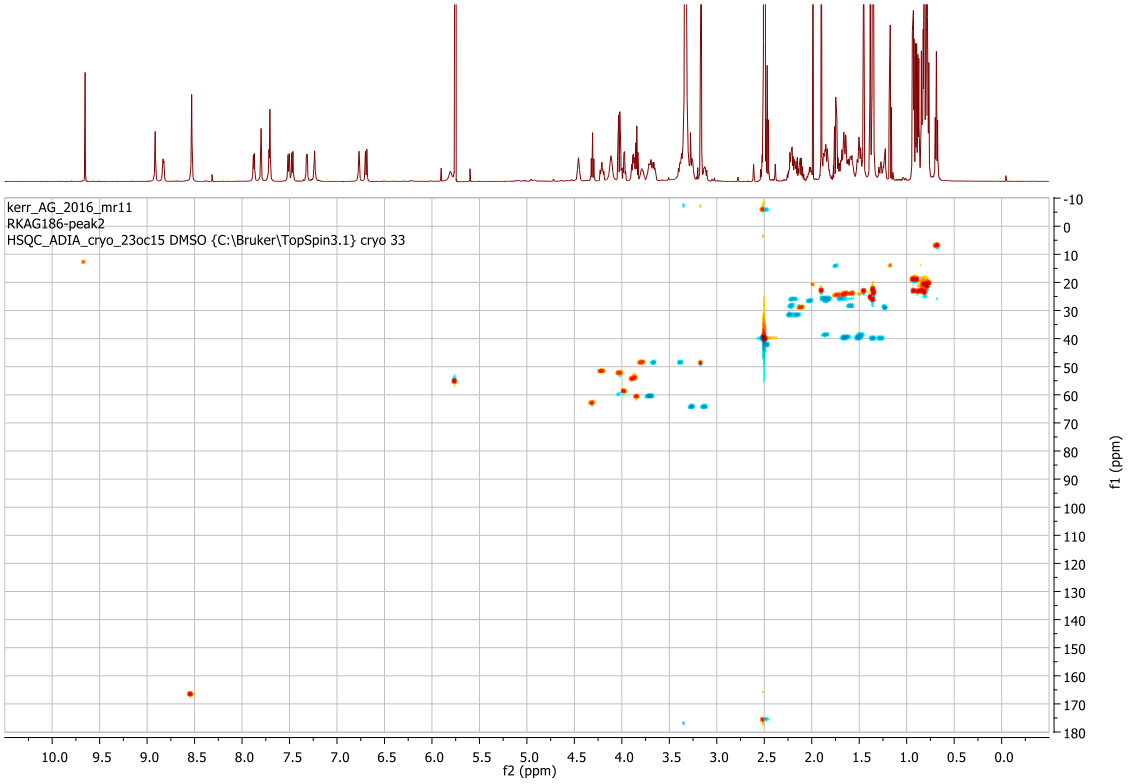

Figure A.32. HSQC spectrum of tariuqin B in DMSO-*d6*.

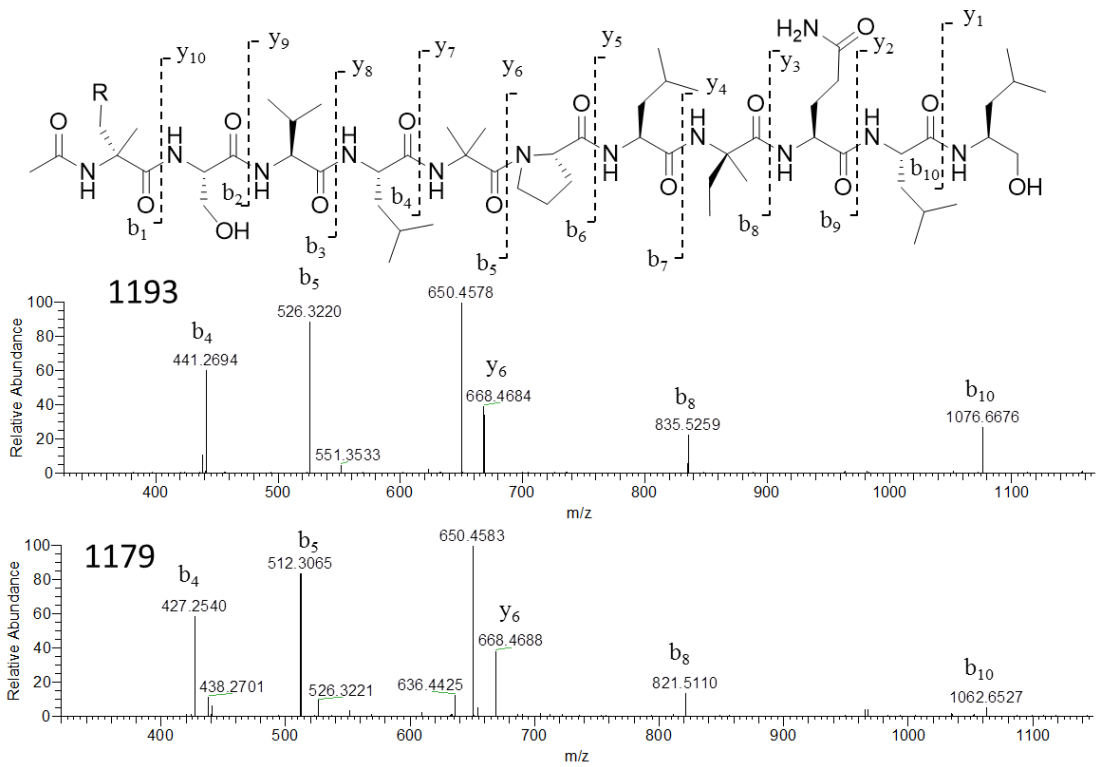

	m/z 1193.7893 $[M+H]^+$				*m/z* 1179.7704 $[M+H]^+$		
b_{10}	1076.6771	y_{10}	1052.7037	b_{10}	1062.6539	y_{10}	N.D.
b_9	963.5864	y_9	N.D.	b_9	949.5751	y_9	N.D.
b_8	835.5258	y_8	866.6064	b_8	821.5111	y_8	866.6075
b_7	736.4570	y_7	753.5139	b_7	722.4438	y_7	753.5247
b_6	627.3283	y_6	668.4685	b_6	609.3590	y_6	668.4688
b_5	526.3226	y_5	N.D.	b_5	512.3066	y_5	N.D.
b_4	441.2699	y_4	N.D.	b_4	427.2542	y_4	458.3330
b_3	328.1855	y_3	N.D.	b_3	314.1704	y_3	359.2649

Figure A.33. MS^n fragments used to determine the structure of tariuqin A and B.

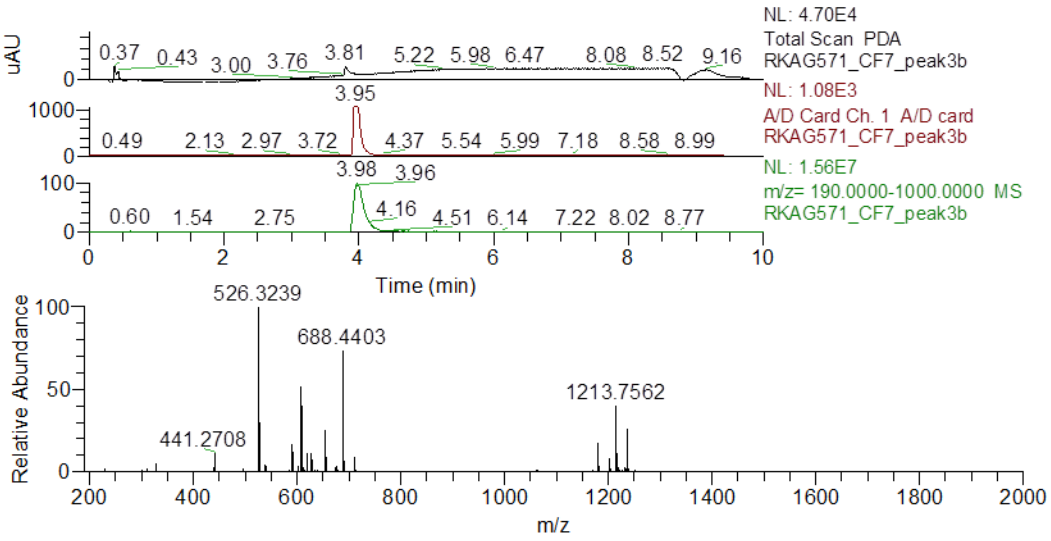

Figure A.34. +ESI HRMS of tariuqin C *m/z* 1213.7562 $[M+H]^+$.

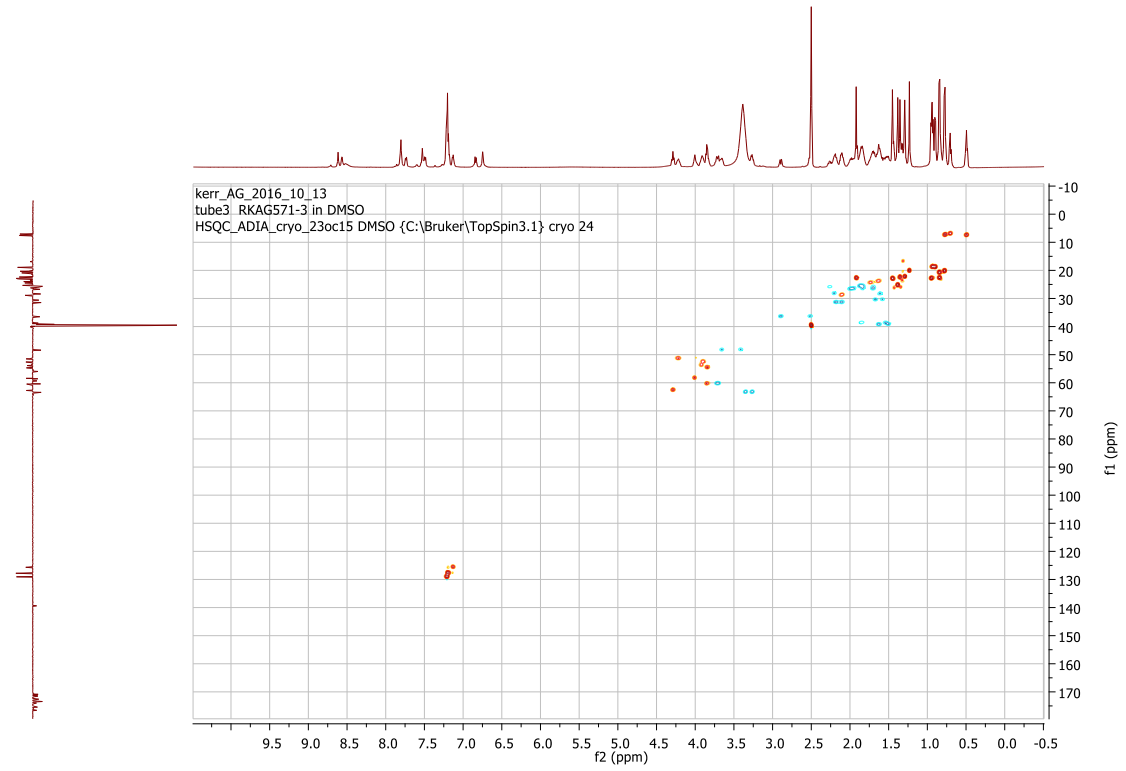

Figure A.35. HSQC of tariuqin C in DMSO-d_6.

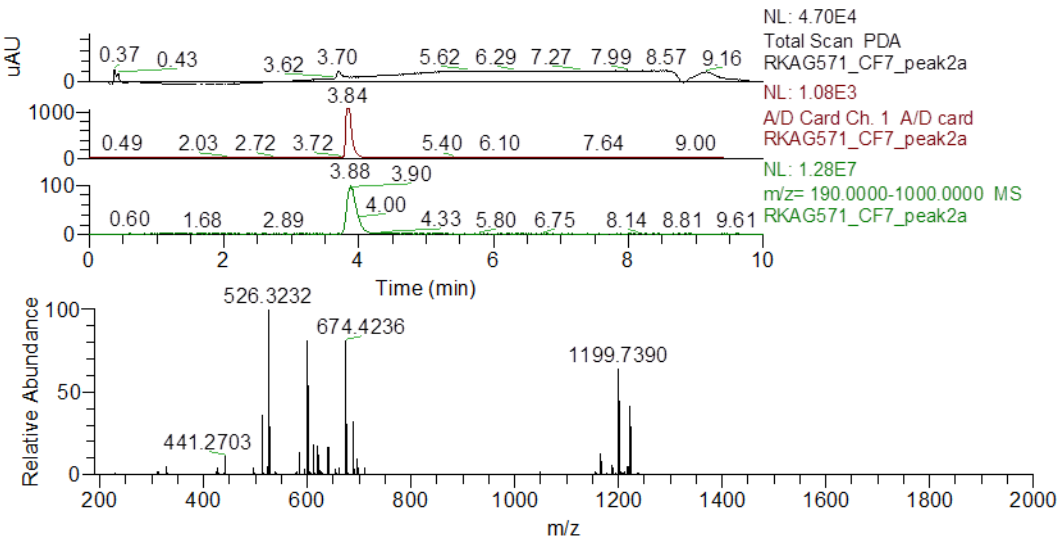

Figure A.36. +ESI HRMS of tariuqin D *m/z* 1199.7390 $[M+H]^+$.

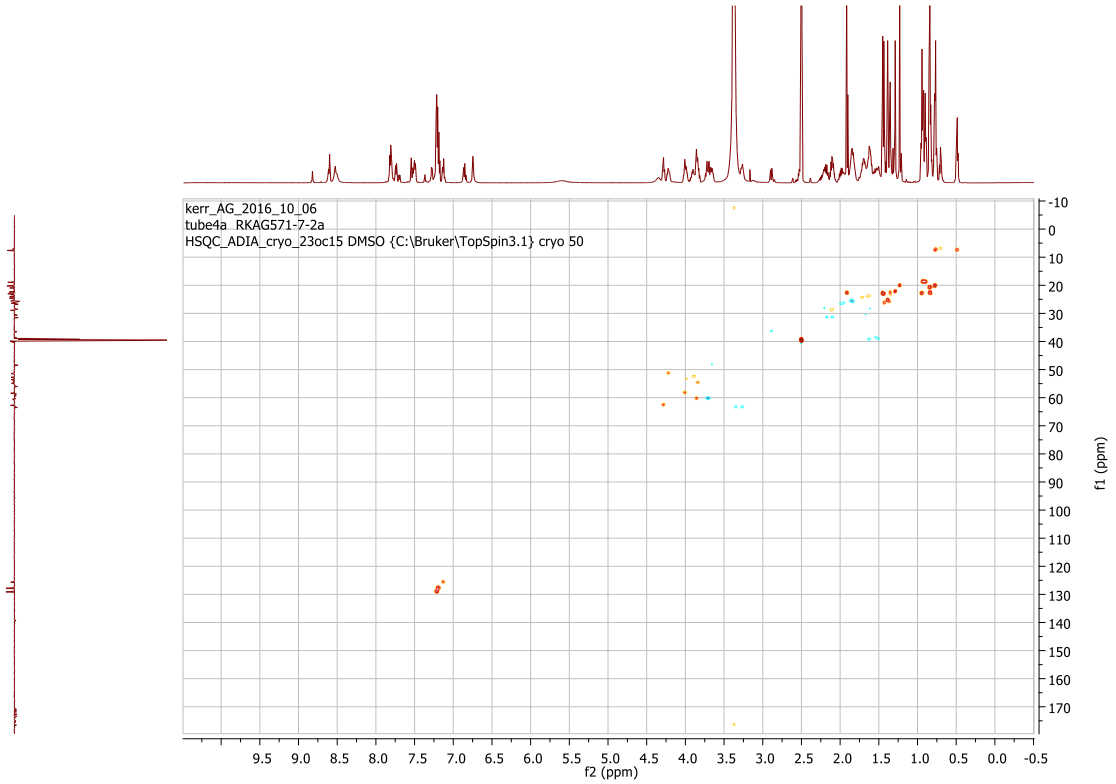

Figure A.37. HSQC spectrum of tariuqin D in DMSO-d_6.

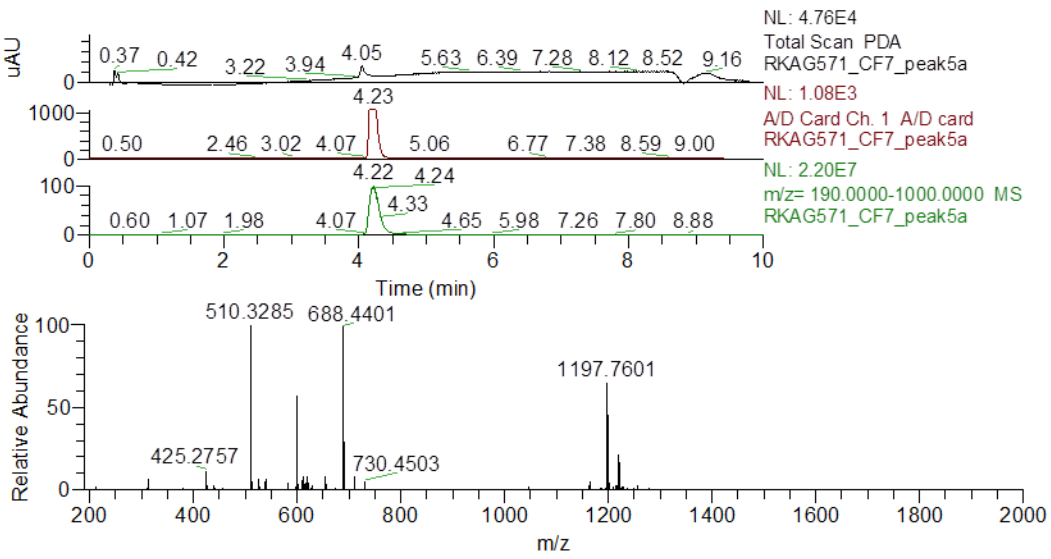

Figure A.38. +ESI HRMS of tariuqin E *m/z* 1197.7601 $[M+H]^+$.

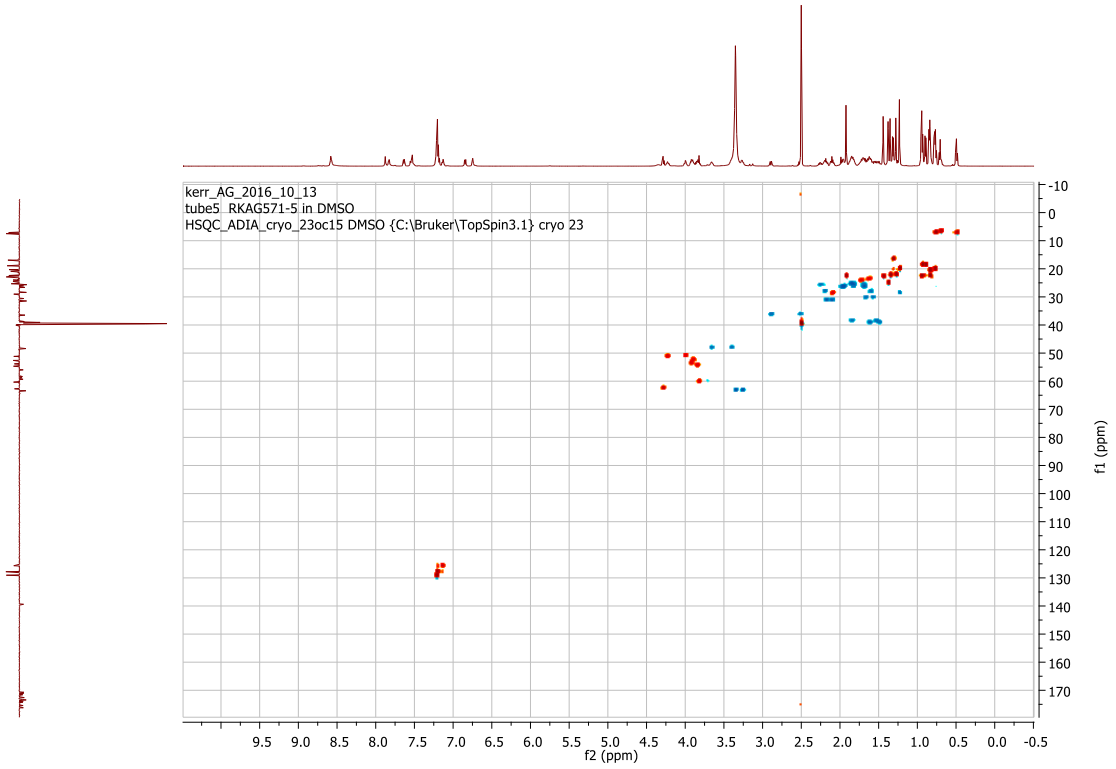

Figure A.39. HSQC spectrum of tariuqin E in DMSO-d_6.

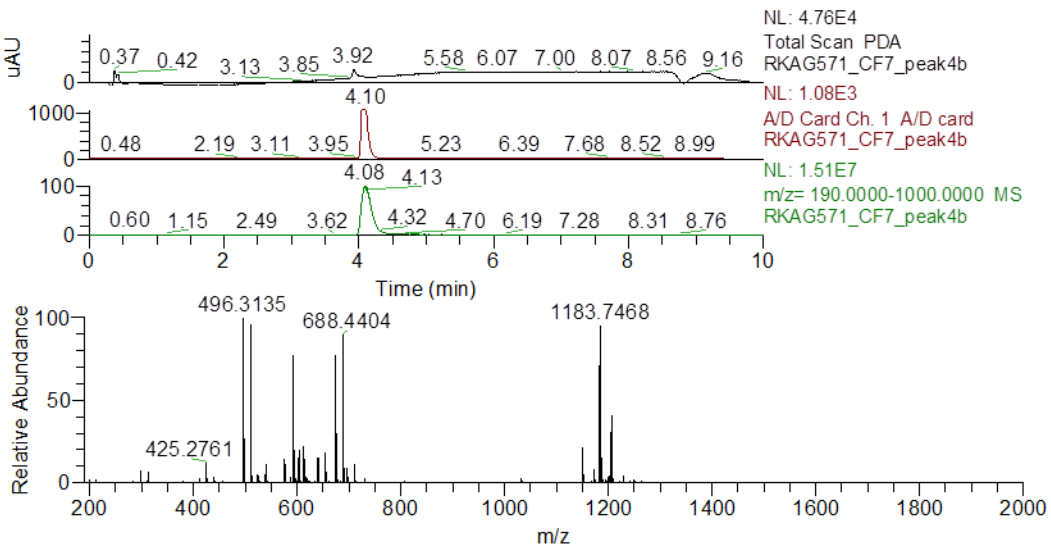

Figure A.40. +ESI HRMS of tariuqin F *m/z* 1183.7468 $[M+H]^+$.

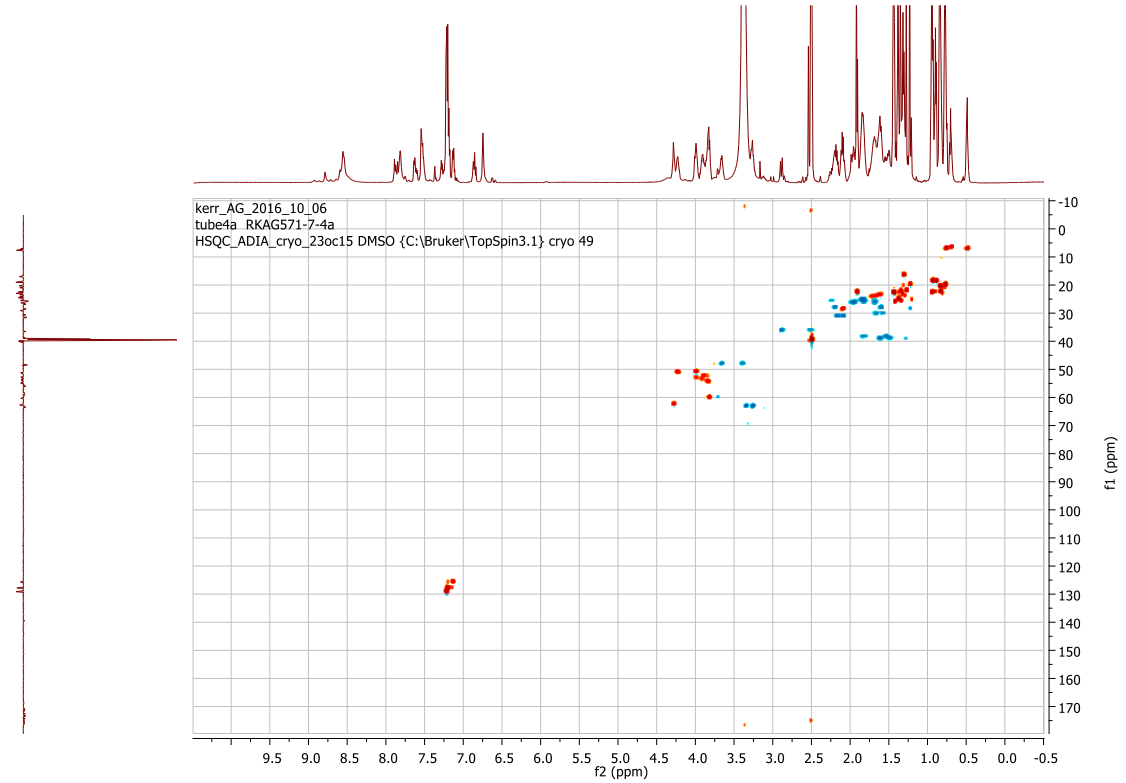

Figure A.41. HSQC spectrum of tariuqin F in DMSO-d_6.

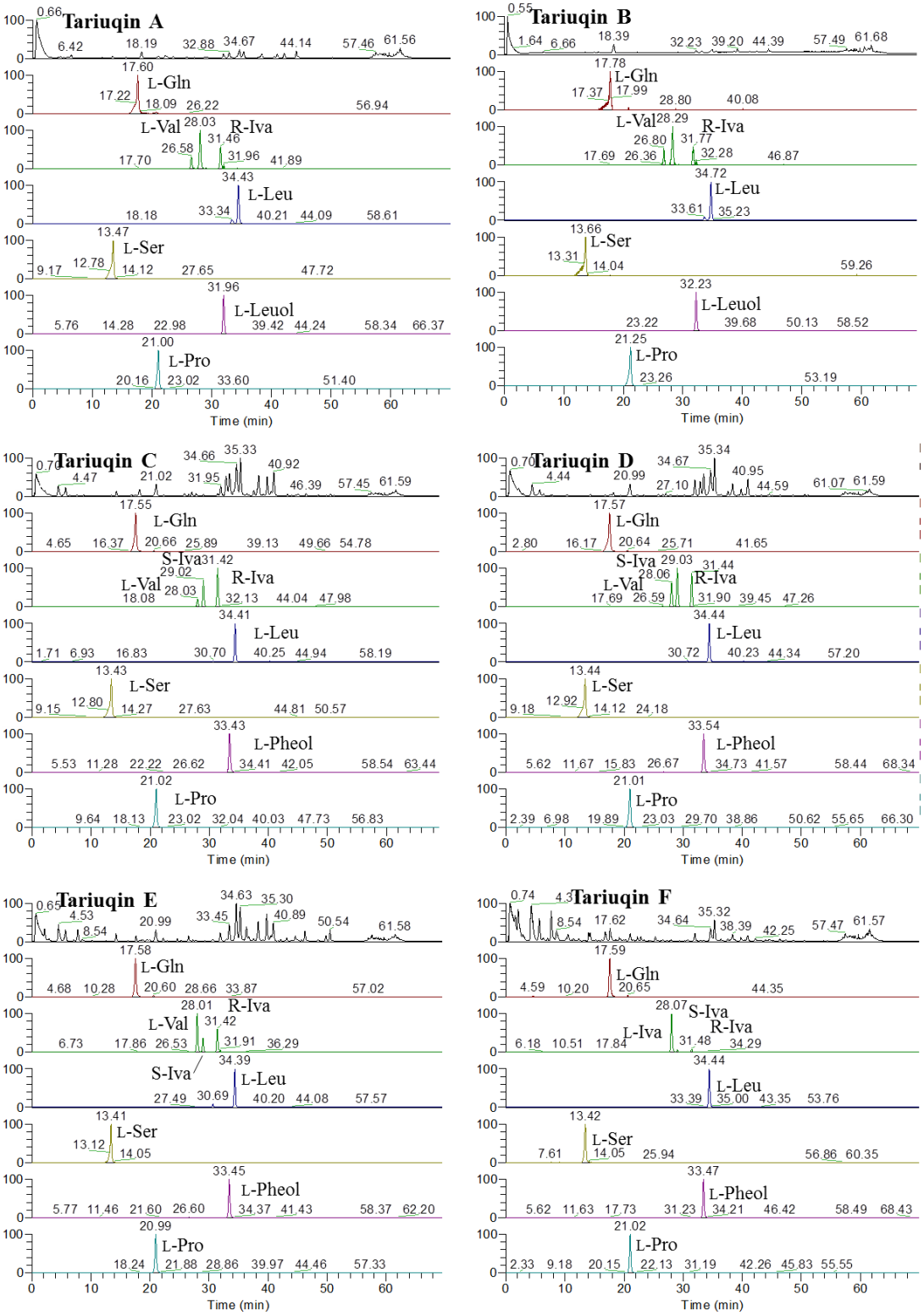

Figure A.42. Marfey's analysis of tariuqin A-F.

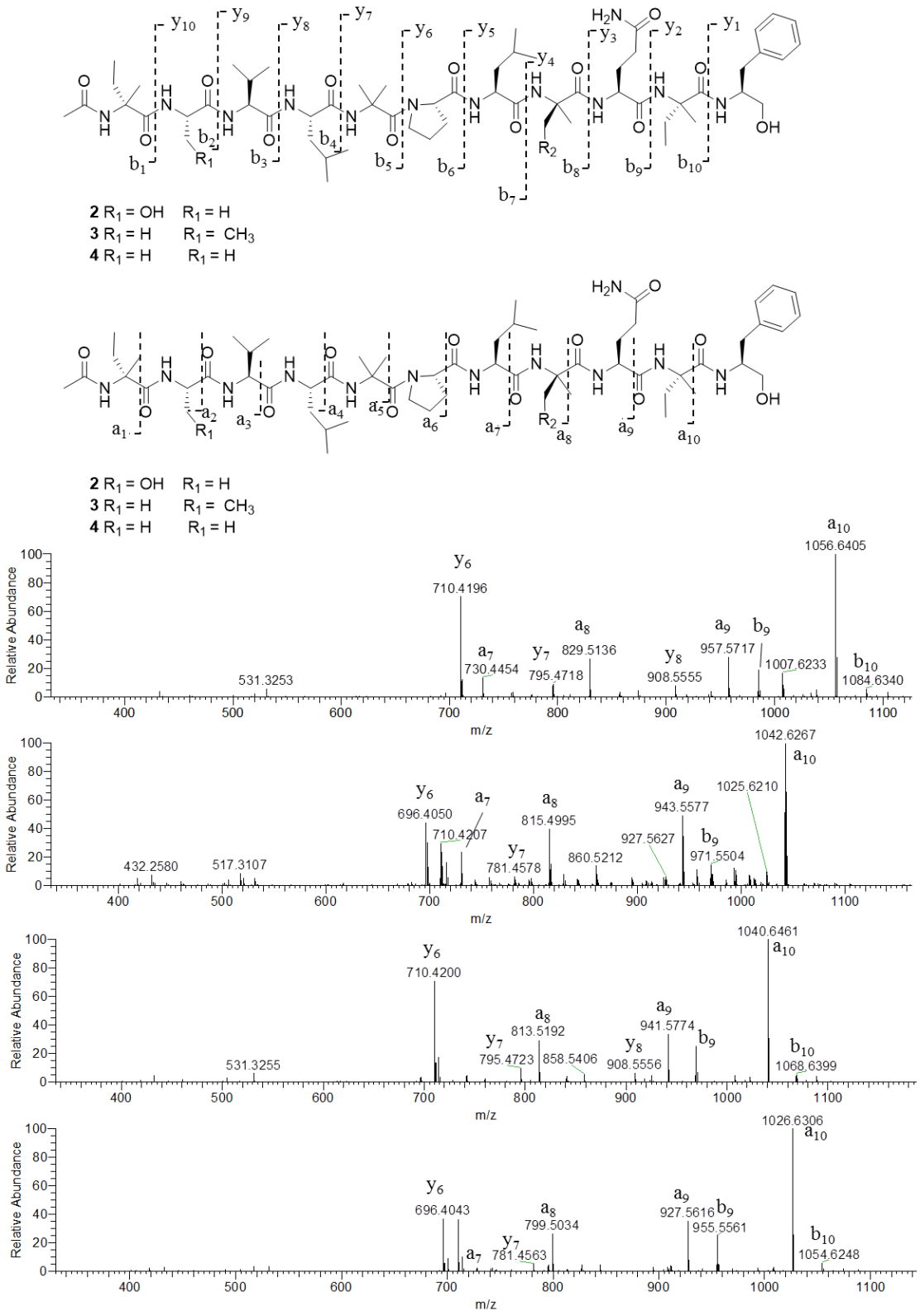

Figure A.43. MS^n fragments used for the structural determination of tariuqin C-F

Figure A.43. continued from previous page

Tariuqin C	***m/z* 1235.7350 [M+Na]$^+$**				
b_{10}	1084.6345	a_{10}	1056.6410	y_{10}	1094.6569
b_9	985.5663	a_9	957.5718	y_9	1007.6240
b_8	857.5073	a_8	829.5139	y_8	908.5555
b_7	758.4395	a_7	730.4457	y_7	795.4722
b_6	644.3727	a_6	616.3779	y_6	710.4198
b_5	548.3043	a_5	520.3096	y_5	613.3669
b_4	463.2520	a_4	432.2572	y_4	500.2833
b_3	N.D	a_3	N.D	y_3	401.2151

Tariuqin D	***m/z* 1221.7198 [M+Na]$^+$**				
b_{10}	1070.6212	a_{10}	1042.6271	y_{10}	1080.6432
b_9	971.5502	a_9	943.5579	y_9	993.6101
b_8	843.4918	a_8	815.4996	y_8	894.5424
b_7	758.4409	a_7	730.4471	y_7	781.4567
b_6	645.3626	a_6	617.3632	y_6	696.4052
b_5	548.3058	a_5	520.3106	y_5	599.3516
b_4	463.2532	a_4	435.2576	y_4	486.2687
b_3	N.D	a_3	N.D	y_3	401.2158

Tariuqin E	***m/z* 1219.7404 [M+Na]$^+$**				
b_{10}	1068.6398	a_{10}	1040.6461	y_{10}	1078.6615
b_9	969.5715	a_9	941.5774	y_9	1007.6240
b_8	841.5128	a_8	813.5192	y_8	908.5557
b_7	742.4453	a_7	714.4509	y_7	795.4724
b_6	629.3627	a_6	601.3683	y_6	710.4212
b_5	532.3096	a_5	504.3148	y_5	613.3674
b_4	447.2576	a_4	419.2620	y_4	500.2834
b_3	N.D	a_3	N.D	y_3	401.2154

Tariuqin F	***m/z* 1205.7252 [M+Na]$^+$**				
b_{10}	1054.6245	a_{10}	1026.6307	y_{10}	N.D
b_9	955.5560	a_9	927.5617	y_9	993.6083
b_8	827.4975	a_8	799.5035	y_8	894.5400
b_7	742.4453	a_7	714.4508	y_7	781.4563
b_6	629.3613	a_6	601.3660	y_6	696.4041
b_5	532.3101	a_5	504.3146	y_5	599.3511
b_4	447.2573	a_4	419.2621	y_4	486.2674
b_3	N.D	a_3	N.D	y_3	401.2149

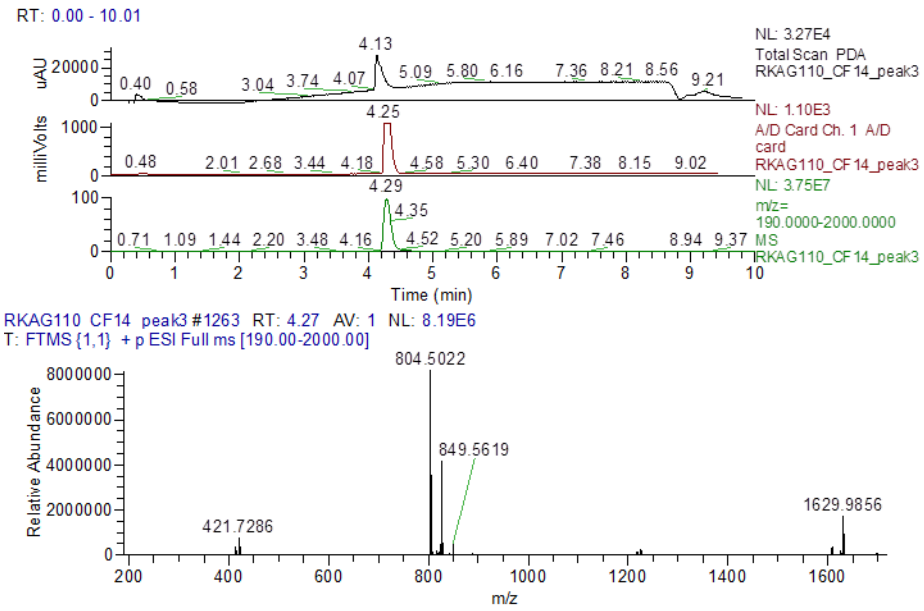

Figure A.44. +ESI HRMS of mortiamide A *m/z* 804.5022 $[M+H]^+$.

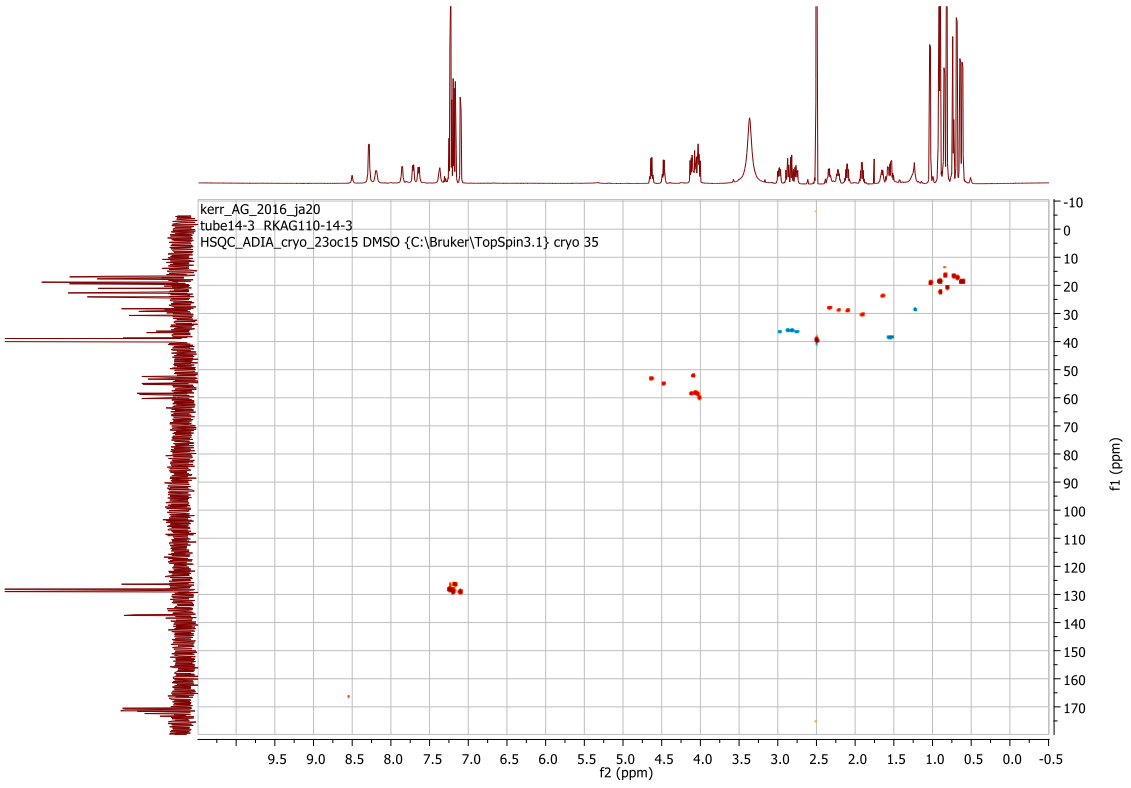

Figure A.45. HSQC spectrum of mortiamide A in DMSO-d_6.

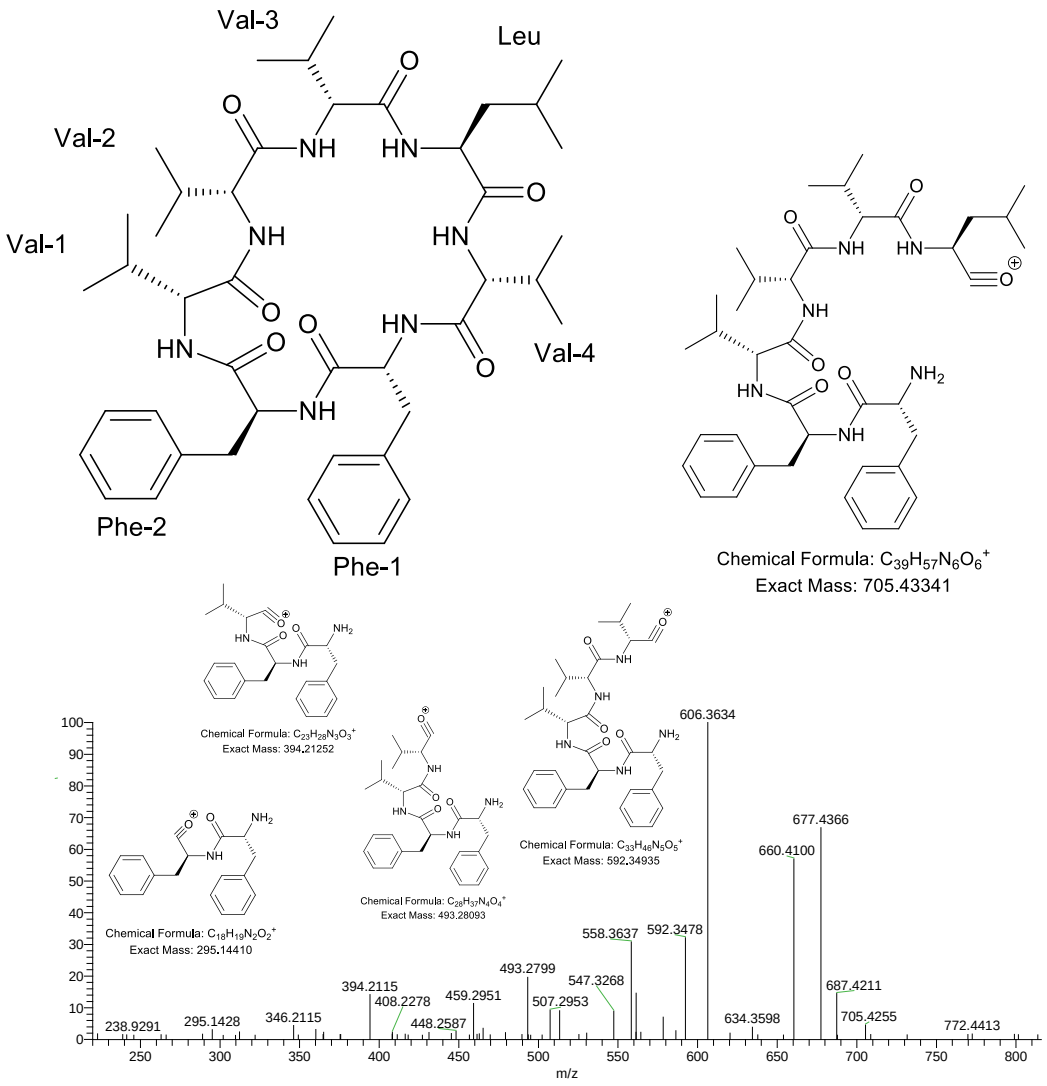

Figure A.46. MSn fragments used for the structural determination of mortiamide A.

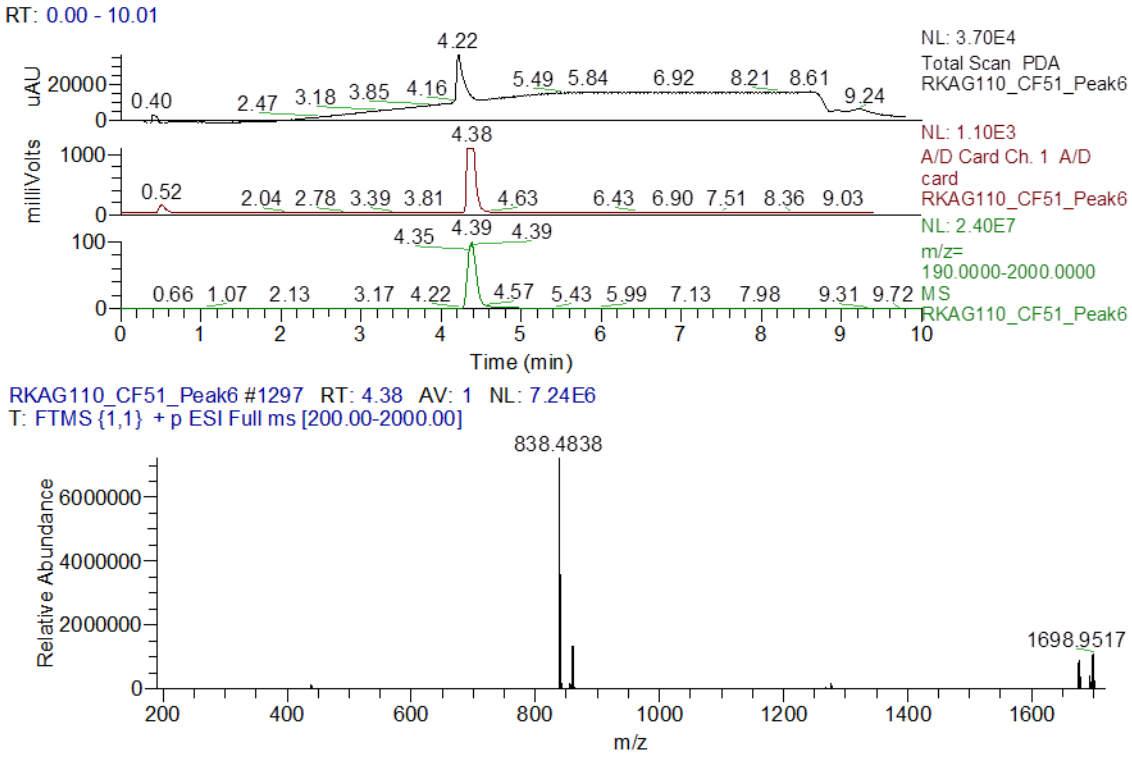

Figure A.47. +ESI HRMS of mortiamide B *m/z* 838.4838 $[M+H]^+$.

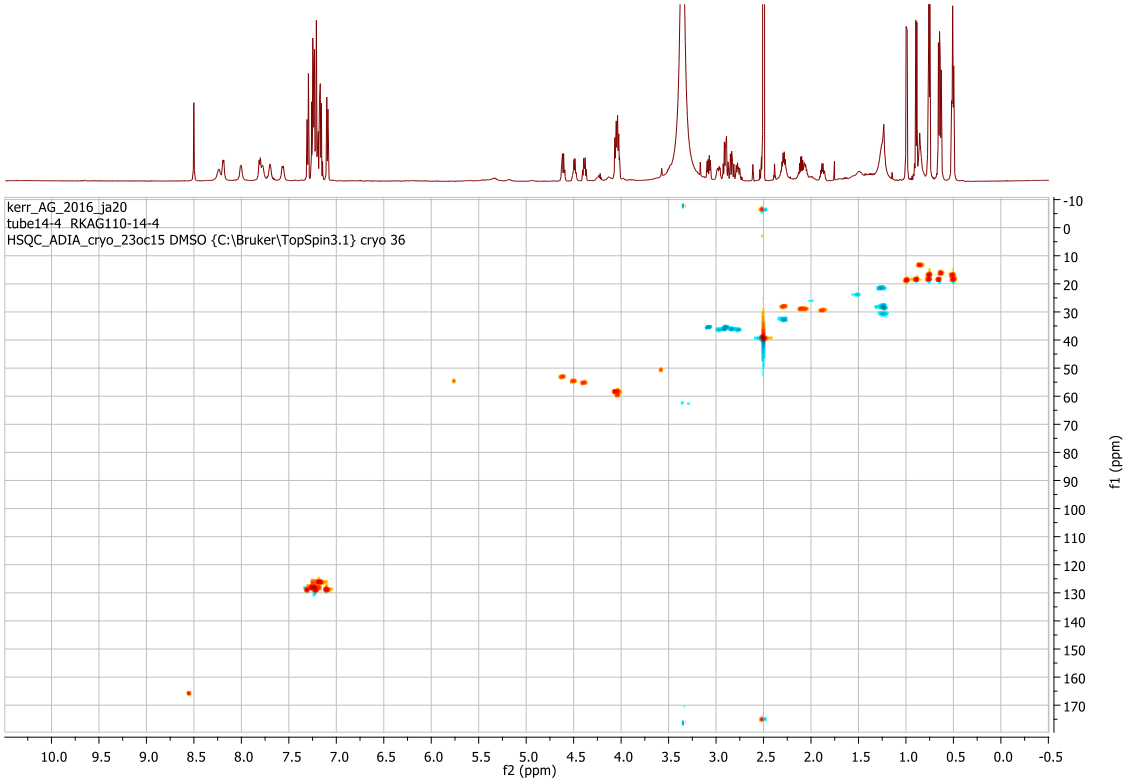

Figure A.48. HSQC spectrum of mortiamide B in DMSO-d_6.

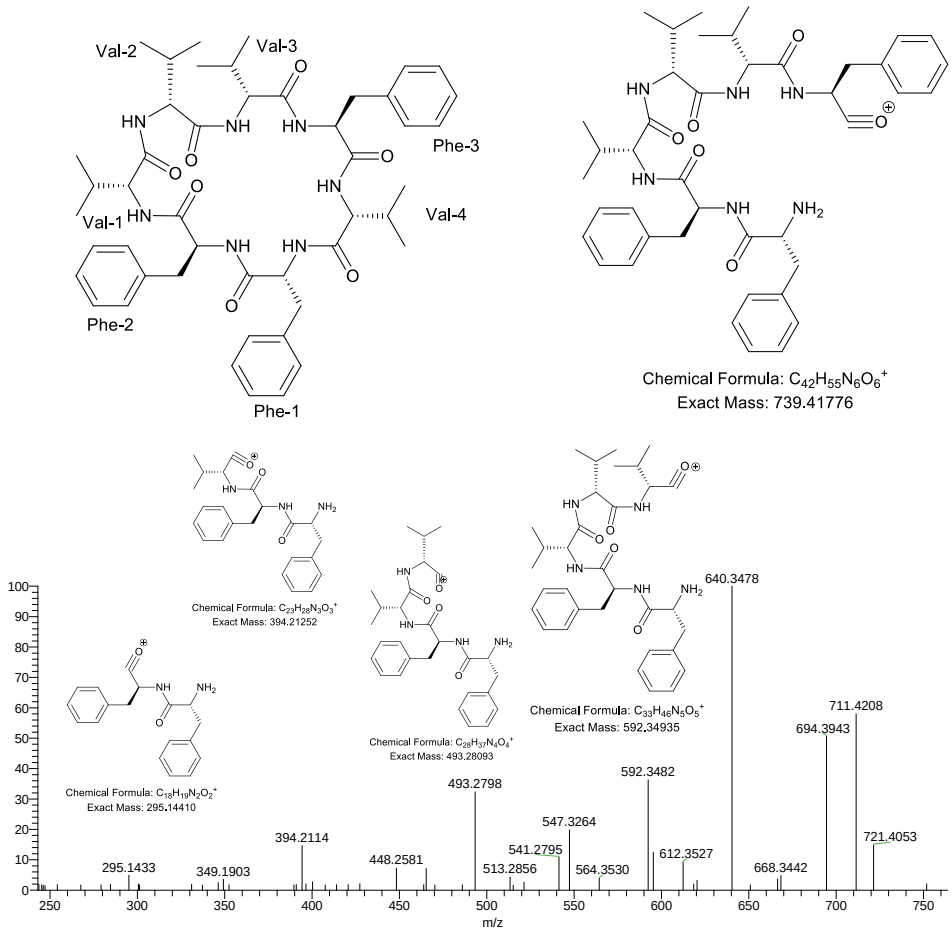

Figure A.49. MSn fragments used for the structural determination of mortiamide B.

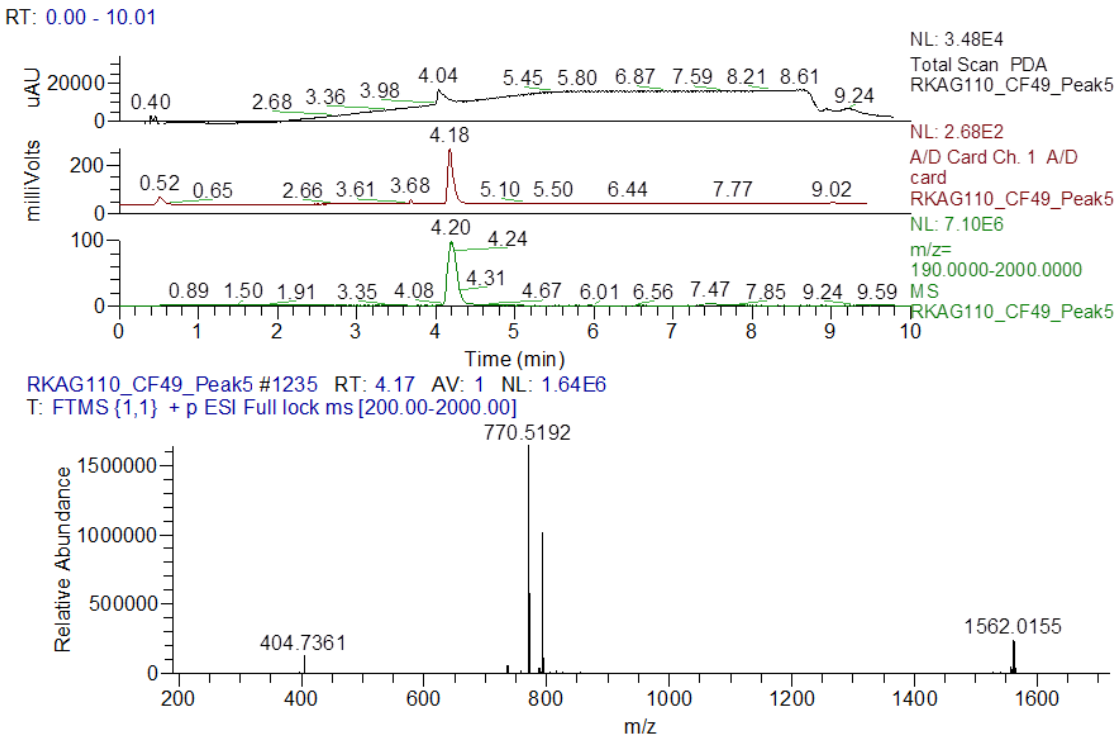

Figure A.50. +ESI HRMS of mortiamide C *m/z* 770.5192 $[M+H]^+$.

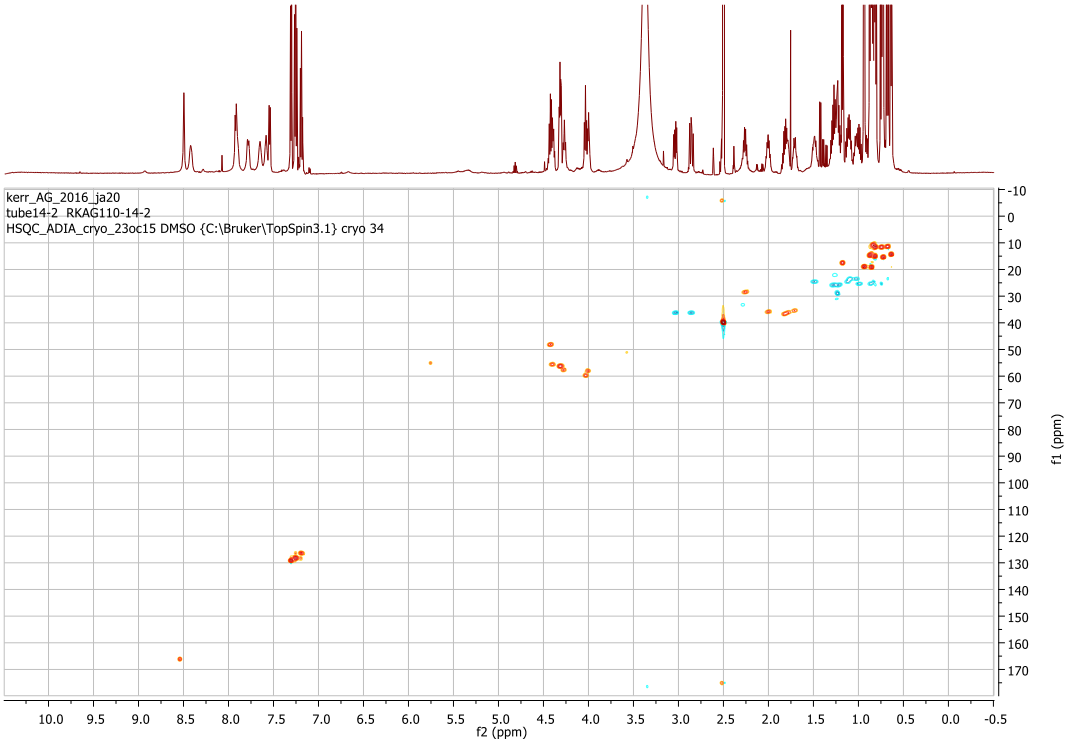

Figure A.51. HSQC spectrum of mortiamide C in DMSO-d_6.

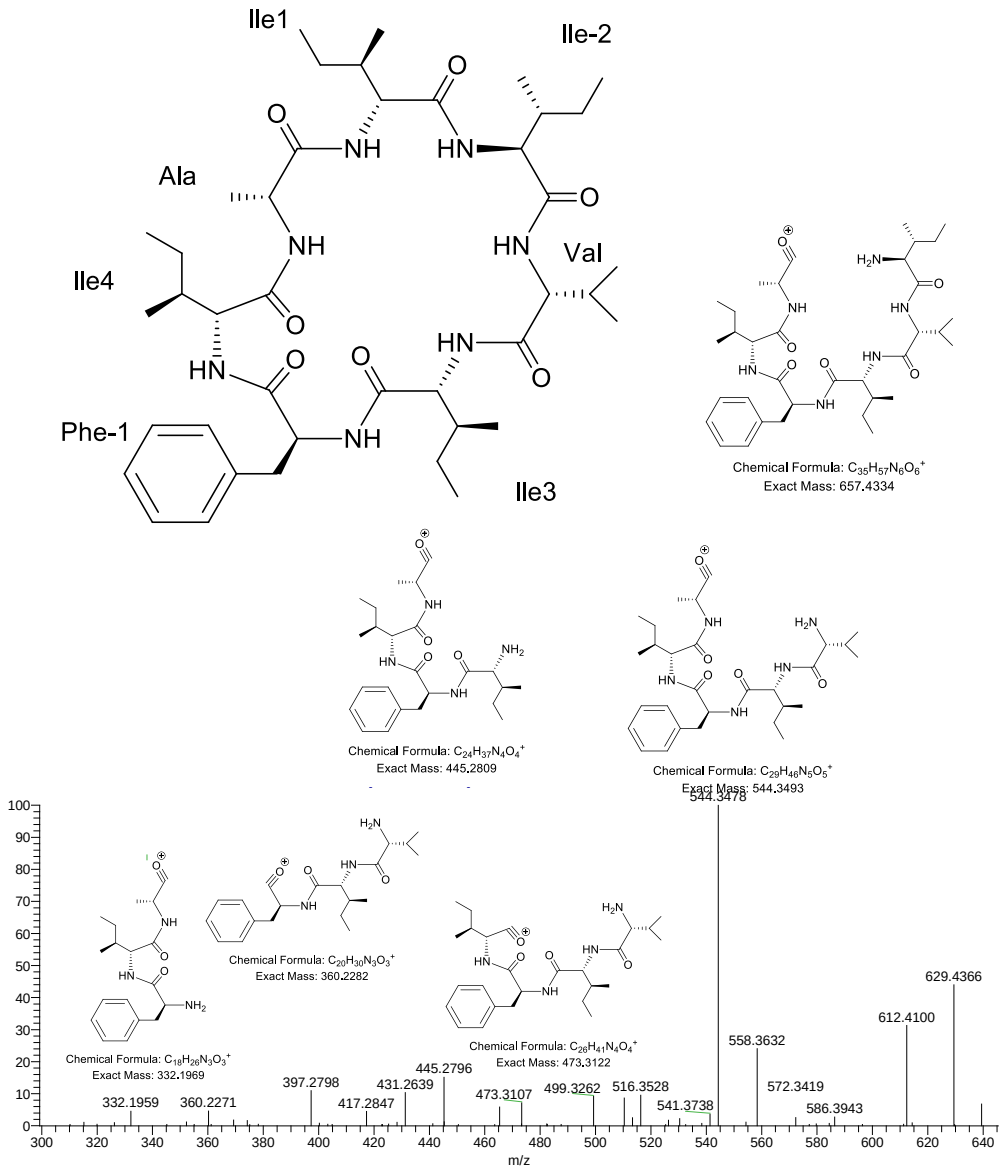

Figure A.52. MS^n fragments used for the structural determination of mortiamide C.

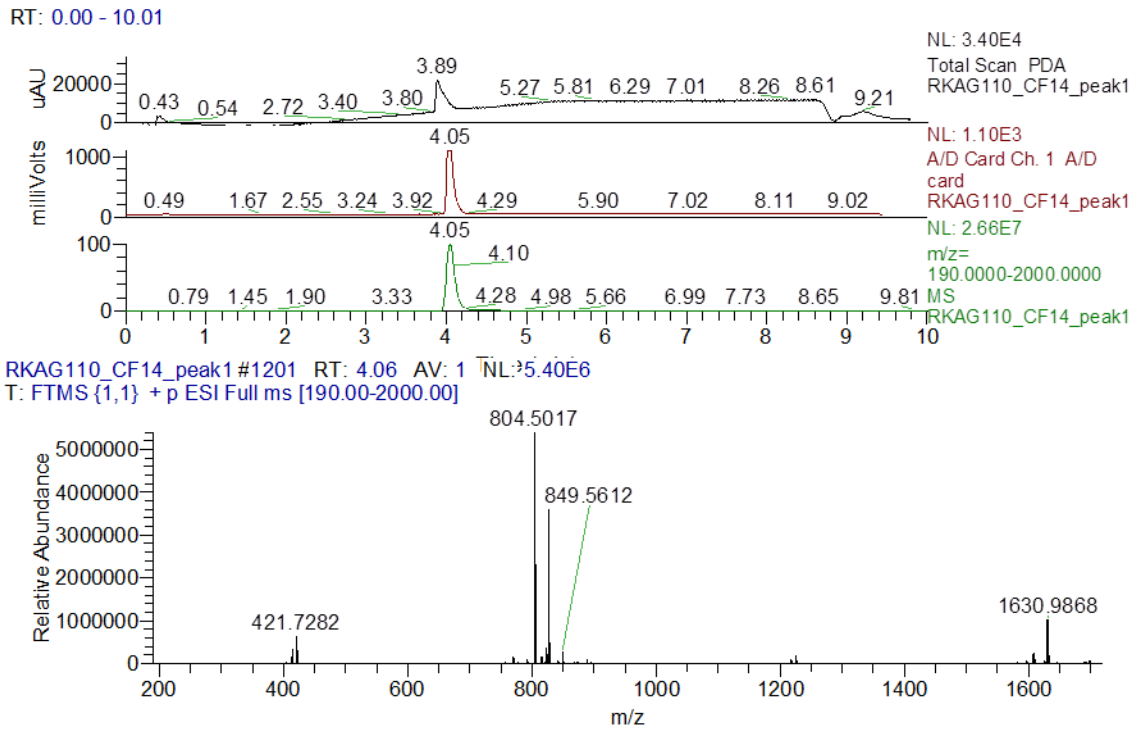

Figure A.53. +ESI HRMS of mortiamide D *m/z* 804.5017 $[M+H]^+$.

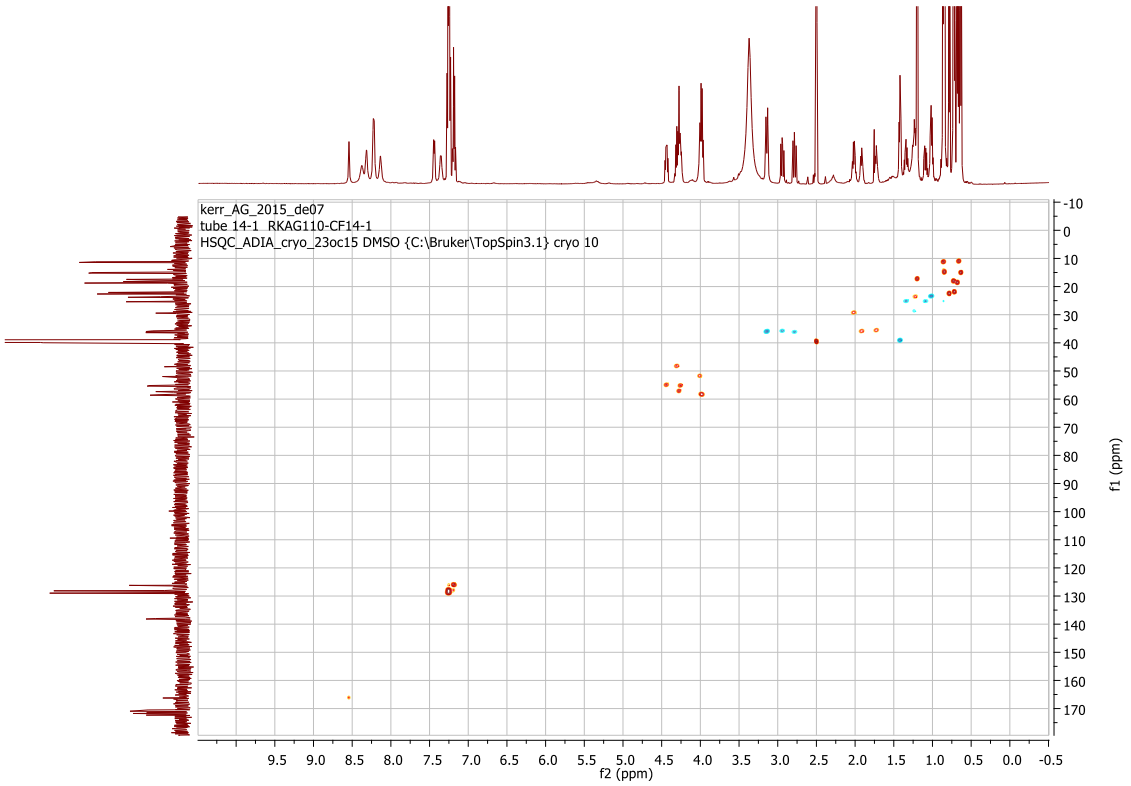

Figure A.54. HSQC spectrum of mortiamide D in DMSO-d_6.

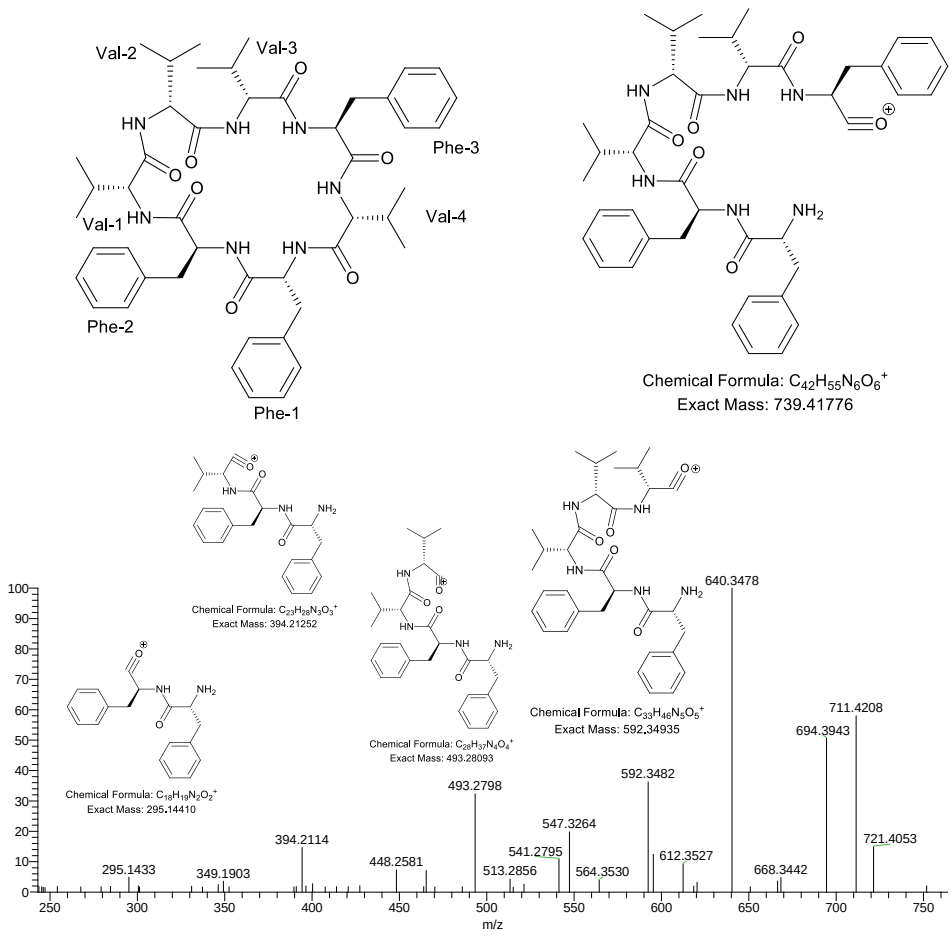

Figure A.55. MS^n fragments used for the structural determination of mortiamide D.

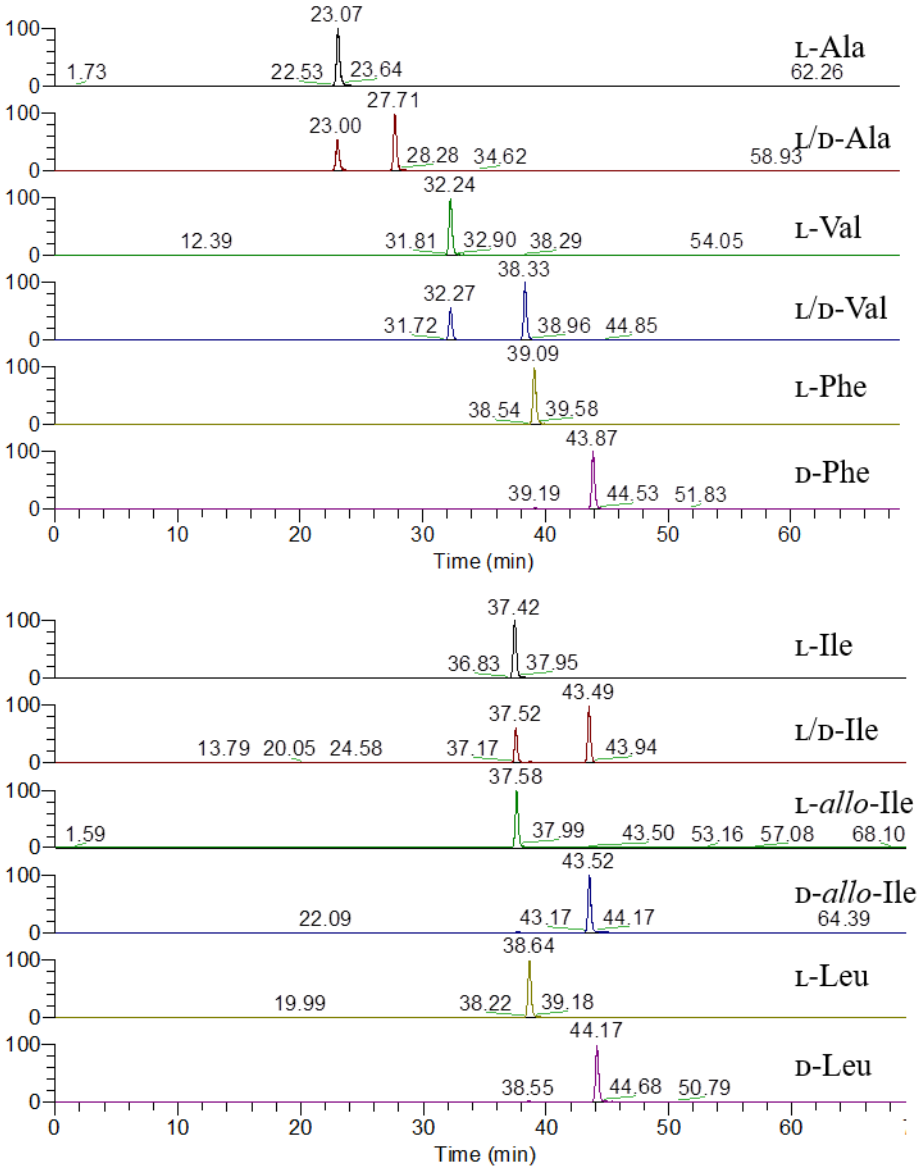

Figure A.56. Marfey's analysis of amino acid standards.

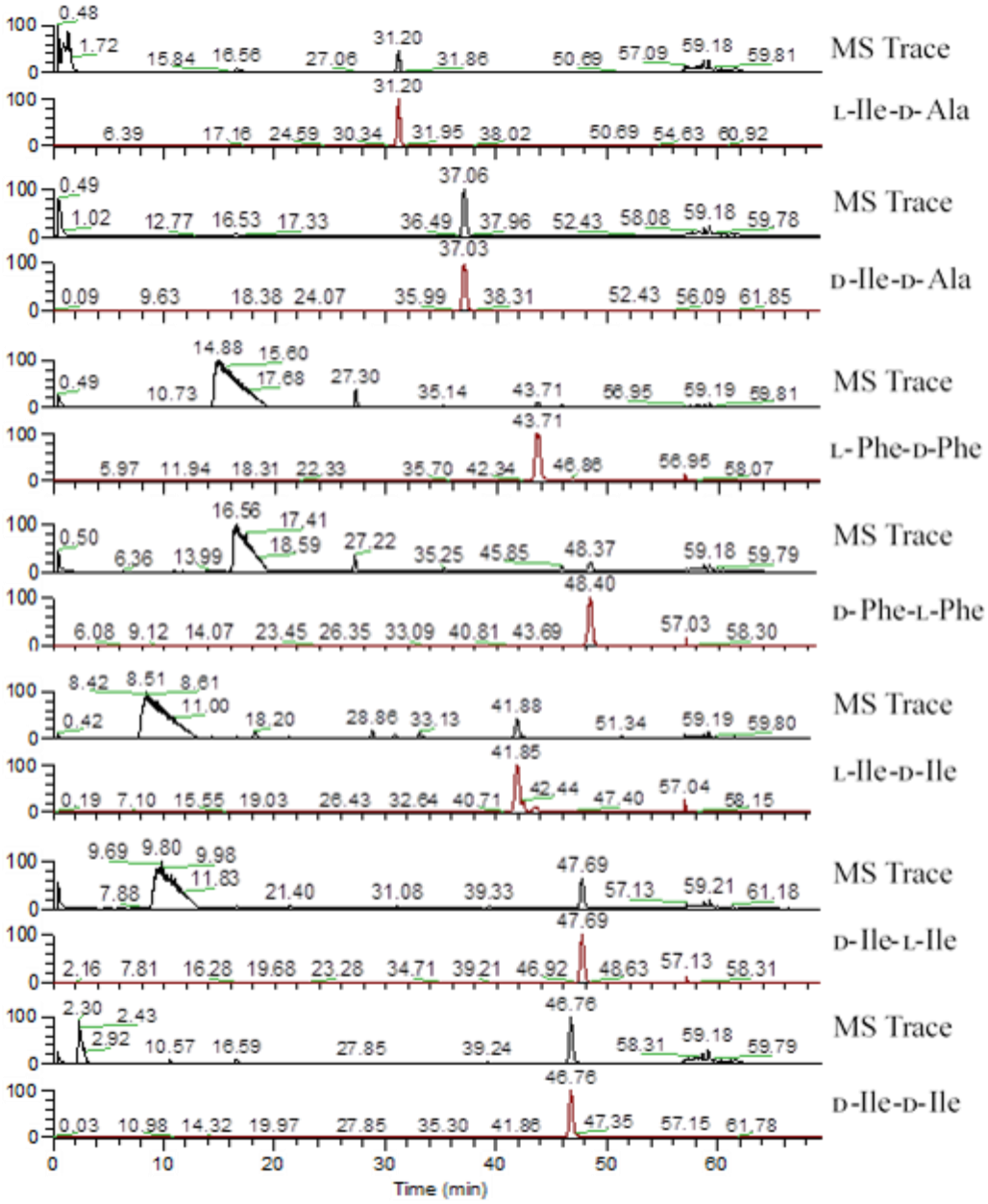

Figure A.57. Marfey's analysis of dipeptide standards.

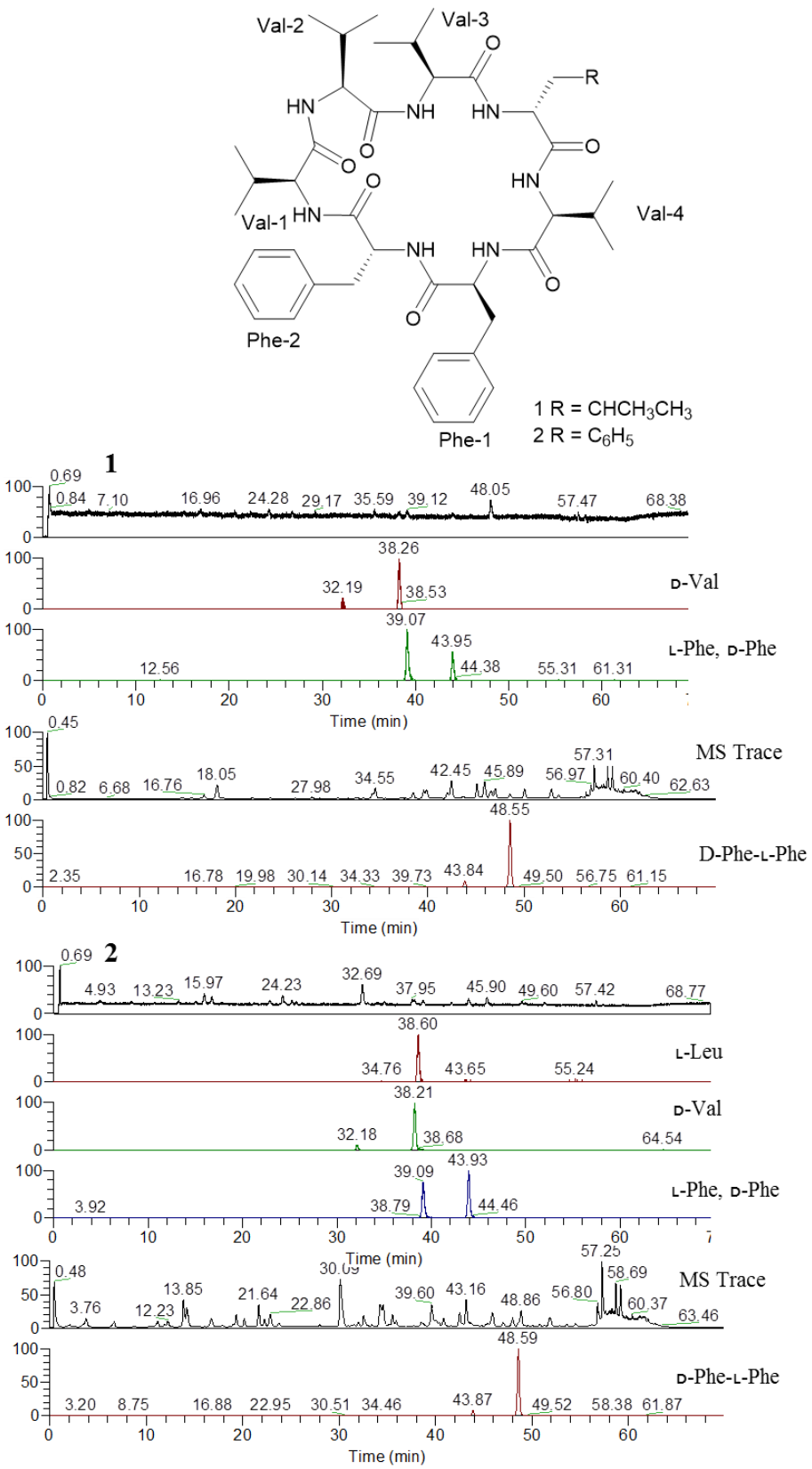

Figure A.58. Marfey's analysis of mortiamide A and B.

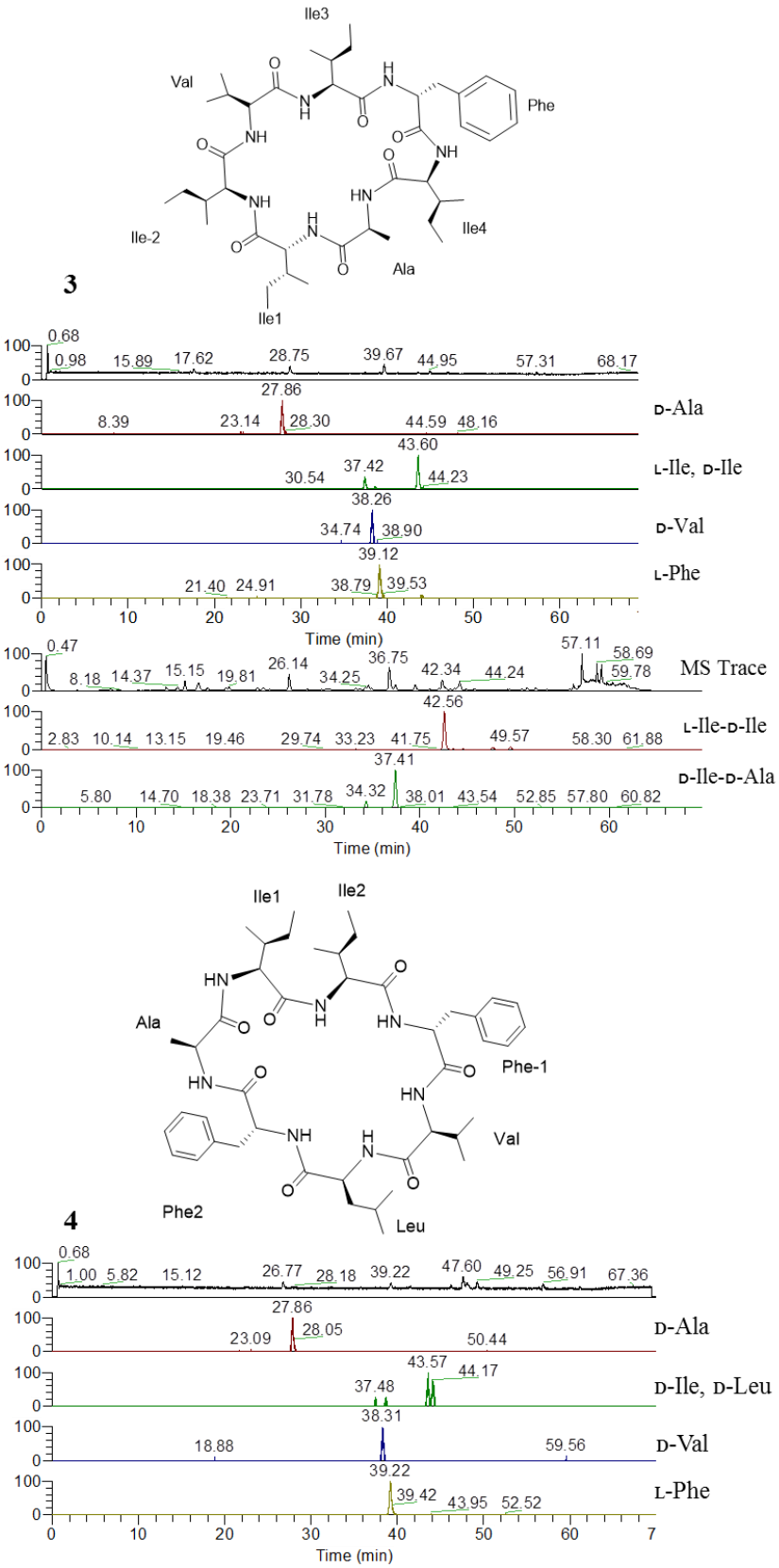

Figure A.59. Marfey's analysis of mortiamide C and D.

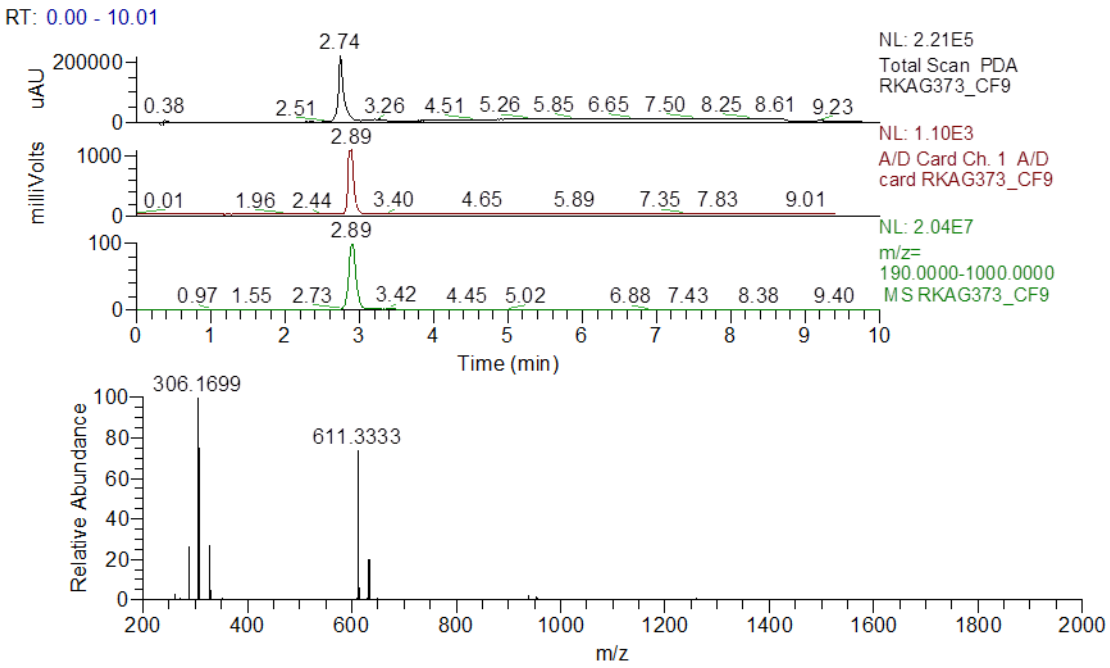

Figure A.60. +ESI HRMS of iqalisetin A *m/z* 306.1699 $[M+H]^+$.

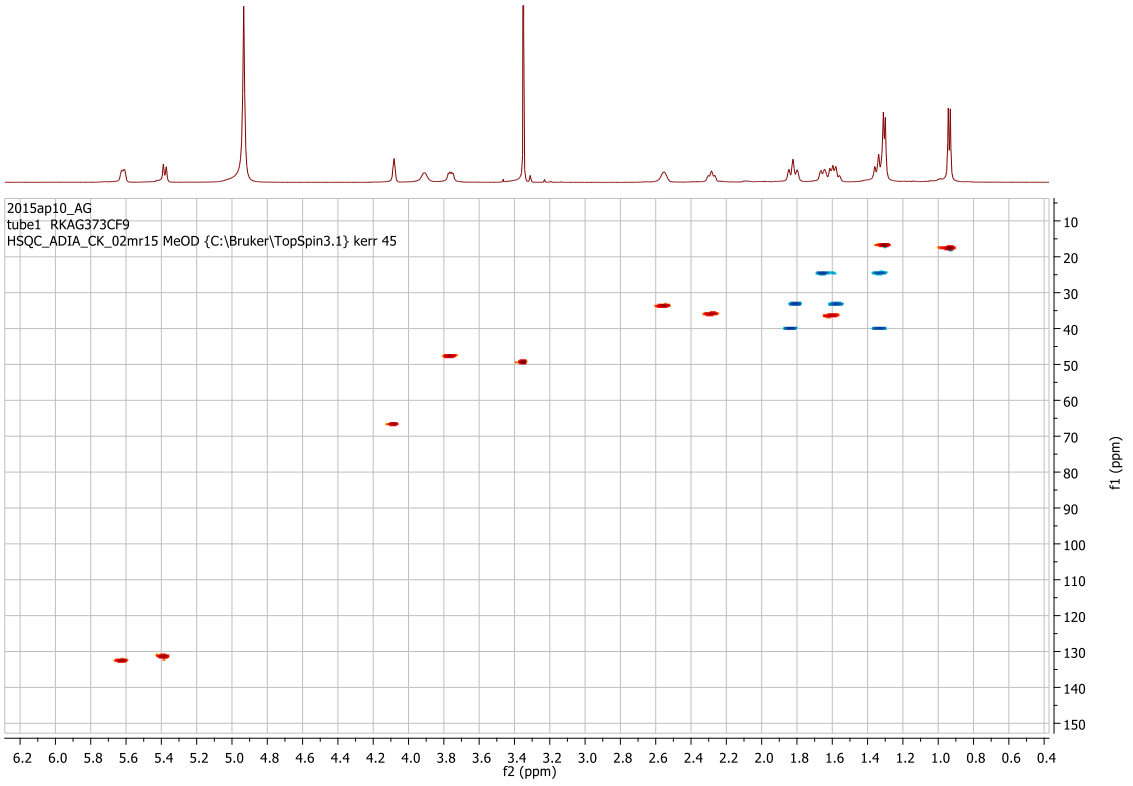

Figure A.61. HSQC spectrum of iqalisetin A in CD_3OD.

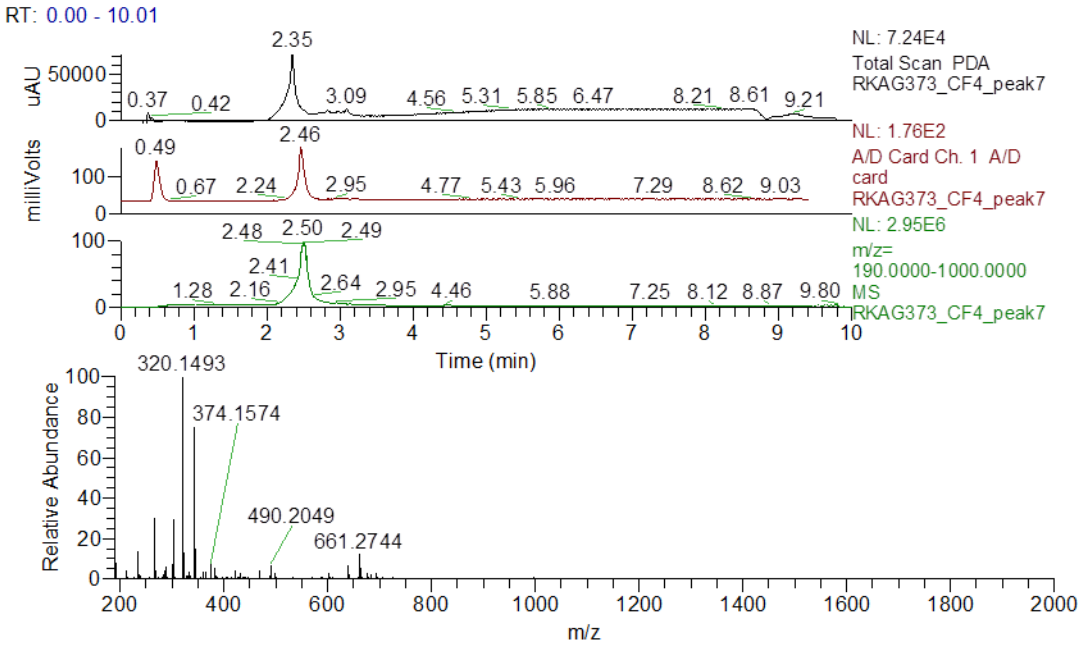

Figure A.62. +ESI HRMS of iqalisetin B *m/z* 320.1493 $[M+H]^+$.

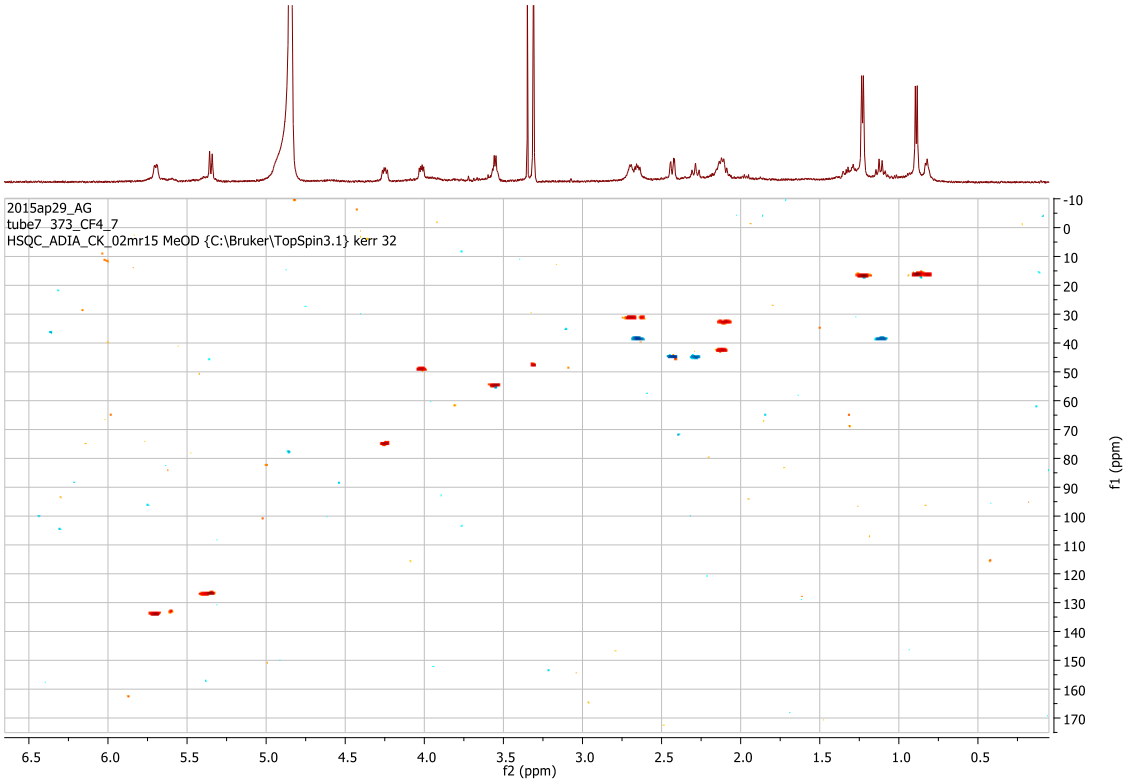

Figure A.63. HSQC spectrum of iqalisetin B in CD_3OD.

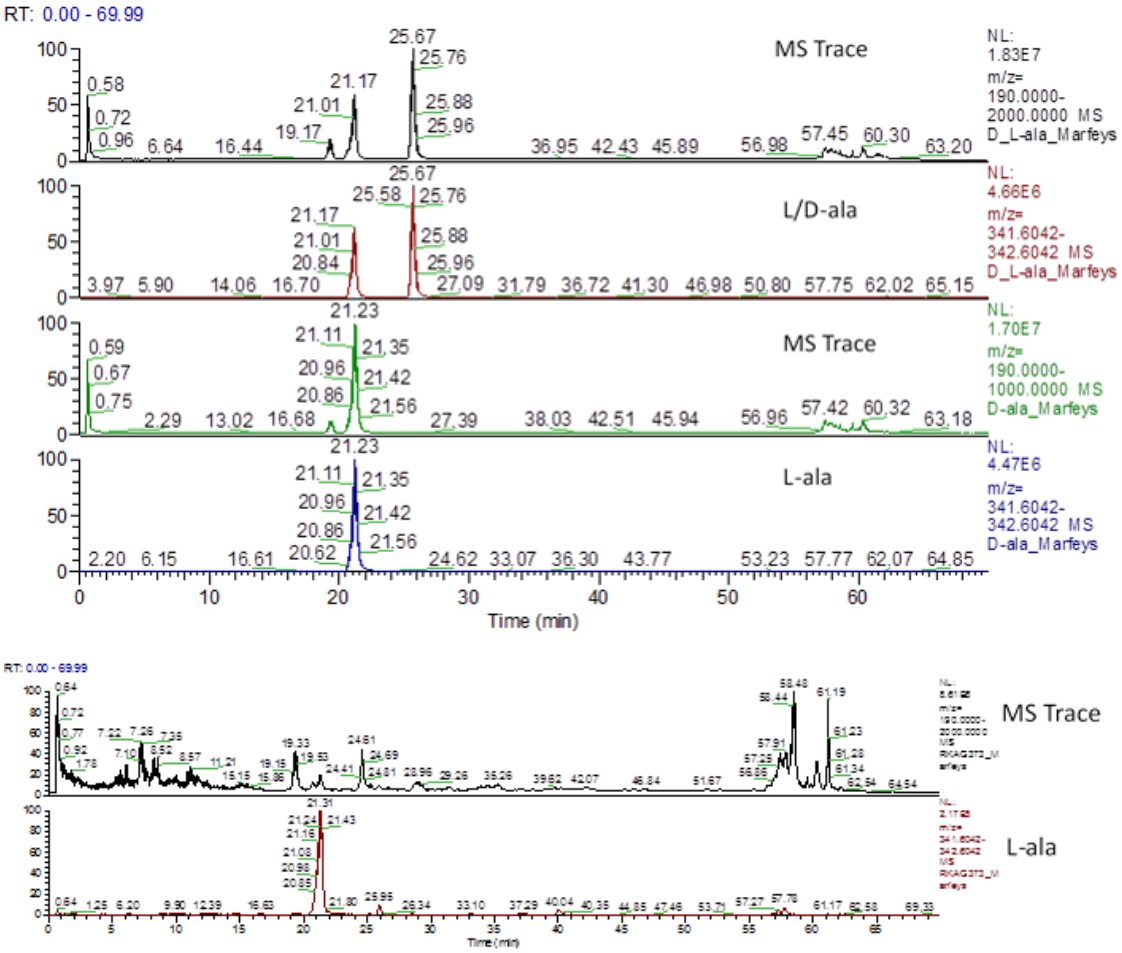

Figure A.64. Marfey's analysis of iqalisetin A.

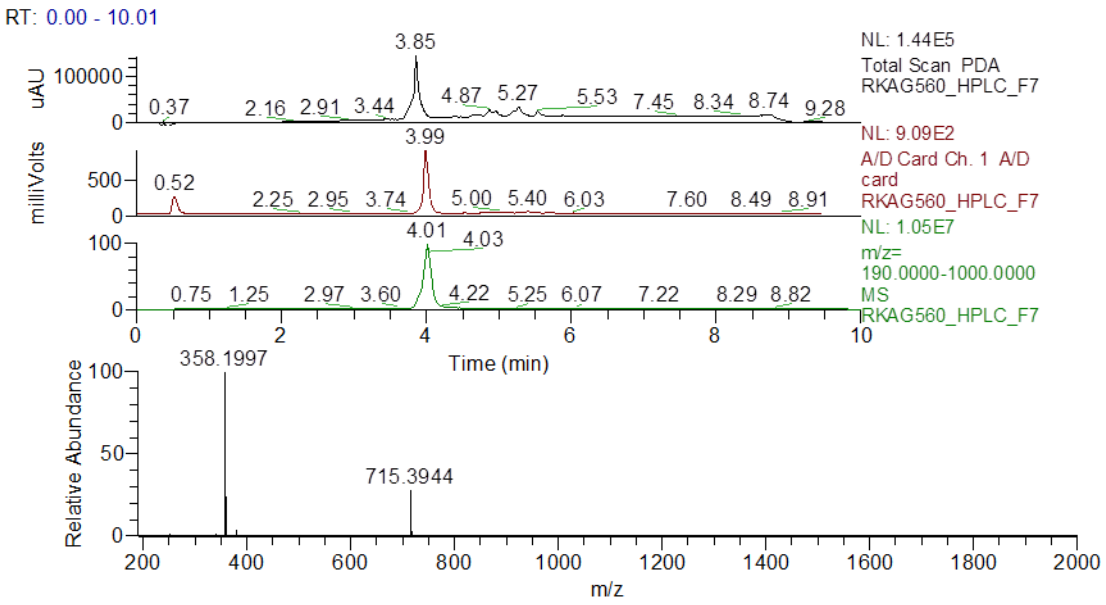

Figure A.65. +ESI HRMS of tolypoalbin *m/z* 358.1997 $[M+H]^+$.

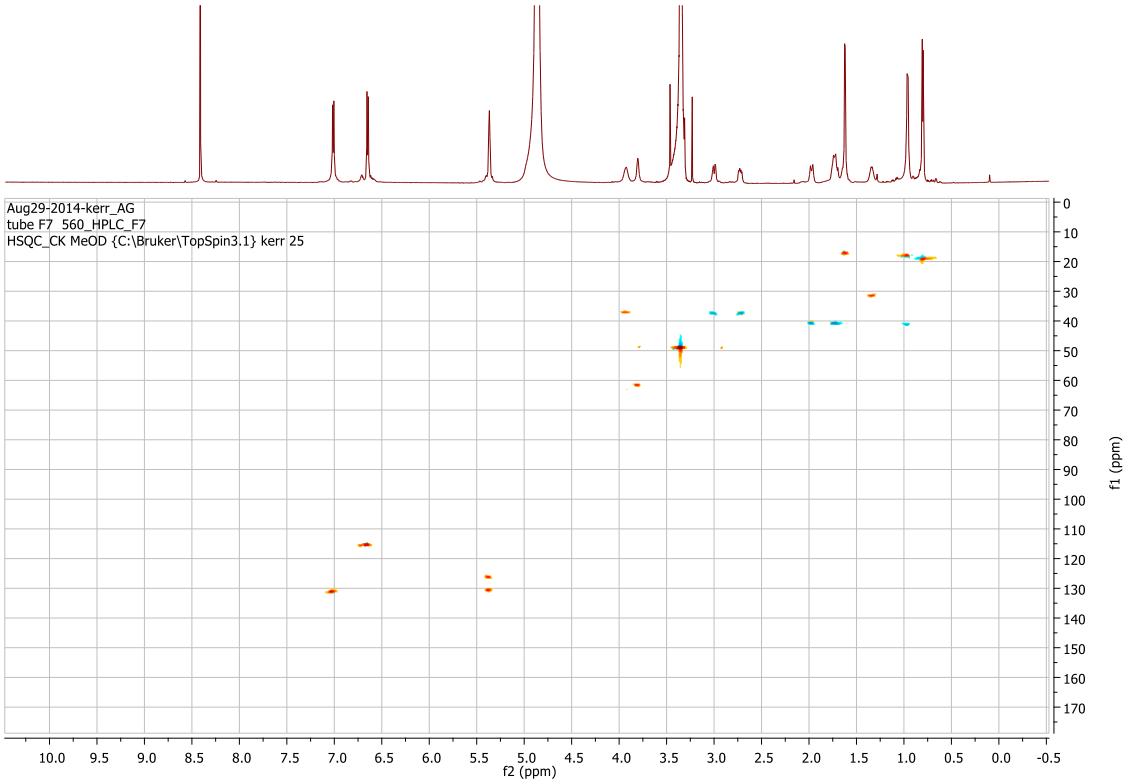

Figure A.66. HSQC spectrum of tolypoalbin in CD_3OD.

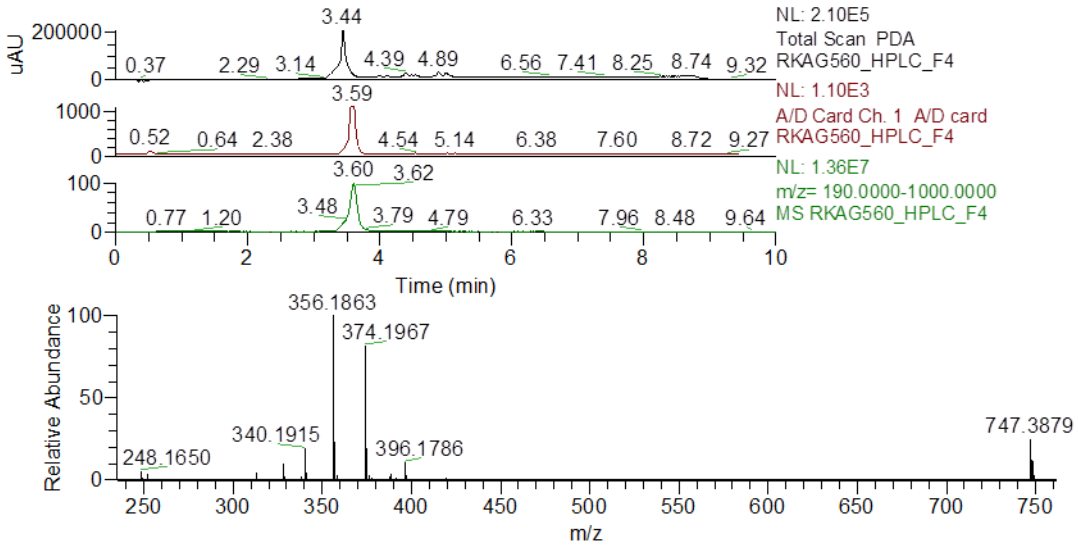

Figure A.67. +ESI HRMS of F-14329 *m/z* 374.1967 $[M+H]^+$.

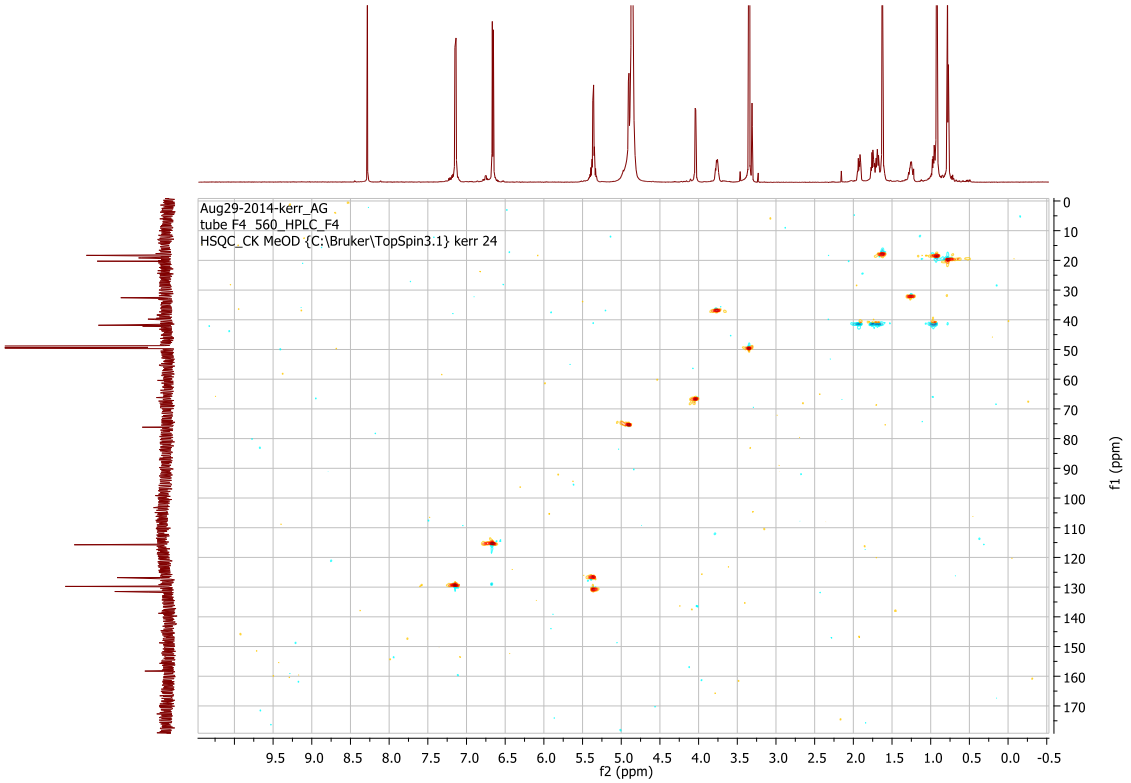

Figure A.68. HSQC spectrum of F-14329 in CD_3OD.

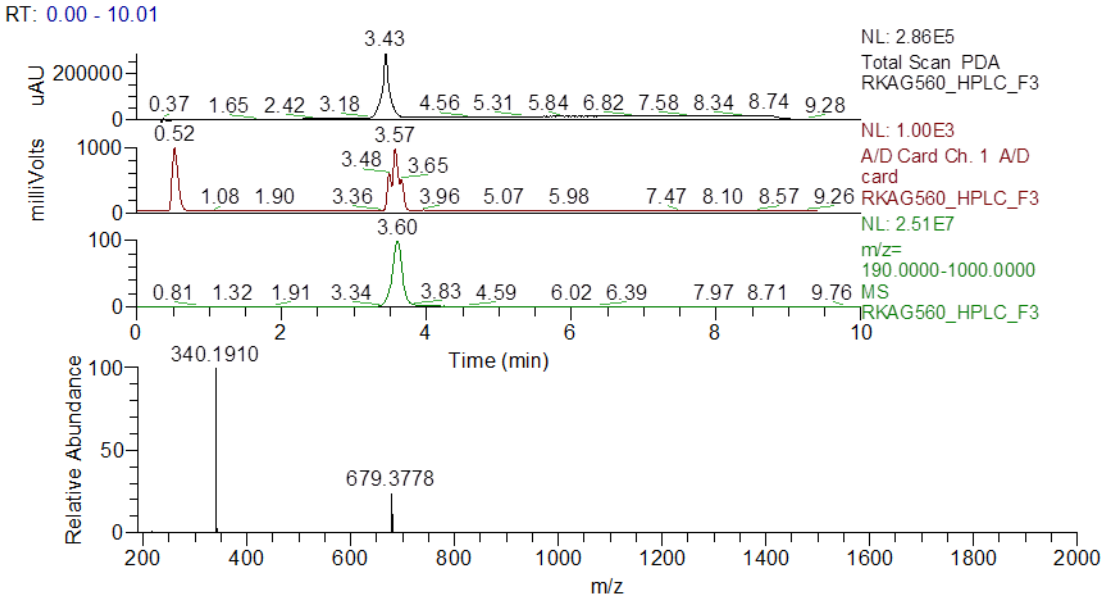

Figure A.69. +ESI HRMS of trichodin A *m/z* 340.1910 $[M+H]^+$.

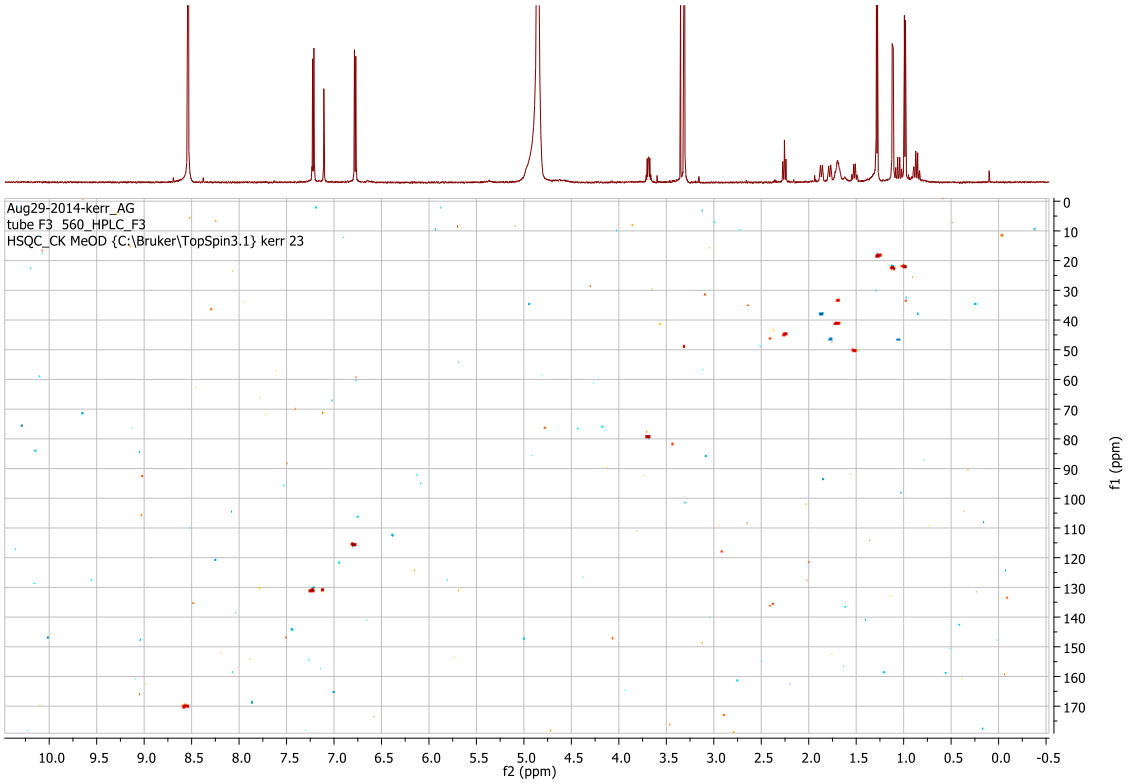

Figure A.70. HSQC spectrum of trichodin A in CD_3OD.